Copyright is owned by the Author of the thesis. Permission is given for a copy to be downloaded by an individual for the purpose of research and private study only. The thesis may not be reproduced elsewhere without the permission of the Author.

Ecology of infectious diseases in wild bats

A dissertation presented in partial fulfilment of the requirements for the degree of

Doctor of Philosophy

in

Veterinary Sciences

Carter Reed Hranac

School of Veterinary Science

Massey University

2019

Abstract

Emerging infectious diseases present significant threats to the health of humans and wildlife. The ecology of emerging infectious diseases is a data hungry field in a world of rare events. Bats are both the source of human pathogens globally and the victims of a novel fungal pathogen causing continent-wide population declines in North America. By using the principals of iterative model design and model guided field work I leverage the mechanistic relationships between seasonally limiting biotic and abiotic factors of wild bats to understand spatio-temporal disease emergence dynamics from and within bat populations.

I first use a novel ecological niche modeling technique to relate the seasonal availability of resources to predict African bat birthing events. I then use these model results to test hypotheses that Ebola virus disease (EVD) transmission to humans and non-reservoir animal hosts are related to the birthing events of bats through the use of a spatiotemporal Poisson point process model. The results suggest EVD emergence in Africa may be driven in part by the pattern of births among bats, especially fruit bats. Further, the identified temporal lag terms between bat birthing terms and EVD emergence are consistent with hypothesized viral dynamics in bat populations. Out of sample testing on the two most recent EVD outbreaks in the Democratic Republic of the Congo reveal a high predictive model performance and suggest the existence of both strong regional seasonality and locations persistently at risk of EVD outbreaks in humans and susceptible wildlife.

Finally, I model North American winter duration and incorporate spatial variation in host traits related to body mass and composition to update survival estimates for hibernating *Myotis lucifugus* infected with *Pseudogymnoascus destructans*, the causative agent of the emerging disease white-nose syndrome (WNS) killing bats in Eastern North American populations. Results indicate that hibernating *M. lucifugus* in the West are likely to suffer populations declines similar to those observed

in the East. All my findings will require further ground-truthing to validate the results, yet demonstrate the predictive power of identified mechanistic relationships on complex infectious disease systems.

I would like to dedicate this thesis to my loving parents, my brother, coffee, Google and all the people who helped me along. I would also like to make a special dedication to Dr. Nathan C. Nieto, a friend and advisor who started be down this path nearly 7 years ago but sadly passed away this June. His wisdom and passion for life will be missed by all those who were lucky enough to have him in their lives.

Acknowledgements

And I would like to acknowledge my co-authors, SERDP working group on white-nose syndrome, Massey University, the School of Veterinary Sciences and all those in the ^{m}EpiLab.

Table of contents

List of figures **xiii**

List of tables **xv**

1 Introduction to emerging infectious disease and their space-time complexities **1**

1.1 General introduction 1

1.2 Sylvatic transmission and the mechanisms of spillover 2

1.3 Dynamical models 3

1.4 Models of spillover processes 4

1.5 Ecological niche models 6

1.6 Barriers to spillover 8

1.7 Establishment and endemicity 10

1.8 Seasonality and temporal dynamics of infectious disease transmission 11

1.9 Ecological scale 12

1.10 Bats and disease ecology 13

1.11 Case Study 1: Ebola virus disease 15

1.12 Case study 2: White-nose syndrome 18

1.13 Where to next? 19

2 Spatial and temporal patterns of birth pulses among African bats **23**

2.1 Introduction 23

2.2 Methods 26

2.2.1 Chiropteran parturition data mining 26

2.2.2 Covariate data . . . 27
2.2.2.1 Mammalian diversity layers . . . 28
2.2.2.2 Land cover . . . 28
2.2.3 African bat birth pulse modeling . . . 28
2.3 Results . . . 30
2.4 Discussion . . . 35

3 Predicting Ebola virus disease risk and the role of African bat birthing 39
3.1 Introduction . . . 39
3.2 Methods . . . 42
3.2.1 Covariate . . . 42
3.2.1.1 Mammalian diversity layers . . . 43
3.2.1.2 Land cover . . . 43
3.2.1.3 Fragmentation index . . . 43
3.2.1.4 Bat birth pulses . . . 43
3.2.2 spatGLM . . . 45
3.3 Results . . . 48
3.4 Discussion . . . 51

4 What is a winter? Addressing data deficiencies for vital overwinter bat models 57
4.1 Introduction: . . . 57
4.2 Methods: . . . 60
4.2.1 Winter duration . . . 61
4.2.1.1 Acoustic and winter duration data . . . 61
4.2.1.2 Spatial covariates . . . 61
4.2.1.3 Modeling framework . . . 62
4.2.2 Spatially varying body mass . . . 62
4.2.2.1 Body mass data . . . 62
4.2.2.2 Spatially varying body mass . . . 63
4.2.3 Spatially variation in hibernation survival . . . 63

4.3 Results . . . 65
4.3.1 Winter hibernation duration . . . 65
4.3.2 Body mass . . . 65
4.3.3 Overwinter hibernation survival . . . 69
4.4 Discussion . . . 72

5 Discussion and concluding remarks 79
5.1 General discussion . . . 79
5.1.1 Future global emerging infectious disease challenges . . . 79
5.1.2 One Heath . . . 80
5.1.3 Data challenges . . . 80
5.1.4 Model guided fieldwork . . . 81
5.1.4.1 Model guided fieldwork in this project . . . 82
5.2 Chapter discussions . . . 83
5.2.1 Chapter 2 . . . 83
5.3 Chapter 3 . . . 84
5.4 Chapter 4 . . . 86
5.5 Concluding remarks . . . 87
5.5.1 Space and time . . . 87
5.5.2 The special place for bats in disease ecology . . . 88

References 89

Appendix A Spatial and temporal patterns of birth pulses among African bats 107
A.1 Data availability . . . 107
A.2 Figures . . . 107
A.3 Figures . . . 109
A.4 Figures . . . 110

Appendix B Spatial and temporal patterns of birth pulses among African bats 111
B.1 Data availability . . . 111

B.2 Tables 111
B.3 Figures 116

Appendix C What is a winter? Addressing data deficiencies for vital overwinter bat models 121

C.1 Tables 121
C.2 Figures 124

Appendix D Bats are not squirrels: Revisiting the cost of cooling in hibernating mammals 129

Appendix E Incorporating evaporative water loss into bioenergetic models of hibernation to test for relative influence of host and pathogen traits on white-nose syndrome 139

Appendix F Statements of contribution and copyright declarations 159

Appendix G Predicting Ebola virus disease risk and the role of African bat birthing 169

List of figures

1.1 BAM model of the biogeography of disease. 5

1.2 Descriptions of multi-disease biogeographic patterns: 7

1.3 Barriers to pathogen spillover and dose-response relationships 9

2.1 Spatial and temporal occurrence of bat birthing records obtained from the literature . 27

2.2 Probability of birth of African bats 36

3.1 Spatial and temporal detection of ebolavirus by host taxonomic group 40

3.2 Model prediction comparison 49

3.3 Risk of Ebola virus disease outbreaks among people 52

3.4 Model results in the context of the most recent EVD outbreaks 54

4.1 Data of *Myotis lucifugus* mass and hibernation duration across temperate North America. 60

4.2 Predicted duration of winter across temperate North America for *Myotis lucifugus* . . 66

4.3 Estimated body mass and component fat across the distribution of *Myotis lucifugus* . 69

4.4 Predicted end of hibernation body fat stores for *Myotis lucifugus* 71

4.5 Percent increase in predicted amount of fat stores required for *Myotis lucifugus* to survive hibernation when infected with *Pseudogymnascus destructans*. 74

A.1 Monthly ensemble probability habitat suitability to African fruit bats giving birth. . . 108

A.2 Monthly ensemble probability habitat suitability for non-Molossid microbats to give birth. 109

A.3 Monthly ensemble probability habitat suitability for Molossid bats giving birth. . . . 110

B.1 Risk of ebloavirus spillover to non-humans spillover hosts 117

B.2 Monthly risk of ebolavirus spillover to non-human spillover hosts 118

B.3 Monthly risk ebolavirus spillover into humans 119

C.1 Compairison of body fat by state for *Myotis lucifugus* 124

C.2 95% Confidence Interval for predicted winter duration. 125

C.3 95% Confidence Interval for predicted mass pre-hibernation. 126

C.4 95% Confidence Interval for predicted fat mass pre-hibernation 127

C.5 Increased fat consumption due to infection for *Myotis lucifugus* when hibernating at $Ta = 2°$, and $RH = 100\%$. 128

List of tables

1.1 Currently recognized Filoviridae members. 15

2.1 Co-variate layers for ecological niche modeling 28
2.2 Reclassification of land cover variables 29
2.3 Data mining results for African bat birthing 30
2.4 Ecological niche model ensemble scores. 34

3.1 Reclassification of land cover variables 44
3.2 Covariate layers for spatGLM modeling 44
3.3 Top two human Ebola virus disease risk model results 50

4.1 Abiotic covariate tested in spatial analyses 62
4.2 Model selection by AIC for alternative spatial models. 67
4.3 Summary of predicted survival capacity for *Myotis lucifugus* 68

B.1 Animal spatGLM Results 112
B.2 Animal spatGLM* Results 113
B.3 Human spatGLM Results 114
B.4 Human spatGLM* Results 115

C.1 Data collection records for the duration of winter for *Myotis lucifugus* 122
C.2 Data collection records for the mass of *Myotis lucifugus* 123

Chapter 1

Introduction to emerging infectious disease and their space-time complexities

1.1 General introduction

Emerging infectious diseases (EIDs) present enormous threats to human and ecological health across the globe [113]. EIDs represent a special subclass of infectious agents whose incidence has increased over the last decades. Emergence of these pathogens is often the result of pathogen introduction into a susceptible population for the first time, commonly through entrance into a new geographic region where they were previously absent. The reemergence of infectious diseases is also possible, often through the evolution of new mechanisms of virulence or resistance to treatment [113]. Some of the most notable recent examples of human EIDs include the 2014 West Africa Ebola virus disease (EVD) outbreak [32], the 2016 Zika virus epidemic [100] or even the re-emergence of Measles virus within un-vaccinated communities [76].

Many of what are now seen as endemic human infections originated within non-human animals, as zoonotic pathogens (defined as pathogens with a animal origin), before establishing as endemic in humans (HIV/AIDS, Malaria)[242]. Zoonotic agents are generally constrained to reservoir populations, however *'spillover'* events occur, where infection jumps between species. While these events are often rare for specific infectious diseases, some zoonotic disease events occur regularly (e.g. food-borne diseases) and greater than 60% of all human EIDs between 1940 and 2003 originated in non-human

hosts, and, of those, 71.8% were of wildlife origin [113]. Frequency of EID and zoonotic events has increased over recent decades in part due to processes like habitat encroachment, land use changes, human population expansion [241, 57]. EID events can also occur within animal populations often leading to complex conservation challenges [131, 66].

Epizootic (within domestic animal or wildlife epidemics) outbreaks of fungal pathogens are responsible for White-nose syndrome (WNS) and chytridiomycosis[62]. Both pathogens have proven to be ecologically devastating [66, 202]. Populations of at least 501 amphibian species are in decline, including as many as 90 species extinctions due to chytridiomycosis [202]. Similarly many species of North American hibernating bats are experiencing large scale population declines and local extinctions, due to the introduction of *Pseudogymnoascus destructans* just over a decade ago [26, 66].

In this chapter I will discuss some of the fundamental tenants of infectious disease ecology with specific focus on bats, the mechanistic relationships between the hosts and pathogens, and how spatial and seasonal dynamics can modify risk and transmission of infectious agents. To provide background I will introduce two case-study examples: EVD, a high consequence zoonotic pathogen that has caused tens of thousands of human deaths [32]; and WNS, a purely enzootic pathogen with conservation implications [66, 67]. Each of these examples are explored more in depth within this thesis. I will be focusing on how seasonal life-history events within bat populations influence infection dynamics, highlighting tools, theories, and frameworks explored in subsequent sections and chapters in this thesis.

1.2 Sylvatic transmission and the mechanisms of spillover

There are an estimated minimum of 320,000 mammalian viruses alone awaiting description [8] and prior to an initial spillover event, these viruses, or any other zoonotic pathogens are constrained by their host-pathogen cellular relationships and sylvatic transmission cycles. Within the simplest of these systems, a reservoir host species is required to maintain and transmit the infectious agent within the population [90]. Sylvatic systems may be composed of a single or multiple species or entire communities of species acting as reservoir hosts [164]. Additional non-reservoir hosts can exist and include: *amplifying hosts*, in which pathogen replication and excretion rises over that within the

reservoir host (generally with deleterious consequences); *paratenic hosts*, in which no replication pathogen occurs yet the host is still capable of transmission; *dead end hosts* that are not capable of further propagating the infection to others; and *phylogenetic hosts*, that contribute to the genetic evolution of the pathogen in some manner. These 'non-reservoir' hosts are by definition not required to maintain the pathogen on the landscape; however through changes in host densities (reservoir or otherwise), infection prevalence, and intensity of infection (e.g. amplifying hosts) all may act to modify pathogen pressure and spillover [190, 137].

1.3 Dynamical models

In order to model how population members or subpopulations move from uninfected to infected and beyond we can to use a compartmental model of infection. For simplicity, one can consider this as a single closed population and ignore entry and exit of members due to births and deaths. Within this framework a randomly mixing population of N individuals is split into three mutually exclusive classes: susceptible (S); infected (I); and recovered (R). In this case, infected individuals are capable of infecting susceptible individuals at the rate of $\beta * SI$, and infected individuals recover from infection where they can not be infected again at the rate of γ. This can be defined by a series of differential equations describing movement between classes over time t and summarized by the system of equations:

$$\begin{aligned} N &= S + I + R \\ \frac{dS}{dt} &= -\beta SI \\ \frac{dI}{dt} &= \beta SI - \gamma I \\ \frac{dR}{dt} &= \gamma I \end{aligned} \tag{1.1}$$

The addition of hosts to the system through births and immigration and loss through death and emigration will modify the rate at which the population shifts between these compartments. Further modifications can be made such as the introduction of different transmission mechanisms, infection dynamics (e.g. a return to susceptible status), or age structure and these are discussed below, when necessary.

Two more critically important parameters derived from this system of equations are R_0 and the critical community size (CCS). The parameter R_0 is the average number of secondary infections to arise from a single infected individual in a totally susceptible population. Using equation 1.1 with its same assumptions R_0 is simply calculated by $R_0 = \frac{\beta}{\gamma}$. In order for an infection to be maintained within a population an outbreak must have an $R_0 \geq 1$, else the number of individuals in the infected compartment will eventually decline as hosts transition to the recovered category more quickly than they can be replaced, resulting in the eventual fade out of infection as susceptible individuals are depleted. Outbreak intervention strategies that target improving hygiene, or establishing quarantine, effectively aim to lower the R_0 value by reducing interaction between susceptible and infected limiting the epidemic. Alternatively, infections with exceptionally high R_0 like measles, with a value 12-18 [78], can rapidly deplete available susceptible individuals and require a large population with a continuous influx of naive hosts to enter an endemic state. This tipping point of population composition is referred to as the CCS. Pathogens with a viable environmental life-stage or that result in chronically shedding hosts can maintain infection at comparatively smaller CCS and R_0 is not as directly interpretable for control measures [136].

1.4 Models of spillover processes

The factors driving and contributing to the spillover or emergence of EIDs from sylvatic maintenance are inherently complex, and, as such, many frameworks have been proposed to decompose the drivers into explicit terms [244]. One such framework within disease ecology is the "BAM" framework (Figure 1.1) proposed by Peterson [185] as "biogeography of disease." [185, 207]. The distribution of any pathogen can be viewed as a standard Grinnellian niche within the larger reservoir host and is defined by the interaction of **B**iology, **A**biological factors and constrained within limitations of a species distribution and **M**ovement. Thereby, the realized niche of any pathogen can be described $A \cap B$, and the complete geographic distribution of a species (P) would be further refined as the joint probability of $B \cap A \cap M$. As the system increases in complexity this can be expanded with each host and pathogen creating a theoretically infinitely expandable equation where the true distribution would

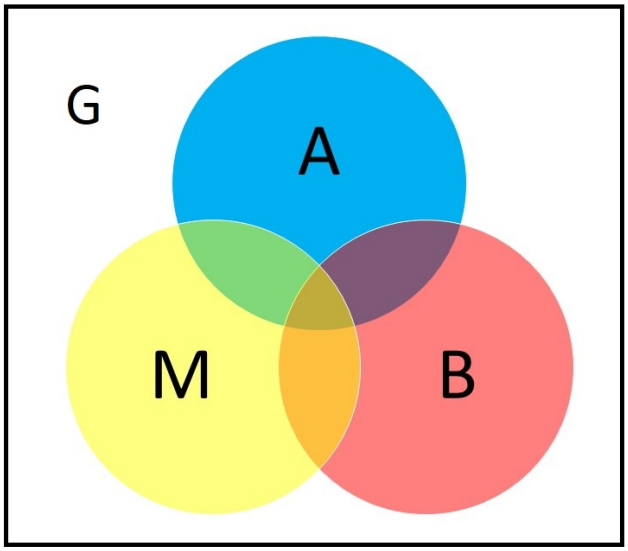


Fig. 1.1 **BAM model of the biogeography of disease.** The area G represents all possible parameter space available on the planet. The blue area **A** represent locations on the landscape with the appropriate abiotic features to support a species, and can be alternatively defined as the fundamental niche. The red **B** zone includes the correct combination of interacting species, and may not completely overlap with the **A** region. The purple area in which $A \cap B$ represents the Realized Niche. The parts of the world accessible to the species is represented as the yellow **M** circle and excludes barriers to movement like oceans and mountain ranges. The central overlap describes a region with correct biotic and abiotic factors for a species survival as well as being accessible and can be though of as equivalent to the geographic distribution of the species. *Adapted from [207]*

be represented as:

$$P = \Sigma(B_1 + ...B_i) \cap \Sigma(A_1 + ...A_i) \cap \Sigma(M_1 + ...M_i). \tag{1.2}$$

In order for spillover to occur, the reservoir species ($_1$) and the spillover host species ($_2$) must both inhabit a subset of G (as defined as all conceptually available habitat space) in equation 1.2 such that $A_1 \cap A_2$, and be close enough biologically that the pathogen can successfully infect both ($B_1 \cap B_2$). The intersection of M between reservoir and spillover host species therefore defines the geospatial context of the interaction between these two species, whether they are community members within the same ecological assemblage, or one of them is merely a migrant passing through.

This framework can be expanded upon to describe the complete 'Pathogeography' of a system by defining relevant covariate structures, e.g. landscape, biogeographical, and observational features as depicted within Figure 1.2.

1.5 Ecological niche models

Core methods at the heart of the BAM methods are ecological niche models (ENM), which attempt to define the fundamental niche that a species occupies, while the closely related species distribution models (SDM) includes movement and dispersion to better reflect the realized niche [185]. Either of these approaches allow us to create correlative relationships between the occurrence of a species and the environmental (abiotic) conditions [185, 55]. The algorithms typically deployed include generalized linear models, generalized additive models and machine learning techniques, such as boosted regression trees. Additionally, more recent model developments have sought to define a species distribution through mechanistic relationships, often relying upon the metabolic physiology of the target species and the habitat space they inhabit [36]. Covariate data is incorporated as environmental data including climate data (e.g. temperature, rainfall), but any available variables defining a limiting relationship could in theory be used [159]. ENMs and SDMs provide powerful platforms to work from as after initial model fitting, distributions can be predicted across novel environmental space, which are of particular use when assessing climate change and habitat loss [159, 36].

Like all models, the results are dependent on the complexity and accuracy of the input data and the modelers knowledge of the underlying relationship of the target system [194]. Correlative ENMs typically use multiple regression, assuming that the species and covariates have been adequately sampled and species' presence and absence data are available [185]. In many cases, true absences are unavailable (see chapter 5 for further discussion), so "random background" or "pseudo-absence" data are often used to fit these models, potentially introducing bias [55]. Correlative ENM are relatively easy and fast to implement, but often do not provide information on causal mechanisms and are less suited to extrapolation. Physiological mechanistic ENMs may use microclimate, body temperature and energy requirements to predict the potential distribution and so may be independent of the species' known or current range [36]. Mechanistic models, however, require substantial understanding of host physiology, which is often not available. While mechanistic models can often be complex, improvements of computational capacity have allowed these models to be used and combined with correlative approaches to provide additional insights [207, 36]. Increasingly, multiple types of models

are used to create ensemble models that combine several model outputs to share the strengths and weaknesses of each constituent member and come to more robust conclusions than each individual model alone.

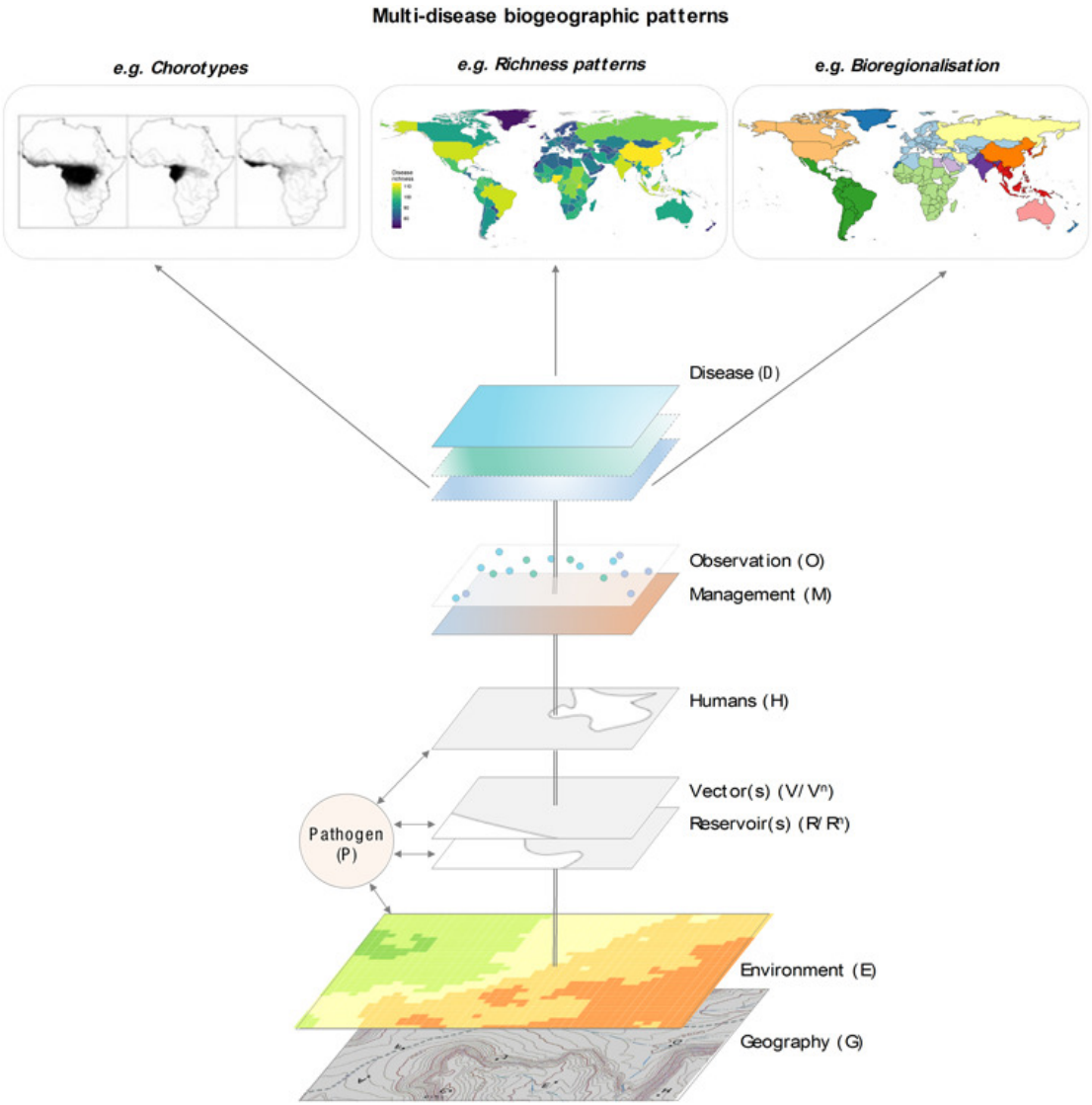


Fig. 1.2 **Descriptions of multi-disease biogeographic patterns:** The observed distribution of a disease D, can be describe in it's multi-dimensional space as the subset of areas across which the geography (G), environment (E), reservoir (R), vectors (V), observations (O), and humans (H) all over lap. Within a generalized system of all potential diseases, hosts, and environments, species richness, bioregionalism and chorotypes can be created to represent large scale patterns potentially useful to the study of infectious disease. *Adapted from Murray et al. 2018*[159] *under the creative commons attribution license.*

1.6 Barriers to spillover

For a pathogen to emerge from a zoonotic host and enter circulation in human populations to causing disease a set of "necessary" and "sufficient" criteria must be met [190, 138, 197]. The presence of an infectious agent alone does not describe the complete mechanism of infection, but rather, a number of individual 'components' act in concert to result in a disease state. These components interact with barriers to infection and Plowright *et al.,* 2017 conceptually visualized these as a series of mechanistic filters that a pathogen must pass through in order to successfully infect and replicate within a spillover host, as shown in Figure 1.3. These filters can be broadly separated into three general themes: 'Pathogen pressure', 'Exposure', and 'Probability of infection'.

Pathogen pressure factors determine the contact duration and intensity of interactions among hosts to modify the quantity of infectious agent on the landscape. The simplest example of this is species distributions. As an extreme example, a pathogen maintained within crustation species living deep in the ocean will have a nearly null probability of transmitting into a Savannah dwelling lion, effectively setting the equation 1.1 β term to 0, as M_1 and M_2 from equation 1.2 do not overlap. Alternatively, hosts sharing a biome may naturally come into contact with one another often through competition for resources. The duration and intimacy of these contact interactions can vary greatly and the prevalence of infection within the reservoir host population functions to quantify this risk. The density of infected individuals on the landscape will further modify that β term, increasing the probability that a spillover host encounters an infected reservoir host.

Conceptually, once contact has been made between an infectious and noninfectious hosts, the next key component is the mechanism of infection transmission. Directly transmitted infections will inherently require a more intimate level contact between individuals to facilitate transmission, reducing the probability of trans-species infection. If, however, the infectious agent can be shed into the environment, persist, and remain infectious for a period of time contact sufficient to transmit from host to host is more relaxed, and needs to be considered as such when both parameterizing models and developing disease control measures.

The mechanism of transmission and interaction between the S and I individuals in equation 1.1 are generally grouped into either a frequency, or density based transmission models. Frequency

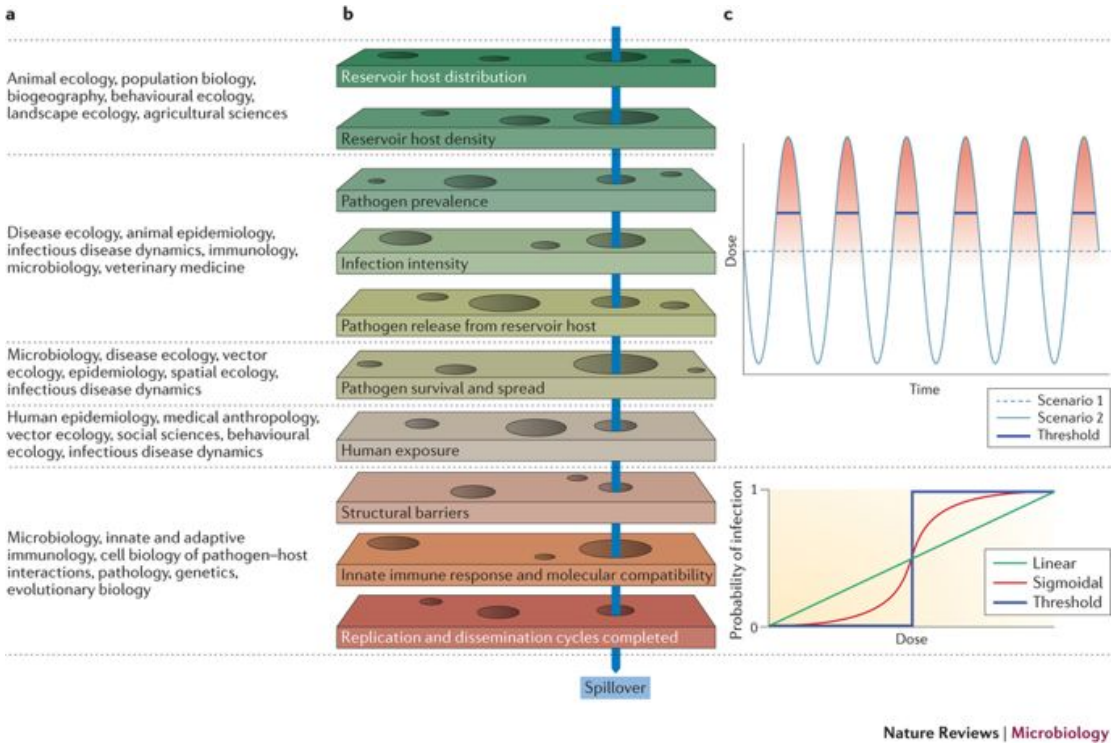


Fig. 1.3 **Barriers to pathogen spillover and dose-response relationships a)** Determinants of spillover are being studied by researchers in many disciplines. **b)** A pathogen must overcome a series of barriers to transmit from one species to another. If any of these barriers is impenetrable, spillover cannot occur. Spillover of some pathogens requires that gaps (depicted as holes) in all of the barriers align within a narrow window in space and time. For other pathogens, protracted survival in the environment, or wide dissemination, may stagger the alignment of barriers to spillover. **c)** Top panel: hypothetical dose available over time for a given pathogen. In scenario 1 (dashed light blue line), the pathogen is excreted consistently from infected reservoir hosts. In scenario 2 (solid light blue line), the pathogen is excreted in regular but short high-intensity pulses over time. In both scenarios, the mean dose over the time interval is the same. Bottom panel: the likelihood that this dose will translate into infection depends on the functional form of the dose–response relationship. If the dose–response relationship is linear (green line), these two excretion scenarios generate the same total probability of spillover over the time interval shown. However, for nonlinear dose–response relationships, the total probability of spillover differs between scenarios. If the relationship is sigmoidal (red line), there is some probability of spillover whenever the dose exceeds zero (indicated by the intensity of the red shading in the top panel), but the total spillover probability in scenario 2 is markedly higher. In the extreme case in which the recipient host can be infected only by a dose that exceeds a sharp threshold, as suspected for *Bacillus anthracis*, the pathogen in scenario 2 will spill over when the dose peaks above the threshold (blue solid line near peak), but the pathogen in scenario 1 will never spill over. *Reprinted by permission from Nature Plowright et al. 2017 [190]* ©2017

based transmission rely on the number of infected individuals withing the populations often requiring intimate contacts to facilitate transmission and best exemplified by sexually transmitted diseases.

Mathematically these are of the general form $\beta \frac{SI}{N}$. Density dependent infections like measles have a term of the general form βSI. Density dependent infections spread rapidly though gregarious populations as they are more reliant on less intimate contacts between individuals for transmission and often through aerosol or fomites. Transmission of most infections however, is neither one extreme or the other and sylvatic maintenance can often shift between contact structures [141, 2, 137, 199].

The *exposure* component of this framework is composed of factors contributing to the dose and route of exposure and often referred to as the 'force of infection' [137]. At one extreme lies aerosol transmission of measles where millions of viral particles are released into the air where they may persist of hours in sufficient quantity to cause infection in a susceptible host [78]. At the other extreme, as few as 25 bacterial cells may be sufficient for transmission of *Francisella tularensis* bacteria [177]. Attempting to parameterize these routes of exposure is complex and requires intimate system knowledge. These factors are rarely known within the sylvatic and primary spillover context. Controlled experimental infection trials are therefore desirable to advance system knowledge, yet these can have considerable logistical and ethical concerns surrounding them.

Finally, once naïve hosts have come into contact with an infected reservoir host and a pathogen is passed through a viable route of transmission in sufficient quantity, a pathogen must overcome the host's barriers to infection in order to successfully invade and establish. The *probability of infection* depends upon route of infection, with barriers to pathogen invasion including physical means such as the skin, mucosal membranes designed to ensnare bacteria, cell membranes with highly specific receptor binding sites or other passive innate immune challenges. To successfully propagate infection to a new host, infecting agents must effectively evade, suppress, or overwhelm the host immune response to reproduce and then be released from the host to reach another susceptible individual.

1.7 Establishment and endemicity

Following the initial spillover event, most zoonotic pathogens do not immediately become endemic within the spillover population, rather these pathogens generally have multiple dead-end transmission events from the reservoir host population [137, 138]. As successive pathogen generations make the trans-species leap, longer stuttering transmission chains are created in which transmission will

temporally persist within the host population prior to stochastic fade out. Selection and drift can allow for accumulation of genetic changes and the development of a phenotype capable of increased onward transmission [183, 138, 137]. Moreover, the novel spillover host may circulate the infection back into the reservoir host community, as reverse zoonosis [150]. Eventually, some infectious agents accumulate enough changes to colonized the new niche and enter endemic maintenance within the formerly naïve population [138].

1.8 Seasonality and temporal dynamics of infectious disease transmission

In the context of disease ecology, seasonality, or "seasonal forcing," can be any periodic event that modifies how infection moves within or between hosts. Drivers of seasonality are often abiotic and affect primary production, including annual cycles in rainfall, temperature and photoperiod [2]. These seasonal events can drive population demographic events, such as synchronous births of mosquito populations following rains [39]. Additionally, seasonal drivers primarily modify components related to R_0, often by altering contact rates within populations, however seasonal variation in susceptibility due to nutritional and reproductive status have been recorded [2].

At a fine temporal resolution, forcing can be incorporated within a single day. Bats are nocturnal, with daily change in both population densities (they may fly alone at night, but roost in clusters of hundreds in hibernacula [122]) and physiological state (their metabolic rates can increase up to 16-fold from resting rates during flight, only to drop below this 'resting' metabolic rate during daily topor [175]). These diurnal changes effectively change intra- and inter-species interactions and providing an unequal probability of contact sufficient to transmit infection throughout the day. In the context of human infectious diseases, daily, weekly and monthly alterations in behavioral patterns can create variance in contact networks, altering rates of transmission and the probability of infection persistence within a population [138]. Events that increase the density, elevate contact rates or bring together sub-populations of susceptible individuals will increase the spread of infection [77, 2, 37]. One of the most famous examples of this is the relationships between measles and the return of children to school following the summer holidays [77]. As these populations of previously dispersed children

aggregate into close quarters the rate of infection increased and an epidemic wave took off through the population. Without the inclusion of seasonal forcing, epidemic peaks for measles were less steep and of lower magnitude then those observed within actual populations [77]. Seasonal forcing can affect each participant host in unique ways and can be difficult to incorporate within dynamic models as drivers may act independently between host types and act across a variety of temporal scales [54].

Within a bat specific context, at tropical latitudes the bi-annual oscillations between wet and dry seasons create pulses in food availability [50]. Transient resources on the landscape have resulted in teh development of migratory and nomadic lifestyles among some species to maximize resource consumption [38, 16]. These life history strategies can create transmission hot spots along migratory corridors and destinations where locally transmitted infections can enter global circulation [37]. Alternatively, exotic infections can enter local circulation through the inverse processes resulting in new local endemic transition of a previously exotic infectious agent [37]. At increased temporal scale, interannual patterns of seasonal oscillations like the El Nino and La Nina events precipitate trophic cascades creating boom and bust cycles within wildlife populations [73]. Spatial and temporal scales interact in both predicable and unpredictable ways, modifying much of what we know about infectious dynamics [2].

1.9 Ecological scale

Much in the way that seasonality can be split by the temporal resolution, ecological scale must be considered. At the finest resolution, intra-host factors define relationships between hosts and pathogens. Infected individuals can be considered as an independent micro-habitat, and need to fulfill all metabolic demands of the pathogen to successfully replicate [207]. Infection status determinants like age, sex, reproductive status and other life history traits modify the susceptibility and disease outcome [190, 2].

Increasing from an individual to populations, several simplifying assumptions are commonly made within dynamic modeling. Populations are often considered to be at equilibrium with equal mortality and replacement rates, population members are considered free mixing, and forcing due to seasonality affects all members equally. These assumptions are rarely met for wildlife [136, 180],

and in more complex scenarios where the populations are better understood, subpopulations can be included to explicitly describe variance between population members.

Meta-populations can be considered as a network of inter-connected nodes, each representing a distinct population, with parameterized movements between one another. Each node will contain some simplifying assumptions, but more importantly each node can be independent, containing unique population sizes and estimations for each term (*e.g.* β, and R_0). Because of the flexibility of this approach, researchers can computationally simulate complex phenomena like unequal seasonal forcing which can act to drive infection across the landscape [54, 77].

In the final level of abstraction we can consider the concept of ecological communities on infectious disease dynamics. These systems are maintained through a variety of animal hosts, and, in some cases, a single pathogen will require multiple reservoir hosts to complete one full life cycle. *Ribeiroria* for instance is a genus of trematode parasites that infects snails, amphibians (or fish) and finally predatory birds that act as the definitive host (where sexual reproduction occurs) all within a single life cycle [112]. If a single one of these members is absent, or resistant to infection, sylvatic maintenance of infection could collapse and disease fade out occur.

In the next section, I introduce bats as exemplars of many of these concepts and conclude with two case studies, Ebola virus disease and White nose syndrome.

1.10 Bats and disease ecology

Bats are the second most diverse mammalian taxa behind rodents and are nearly globally distributed, playing an imperative role in environmental health by pollinating plants, predating pest species, and other ecological services [166]. Bats have been implicated as potential ancestral hosts for some important mammalian viruses including Severe Acute Respiratory Syndrome (SARS) coronavirus [79] and Rabies virus [134], and novel viruses are continually described from bat hosts [75, 91]. Traits linked to the ecology, evolution and life history of bats make them 'special' reservoir hosts for pathogens [173, 141, 33]. Viruses associated with bats were found to be hosted by more species than their rodent counterparts and sympatry of taxonomic members is thought to explain much of this relationship [140]. Evidence suggests that dense, pathogen permissive communities with high

dispersion and connectivity between one another facilitated by migratory and nomadic behavior allow bat populations to sustain even acute viral pathogens [93, 4].

The evolution of flight is hypothesized to facilitate the competency of bats to act as pathogen reservoirs [173, 134]. During flight metabolic expenditure increases 15-16 fold, increasing body temperatures to 40°C and consuming double the energy over the course of a lifetime when compared it an equal non-volant counterpart [208]. To account for increased metabolic demand, bats have been discovered to have evolved additional molecular mechanisms to handle oxidative stress at the site of production, including, by redirecting 'Reactive oxygen species' (ROS) chemicals to activate 'self-destruct' pathways when appropriated [33]. Limitations of intracellular pathogens (and tumour genesis) through autophagy and apoptosis triggered by these intracellular mechanisms rather than adaptive immune cascades are hypothesized to reduce the occurrence of immunopathologically induced mortality [229]. These virtually ever-present innate 'hyper-vigilance' mechanisms may not only have selected for incomplete clearance of viral pathogens, but also increased metabolic tolerance, improving the fitness of viral agents [173]. Resultantly, this may in part explain the virulence and lethality of bat-derived infections like Ebola virus (see below), to humans and other mammals. Once cross-species spillover occurs viruses may be already tolerant to many generic innate immune responses used to suppress viral infection.

While bats as a whole have evolved the ability to drastically increase metabolic rates, some species are also capable of hibernation by repressing metabolic rates through the use of torpor. Torpor reduces energy consumption by dropping the body temperature to ambient (or near ambient) temperatures, resultingly reducing intracellular metabolism [208]. This decreased intracellular metabolism leads to decreased viral replication, however extended bouts of torpor also suppresses immune function providing an exploitable weakness for opportunistic extra-cellular pathogens [157]. The lethality of extracellular fungal pathogens to bats, and in particular WNS, far exceeds that of other infectious agents and is causing broad population declines among some hibernating bat species across North America [67, 174].

1.11 Case Study 1: Ebola virus disease

Ebola virus disease (EVD) is caused by members of the genus *Ebolavirus* (Family Filoviridae) and is composed of 5 current members, of which 4 are known to cause EVD in humans (henceforth referred to as "ebolaviruses") and summarized in Table 1.1 [120]. In 1979 EVD first emerged along the Ebola river in what was Zaire, presenting as an acute febrile illness with hemorrhaging and high case fatality rates [191]. Since then ebolaviruses have emerged sporadically across central and western Africa [187]. The largest event to date started in 2013 in Guinea, West Africa, ultimately resulting in 26,000+ infections, and 10,000+ deaths [32]. Currently, the second largest outbreak of EVD continues in the extremely politically turbulent Northern region of the Democratic Republic of Congo (DRC) [239, 46].

Table 1.1 **Currently recognized Filoviridae members by the International Committee on Taxonomy of Viruses.**

Genus	Species	Abbreviation
Marburgvirus	*Marburg virus*	MARV
	Ravn virus	RAVV
Ebolavirus	*Bundibugyo*	BDBV
	Reston virus	RESTV
	Sudan ebolavirus	SUDV
	Tai Forst ebolavirus	TAFV
	Zaire ebolavirus	EBOV
Cuevavirus	*Lloviu cuevairus*	LLOV

While EVD outbreaks have caused many human deaths, EVD is also suspected in large scale die-offs of gorillas and chimpanzees throughout central Africa causing additional conservation concerns [131]. Despite decades of research and numerous epidemiological investigations all components of the **BAM** framework are still unclear. Reservoir host(s) have yet to be confirmed [210] and while there seems to be some seasonality to viral emergence no mechanistic driver has been proven [188]. The sporadic nature of EVD outbreaks on the landscape suggests complex dynamics either in the spillover process and/or the maintenance and propagation of the virus across the landscape.

To date no full viral genomes for EVD causing ebolaviruses have been sequenced from bat species, yet several key facts point in the direction of a ‘Chiropteran’ host [170]. within non-bat mammalian species the ebolaviruses have been detected in, with EVD-causing species results in

acute febrile illnesses with rapid progression to mortality [94]. In contrast, experimental infection studies have demonstrated the ability of some bat species to mount an effective immune response, and clear the pathogen with little pathogenesis [210]. Most recently, a full viral sequence was recovered for a proposed 6th *Ebolavirus* species hosted by a molossid bat, however the ability of this virus to cause EVD is still unknown [75]. Several EVD outbreak events are anecdotally connected with bats, but no definitive evidence of the primary spillover event exist [191]. In the few traceable cases of spillover, contact with deceased gorillas, chimpanzees or duikers were noted along with their mortality, suggesting epizootic events may have originated from some primary spillover event [94]. Many questions still remain concerning the competency of bats to propagate the infection in nature, shed infectious numbers of viral particles, and the mechanisms of spillover into human and non-human spillover hosts remains undetermined [170].

While many questions still remain unanswered about the sylvatic ecology of ebolaviruses, inferences can be drawn from a sister taxa. *Marburgvirus marburgvirus* (MARV, family Filoviridae) emerged in clinical research primates imported from Africa into research facilities in Marburg, Germany, infecting staff [98]. Since then sylvatic maintenance of MARV has been linked to the large cave dwelling populations of *Rousettus aegyptiacus* [192]. Similar to Ebola virus in bats, MARV infection in *R. aegypticus* results in the production of an immunizing response with a short window of viral shedding [211, 5]. Temporal analysis of MARV infections and virological work suggest that despite the narrow window of viral shedding, synchronous shifts in population demographics enable viral maintenance [4]. The highly synchronous bi-annual birthing of *R. aegyptiacus* would large numbers of individuals becoming susceptible simultaneously, however this may be partially dampened by the waning of maternally derived antibodies providing a more sustained pool of susceptible hosts [180]. These younger bats inhabit sub-optimal roosting space where they are constantly in direct contact with excreta from adults roosting above them, and presumably resulting in MARV transmission [4].

In contrast to the MARV system, serological evidence of ebolaviruses implicates foliage roosting species of fruit bat with far less gregarious populations than *R. aegyptiacus* [170]. Computational simulations have suggested that the same synchronous pulses in population demographics observed within the MARV system may allow for the endemic persistence of ebolaviruses with achievable CCS [93]. Separate machine learning analyses correlated specific host traits including the biannual birth

pulses and synchronous birth events with filovirus hosts [84]. While locally synchronous, spatial heterogeneity in the timing of the birth pulses is capable of causing a complex enzootic (endemic) state, and theoretically responsible the sporadic EVD spillover events observed.

In the context of the *SIR* disease dynamic modeling this case study brings many new facets to the system of equations. The maternally derived antibodies (MDA) acquired *in utero* are believed to functionally protect the fetus during gestation and may be continually replenished while the pup continues to suckle off the mother [56]. This period, represented by M, is a new state, thus creating a linear *MSIR* structure of the form:

$$\begin{aligned} N &= M + S + I + R \\ \frac{dM}{dt} &= B_t * R - \sigma_t * M - \mu * M \\ \frac{dS}{dt} &= B_t * S + \sigma_t * M - \beta_t * S * I - \mu * S \\ \frac{dI}{dt} &= \beta_t * S * I - \gamma_t * I - \mu * I \\ \frac{dR}{dt} &= \gamma_t * I - \mu * R \end{aligned} \tag{1.3}$$

In addition to the inclusion of a M category, population demographics are included as the terms B representing the birth rate, and μ, the mortality rate. A time varying birth pulse can take many forms. One recent one allows births to be modeled as a 'periodic Gaussian' function, so that birthing can be seasonally pulsed, but does not stop and start abruptly like a step function [93, 180]:

$$\beta_t = \kappa \sqrt{(\frac{S}{\pi})} * exp^{s*cos*\pi*t*\omega - phi^2} \tag{1.4}$$

While the high synchrony of births allows for large swings in the susceptible population, this is tempered by the more steady introduction of the M class animals, as maternally derived antibody is lost at rate σ. This structure can be further developed by including factors such as age structure and density-dependent mortality, similar to [93].

1.12 Case study 2: White-nose syndrome

The emergence of *Pseudogymnoascus destructans* (*Pd*), the causative agent of WNS in 2006-2007 has severely impacted the hibernating bat species of eastern North America [26, 66]. The psychrophilic (cold-loving) fungus infects hibernating bats, disrupting the delicate energy balance required for overwinter hibernation and causes the premature depletion of overwinter energy reserves. Northeastern bat populations have seen severe population declines, local expatriations, and changes in community structure [67]. During the winter of 2016 the fungus was detected in Washington state, signifying the arrival of WNS to the more biodiverse western bat populations [83]. As the fungus continues to spread through western North America, researchers are working diligently to better understand what measures can be taken to protect these at risk communities. Interestingly, and importantly for understanding the potential long term impacts, *Pd* appears to be an introduced clone from Eurasia [53], where the bats have apparently co-evolved to live with this environmentally persistent fungus [106].

At the scale of a single hibernating bat infected with *Pd*, we can again return to the **BAM** framework. The disease state of WNS is largely due to the interaction between the bats' hibernation physiology and the abiotic conditions required for hibernation [229, 237]. In order to survive the resource poor winter period, bats rely on the use of torpor to manage available energy resources [108, 208, 234]. By dropping their metabolic rate and body temperature to ambient temperatures, bats minimize their energy consumption [215, 208]. This biological conformation to the abiotic conditions for hibernation affect infection by the *Pd* fungus in two ways: 1) fungal growth on the dermis would be inhibited at normal euthermic temperatures [228, 42], and 2) during torpor the immune functionality of bats is severely diminished, eventually leading to the colonization of the bats most vulnerable areas, the wings and snout [237]. If an infected bat can make it through the duration of hibernation, the bats' return to euthermic body temperatures in the spring will inhibit fungal growth and an up-regulated immune systems will work to clear infection and heal lesions [228, 42]. While the fungus may permanently live in the environment [65], it is only by the seasonal reduction in the hosts barriers to infection that infection is possible [190].

To scale up from a single bat infected with *Pd* into a single population we can return to a system of differential equations. Bats on the landscape during the summer could be considered a 'resistant' population (R), as they do not seem to be infected at pathogenic level [228], so we can create a periodic *RIS* model to describe the movement of bats in and out of the susceptible state. Bats in the summer give birth at rate B_t and die at their natural rate μ_n. As uninfected bats enter hibernation at the rate of α, they can become infected from the environmentally persisting fungus at rate ε, or by contact with an infected individual at the rate γ. These bats remain infected by *Pd* over winter, dying at a rate (μ_i), likely determined by fungal load [236]. As spring arrives, bats exit hibernation back onto the landscape and re-enter the resistant population at the rate β. Prior to WNS, most bat mortality overwinter in hibernation was close to 0 [209], yet to balance populations natural mortality (not due to infection) would be included as μ_n.

$$\begin{aligned}
\frac{R}{dt} &= B_t * R - \mu_n * R - \alpha * R + \beta * (S + I) \\
\frac{dS}{dt} &= \alpha * R - \beta * S - \varepsilon * S - \gamma * I * S - \mu_n * S \\
\frac{dI}{dt} &= -\beta * I + \varepsilon * S + \gamma * I * S - \mu_I * I - \mu_n * I
\end{aligned} \tag{1.5}$$

This model is a gross simplification of a complex system. The integration of host energetic physiology, overwinter torpor dynamics coupled with temperature and humidity dependent fungal growth dynamics leads to a complex system of equations that remain an area of active research [96, 80, 81]. Later in this thesis, I use a series of coupled models [81] with spatially explicit covariates to model the impacts of spatially varying phenotypic traits (body mass) and behavioral traits (overwinter hibernation duration), to determine the possible impact of *Pd* on an at risk North American bat species.

1.13 Where to next?

Ecological and infection dynamic modeling are data hungry processes, requiring simplification where necessary, and high quality parameter value estimation where available. However, both can be used in

scenarios with limited data to test and/or develop hypothesis (e.g. [93, 176]). Depending upon the data type and resolution available ecological methods can be employed to tease apart complex reservoir systems [164, 69], determine abiotic drivers of infection [184], or provide spatially and temporally defined risk maps [187, 188, 203]. Despite these 'successes', there are numerous challenges and caveats to the analysis of infectious disease data, often relating to low sample sizes, and unequal sampling of available species. These deficiencies are highlighted within the research chapters where necessary and more conceptually within the final discussion of this dissertation. More generally, however, there are two main research gaps. First, many studies address ecological and infectious disease processes in either space or time, but not both. Second, many studies use correlative analyses to understand disease dynamics using phenomenological models, but often miss the underlying mechanistic processes of the infection or disease processes. In the rest of this thesis, my work aims to address these gaps by: 1) using statistical approaches to address data gaps in spatially and temporally varying data sets, and 2) developing spatio-temporal models that integrate necessary and sufficient causes that can explain disease dynamics.

I explore spatio-temporally varying processes relating to Ebola virus disease outbreaks, thought to be derived from bat reservoirs in Africa, and white-nose syndrome killing bats themselves in North America. Both research projects are extensions and developments of previous modeling works guided by the ideas of iterative model development and model guided fieldwork (MFG) [194]. Within the first two chapters of this dissertation I continue work on the hypothesis that the seasonality of bat birthing events drives ebolavirus spillover events, dynamically modeled within Hayman, 2015 [93]. In order to accomplish this I first creating a spatial and temporal model of bat birthing events in Chapter 2. The results of this work are subsequently used in Chapter 3 to find correlative relationships between these birthing events and known ebolavirus spillover. Both Chapters 2, and 3 combined within a single manuscript recently published in the journal *Epidemics* and included as the final Appendix G. The last research chapter, Chapter 4, focuses on the spatial variations in seasonal forcing and host traits to refine a predictive model of WNS disease outcome initially published within Hayman *et al.,* 2016 [96] and is being prepared for submission to *The Proceeding of the Royal Society B*. By challenging *a priori* definitions and altering the model framework to account for variance in host traits we create updated estimates of the impact that WNS may have on hibernating bats in western North

America. Additionally, Appendix D and E are included to better define the hibernation energetics model deployed in chapter 4 and represent work completed that I was a co-author on, developing and refining methodology. All statements of contribution for publication are collected and presented in Appendix F.

Chapter 2

Spatial and temporal patterns of birth pulses among African bats

2.1 Introduction

Bats, of the order Chiroptera, are an ancient mammalian lineage covering every continent aside from Antarctica, and inhabit remote islands such as Hawaii and New Zealand [166]. Body sizes covers nearly 3 orders of magnitude from the smallest insectivores weighing a couple grams all the way to the flying foxes that can weigh in at 1Kg+ [166]. While many people do not realize it, bats play critical environmental roles in crop pest control, seed dispersion, and pollination and are in fact the sole pollinators for such vital crops as the blue agave (which is then fermented into tequila and mescal!). Bat species inhabit diverse environmental niches and have diverse dietary requirements to match including carnivorous, piscivorous, frugivorous, insectivorous, nectivorous, and sanguivorous lifestyles [166]. Due the high energy usage of flight the life histories of bats are intimately tied to the seasonality of the food resources they rely on [208, 50].

In sub-Saharan Africa resource availability is transient across the landscape, driven by cyclical patterns of wet and dry seasons [50]. Within equatorial Africa the year is defined by the long and short dry periods, and intense wet periods following each. These climatic shifts cause peaks and troughs in the availability of both fruits and insects, two of the primary foodstuffs for African bats. At more southern latitudes only a single annual cycle of wet and dry seasons exists, with the rains following the

long dry season contributing most of the rainfall for the year. The resulting "green wave" oscillating between tropical and subtropical Africa creates a dynamic landscape of food availability that many species of bat have exploited though the development of migratory or nomadic strategies and seasonal birthing life histories [50]. Some bat species to traverse great distances for food,including the African-straw colored fruit bat, *Eidolon helvum*, is recorded to travel 2518 km in 149 days following the fruit pulse in northern Zambia to the Democratic Republic of the Congo (DRC) [196]. *Eidolon helvum* and species like the hammer headed bat (*Hypsignathus monstrosus*) show very little population structure across western and central African populations and are considered panmictic across their distributions [89, 181].

The reproductive period in bats represents a life history events under strong selection pressure and can be limited by factors including calcium demand [10], water availability [12], predation levels [59], and parasitism. Bat species use complex environmental cues to time the parturition of young and subsequent weaning of the young pups with peak resource abundance across this dynamic landscape [193, 50]. Accordingly African bats species tend to have synchronous birthing events just prior to the seasonal rains such that the following periods of peak resource availability correlates with weaning of the pups. To achieve this bats have evolved a series of reproductive delay mechanisms, including delayed implantation, delayed fertilization, or retarded fetal growth to postpone parturition until still undefined environmental cues foretell the coming resource abundance [50]. Previous research has proposed the division of the Chiropteran family into three useful sub groups based upon shared reproductive features: African fruit bats (pteropodid bats, family: Pteropodidae); molossid bats (family: Molossidae); and non-molossid microbats [50]. At equatorial latitudes African fruit bat and non-molossid microbat species are generally biannually polyestrous, yet at more temperate latitudes species shift to a monoestrous with a single annual birth pulse. Insectivorous molossid bats reproduce nearly continuously through the equatorial region with strong bi-modal seasonally polyestrous in the seasonal climates $>\sim 10^{\circ}$S. Within the African fruit bat sub-group, variation further complicates things. The Straw-colored fruit bat (*E. helvum*) and other monoestrous fruit bat species only display a single annual birth pulse following the long dry period, while other species capitalize on the biannual pulse of resources to rear another litter of young. Populations that span both equatorial and temperate Africa, like the Egyptian fruit bat (*Rousettus aegypticus*), display reproductive trait plasticity with

2 birth pulses through central and western Africa and a single pulse at more southern latitudes. Seasonal shifts in resource availability and reproductive status impact the health of poulations and are believed to contribute to the spillover of dangerous pathogens from their sylvatic bat hosts into humans [93, 4, 84].

As the human population continues to grow, shifts in land use, deforestation, swamp reclamation, wind power generation and human encroachment are increasingly identified as conservation concerns [174] .Globally increased interactions between human and bat populations have resulted in the spillover of several notable pathogens including Hendra virus, Nipah virus, and filoviruses (e.g. Marburg virus and Ebola virus)[113]. *Ebolavirus* (family Filoviridae) have been sporadically emerging across sub-Saharan Africa since 1979, and while anecdotal evidence from a number of outbreak events implicates bats, limited direct evidence corroborates this [200, 191]. Cross-sectional serological studies have implicated several species of African fruit bats, yet no live virus has been isolated from these bats [187] despite the detection of viral fragments from some bat species [75, 192]. With the exception of the Asian *Reston ebolavirus* (RESTV), all recognized viral species are highly pathogenic to most mammalian hosts causing Ebola Virus Disease (EVD), an acute, sometimes hemorrhagic fever with high rates of mortality [32]. Experimental infection studies have demonstrated mortality in fruit bat species is limited by the production of an immunizing response to infection, yet their true competency as an ecological maintenance reservoir is still very much in question [210, 130].

Infection dynamic simulations and machine learning analyses have independently identified traits associated with fruit bat species as correlative with traits required to maintain filoviruses in sylvatic transmission [93]. Chief among these traits is a highly synchronous, biannual birthing pattern and the inhabitation of dense forest patches [84]. Research into *Marburgvirus marburgvirus* (MARV), a sister genus to *Ebolavius* has identified *R. aegypticus* as the reservoir host, and spillover events are seemingly correlated with the timing of birth, and the waning of maternally derived antibodies [4, 180].

Previous studies on the spatio-temporal occurrence of EVD spillover have used environmental covariates in their correlative approach [187, 188]. These are useful, because they provide continuous data and show the seasonal change in risk for EVD outbreaks. However, a gap exists on the linkages between seasonality in bat birthing and EVD outbreaks and on bat birthing itself [50]. One reason for

this gap is an absence of bat birthing data in space and time. Within this work, I create a framework by which I can test the hypothesized mechanistic relationship between the environmental factors driving bat birthing and ebolavirus spillover occurrence, which I present in Chapter 3. In this Chapter I compress decades of bat reproductive ecology into a single recirculating year and use ecological niche modeling (ENM) techniques to create predictions of when and where African bats will give birth.

2.2 Methods

2.2.1 Chiropteran parturition data mining

Bat species that have been implicated in filovirus transmission either through RNA or antibody detection methods [84, 232] were systematically queried through Walker's Bats of the World [166], Scopus, Web of Science, and Google Scholar. Generalized search terms including: "Birth*"; "Breed*"; "Reproduc*"; "Partur*" along with the Latin binomial and common species names were used. Bat species that had undergone taxonomic reassignment were queried under all names. Species that had been implicated in global filovirus transmission, but did not reside in Africa, were queried at the genus level to identify representative sister species. Preliminary results suggested insufficient sample sizes to model parturition on a consistent per species, or per genus basis. Species were then aggregated into three taxonomic clusters: African fruit bats (family: *Pteropodidae*), molossid bats (family: *Molossidae*, and non-molossid microbats, according to Cumming and Bernard [50]. Publications were accessed by hand and the location and month of parturition events were extracted. Data points were restricted to those within mainland Africa. Studies that reported suckling neonates, lactating females, or attached pups were excluded as parturition events as they did not provide accurate indication of the date or location of parturition. Additional points for non-implicated species were added opportunistically as discovered and an African bat specialist (A. Monadjem) was consulted to help fill holes in the dataset primarily by identifying additional species reassignments, and to identify overlooked literature in attempt to expand the data set to all mainland African bats. All gathered data was then compiled into a single, recirculating year for further analysis.

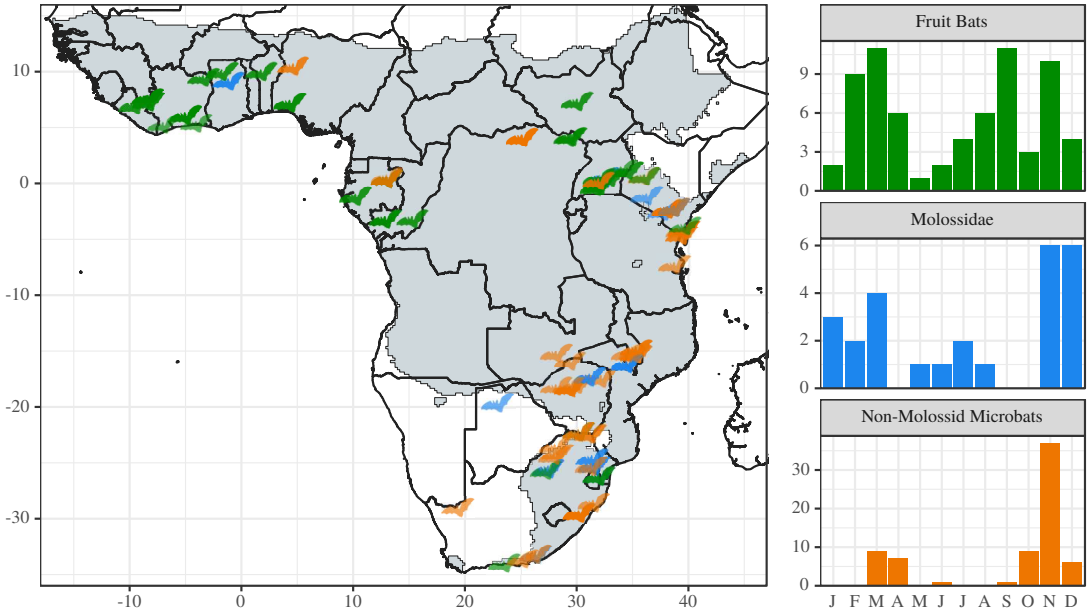


Fig. 2.1 **Spatial and temporal occurrence of bat birthing records obtained from the literature.** All results from mainland sub-Saharan Africa for the date and location of bat birth events. African fruit bat species are in green, molossid species in blue, and non-molossid microbats in orange. The gray background represents the study region and regions in white were excluded from this analysis. *Left:* Spatial locations of recorded observations. *Right:* Number of birthing observations in the literature by taxonomic group collapsed into a single year and aggregated by month.

2.2.2 Covariate data

Covariate data was assembled and is summarized in Table 2.1. Covariate layers were blocked into static variables and temporally dynamic variables depending on the data availability and hypotheses being tested. The static covariate layers used included those describing mammalian species biodiversity (both bat and non-bat) [109], land cover [172], and four of the 19 Bioclimatic variables representing 30 year average for precipitation seasonality, mean diurnal range, temperature seasonality, and temperature annual range [64]. Temporally dynamic covariate layers were used to describe mean monthly temperature, average monthly precipitation, potential evapo-transpiration [219] and an enhanced vegetative index [107].

Considering the vast size of Africa the study extent was restricted to locations in Africa receiving more than 500mL of precipitation annually as suggested by Schmidt *et al.* 2017 [203]. All covariate layers were cropped and masked to the precipitation layer, resolution was aggregated to 25km raster blocks and temporally dynamic covariates were normalized (mean zero and standard deviation of 1).

Table 2.1 **Co-variate layers for ecological niche modeling** Static co-variate are stationary across the landscape while temporal variables were collected for all months.

Description	Variable Type	References
Non-volant mammalian biodiversity	Static	[109]
Land cover (modified)	Static	[172]
Precipitation seasonality	Static	[64]
Mean diurnal range	Static	[64]
Temperature seasonality	Static	[64]
Temperature annual range	Static	[64]
Mean monthly temperature	Temporal	[64]
Mean monthly precipitation	Temporal	[64]
Potential evapo-transpiration	Temporal	[219]
Enhanced vegetative index	Temporal	[107]

All spatial handling was preformed within R [213], using tools in the `sp` [179], `raster` [101], and `rgdal` [25] packages.

2.2.2.1 Mammalian diversity layers

Covariate layers describing non-bat mammalian, African fruit bat, molossid, and non-molossid microbat diversity were created using the IUCN Red List terrestrial mammal distribution database [109]. Classification by taxonomic rank was performed by `taxize` package [41] and manually checked by hand (see `DiversityRasters.R`) and the number of overlapping distributions for each cell within the study area were counted to create the diversity raster layers.

2.2.2.2 Land cover

The global land cover database [172] was obtained for the year 2009 and custom aggregation was used to reduce the number of classes from 23 to five as described by Table 2.2.

2.2.3 African bat birth pulse modeling

The birth pulses for each of the taxonomic clusters were modeled though a modified ecological niche modeling (ENM) procedure devised for this analysis. Standard ENMs use occurrence (or occurrence/absence) and covariate data to create regressive correlations between observed environmental

Table 2.2 **Reclassification of land cover variables originally included in the global land cover data set [172]**

Value	Label	Class
11	Post-flooding or irrigated croplands (or aquatic)	crop
14	Rainfed croplands	crop
20	Mosaic cropland (50-70%) / vegetation (grassland/shrubland/forest) (20-50%)	crop
30	Mosaic vegetation (grassland/shrubland/forest) (50-70%) / cropland (20-50%)	grass
40	Closed to open (>15%) broadleaved evergreen or semi-deciduous forest (>5m)	forest
50	Closed (>40%) broadleaved deciduous forest (>5m)	forest
60	Open (15-40%) broadleaved deciduous forest/woodland (>5m)	forest
70	Closed (>40%) needleleaved evergreen forest (>5m)	forest
90	Open (15-40%) needleleaved deciduous or evergreen forest (>5m)	forest
100	Closed to open (>15%) mixed broadleaved and needleleaved forest (>5m)	forest
110	Mosaic forest or shrubland (50-70%) / grassland (20-50%)	forest
120	Mosaic grassland (50-70%) / forest or shrubland (20-50%)	grass
130	Closed to open (>15%) (broadleaved or needleleaved; evergreen or deciduous) shrubland (<5m)	grass
140	Closed to open (>15%) herbaceous vegetation (grassland; savannas or lichens/mosses)	grass
150	Sparse (<15%) vegetation	grass
160	Closed to open (>15%) broadleaved forest regularly flooded (semi-permanently or temporarily)	forest
170	Closed (>40%) broadleaved forest or shrubland permanently flooded - Saline or brackish water	forest
180	Closed to open (>15%) grassland or woody vegetation on regularly flooded or waterlogged soi	grass
190	Artificial surfaces and associated areas (Urban areas >50%)	urban
200	Bare areas	other
210	Water bodies	other
220	Permanent snow and ice	other
230	No data (burnt areas; clouds;...)	NA

phenomena and species observations. In this instance, we re-purposed these models to correlate phenological environmental signals with bat birthing events within a temporally dynamic framework.

Birthing events identified through the data mining were split by taxonomic grouping as described above and observation/absence matrices were generated to a sliding two month window. Records of a birth within the window were recorded as an occurrence within the 25x25km cell in which it was observed. All locations for which there was a recorded birth for within the taxon group, but no births were observed in those months were deemed "absence points" and were entered back into the dataset for modeling. The two month sliding window was chosen to reflect the non-discrete nature of birthing within wild animals and to help account for deficiencies in the source data. An additional ten, randomly generated, down-weighted (0.001) points (five occurrence and five absence points) were added to all models. This measure was taken to ensure the representation of all land cover categories in all models, and provide necessary pseudo-absence points in a small number of cases in which an insufficient number of absence points existed, while having minimal impact on the model outcomes.

Temporal covariate data was selected using a wider six month sliding window centered on the same two month window used for the occurrence/absences and included the two preceding, and two following months. Due to the inherent correlation of the covariate layers (especially the temporally dynamic covariate layers) and general non-independence of all selected environmental metrics, a raster based principal components analysis (PCA) method was used to reduce the dimensionality of

all continuous predictors into six orthogonal principal components using the `rasterPCA` function of the package RStoobox [133]. The categorical land cover variable was then added to the other dimensionally reduced covariates and occurrence/absence data were fed into the `biomod2` [218] framework.

ENMs were procedurally generated for all taxonomic clusters and all pairs of consecutive months where the number of combined observations was greater than 7. Ten iterations of the potential eight preliminary models (generalized linear model, generalized boosted model, classification tree analysis, artificial neural network, surface range envelope, flexible discriminate analysis, random forest and maximum entropy) were computed using a standard 70:30 training:test ratio. Ensemble models were then compiled based on the weighted mean of the receiver operating characteristic (ROC score) to create a single consensus layer with the probability of event occurrence between 0 and 1.

2.3 Results

A total of 63 articles provided information on 14 African fruit bat species, 7 molossid species, and 43 non-molossid microbats at 75 unique locations, totaling 164 event records (Figure 2.1, Table 2.3). Of these, 89% were retained with 8 records discarded as outside of our study extent within mainland Africa. The African fruit bats were the only bats with births observed in every month with a maximum of 104 of the total 159 unique observation locations giving birth in the month of March. There were no observed births within our data set for the month of October for the molossid bats. There were no recorded births for non-molossid microbats within the months of January, February, July or August within the literature queried.

Table 2.3 **Data mining results for African bat birthing. Species are categorized as members of the *Pteropdidae* (African fruit bats), Molossid bats, or non-Molossid microbats. The column "Annual Births" describes the number of esterus cycles the species exhibits. Depending on geographic location this may vary within a single species. "Locations" details the number of unique geographic points were births were described within the literature.**

Species	Annual Births	Locations	References
Pteropodidae			
Continued on next page			

Table 2.3 – continued from previous page

Species	Annual Births	Locations	References
Casinycteris ophiodon	1	1	[243]
Eidolon helvum	1	3	[160, 214, 70, 58]
Epomophorus gambianus	1-2	3	[45, 142, 217]
Epomophorus labiatus	2	1	[168]
Epomophorus wahlbergi	1-2	2	[155, 240]
Epomopos buettikoferi	2	2	[217, 119]
Epomopos franqueti	2	3	[14, 115, 168]
Hypsignathus monstrosus	2	3	[30, 116, 243]
Micropteropus pusillus	1-2	6	[13, 169, 230, 142, 102, 217]
Myonycteris angolensis	1	2	[45, 243]
Myonycteris leptodon	1-2	3	[214, 243]
Myonycteris torquata	2	1	[13]
Nanonycteris veldkampi	1	2	[243, 142]
Rousettus aegyptiacus	1-2	12	[243, 142, 99, 110, 1, 116, 169, 45, 6, 161]
Molossidae			
Chaerephon pumilas	2-3	4	[221, 85, 162, 147]
Chaerephon pumilus	1	1	[154]
Mops condylurus	2	5	[231, 85, 175, 162]
Mops midas	1	1	[205]
Otomops harrisoni	1	2	[162]
Tadarida aegyptiaca	1	1	[23]
Tadarida fulminans	2	1	[48]
Non-*Molossidae* Microbats			
Cardioderma cor	2	1	[226]

Continued on next page

Table 2.3 – continued from previous page

Species	Annual Births	Locations	References
Coleura afra	2	1	[147]
Eptesicus hottentotus	1	1	[87]
Hipposideros abae	1	1	[230]
Hipposideros beatus	1	1	[34]
Hipposideros caffer	1	3	[17, 7, 149]
Hipposideros caffer rubber	1	2	[230, 243]
Hipposideros cyclops	1	1	[230]
Hipposideros gigas	1	2	[146, 35]
Hipposideros rubber	1	1	[105]
Hipposideros vittatus	1	1	[49]
Lavia frons	1	2	[230, 227]
Miniopterus fraterculus	1	1	[15]
Miniopterus inflatus	1	1	[35]
Miniopterus minor	1	1	[148]
Miniopterus natalensis	1	4	[22, 15, 19, 225]
Myotis bocageii	2	1	[34]
Myotis tricolor	1	1	[20]
Neoromicia capensis	1	1	[220]
Neoromicia nanus	1	4	[223, 129, 16, 175]
Neoromicia somalicus	1	1	[175]
Neoromicia zuluensis	1	1	[86]
Nycteris grandis	1	1	[60]
Nycteris hispidar	2	1	[230]
Nycteris nana	1	1	[230]
Nycteris thebaica	1	1	[17]

Continued on next page

Table 2.3 – continued from previous page

Species	Annual Births	Locations	References
Nycticeinops schlieffeni	1	3	[224, 175, 86]
Pipistellus rusticus	1	1	[222]
Rhinolophus basii	1	1	[86]
Rhinolophus capensis	1	1	[21]
Rhinolophus clivossis	1	1	[21]
Rhinolophus darlingi	1	1	[206]
Rhinolophus fumigatus	1	1	[86]
Rhinolophus landeri	1	1	[149]
Rhinolophus mossambicus	1	1	[47]
Rhinolophus simulator	1	2	[47, 175]
Scotoecus hirundo	1	1	[175]
Scroptophilus borbonicus	1	1	[224]
Scroptophilus dinganii	1-2	3	[175, 223, 169]
Scroptophilus leucigaster	1	1	[10]
Scroptophilus vividis	1	1	[224]
Taphozous hildegardeae	2	1	[148]
Taphozous mauritianus	2	2	[86, 175]

EMNs were generated for all three bat taxonomic groups for 34 of 36 possible month pairs, and full model results are summarize in Table 2.4 and Figure 2.2 as well as Appendix A A.1- A.3. Models were not made for January-Febuary and July-August for the non-molossid microbats as all months had no birth observations with our dataset. ROC, sensitivity and specificity scores were high across all models as expected through ensemble modeling techniques, with most scores within 5% of maximal values and virtually all scores within 15% (Table 2.4).

At equatorial latitudes ($\pm$ 10°) African fruit bats and non-molossid microbats were predicted to experience conditions suitable for biannual birthing seasons. For the non-molossid microbats results suggest 2 three month birthing windows centered in April and November. Fruit bats results predicted a

Table 2.4 **Ecological niche model ensemble scores.** The abbreviations abr, mic, and mol, represent African fruit bats, non-molossid microbats and molissid bats respectively. The numbers included within the model names are the calender months over which the model was produced. No models were created for January-February, and July-August for the non-molossid microbats.

Model	ROC	Sensitivity	Specificity
mic2.mic3	0.986	96.296	96.97
mic3.mic4	0.979	97.959	87.013
mic4.mic5	0.985	97.561	89.412
mic5.mic6	0.993	97.222	98.889
mic6.mic7	0.995	100	98.131
mic8.mic9	0.997	100	97.368
mic10.mic11	0.994	96.154	100
mic11.mic12	0.993	92.683	100
mic12.mic1	0.985	98.551	91.228
mol1.mol2	0.969	100	82.222
mol2.mol3	0.993	100	90.625
mol3.mol4	0.993	100	93.75
mol4.mol5	0.983	96.296	93.939
mol5.mol6	0.952	95.238	84.615
mol6.mol7	0.96	95.238	84.615
mol7.mol8	0.962	90.476	89.744
mol8.mol9	0.976	84.211	100
mol9.mol10	0.972	84.211	100
mol10.mol11	0.952	92.308	88.235
mol11.mol12	0.961	90.244	100
mol12.mol1	0.969	93.478	92.857
afb1.afb2	0.987	97.015	91.589
afb2.afb3	0.988	99.01	93.151
afb3.afb4	0.991	96.124	95.556
afb4.afb5	0.994	97.248	95.385
afb5.afb6	0.992	94.643	96.61
afb6.afb7	0.988	96.364	94.958
afb7.afb8	0.983	94.444	94.118
afb8.afb9	0.982	92.553	96.25
afb9.afb10	0.991	93.75	100
afb10.afb11	0.994	95.918	100
afb11.afb12	0.991	94	98.387
afb12.afb1	0.989	95.349	96.183

particularly broad and temporally meandering peak of habitat suitability associated with the cessation of the long dry period, potentially influenced by the monoestrous species. Molossid species had predicted suitable conditions for birth nearly continuously throughout the year (Figure 2.2) within these latitudes.

Above $\sim$10°N the signal of habitat suitability were modified for all taxonomic groups. Non-molossid microbat patterns changed the least and suggested a halving of the duration of habitat suitability during the first birth pulse of the year. The magnitude for the second annual pulse was reduced, but temporally consistent with predicted habitat suitability across all other latitudes. The predicted suitability for fruit bat birthing lost much of the bimodal signal which was replaced by a single broad suitable period between May and November. Molossid bat birthing patterns were also predicted to shift to bimodal with peaks centered in March and October.

At more southern latitudes (>$\sim$10°S) predicted molossid species results again suggested a reduction in habitat suitability to a biannual birthing pattern with a high degree of synchronicity following to the long dry season. Both fruit bats and the non-molossid microbats were predicted to reduce births at southern latitudes to a monoestrous reproductive cycle with births prior to the end of the long dry season. Results for the fruit bat species suggest transient suitability during the first half of the year, yet model results and previous research [16] suggest that the majority of births take place in association with end of the long dry season. These results are largely consistent with previous work [16, 86, 156, 87], but critically provide a continuous metric describing both the spatial and temporal aspects of the phenomenon.

2.4 Discussion

Evolutionary, environmental, and phenological processes undoubtedly drive the timing and location of bat breeding and birthing, yet these intricacies have yet to be fully and mechanistically described. Sparse data exist for the timing bat births, especially in mainland tropical Africa [50, 156]. Within this work we combine 50+ years of ecological research into a single, recirculating year of spatio-temporally defined bat birthing events. Using these records, and spatially explicit covariates describing seasonality of rainfall and primary production, we created a series of EMNs to capture the monthly probability of suitable habitat for bats to give birth in across sub-Saharan Africa.

For the simplification of interpretation we have assumed that our areas of predicted habitat suitability correspond to the actual occurrence of bat births. Patterns observed in this analysis are largely consistent with latitudinal patterns previously published [50, 16], yet represent a significant

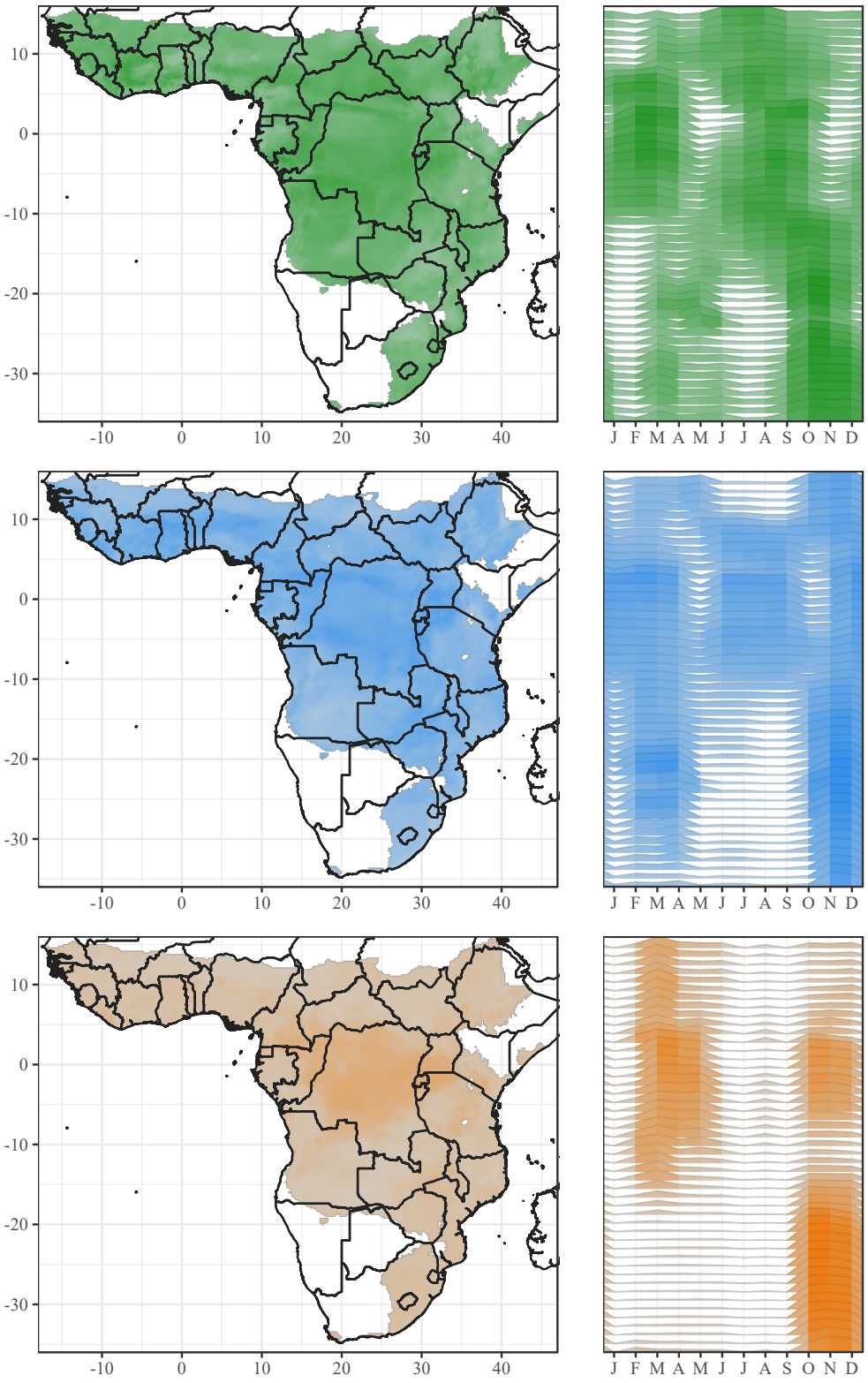


Fig. 2.2 **Probability of birth of African bats** *Top row:* African fruit bats *Middle row:* Molossid bats *Bottom row:* Non-molossid microbats *Left:* Mean annual probability of a bat giving birth spatially. Grey represents low values while more intense colors denotes regions where a environmental conditions correlated with bat birth events are met. White regions were excluded from this study. *Right:* Probability of birth by latitude and month. Height and color intensity are proportional to relative number of species giving birth within the latitudinal window.

contribution to the literature due to the spatial and temporal extent of predictions. Both fruit bats and non-molossid microbats are predicted to experience habitat suitability for biannual birth pulses within $\sim 10^{\circ}$ of the equator. Previous work found partition of African fruit bats $\sim$2 weeks to a month before non-molossid microbats [50], which was further supported by our findings. Suitable birth conditions for molossid bats were present nearly year round and was consistent with previous descriptions. However, our models predict a reduction to a bi-modal breeding pattern at more temperate latitudes $\geq \sim 10^{\circ}$. Additionally, our model predicts a single and more broad time of suitability for fruit bat birthing above $\sim 10^{\circ}$, a phenomena not previously reported.

The timing of bat births are thought to correspond with maximal resource abundance, likely driving the spatial and temporal heterogeneity in birth events across the landscape [50]. Global studies of bat reproductive patterns suggests the weaning of young as the most evolutionary selective period during early life history [121], and as such bats have evolved mechanisms by which to maximize resource availability for their during this period [193, 50]. Insects reach peak abundance $\sim$1 month after the onset of seasonal rains in equatorial Africa [50], with the duration of lactation typically averaging 6 weeks for insectivorous bats[193]. This places insect peak abundance squarely withing the expected period of weaning. Maximal flowering occurs at about the same time as insect abundance yet peak fruit availability follows sometime after [50]. Accordingly, lactation for fruit bat species typically lasts sometime between 10 and 13 weeks [217], and again placing weaning and learning to forage into the periods of high resource abundance. These patterns of habitat suitability are broad, and intra-species variation in prey/ foraging preference and time to neonate independence will ultimately define where within the predicted suitability peaks each specific species give birth.

Data availability ultimately required the use of several simplifying assumptions, most notably the consolidation of species into the taxonomic groups. This simplification creates scenarios in which within a single location and pulse of habitat suitable for birth, two taxonomic members may give birth at different, non-overlapping times. Additionally, a single species at two separate locations could conceivably give birth at different times within a broader birth pulse due to localized resource preference/ availability patterns. A considerable amount of investment is required to discern these patterns for each species and to date most work has been focused on a few, widely distributed fruit bat species (*e.g. Eidolon helvum*, *Rousettus aegyptiacus*, and *Micropterpous pusillus*). Only three

species of non-fruit bat species included records from more than three separate publications and the rates of species representation per taxon were much lower (species represented/total species within the taxonomic cluster). The over representation of just a few species within the dataset may be disproportionately influencing the definition of birth habitat suitability, but without increased record availability this work still represents the most complete description available.

Going forward there are three main areas to be addressed. First, as additional museum records are digitalized, gray literature becomes more search-able and additional field observations are made, species specific (or even genus specific) models may become viable. Increased acknowledgment towards the roles of bats as potential reservoirs for viral pathogens has already increased study into the natural history of several fruit bat species [204], yet the sylvatic role of more rare and difficult to capture species will likely remain undefined for an extended period. Second, with the currently available data there are no ways by which to establish abundance estimates. Incorporation of relative abundance and/or community compositions would be a boon to infectious disease and ecological researchers alike providing insights to effectively manage resources and health at the human wildlife interface. Lastly, the period at which these records were collect spanned nearly a century. This fact necessitated the use of a recirculating year, yet inner-annual weather patterns and intra-annual variation are likely to influence results in so far undetectable ways. As global climate change accelerates, along with land-use changes, the use of a "standard" year may no longer be relevant approach as environmental metrics drift away from historical averages and more chaotic patterns may emerge.

In the next Chapter 3 I use the results of this work to test the hypothesis that bat birthing is linked to EVD outbreaks.

Chapter 3

Predicting Ebola virus disease risk and the role of African bat birthing

3.1 Introduction

Ebola virus disease (EBD) is a highly pathogenic public health threat to equatorial Africa and outbreaks have been considered Public Health Emergencies of International Concern [32]. This zoonotic emerging infectious disease (EID) results from infection from all of the recognized *Ebolavirus* species (family Filoviridae) with the exception *Reston ebolavirus* (RESTV) [152]. Most recently a proposed sixth *Ebolavirus* species was described with unknown ability to cause EVD [75]. Since the first recorded viral spillover events in 1979, EVD agents (referred to henceforth as "ebolaviruses") have emerged sporadically [187], with 34 identified human index cases to date (Figure 3.1). The most notable of these events occurred in West Africa between 2013–2016, during which EVD was directly responsible for the death of at least 11,300 people [32]. The second largest human outbreak currently continues in the Democratic Republic of Congo (DRC) [239] and political and social instability within the region have hampered public health interventions to control viral transmission [46]. In addition to human health concerns, EVD has been implicated in large scale great ape die-offs in central Africa, suggesting potential conservation concerns for forest dwelling mammals [132].

Despite decades of intense epidemiological investigation, little is known about the ecological reservoir, sylvatic maintenance or mechanisms of spillover for ebolaviruses. Mounting evidence

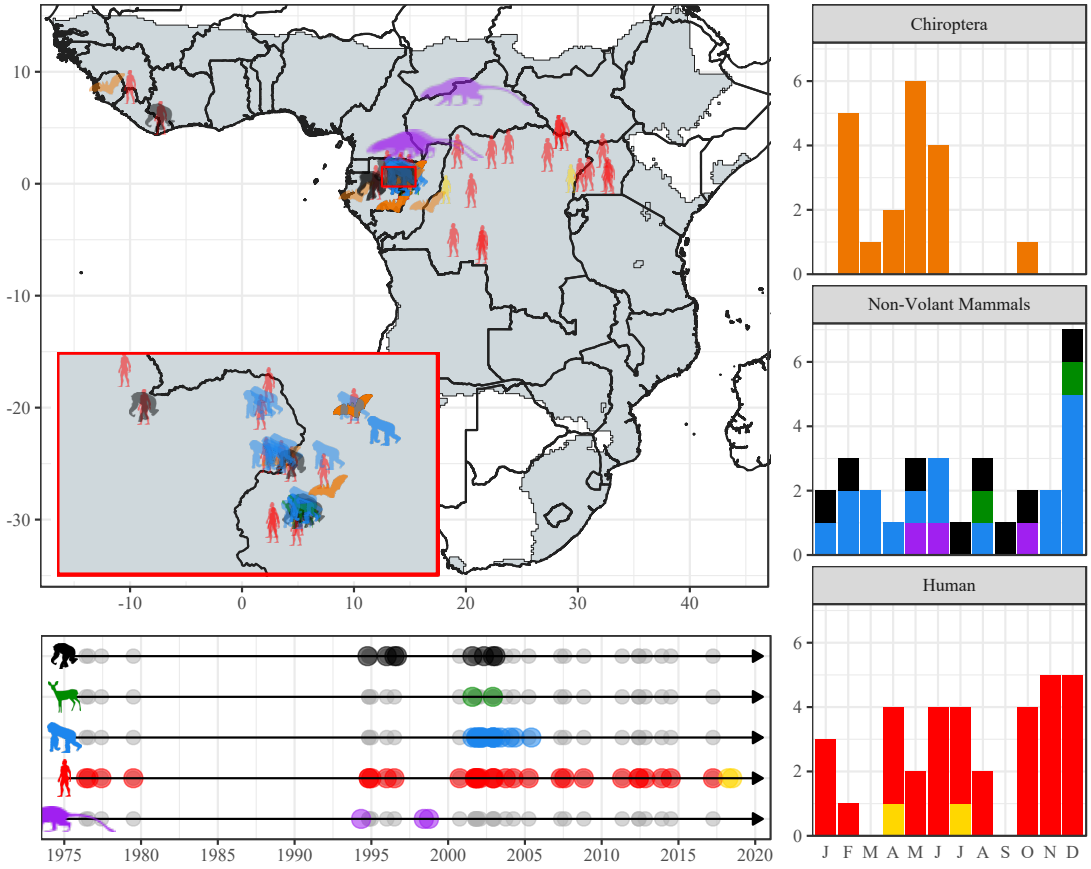


Fig. 3.1 **Spatial and temporal detection of ebolavirus by host taxonomic group.** *Top left:* Location of all EVD index spillover events and detections within bat populations. Zoom panel focuses in on the border of Gabon and Republic of Congo. *Bottom left:* Viral detection by taxonomic classes (non-human time-line gray points are human events for reference). *Right:* Frequency of viral detection by taxonomic host collapsed into a single year and aggregated by month. Bats are orange, chimpanzees black, duikers green, gorillas blue, rodents purple and humans red. In all cases except for the bats detections represent unique spillover events. The two most recent outbreak in the DRC are denoted in gold. All references, are available within the online material.

implicates African Old World fruit bat species (Order Chiroptera; family Pteropodidae) as potential reservoirs, as defined by Haydon *et al.* [90], in maintaining and propagating infection on the landscape [52, 131, 84, 192]. To date no full EVD-causing *Ebolavirus* has been isolated from a bat host. Possible reasons for this, if they are true maintenance reservoir hosts, include: the remote geographic locations of the EVD outbreaks; nomadic or migratory nature of bats [166]; potentially acute viremic periods [210]; spatio-temporal extinction and recolonization dynamics, the unknown role of viral persistence and intermittent viral shedding [204], and possibly biased samples unrepresentative of

true bat diversity [130]. However, RNA viral fragments of ebolaviruses causing EVD have been recovered from three African fruit bat species: Franquet's epauletted fruit bat (*Epomops franqueti*), the Hammer-headed bat (*Hypsignathus monstrosus*), and the Little collared fruit bat (*Myonycteris torquata*) [131]. *Ebolavirus* fragments were also detected in four rodent species: two *Praomys sp.*, two *Mus sp.* and one shrew *Sylvisorex ollula* (family: Soricidae) [158], although there is some contention whether these species could effectively act as reservoir hosts [210] and whether these were in fact active infections [212]. Phylogenetic analyses have also suggested that fruit bats have played some role in the recent evolutionary history of *Zaire ebolavirus* (ZEBOV) [232, 24].

Empirical and experimental studies have left much to be discovered within the ecology of ebolaviruses, however research on the sister genus *Marburgvirus marburgvirus* (MARV) and computational research help to fill the gaps. MARV circulates within cave dwelling Egyptian fruit bat (*Rousettus aegyptiacus*) colonies with seasonal increases in viral shedding among juvenile bats and the high birthing synchrony [4]. Anti-MARV antibodies have also been detected within co-roosting insectivorous bats which to-date play an unknown role in sylvatic maintenance. Machine learning and infection dynamic simulations have both identified biannual, synchronous birth-pulses as potentially important host life history traits for filovirus maintenance [84, 93], all traits found within African bat species .

While there are many similarities between MARV and ebolavirus systems, the principal suspected ebolavirus reservoirs are primarily tree roosting species with far lower colony densities compared to the Egyptian fruit bat. The sporadic occurrence of outbreaks, lifestyles of putative reservoirs, viral dynamics and subsequent antibody production in bats [210] suggest a potential reliance on meta-populations within a larger reservoir community to sustain sylvatic ebolavirus *Ebolavirus* [37, 77, 84, 89]. Strong, spatially asynchronous seasonal forcing events including birthing likely drive additional layers of complexity in disease outbreak events [54] and spatial risk models have previously identified regions of realized, and unrealized risk throughout equatorial sub-Saharan Africa, linked to a variety of drivers including forest fragmentation, and vegetation index [198, 186, 187]. Furthermore, temporal risk models have suggested that EVD spillover risk across the region is greatest during transitions between wet and dry seasons [203], periods also associated with African bat species birthing events [50]. One hypothesis of filovirus spillover risk posits that synchronous shifts in

population demographics may be responsible for periods of increased viral shedding similar to those witnessed in the MARV system [93, 192].

In this work I test the hypothesis that birthing among some African bat species is linked to EVD spillover events to humans and forest dwelling animals susceptible to EVD, hereafter referred to as "non-human spillover hosts." Due to the rarity of EVD outbreak events I was not able to model each EVD-causing *Ebolavirus* species separately, and therefore combined them all together to represent a single, general, "ebolavirus" capable of infecting, and causing EVD in mammalian hosts. Using previously described models of African bat birthing patterns I create statio-temporal models to describe the relative spillover risk. I assumed bats were reservoir hosts and that non-human spillover hosts have different habitat use, risk factors and contact patterns with the potential reservoir host(s) than humans. Subsequently I modeled spillover into non-human spillover hosts independently of humans. I then used the two most recent outbreaks of EVD in the DRC [11, 239], which were excluded from the modeling procedures (but see methods), to test the predictive power of the generated models.

3.2 Methods

The true distribution of ebolaviruses across the landscape is likely driven by complex patterns of seasonality and host behavior. To test the hypothesized link between spillover events and bat birthing we collapsed the 42 year history of EVD outbreaks into the same recirculating year used in the birthing ENM. We then treated outbreaks as a spatio-temporal Poisson point process, with rate (herein, risk) estimated using a spatially weighted, over-dispersed general linear model (spatGLM). Covariate describing bat birthing, mammalian diversity, human population demographics, forest fragmentation, and the occurrence of bats infected with ebolaviruses were included in various combinations to create a series of alternative spatGLM models.

3.2.1 Covariate

Considering the vast size of Africa the study extent was restricted to locations in Africa receiving more than 500mL of precipitation annually as suggested by Schmidt *et al.* 2017 [203]. All covariate layers were cropped and masked to the precipitation layer, resolution was aggregated to $\sim$25km raster

blocks. All spatial handling was preformed within `R` [213], using tools in the `sp` [179], `raster` [101], and `rgdal` [25] packages.

3.2.1.1 Mammalian diversity layers

Covariate layers describing non-volant mammalian, African fruit bat, molossid, and non-molossid microbats diversity were created using the IUCN red list terrestrial mammals distribution database [109]. Classification by taxonomic rank was performed by `taxize` package [41] and manually checked by hand (see `DiversityRasters.R`) and the number of overlapping distributions for each cell within the study area were counted to create the diversity raster layers.

3.2.1.2 Land cover

The global land cover database [172] was obtained for the year 2009 and custom aggregation was used to reduce the number of classes from 23 to five as described by Table 3.1.

3.2.1.3 Fragmentation index

A binary mask of the aggregated 'forest' class (as described above) from the Globcover 2009 dataset [172] was used to define forest patches using 4-connectivity. A fragmentation index was then calculated for each pixel by counting the number of unique patches within a 20x20 sliding window using tools in the `EBImage` package [178].

3.2.1.4 Bat birth pulses

Birth pulses were modeled for African bats and a full description resides in Chapter 2. In brief, African bats were separated into three mutually exclusive taxonomic clusters, African fruit bats, molossid bats, and non-molossid microbats. Occurrence of bat birthing events were mined from the literature and a series of procedurally generated ecological niche models (ENMs) were generated to describe the probability of a bat giving birth at any place and time within the study region. The ENM results were then used and combined with bat diversity in a number of different ways. First and most intuitively, the probability of birthing for the three different taxonomic class were used as covariates where probability of birth occurrence is $P_{T,i,t}$ for each taxonomic group T, at location i and

Table 3.1 **Reclassification of land cover variables**

Value	Label	Class
11	Post-flooding or irrigated croplands (or aquatic)	crop
14	Rainfed croplands	crop
20	Mosaic cropland (50-70%) / vegetation (grassland/shrubland/forest) (20-50%)	crop
30	Mosaic vegetation (grassland/shrubland/forest) (50-70%) / cropland (20-50%)	grass
40	Closed to open (>15%) broadleaved evergreen or semi-deciduous forest (>5m)	forest
50	Closed (>40%) broadleaved deciduous forest (>5m)	forest
60	Open (15-40%) broadleaved deciduous forest/woodland (>5m)	forest
70	Closed (>40%) needleleaved evergreen forest (>5m)	forest
90	Open (15-40%) needleleaved deciduous or evergreen forest (>5m)	forest
100	Closed to open (>15%) mixed broadleaved and needleleaved forest (>5m)	forest
110	Mosaic forest or shrubland (50-70%) / grassland (20-50%)	forest
120	Mosaic grassland (50-70%) / forest or shrubland (20-50%)	grass
130	Closed to open (>15%) (broadleaved or needleleaved; evergreen or deciduous) shrubland (<5m)	grass
140	Closed to open (>15%) herbaceous vegetation (grassland; savannas or lichens/mosses)	grass
150	Sparse (<15%) vegetation	grass
160	Closed to open (>15%) broadleaved forest regularly flooded (semi-permanently or temporarily)	forest
170	Closed (>40%) broadleaved forest or shrubland permanently flooded - Saline or brackish water	forest
180	Closed to open (>15%) grassland or woody vegetation on regularly flooded or waterlogged soi	grass
190	Artificial surfaces and associated areas (Urban areas >50%)	urban
200	Bare areas	other
210	Water bodies	other
220	Permanent snow and ice	other
230	No data (burnt areas; clouds;...)	NA

time t. Next the ENM results were combined with local species diversity estimates to create a "force of birthing" ($\lambda_{T,i,t}$) metric, representing the relative number of taxon member species giving birth at any time and space (as described by raster months), as defined by:

$$\lambda_{T,i,t} = P_{T,i,t}\mathrm{D}_{T,i} \tag{3.1}$$

Table 3.2 **Covariate layers for spatGLM modeling**

Description	References
Non-volant mammalian biodiversity	[109]
Land cover (modified)	[172]
Vegetation fragmentation index	This study
Human population density	[44]

where the number of taxonomic members is given by $D_{T,i}$. The abbreviations afb, mic and mol were used to represent African fruit bats, non-molossid microbats, and molossid bats respectively. Third, the total conditional probability $P_{total,i,t}$ of any bat birthing from any of the three taxonomic groups at location i and time t, assuming independence, defined by:

$$P_{total,i,t} = 1 - \prod_{T=1}^{n}(1 - P_{T,i,t}) \tag{3.2}$$

A total "force of birthing" ($\lambda_{total,i,t}$) metric representing the number of bats of all taxons giving birth at any time and space as defined by:

$$\lambda_{total,i,t} = P_{total,i,t} \sum_{T=1}^{n} D_{T,i} \tag{3.3}$$

Finally, a modified version of the probability of birth was made for the African fruit bats in which we accounted for variation within taxonomic classes in the first annual birthing pulse of the year. Previous work has indicated that the bi-annually polyestrous breeding African fruit bats will have a birth pulse proceeding the start of the short dry period in addition to giving birth following the long dry season like all monoestrous species. Historically phenomena was only seen above $\sim$18°S, south of which all fruit bat populations only had a single annual birth associated with the long-dry season [50]. However, our modeling results suggested a threshold of $\sim$10°S and therefore we used this value. We accounted for this by down-weighting the probability of birth on the first six months of the calendar year by a ratio of biannual genera:total genera ($\frac{5}{9}$), as determined by our data-mining results. This information was not available on a comparable scale for any other taxonomic group. This modification allowed us to further probe the involvement of African fruit bat births on ebolavirus spillover events and is denoted throughout with the * symbol.

3.2.2 spatGLM

To assess the hypothesized temporal lags between birth pulses and outbreak events due to shifting population demographics we included lag terms for bat birthing terms. Because of the two month aggregation used within the ENMs, each lag term included represented a two month period. In the

model with most parameters, the risk of EVD spillover into non-human spillover hosts was defined as:

$$\begin{aligned}
&\log(R_{\text{an},i,t}) \sim \\
&\quad \beta_1 P_{\text{afb}*,i,t} + \beta_2 P_{\text{mic},l,i,t} + \beta_3 P_{\text{mol},i,t} \\
&+\beta_4 P_{\text{afb}*,i,t-2} + \beta_5 P_{\text{mic},i,t-2} + \beta_6 P_{\text{mol},i,t-2} \\
&+\beta_7 P_{\text{afb}*,i,t-4} + \beta_8 P_{\text{mic},i,t-4} + \beta_9 P_{\text{mol},i,t-4} \\
&+\beta_{10} P_{\text{afb}*,i,t-6} + \beta_{11} P_{\text{mic},i,t-6} + \beta_{12} P_{\text{mol},i,t-6} \\
&+\beta_{13} \text{D}_{\text{afb},i} + \beta_{14} \text{D}_{\text{mic},i} + \beta_{15} \text{D}_{\text{mol},i} + \\
&+\beta_{16} \text{NBMdiv}_i + \beta_{17} \text{PopDen}_i + \beta_{18} \text{fragIndex}_i \\
&+\beta_{19} \text{BVD}_{i,t}
\end{aligned} \tag{3.4}$$

where $R_{\text{an},i,t}$ represented the risk of EVD spillover at spatial location i, and month t. Potential sources of infection on the landscape were defined as times and locations where RNA fragments had been recovered from wild bats, our hypothesized reservoir hosts, and were included by the term $\text{BVD}_{i,t}$. Sero-positive animals were not included because the timing of infection is unknown. Non-bat mammalian diversity and a forest fragmentation index [241] were also included as the terms NBMdiv_i and fragIndex_i. Human population density, PopDen_i was included to represent the human-wildlife interface [189]. The transformation $\log(x+1)$ was used to treat all variables (with the exception of $\text{BVD}_{i,t}$) on the log scale while allowing that they might be zero.

Human outbreak events are not exclusively linked to direct exposure to proposed bat reservoir host(s) [191] and so outbreaks in non-humans were included within the human spillover model to capture these transmission chains. A lag term of a single month was included for non-human outbreaks to describe the transmission chain and incubation periods of non-human spillover hosts acting as amplifying hosts and transmitting virus to humans [210]. The risk of EVD spillover into humans

(R_{hum}) was therefore described as:

$$\begin{aligned}
&\log(R_{\text{hum},i,t}) \sim \\
&\quad \beta_1 P_{\text{afb}*,i,t} + \beta_2 P_{\text{mic},l,i,t} + \beta_3 P_{\text{mol},i,t} \\
&+\beta_4 P_{\text{afb}*,i,t-2} + \beta_5 P_{\text{mic},i,t-2} + \beta_6 P_{\text{mol},i,t-2} \\
&+\beta_7 P_{\text{afb}*,i,t-4} + \beta_8 P_{\text{mic},i,t-4} + \beta_9 P_{\text{mol},i,t-4} \\
&+\beta_{10} P_{\text{afb}*,i,t-6} + \beta_{11} P_{\text{mic},i,t-6} + \beta_{12} P_{\text{mol},i,t-6} \\
&+\beta_{13} \text{D}_{\text{afb},i} + \beta_{14} \text{D}_{\text{mic},i} + \beta_{15} \text{D}_{\text{mol},i} + \\
&+\beta_{16} \text{NBMdiv}_i + \beta_{17} \text{PopDen}_i + \beta_{18} \text{fragIndex}_i \\
&+\beta_{19} \text{BVD}_{i,t} + \beta_{20} OB_{\text{an},i,t} + \beta_{21} OB_{\text{an},i,t-1}
\end{aligned} \tag{3.5}$$

where OB_{an} is the occurrence of an EVD spillover into a non-human spillover host at spatial location i, and month t.

Within alternative models, bat diversity terms were tested as both combined (read: any bat species), and separated by taxon to test the relative contribution of each tax group to overall spillover risk. "Null" models in which all bat birth associated terms ($P_{T,i,t}$, $P_{toal,i,t}$, $\lambda_{T,i,t}$, and $\lambda_{total,i,t}$) were excluded were also computed and model comparison and selection were completed though qAIC (see SI Methods for details).

Additional validation was provided by testing our model predictions using the two most recent EVD outbreaks in the DRC, which were not included in the analysis. To do so, we estimated relative risk as ($R_{\text{hum},i,t}/\text{g}_{\text{mean}}(R_{\text{hum},i,t})$), where g_{mean} is the geometric mean, and percent risk rank, where each cell was against all cells across the entire 12 months available. Values were extracted for all cells covering the health districts where the spillover cases were purported to have occurred [11, 239] and visually compared. Because the outbreak numbers are low, we also checked the model sensitivity to the inclusion of these two data points, and performed the same analyses as above.

Model forms for both human, and non-humans spillover host spatGLMs are available from Appendix B B.1 - B.4 All work was completed using custom code written for R (version 3.4.3 [213]) and is available at github.com/cReedHranac/FS.

3.3 Results

The inclusion of bat terms improved the qAIC and predictive ability of our spatGLM models compared to the "null" models without bat terms for all human and the majority of animal models (Figure 3.2, Appendix B B.1 - B.4). The top animal spillover model by qAIC included product terms of the conditional probability of bat birth (including the modified fruit bat term) and total bat diversity. The terms describing bat birthing events 5-6 months prior and the month before and the month of spillover events were both significant and positively related to spillover risk to other mammals. Diversity of non-volant mammals was identified as a significant predictor and human population density had the only inverse significant relationship identified with spillover risk (see Appendix B Table B.1). The spatial and temporal locations of viral RNA detections in bats was also found to be a significant term providing credence to some of our hypotheses. Risk of EVD spillover to non-human spillover hosts was largely focused on Central Africa with high annual probability of infection across Gabon and the Republic of the Congo (RoC), the Eastern region of the Central African Republic (CAR), Northeastern DRC and included pockets in Western Africa covering Liberia, northern Côte d'Ivoire, and Ghana (Appendix B Figure B.1). Additional regions of potential risk were predicted throughout South Sudan, Uganda, parts of Kenya. At equatorial latitudes risk was constantly elevated over the rest of the study area with seasonal peaks centered around May and September. Another region of elevated annual risk was predicted at 25°S covering Angola, Zambia, eastern Mozambique and Northern South Africa despite no known occurrences of eboalviruses south of 10°S. Seasonal fluctuations in risk peaked between May to July in a single annual pulse rather then the bi-modal pattern observed further North.

The top model for human spillover risk by qAIC used the taxonomically separated probability of birth terms and included the down-weighted fruit bat modification (*). Significant terms identified included EVD spillover into a non-human host in the month of and month prior to an outbreak, suggesting the model's sensitivity to the stuttering infection chains within the system and supporting observed patterns of infection transmission [131]. The down-weighted probability of birthing term for the African fruit bat group 5-6 months prior, and the month of and month proceeding spillover events for both the fruit bats and non-molossid microbats were significant to predictions and top two models are summarized in Table 3.3 (See Appendix B). Diversity of non-bat mammals was

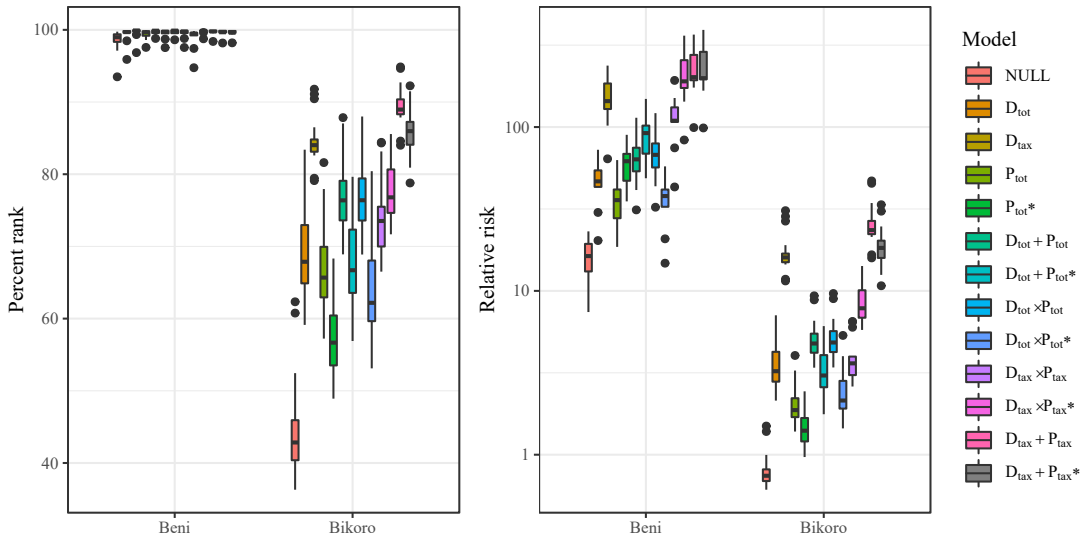


Fig. 3.2 **Model prediction comparison** All proposed models predictive scores for the cells covering the health districts in which the two most recent DRC outbreaks occurred for the month of outbreak occurrence (July and April respectively). *Left:* Percent rank against all cells in all months, *Right:* relative risk of *Ebolavirus* spillover in to human populations. Models contain different covariate combinations of bat diversity (D), and bat birth terms (B) with were either separated by taxonomic group ($_{tax}$) or combined as ($_{tot}$). Alternative models that contain the down-weighted fruit bat term are denoted by *

again identified as a significant predictor although neither viral detection in bats, nor the effect of forest fragmentation were identified as significant predictors of ebolavirus spillover to humans within this analysis. Risk of EVD spillover to humans was somewhat different to that of spillover into the non-human spillover hosts, as annual risk was more diffuse across Central Africa and more evenly distributed across areas of Western Africa (Figure 3.3). Similar to the non-human spillover hosts, the highest risk zones occurred around the border of Gabon and the RoC, although Cameroon was included and the high risk of spillover within the CAR were missing from the human model results. The associated temporal analysis (Figure 3.3 *right*) suggest seasonality within the system with two distinct periods of increased risk centered around the months of June and November just north of the equator. Acknowledging possible surveillance bias, the difference in peak relative risk between the human and non-human spillover host models suggest potential differences in spillover mechanisms between human and non-reservoir mammal host systems.

The two most recent EVD outbreaks in the DRC provided a test of the predictive power of our model (Figure 3.4). The EVD outbreak announced by the WHO in July likely started in April within

Table 3.3 **Top two human Ebola virus disease risk model results**

Model:	$D_{tax} + P_{tax*}$			$D_{tax} + P_{tax}$		
	Estimate	±95 CI	P value	Estimate	±95 CI	P value
Intercept)	-30.63	10.04	<0.001	-31.62	10.00	<0.001
P_{afb}	-2.41	2.16	0.04	-1.49	1.98	0.14
P_{mic}	1.83	1.53	0.02	1.48	1.51	0.06
P_{mol}	-0.19	2.00	0.84	-0.45	2.02	0.66
P_{afb_2}	0.91	2.04	0.29	1.39	1.88	0.15
P_{mic_2}	-0.06	1.55	0.93	-0.37	1.51	0.63
P_{mol_2}	0.29	2.14	0.73	0.11	2.18	0.92
P_{afb_4}	-0.39	1.96	0.9	-0.02	1.84	0.98
P_{mic_4}	-0.78	1.84	0.35	-0.95	1.80	0.3
P_{mol_4}	0.20	2.16	0.85	0.38	2.16	0.73
P_{afb_6}	1.60	1.88	0.05	1.29	1.94	0.19
P_{mic_6}	-0.27	1.61	0.67	-0.23	1.63	0.78
P_{mol_6}	1.34	1.98	0.2	1.48	1.94	0.13
D_{afb}	2.87	1.59	<0.001	2.88	1.63	<0.001
D_{mic}	1.86	2.76	0.18	1.92	2.78	0.18
D_{mol}	-0.59	1.57	0.46	-0.63	1.57	0.43
PopDen	-0.23	0.25	0.07	-0.23	0.25	0.08
fragIndex	-0.39	0.51	0.12	-0.4	0.51	0.12
BVD	-11.54	937.31	0.98	-11.43	944.88	0.98
D_{MNB}	3.23	2.31	<0.001	3.36	2.33	<0.001
OB_{an}	4.56	1.57	<0.001	4.5	1.59	<0.001
$\text{OB}_{\text{an}_{l-1}}$	2.89	2.20	0.01	2.71	2.23	0.02
qAIC		454.93			457.58	
$\hat{c}$		0.78			0.79	

the Bikoro health district in the northeastern part of the country close to the border with RoC [11]. This health district showed seasonality with peaks and troughs in the relative risk of viral spillover into humans (Figure 3.4). Of the 16 cells that covered the Bikoro health district there was a median percent rank scores of 88.3% compared to all cells in all months. Relative risk of ebolavirus spillover fluctuated between minimum, median, and high of 14.9, 21.3 and 50.4 respectively. The more recent EVD outbreak occurred in the district of Beni, a persistently highly ranked region. The district in northwestern DRC near the border with Uganda announced the outbreak on first of August with the index case was presumably in July or June [239]. The smaller region was covered by only nine cells and risk percent rank values extracted from the model covering July were among the highest ranking of all cells with a median of 99.6%, minimum of 98.0% and maximum of 99.8%. Relative risk for the region was considerable with minimal values of 93.0, a median of 195.0 and a high of 273.0 across the

year. Percent rank and relative risk scores were very similar between $D + B_{tax}*$ and $D + B_{tax}$ models with the later preforming slightly better in both metric at the Bikoro site. We ultimately chose the $D + B_{tax}*$ model as our top model due to it's inclusion of more precise information related to our *a priori* hypotheses, and its comparable predictive power over all other alternative models.

3.4 Discussion

The spatial and temporal occurrence of ebolavirus on the landscape is complex, with seasonal drivers likely modifying the behaviors of both the (yet unidentified) maintenance reservoir host(s) and susceptible non-maintenance host populations. The inability of outbreak investigation teams to determine a definitive source of infection in all but a small number of cases has severely hindered the ability of public health officials to generate actionable measures against future EVD outbreak events. Infections from non-human spillover hosts to humans have occurred but only been confirmed from great apes and duikers, despite ebolavirus sequence detection in some rodent species [158], bat species and the wide diversity of susceptible species within the biome [132, 210]. Here I predict the continental birthing patterns of African bats and find some statistical support for bats births, and African fruit bats in particular, being correlated with EVD outbreaks. Furthermore the inclusion of the proportionally down-weighted birth term for the African fruit bats species improved predictive ability in most cases. Together these are used to predict the spatio-temporal risk of EVD outbreaks in non-human mammals and humans across the African continent.

The discovery of statistical support for some African fruit bats species being correlated with ebolavirus outbreaks supports a number of previously disparate hypotheses [93, 232, 84]. In particular the improved predictive ability (by *qAIC*) of the modified fruit bat term suggests the importance of seasonally polyestrous birthing on the occurrence of EVD. The historical association of EVD spillover events and African fruit bats has been more anecdotal than factual in most cases, and to date no hunters targeting fruit bats have been index cases despite the widespread practice [114, 151, 182]. This may be because the species most hunted, *Eidolon helvum* [114, 151], is likely not a reservoir species, possibly due in part to its single annual birth pulse [97, 95] and unique cellular mechanisms [163]. The large geographic spread by viral subtypes, such as that observed in the 2013–2016

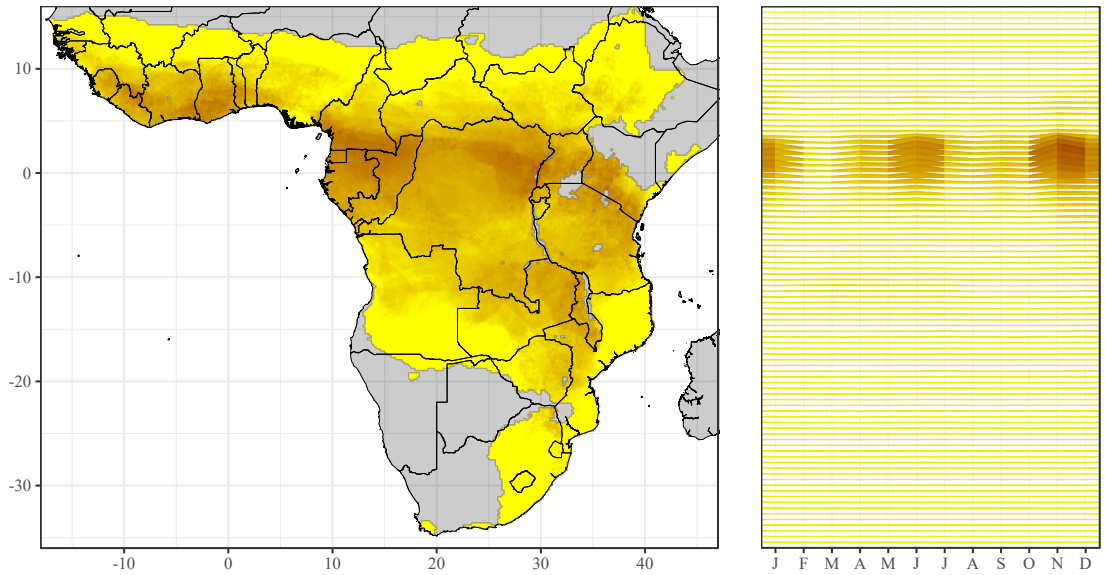


Fig. 3.3 **Risk of Ebola virus disease outbreaks among people** Left: Mean annual risk of EVD emergence in humans across the study area. Low values are in yellow, high values in red, and grey zones were not included in the analysis. *Right:* Risk of EVD aggregated by latitude and month. Height and color intensity are proportional to the risk of EVD within the latitudinal window.

outbreak in West Africa, could be facilitated by other broad ranging African fruit bats such as the *H. monstrosus*, a seasonally polyestrous species whose population spans both Central to West African regions with little measurable population genetic structure [89]. Until recently the only potential reservoir species from which EVD causing Ebola virus viral fragments have been recovered were Pteropodidae members [131, 170]. Serological surveys have implicated molossid and non-molossid microbat species, however serological data are difficult to interpret for a range of reasons from unknown true negatives, cross-reactivity, and unknown within host infection dynamics [72]. Our analysis also identified molossid birthing events as a potential contributer to human risk of EVD spillover and both serological and molecular findings are consistent with the patterns observed in MARV infected *R. aegyptiacus* [192, 4]. Recent detections of ebolavirus fragments in molossid species and our analyses suggest the role of molossid bats in ebolavirus sylvatic maintenance is an important area for potential research within both systems [124, 75].

Seasonality of EVD events has been noted [203], however the abiotic conditions (such as rainfall) used within these analyses are likely not to be directly driving spillover, especially for environmentally unstable RNA viruses in tropical environments [61]. We hypothesized viral persistence within bat

populations themselves, meaning viral sylvatic dynamics, are also unlikely to be directly attributable to exogenous pressures. By exchanging the traditional abiotic metrics of seasonality with a derived metric such as seasonality of birth we are able to explore a mechanistically plausible driver of seasonality within the sylvatic EVD system [2]. Temporally varying bat birth terms identified by both our non-human spillover host and human risk models support the hypothesis that birthing may facilitate transmission into non-human mammals [192, 204]. In our best models for ebolavirus spillover the birthing term for both fruit bats and non-molossid microbats were significant. The later of the lag terms identified for the African fruit bats is consistent with the maternally derived anti-body (MDA) hypothesis of Pourrut *et al.* [192] and Peel *et al.* [180], dynamics predicted by generic filovirus models [93], and observed in empirical MARV data [4].

Risk of spillover to non-human spillover hosts was strongly driven by human population density and responsible for much of the patchy geographic risk distribution (see Appendix B Figure B.1 and B.2). This negative human population density-EVD risk relationship was borderline significant and effect size was much smaller within the human system. This may be expected given many outbreaks in animals are identified in forest-dwelling species, such as gorillas, and concurrently with human cases where index cases are reported to have had contact with other species such as gorillas [132]. The correlation of non-bat mammalian diversity in both spillover models could indicate simply that both the bat hosts and the non-reservoir spillover hosts live in the biodiverse tropical forests. Temporally lagged terms that describe chains of infection, both from bats to non-humans spillover hosts and from them to humans, were significant in our models as expected. In contrast to other work, however, we did not find habitat fragmentation to be predictive of EVD spillover risk [198], perhaps because we are modeling risk at a much larger scale than those studies (but see also [241]) and not accounting for temporal changes. This may be an example of Simpson's paradox, or alternatively, our use of slightly different methods may be highlighting the importance of other model terms. It is difficult to consider how instances of Simpson's paradox may be influencing our results, but clearly the interactions between habitat change, bat birthing, ebolavirus emergence and disease emergence in general are areas for future research [198, 241, 84]. Data sets to test these relationships, such as one populated with animal infections independent of human outbreak events, however, present serious hurdles in these regards.

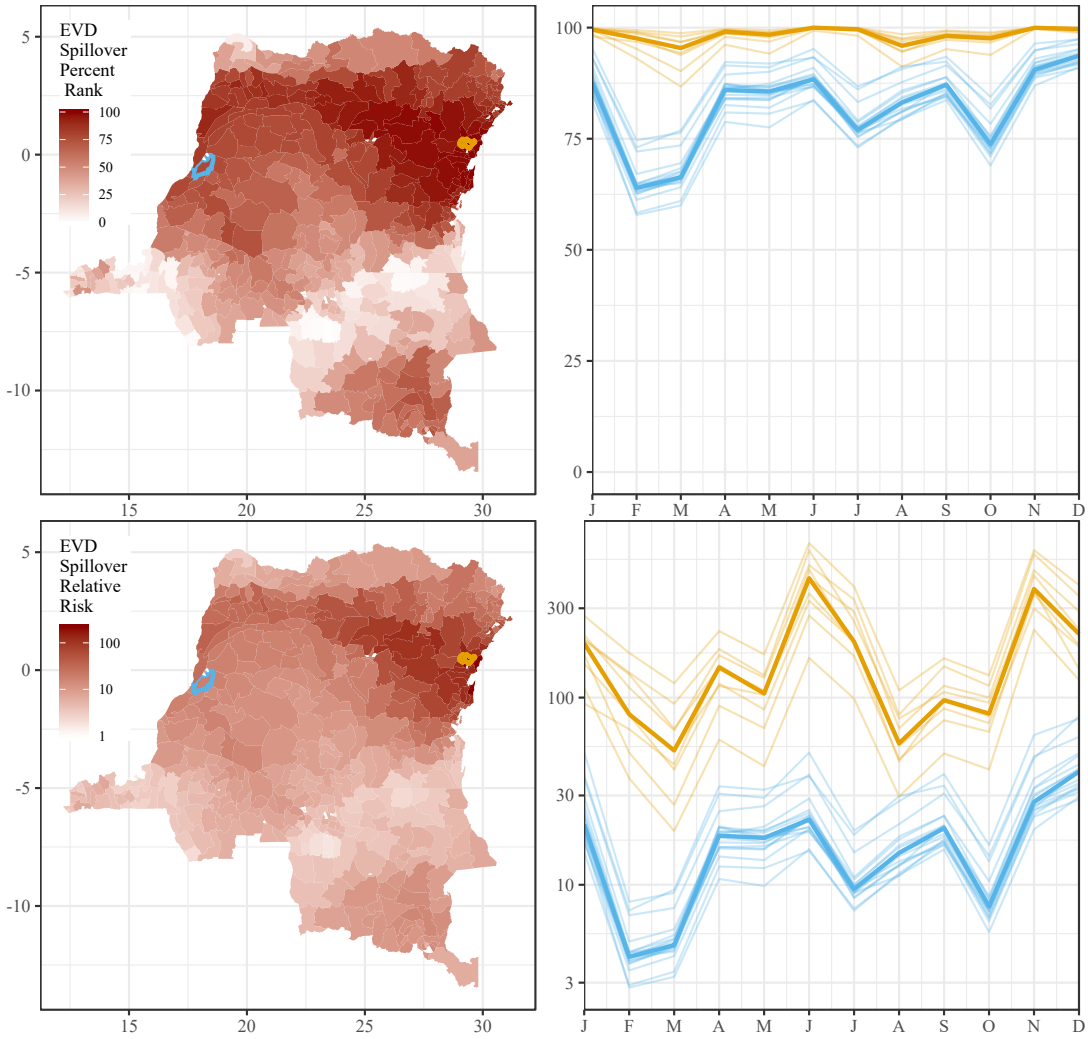


Fig. 3.4 **Model results in the context of the most recent EVD outbreaks** In 2018 there were two recognized EVD outbreaks in the Democratic Republic of the Congo (DRC).The district of Bikoro where the July 2018 outbreak occurred is highlighted in blue, and highlighted in orange is the district of Beni where the outbreak announced in August 2018 started. The index case for the Bikoro epidemic was believed to be in April, while the Beni outbreak is believed to have begun in July. *Upper:* Percent risk ranking against all cells and all months (not just the DRC). *Lower:* Relative risk of viral spillover. *Left:* Annual average risk by district health zone. *Right:* Risk with in the health districts throughout the year. Each lines represents a cell within the district and the median value is bolded.

The DRC has seen more EVD outbreak events than any other country, and the two most recent outbreaks exemplify the countries ongoing struggle to combat a complex system. While the seasonality of relative risk is largely similar between the two locations, there are distinct and potentially important local peaks and troughs within the local seasonality of risk for each location and both outbreaks occurred at, or close to, local maximal values of relative risk. These seasonal patterns may be linked to

the biannual birth pulses of the local fruit bat or molossid species, but are also likely tied to extremely local shifts in behavioral, phenological, and climatic factors that modify both the reservoir host(s) and susceptible populations.

Analyses of EVD emergence, including ours, are clearly limited by sparse data. This includes information on other possible host species such as apes, swine or other small mammals, which may warrant further investigation if data become available. Recent serological analyses of African primates, however, support our assumptions that they are unlikely to be maintenance hosts [9, 94]. The lack of detailed species specific bat birthing data hampered our ability to test some hypotheses and necessitated the aggregation of data by host taxonomic traits rather then by species, or genus. While these groupings have proved useful [50], we do acknowledge that the patterns discussed may not be fully representative for all members (i.e. *E. helvum*) and was our primary motivation for creating down-weighted variation. Despite the significance of only fruit bat associated diversity terms, non-molossid microbats are under sampled virologically [130] and ecologically (this study) for such a diverse taxonomic group. Increased data may change our understanding of their role in EVD, especially in light of the recent news of ebolavirus viral fragments in the *Miniopterus inflatus* microbat and isolation of a potentially new *Ebolavius* species by Goldstein *et al.* [75]. These finding represent a previously undiscovered viral diversity within the system and warrant further investigation into the role of molossid species in Filovirus transmission. Finally, because of our research methodology and the low number of bat birthing records I was required to make the assumption that bat reproductive patterns have not changed over the last half century. While these patterns are often highly conserved, human population encroachments, seasonal variations forest usage, and anthropogenic climate disruption may be modifying bats' selection of locations to give birth in ways that our models cannot capture. Further, seasonal human and other behaviors may also affect spillover risk. These could have be modeled by using a dummy variable (e.g. months) in the absence of data to understand the contribution of such factors, but that bat birthing terms are present in both animal and human spillover models suggests these are plausible mechanistic covariates to include. However, caution is needed before overinterpreting these results and these are potential avenues of future research.

I was also unable to include bat abundance terms, and clearly host abundance will affect the likelihood of viral persistence in populations [93, 192]. These ecological gaps, however, can be filled without additional virological work, although contemporaneous ecological and virological data collection will provide advantages for data integration and improved system understanding [198, 192, 4, 194]. Because of the limited number of viral detections, all *Ebolavirus* species were combined into a generic definition of ebolavirus despite the probably that each species has its own intricacies of sylvatic persistence, distribution, reservoir host and spillover. Further, the reliance on symptomatic EVD can increased these biases especially if a species disproportionately causes asymptomatic infections. Only increased virological studies in hosts and unfortunately outbreaks in people will allow us to disentangle these species level intricacies. Despite these weaknesses, I believe these analyses have successfully captured the overall patterns of birth pulses of African bats and provide potentially useful insights in the ecology of ebolaviruses and how seasonal changes in EVD risk may be driven by bat reservoir host ecology.

Chapter 4

What is a winter? Addressing data deficiencies for vital overwinter bat models

4.1 Introduction:

Following the end of summer in the temperate zones of North America, hibernating animals, including the little brown bat (*Myotis lucifugus*), bridge the resource poor winter months through strict energetic budgeting and behavioral changes [71, 103, 209, 233, 234]. The overwinter survival of a hibernator depends upon three facets: 1) the amount of its energy stores, primarily body fat; 2) its energetic expenditure (rate of metabolic consumption); and 3) the duration of winter hibernation [108, 208]. Hibernation is composed of bouts of torpor, during which body temperature matches ambient (or near ambient) temperatures to limit the consumption of finite metabolic resources. These bouts of torpor are periodically interrupted by energy intensive periods of arousal during which hibernators return to euthermic body temperatures. Hibernators need to arouse periodically for a variety of proposed reasons (for a review see [40] and citations within), including the need to flush metabolic waste, regain water balance, or mate [92]. While these arousals represent a small fraction of the total time spent in hibernation they account for the majority of energy consumed, with a single arousal costing as much as 5% of total overwinter energetic costs [216].

Microclimate selection is critical for hibernators [29]. By allowing body temperatures to drop, *M. lucifugus* is able to consume up to 80 times less energy per unit time compared to resting metabolic rate during torpor due to the exponential relationship between metabolic rate and temperature [103, 208]. In order to maximize the utility of these metabolic reductions, hibernating bats seek out caves, mines, scree slopes or other locations generally referred to as "hibernacula" where they can overwinter [208]. These often subterranean locations provide excellent habitat for hibernators due to their consistently low, but not freezing temperatures (0°> & <10°C) and high humidity relative to the surface landscape [208, 215]. Appropriate microclimate selection within hibernacula is also critical for hibernators to minimize frequency and duration of arousals from torpor [51, 81, 108]. Species such as *M. lucifugus* appear to consistently choose saturated, or nearly saturated, environments with stable temperature to ameliorate relatively high rates of evaporative water loss (EWL), while other bat species utilize more arid, and less thermo-stable hibernating environments [68, 118, 117]. Within a cave or mine system, conditions may not remain stationary throughout the duration of winter and some bats will follow specific conditions within the hibernaculum as they shift [92]. A series of complex interactions between surface features (e.g. slope, aspect, elevation) and cave features (e.g. number of entrances, air flow, depth) will ultimately define when and where microclimatic conditions will be available within the hibernaculum and most will contain a variety of conditions [143, 184].

The duration of winter hibernation is another critical determinate to the survival of hibernators. The stimuli that drive immergence (entrance) to and emergence (exit) from hibernation are under-described, especially when considering the geographic variation in the timing of such events [51, 127, 165]. Moreover, the onset and duration of winter in Northern latitudes is difficult to spatially quantify. The duration of winter hibernation presents a strong selective pressure, placing an energetic and temporal constraint on hibernating populations by limiting pre-hibernation weight gain [123]. While animals that hibernate at more southern latitudes may be able to capitalize on breaks in the winter weather to opportunistically feed [18], this is not always an option, as some hibernaculum entrances may be blocked by snow for the majority of the hibernation period (C. Lausen, personal communication). Because North American hibernating bats feed on insects, researchers have estimated effective winter duration based upon the number of freezing days on the assumption freezing prevents widespread insect emergence in spring [96, 108]. Yet, some populations of bats may emerge from hibernation

when freezing temperatures still occur, suggesting that there may be more complex determinants of emergence times than solely the number of freezing days [111]. Additionally, site level differences, such as the density of prey insects, will also influence traits like body condition, leading to variation in the amount of energy stores that bats take into hibernation.

Beyond the normal challenges of hibernation, the epizootic of white-nose syndrome (WNS) caused by the psychrophilic fungus *Pseudogymnoascus destructans* (*Pd*), in eastern North America has created additional energetic demands for many hibernating bats [26]. The fungal pathogen responsible for the disease has spread rapidly through North America since 2006 and has killed millions of hibernating bats [66, 67]. Bats become infected by the pathogen during hibernation, when skin temperatures are reduced and immune functionality is repressed to conserve energy [228]. Mortality due to WNS has been linked to the increased frequency of arousals of infected bats, ultimately resulting in the depletion of overwinter fat stores prior to the end of winter and subsequent starvation [135, 236]. By spring of 2017, *Pd* had been detected in Washington state [83] yet it is uncertain if western North American (herein Western) bat populations will suffer the same mortality observed in eastern populations (herein Eastern) [96].

Here, we re-examine two of the three most critical parameters governing overwinter survival for hibernators: the duration of winter hibernation and the amount of fat stores taken into this period. Previous model iterations [96], while flawed (especially in up-scaling results to the landscape level) did allow for spatial variation in duration of winter; however, this definition was made *a priori* [108]. Instead, we used data collected from the field, compiled data available from the literature, and reached out to bat researchers across North America to create a spatially defined database of winter duration and body mass for *M. lucifugus*. We then fit a set of linear models to 1) estimate winter duration, 2) relate body mass to pre-hibernation fat stores, and 3) predict body mass across the species' distribution. Additionally, our team also employed a refined mechanistic model of hibernation energetics [81] to provide species-specific estimates of the total metabolic costs of hibernation, which allowed us to predict overwinter survival with and without the effects of WNS. We chose to focus model development and parametrization on *M. lucifugus*, due to the high impact of WNS on Eastern *M. lucifugus* populations and the abundance of published data available for this species. Using these

improved definitions of winter duration and available fat stores, we updated the predicted survival outcomes for infected *M. lucifugus* made in Hayman *et al.*, 2016 [96].

4.2 Methods:

We re-examined the estimates of winter hibernation duration within previous published by Humphries, and Hayman *et al.*, [96, 108] and created the first spatial estimates of body mass and pre-hibernation fat stores for *M. lucifugus*. We compiled body mass and emergence data from a variety of sources including the literature, acoustic surveys, publicly available datasets, and solicited estimates from local bat researchers across North America (Figure 4.1).

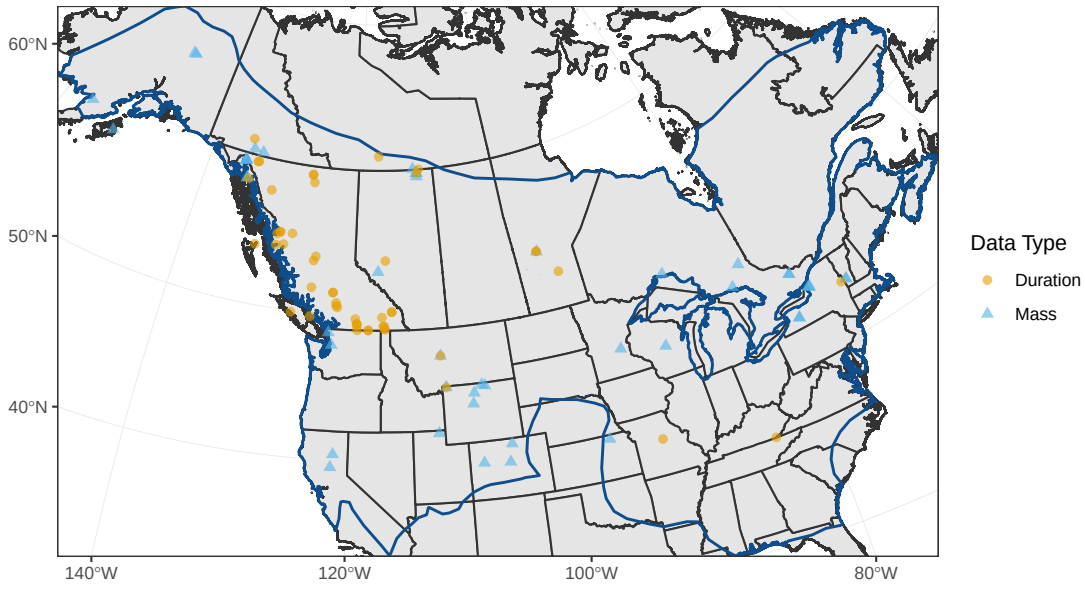


Fig. 4.1 Locations of *Myotis lucifugus* body mass and hibernation duration as estimated by immergence and emergence dates data sources across temperate North America. Records of the duration of hibernation (○), pre-hibernation mass (△) and the current IUCN species distribution (blue outline) [109]

4.2.1 Winter duration

4.2.1.1 Acoustic and winter duration data

Songmeters (SM2+BAT; Wildlife Acoustics, MA, USA) were deployed by the Wildlife Conservation Society (WCS) to passively record bat activity across Western Canada between 2008 and 2016. Microphones (either SMX-US or SMX-U1) were placed on 12-18' tall telescoping poles above likely hibernation or commuting areas (e.g. river banks, cliff ridge tops) in mid-August. Acoustic activity was typically recorded throughout the duration of the winter and data were retrieved sometime between mid-March and mid-May. Recordings were manually analysed using AnalookW software (www.hoarybat.com; C. Corben) and customized noise-filters were used to pull files containing bat calls which were identified to species groups (e.g. 40 kilohertz recording, 25 kilohertz recording, etc.). If diagnostic echolocation features were present, a species-level identification was made. The occurrence of at least 2 bat echolocation pulses in a file was required to identify the recording as a 'bat pass', and the number of passes were summed nightly. The 'start' of the winter hibernation period was defined by the last 3-night window between August 15 and December 31, in which 10 or more bat passes were identified, while the 'end' of the winter hibernation period was defined by the first 3-night window between March 1 and May 15 in which 10 or more bat passes were identified. In locations where bat activity was consistently low throughout the year, winter hibernation 'start' and 'end' points were defined by date of the last and first bat passes during the same time periods. Average immergence and emergence date estimations were computed for sites with more than one year's worth of data. Additionally, records of the location, date of entry into, date of exit from and/or duration of hibernation were collected from the literature and solicited from bat researchers across northern North America as described in Appendix C.

4.2.1.2 Spatial covariates

Due to the correlation between ambient temperature and insect activity, we used climatic covariates to explain the relationship between food resources and the onset of hibernation rather than photoperiod-based metrics hypothesized in migratory studies. Spatial covariate layers hypothesized to be related to the duration of winter are summarized in Table 4.1. All spatial data were re-projected to the same

1km resolution, cropped and masked to the extent of temperate North America (above the Tropic of Cancer and below the Arctic Circle) to represent the full extent that these bats could conceivably disperse to naturally.

Table 4.1 **Abiotic covariate tested in spatial analyses**

Covariate Name	Description	Data Source
$Northing$	Degrees latitude North	[64]
DEM	Elevation	[235]
Day_{frost}	Number of annual days in frost	[235]
Day_{freeze}	Number of annual days below freezing	[235]
Day_{Ngrow}	Number of annual days outside the growing season	[235]
$Original$	Number of nights below 0 between Nov-Feb	[96]

4.2.1.3 Modeling framework

All potential covariates were regressed against the duration of winter hibernation in univariate models and in models adjusting for $Northing$ or $Northing + DEM$. From initial model fits, externally studentised residuals were computed to assess outliers. These residuals were converted to p-values and adjusted for multiple testing using Holm's method [104]. Those observations that had low adjusted p-values (<0.5) across multiple models were then excluded, and models refitted using reduced data. A second round of linear regression was then fit with the modified data set and model selection was assessed by Akaike information criterion (AIC). The top model was predicted back across the study extent to create a complete estimate for the duration of winter. A variogram was created for the top model by AIC to assess the impact of spatial auto-correlation and to determine if more spatially explicit models were needed.

4.2.2 Spatially varying body mass

4.2.2.1 Body mass data

The data required to directly assess the spatial variation in body fat for *M. lucifugus* prior to hibernation do not exist, so instead we relied upon scaling fat with body mass. To do this, we 1) confirmed that separate geographic groups have significantly different body masses; 2) identified a relationship between body mass and composition body fat; and, 3) defined a relationship to predict

these phenomena spatially. Pre-hibernation masses of Eastern (New York, Vermont [144]) and Western (Montana, this study) *M. lucifugus* populations were assessed for equal means using a Tukey's contrast test. These data were selected as they contained detailed measurements of body composition including fat mass obtained through the use of quantitative magnetic resonance. Using the estimates of body composition, we fit a linear model to predict fat mass from body mass with the form:

$$Mass_{fat} \sim \beta_0 + \beta_1 * Mass_{body} + \varepsilon \tag{4.1}$$

where $Mass_{fat}$ was the fat component of total body mass and $Mass_{body}$ was the total body mass.

4.2.2.2 Spatially varying body mass

We then applied this relationship across the spatial species distribution of *M. lucifugus*. We compiled mass data for *M. lucifugus* from VertNet (vertnet.org), existing literature (see Appendix C C.2), our own study, and solicited the same Western researchers mentioned above. Records obtained from VertNet were filtered to include only those with spatial referencing, mass and those that were observed between September and December in attempt to select only records from the swarming period just prior to the start of the hibernation period. Using the same two-step linear modeling methodology described above for the winter duration, we fit a new series of models to predict the pre-hibernation mass of *M. lucifugus* across their distribution. Model selection was again determined by AIC, and the top model was projected back across the species distribution. The linear relationship between pre-hibernation fat mass and body mass was then applied to create a spatial data layer representing estimated fat stores across the species distribution.

4.2.3 Spatially variation in hibernation survival

The new estimates for the duration of hibernation and the amount of fat that *M. lucifugus* take into hibernation were then used as parameters within a previously described mechanistic hibernation energetics model ($Hib_{species}$) [80, 80]. The details of these models are explained in full in both these publications [80, 81] and induced in the two Appendices D and E. In brief, the energetics model uses species specific metabolic and morphometric parameters to estimate the required amount of energy

(in grams of fat G_{fat}) to overwinter a winter of duration Win at location $_i$, defined as any 1km^2 cell, using a series of energetic functions, where ambient temperature is Ta and relative humidity is RH. Together, this takes the form of:

$$G_{fat} = Hib(Ta, RH, Win)_{i,d} \tag{4.2}$$

and disease status is taken into account through the parameter d. Survival capacity, $Surv$, is therefore defined as:

$$Surv_{i,d} = Mass_{fat,i} - Hib_{species}(Ta, RH, Win)_{i,d} \tag{4.3}$$

Constant hibernaculum conditions of $Ta = 4°C$ and $RH = 98\%$ were used as *M. lucifugus* tend to select, or modify microclimate conditions to meet those parameters [215]. These microclimatic conditions are thought to provide for the longest possible hibernation and is supported by findings from Haase *et al.*, [81]. An additional model was run using the hibernaculum conditions of $Ta = 2°C$ and $RH = 100\%$ as Canadian *M. lucifugus* have been observed using these conditions when preferred conditions are not available (C. Lausen, *personal communications*) to exemplify how the subtle differences in microclimate selection can change energy requirements and alter survival estimation predictions when infection is taken into account.

Positive $Surv$ values, measured in grams of fat, indicate that a bat is predicted to be capable of surviving the duration of winter hibernation in that location and having $>$ 48 h worth of additional fat stores to begin foraging for food on the landscape. Negative $Surv_{i,d}$ values indicate that the $Mass_{fat,i}$ is insufficient and the bat is predicted to starve prior to the end of winter. Specific parameter changes from package defaults for *M. lucifugus* were made including an average arousal duration estimate of 2.2 hours ([63] C. Lausen *personal communication*).

Finally, the amount of fat required for overwinter survival was compared between uninfected bats and those infected with Pd within the same hibernacula conditions. To illustrate the difference in fat stores needed between these two, the amount of additional fat required to survive hibernation when infected was computed as a percent by $\frac{G_{fat,I}}{G_{fat,N}} * 100$ where I and N represent infected and uninfected (Null) respectively, and mapped back across the species distribution.

All analyses were preformed through R [213], with spatial handling tools from the raster [101] and sp packages [179]. All custom code and data are available at github.com/cReedHranac/winTor, and the winter hibernation model is available at github.com/cReedHranac/batwintor.

4.3 Results

4.3.1 Winter hibernation duration

The WCS acoustics dataset provided 34 estimates for the duration of witner hibernation across Western Canada, an additional 7 estimates were gleaned from the literature and 11 researchers or research groups provided an estimate of the duration of hibernation for *M. lucifugus* within their locality (Figure 4.1, Appendix C.1). After the leave-one-out round of model fitting, no observations were identified as outliers and the second round of models was fit to all 52 hibernation location estimates.

The top model for predicting duration of hibernation selected through AIC included the covariate terms $Northing$, DEM, and Day_{frost}. DEM and Day_{frost} were the only two significant terms (model summary in Table **??**) and the model had an adjusted R^2 of 0.54. The selected model significantly out preformed the original *a priori* estimate of the duration of winter [96] (full results in Table 4.2). The results were projected back across the study extent and visualized in Figure 4.2. Maximal winter length across the study extent was estimated at 276 days in Alaska, 32 days longer than our longest record in our observation data set in Manitoba Canada. Minimal winter durations of 58 days occurred southern end of the distribution and it's not certain how many of these days would be consecutive.

4.3.2 Body mass

There were site level differences between the body mass of Eastern and Western *M. lucifugus* populations. Population mass means between the Eastern Bats in New York and Vermont were not-significantly different from one another (p= 0.387), however, bat masses from Western bats in Montana were 1.02g and 0.84g below the Eastern populations respectively (both p <0.001), suggesting variance in fat required between Eastern and Western populations. The allometric relationship between pre-hibernation fat stores and body mass was strong with an adjusted R^2 of 0.765 (See Appendix C.1).

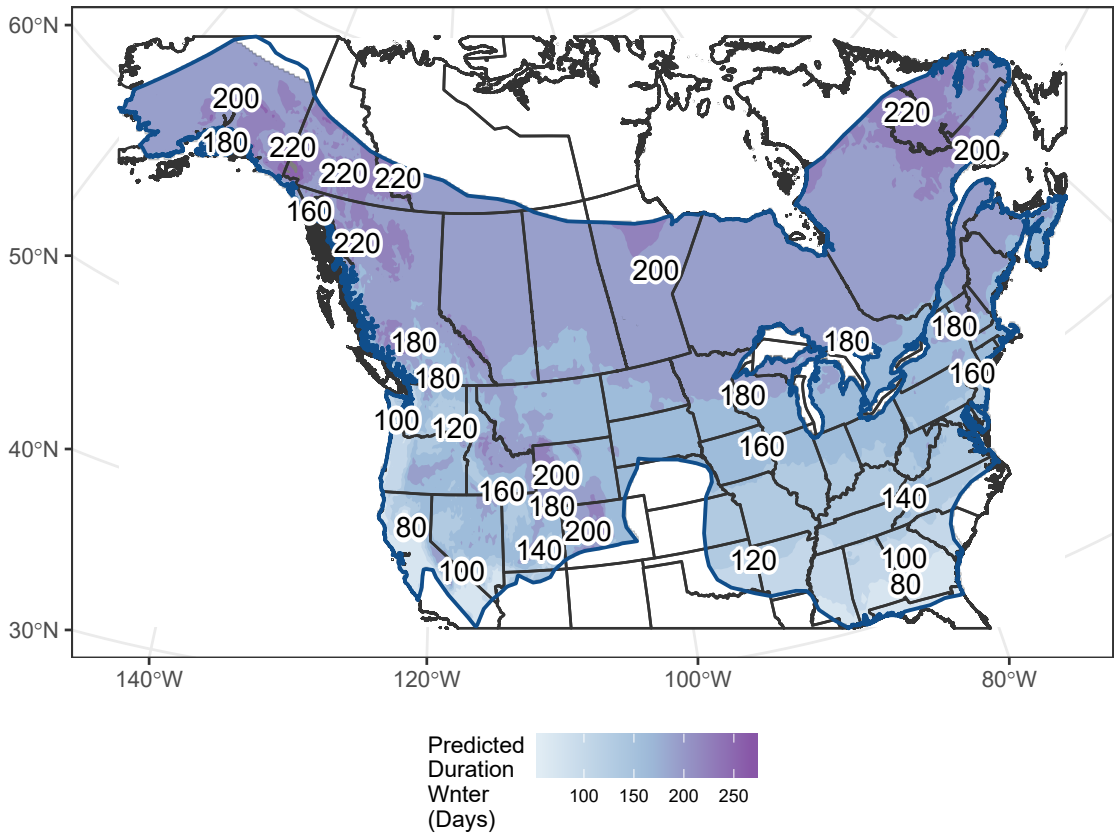


Fig. 4.2 **Predicted duration of winter across temperate North America for *Myotis lucifugus*.**

Table 4.2 **Model selection by AIC for alternative spatial models.** Terms included in the analysis included: degrees of latitude North (*Northing*); Elevation as represented by a digital elevation model (*DEM*); number of days in frost per year (Day_{frost}); number of days below freezing during a year (Day_{freeze}); the number of days not within the growing season (Day_{Ngrow}), and the original *a priori* estimate from Hayman et *al*. 2016 (*Original*). Best model AICc and ΔAICc values are underlined.

	Duration		Body Mass	
Covariate Structure	AICc	ΔAICc	AICc	ΔAICc
$Original$	531.16	21.95	180.01	7.02
$Northing$	538.70	29.49	184.71	11.72
DEM	546.45	37.24	184.78	11.80
Day_{Ngrow}	530.86	21.65	181.53	8.55
Day_{frost}	511.43	2.22	175.24	2.26
Day_{freeze}	514.97	5.76	174.95	1.97
$Northing + Original$	533.23	24.02	179.25	6.27
$Northing + DEM$	538.63	29.42	187.08	14.10
$Northing + Day_{Ngrow}$	532.85	23.64	181.95	8.97
$Northing + Day_{frost}$	513.01	3.80	177.44	4.45
$Northing + Day_{freeze}$	516.87	7.67	<u>172.98</u>	<u>0.00</u>
$Northing + DEM + Original$	535.64	26.44	178.13	5.14
$Northing + DEM + Day_{Ngrow}$	535.64	26.44	179.58	6.60
$Northing + DEM + Day_{frost}$	<u>509.21</u>	<u>0.00</u>	174.28	1.30
$Northing + DEM + Day_{freeze}$	519.14	9.93	174.31	1.33

Table 4.3 Summary for survival capacity (g) results limited to the species distribution of *Myotis lucifugus*. Negative values represent a predicted short fall in the fat require to survive the duration of winter hibernation while positive values indicate a surplus of fat stores remaining after the conclusion of the hibernation period.

	Winter Duration	Mass	Fat	Fat Required (g)				Survival Capacity (g)			
	(days)	(g)	(g)	2°C;100 % RH		4°C; 98 % RH		2°C; 100 % RH		4°C; 98 % RH	
				Uninfected	Infected	Uninfected	Infected	Uninfected	Infected	Uninfected	Infected
Minimum	58	6.11	0.78	0.1	0.19	0.11	0.18	0.55	-1.19	0.52	-0.34
1st Qu.	166	7.81	1.79	0.28	1.33	0.31	1	1.54	0.46	1.51	0.84
Median	187	8.45	2.17	0.31	1.65	0.35	1.22	1.85	0.71	1.81	1.04
Mean	179	8.64	2.28	0.3	1.56	0.34	1.16	1.98	0.72	1.95	1.12
3rd Qu.	202	9.38	2.72	0.34	1.91	0.38	1.4	2.39	0.99	2.35	1.41
Maximum	276	16.88	7.17	0.46	3.45	0.52	2.44	6.71	3.72	6.65	4.73

A total of 46 observations of *M. lucifugus* pre-hibernation body mass were obtained from the literature, VertNet, and various field teams in contact with our research group (See Appendix **??**tab:SI3mass)). Only a single observation was removed during the first round of leave-one-out cross validation and the remaining 45 observations were fit during the second round. The top preforming model contained only the *Northing* and Day_{freeze} covariates, although models including combinations the Day_{frost}, and *DEM* terms had very similar AIC values (Table 4.2). The linear relationship to explain body mass over space was the least predictive of top models selected within this study, with an R^2 of 0.239. Body mass was predicted back across the species distribution and using the relationship between body mass and body fat described above and we created a spatial prediction of pre-hibernation body fat (Figure 4.3). Maximum body mass was predicted to be 16.88g of which 7.17g (42.3%) was predicted to be body fat while minimum predicted mass was as low as 6.11g, with only 0.78g of body fat available (12.8%).

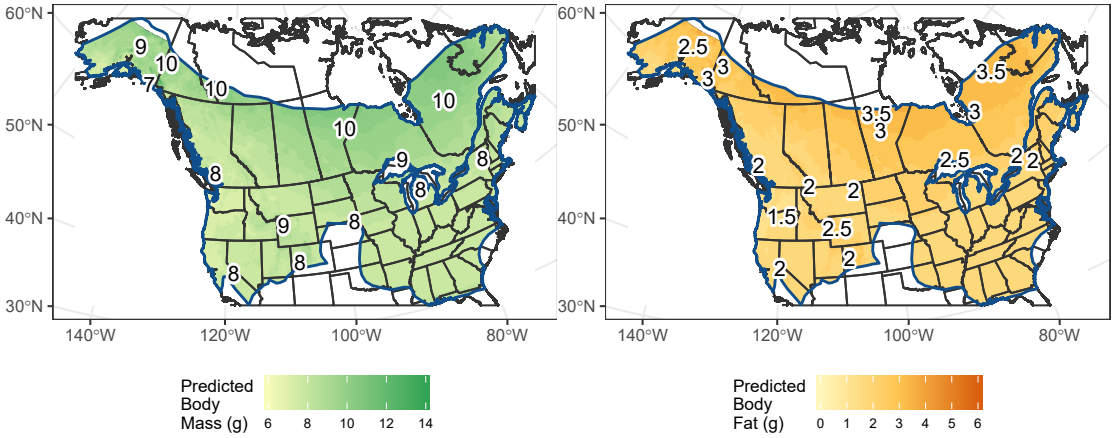


Fig. 4.3 **Estimated body mass and component fat across the distribution of *Myotis lucifugus***

4.3.3 Overwinter hibernation survival

Using the new estimates of hibernation duration and pre-hibernation energy stores, we predicted survival estimates for infected and uninfected *M. lucifugus* (Figure 4.4). Uninfected bats hibernating at $Ta = 4^{\circ}C$ and $RH = 98\%$ required a maximum of 0.52g of fat to survive the longest winter duration;

however most hibernating bats only required between 0.31 g and 0.38 g of body fat. At constant microclimate conditions, some bats exited hibernation with as much as 6.65 g of fat, although this was notably >3x more than the median value predicted across the species distribution. With the added energetic demands of *Pd* infection *M. lucifugus* hibernating at a steady $Ta = 4°C$ and $RH = 98\%$ were still predicted to have sufficient energy stores to survive the duration of winter hibernation. In some areas of British Columbia and Alaska, *Surv* values approached 0g for bats infected with *Pd*, which could indicate mortality in these regions.

When considering hibernation at $Ta = 2°C$ and $RH = 100\%$, all uninfected bats were predicted to survive the duration of hibernation with a surplus of body fat. However, when infected with Pd, bats East of the Appalachian Mountains and throughout most of the West were much closer to the 0 g survival threshold. We predicted mortality due to the premature exhaustion of overwinter fat stores in areas of western and coastal British Columbia, where some bats missed the required fat needed for survival by up to 1.19 g.

Clear differences in fat consumption were observed when comparing survival of *M. lucifugus* with and without Pd infection (Figure 4.4). At $Ta = 4°C$ and $RH = 98\%$, bats consume a minimum of 165% more fat when infected with Pd and >75% of the species distribution was predicted to require $\geq$ 320% more body fat stores for the same duration of winter hibernation. For hibernation at $Ta = 2°C$ and $RH = 100\%$, the increased rate of fat consumption due to fungal infection was even more dramatic, with a median of 526% more fat required and some locations demanding as much as 744% more body fat to survive hibernation (See Appendix C C.5).

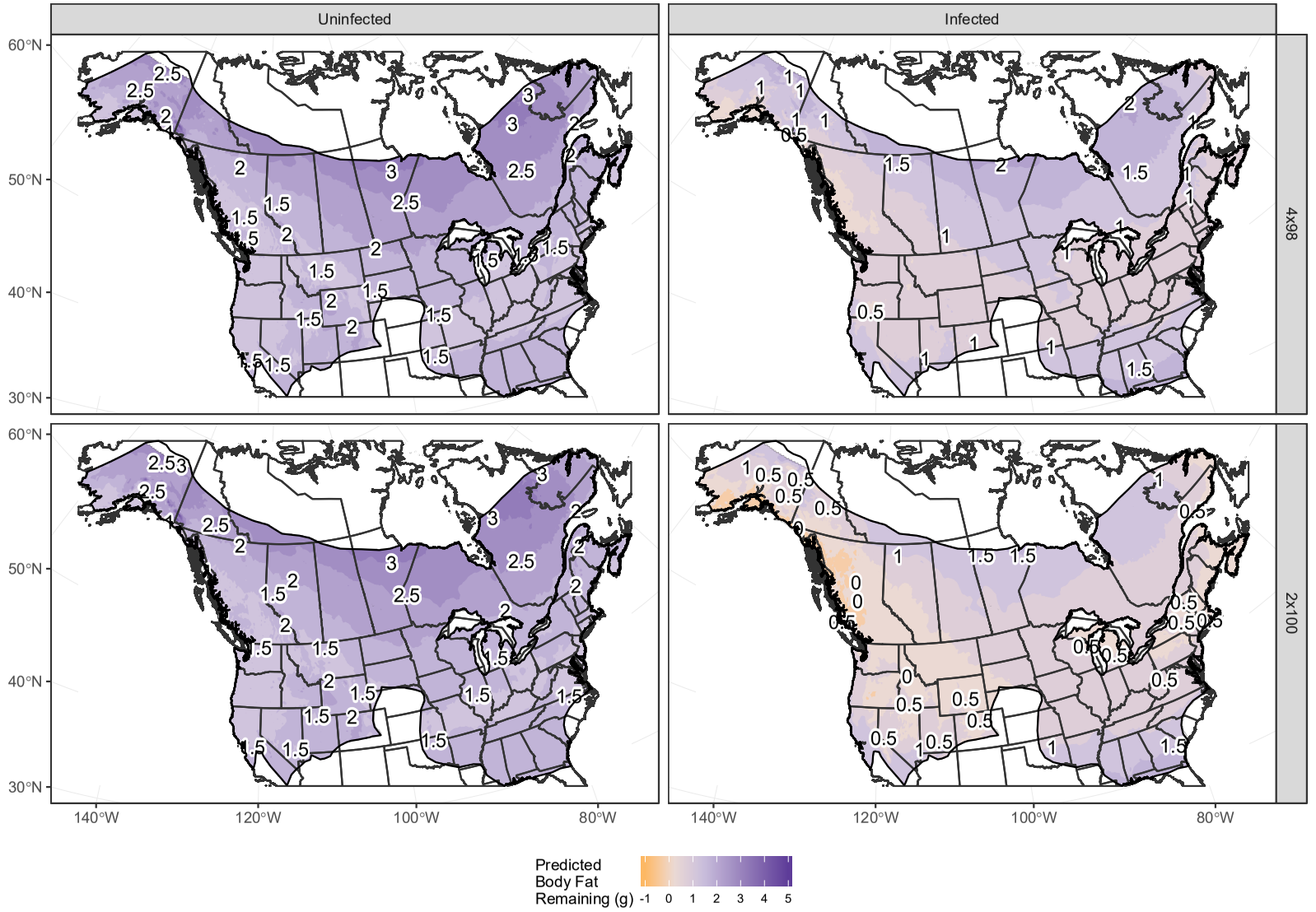


Fig. 4.4 **Predicted end of hibernation body fat stores for *Myotis lucifugus*.** Uninfected (*left*), and and bats infected with *Pd* (*right*) at the stable microclmatic conditions of $Ta = 4°C$ (*top*) and $RH = 98\%$, and $Ta = 2°C$ and $RH = 100\%$ (*bottom*). Values below 0 represent predicted morality prior to the end of winter hibernation due to insufficient fat stores.

4.4 Discussion

Since the emergence of WNS in North America in 2006, many hibernating bat species, including *M. lucifugus*, have suffered severe population declines as infected bats exhaust hibernation fat stores before the end of winter [26, 66, 67]. The overwinter survival of *M. lucifugus* relies upon a complex set interactions between physiological and abiotic factors [36, 96, 108]. A number of studies have investigated the influence of species level physiological traits, temperature and humidity on torpor metabolic rates and torpor bout duration [82, 80, 145], yet none have examined broad scale geographic intraspecies variation as predictors for survival. Here, we re-examined the variation in winter hibernation duration and identified relationships between the geographic distribution of body mass and pre-hibernation fat stores for *M. lucifugus*. We used these spatial estimates and an updated model of hibernation energetics [80, 81] to create survival estimations for Western bat populations currently unaffected by *Pd*.

Winter hibernation duration is a key determinate of the overwintering survival of any hibernating species. While local variation in winter onset due to unique landscape features may create refugia where bats may persist later than or emerge from hibernation earlier than average, the lack of any previous broad scale estimations for this critical parameter highlights the need for this study. Prior work ([96, 108]) has defined the duration of winter hibernation period *a priori* as the yearly number of nights with an average temperature below freezing. Our results suggest that significant improvements in predictive ability can be made by including elevation (*DEM*), northing (*Northing*), and the number of days in frost per year ($Days_{frost}$). Selection of the number of $Days_{frost}$ rather than $Days_{freeze}$ suggest that there is more nuance to the relationship between bats and low (but not freezing) temperatures than currently understood. The counter-intuitive coefficients for both the *Northing* and *DEM* terms are potentially due in part by the over-representation of Canadian data, low elevation sites, and the inherent co-linearity of these two variables. Notably, when included alone, the coefficients signs regress as expected; yet the models do not predict winter hibernation duration as well and had higher AIC scores. Hibernation duration estimates from the western US were rare, especially at southern latitudes, and this likely impacted model results in unpredictable ways and highlights the need for additional data collection.

Species such as *M. lucifugus* likely do not hibernate across their broad summer distribution, but rather seek out locations where more favorable conditions exist to overwinter. The maximum winter hibernation duration that was predicted within the distribution of *M. lucifugus* is a month longer than the longest observation within our dataset. In all probability, this does not likely represent an area where bats would over winter for multiple of reasons. First, while our survival models predict that an uninfected bat could survive the duration of hibernation at the examined microclimatic conditions, those sets of conditions may not exist on the landscape especially within the extreme Northern portions of the species' distribution [143]. Second, and perhaps more importantly, reducing the summer active period to <100 days creates significant challenges to the success of the next generation. With a gestation period of 60 days [125, 167], a female bat would be hard pressed to gestate, nurse, and wean young, while still providing adequate time for the young of the year to fatten sufficiently to survive such an extended hibernation period. Theoretically, these bats could break thermal conformation of hibernation and return to euthermia prior to the conclusion of the predicted duration of hibernation, however this would be extremely energy intensive. These results highlight the fact that only a subset of summer distributions may be suitable for overwinter survival.

Localized clines in body size and body mass of *M. lucifugus* have been recorded and published before [126], yet no continental scale model exists. Model selection suggests that variation in the duration of winter hibernation may be driving variation in both body size and body fat stores across the landscape. The positive relationship between both *Northing* and the Day_{freeze} may also suggest stronger selection pressure for larger bats in more extreme conditions. While still useful the relationship between the selected abiotic variables and body mass of bats was not as strong as the relationship between the spatial covariates and winter hibernation duration, suggesting additional continental scale drivers or local determinants not investigated in this study are truly driving the relationship.

The scaling identified in this study between pre-hibernation fat stores and body mass is a significant departure from the fixed 30% value used in previous studies [96, 108], and is supported by contemporary findings [43]. More localized relationships likely exist, yet without increased data resolution drivers of the true relationship may remain difficult to assess. Our model constantly predicted uninfected bats exiting hibernation with fat stores greater than those required to survive the

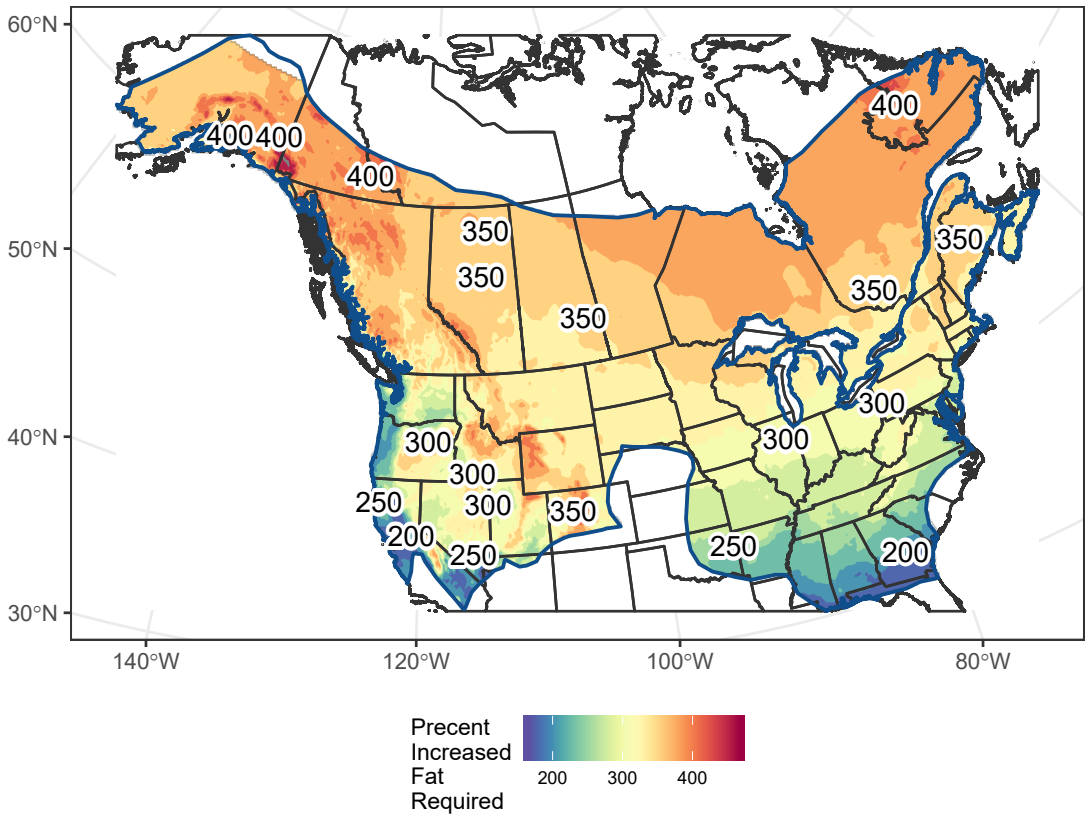


Fig. 4.5 **Percent increase in predicted amount of fat stores required for *Myotis lucifugus* to survive hibernation when infected with *Pseudogymnascus destructans*.** Hibernation was assumed to occur in a steady state with microclimatic conditions of 4°C and 98% relative humidity.

total duration of winter (if one assumes a stead state torpor). These residual fat stores may be retained as a buffer, and allow emergent females leaving hibernation sites before the complete cessation of winter conditions to begin their summer reproductive cycle [111]. This early departure would provide a significant selective advantage to the young of the year as even an extra week or two foraging on the landscape could increase fat stores, making them more likely to survive their first hibernation [195]. Additionally, the absolute reliance of bats solely upon pre-hibernation fat stores for overwinter survival is tenuous, as some bats (primarily within southern hibernacula) have been known to forage over winter to supplement food or water intake [215].

Within both micro-hibernaculum conditions examined, all uninfected *M. lucifugus* were capable of surviving the estimated duration of winter. These results confirm previous work as observed rates of survival among uninfected overwintering bats is high [28] and suggests that bats are likely capable of overwintering across most of their summer distribution where as long as suitable microclimates hibernacula exist. These results are a notable improvement, for previous model iterations had predicted overwinter demise of uninfected bats in regions with long winters exceeding six months [96]; although it must be noted that within that previous framework, microclimatic space was derived from surface metrics which were more energetically costly and a significant departure from the "optimal" conditions used within this work. The use of static hibernation is more biologically relevant for species like *M. lucifugus* that preferentially selects conditions around our chosen parameter values and especially within areas where maximal duration of hibernation is needed [215]. The selection of steady state conditions does have its limitations however. More than likely, bats may drift in and out of "optimal" hibernation conditions as hibernaticula conditions change throughout the duration of winter. Even relatively small changes in microclimatic values can vary the rate of fat consumption as highlighted by the differences in our two uninfected model results.

At $Ta = 4\circ$C and $RH = 98\%$ and when considering infection with Pd, modeled survival predictions did not match observations from the eastern United States where mass mortality events have occurred among infected bats [26, 66, 67]. Despite this, our analysis predicted a dramatic increase of energy expenditure to survive the duration of winter hibernation yet >75% of all cells in the analysis predicted a residual >0.8g of body fat remaining. Even when considering hibernation at the more fungal permissive conditions of model prediction made for $Ta = 2\circ$C and $RH = 100\%$ most bats were not

predicted to exhaust fat supplies before the end of winter hibernation but instead were at or around the point of fat exhaustion. As of yet little is know about the energetic demands of the emergent bats as they return to the landscape and accurate parameterization of this factor could significantly change our definition of survival capacity.

During the peak of WNS declines, bats were observed leaving hibernacula emaciated. Due to individual variance in deposition of pre-winter fat stores, and over-winter microclimate selection our model can not exclude this outcome but rather the "average" bat is not likely to experience. When comparing these results to Western bat populations that have not yet experienced large scale infection, predicted *Surv* values were further reduced with large geographical regions at or below the 0 g threshold suggesting that the impacts of WNS may be severe.

Model results are sensitive to a number of parameters (see Haase *et al.*, [82]), and our group has identified three key areas for work going forward. First, we found that microclimates of hibernaculum were important to survival predictions. While hibernation in a cooler and more saturated environment reduces fat consumption due to decreased rates of evaporative water loss, and subsequent longer torpor bout duration, the inclusion of fungal growth dynamics can mean that these regions may become ecological traps as fungal growth is accelerated in saturated environments, presumptively increasing fungal load and associated pathology. Despite this, hibernation in more arid zones could increase the frequency of torpor bout arousals, which is one of the proposed mechanisms of mortality [237] and so determining where and exactly how long bats are spending in specific sets of microclimatic conditions is vital to predicting total overwinter survival. Secondly, bouts of arousal account for > 90% of total energy expended during the hibernation period, and thus variation in the period of time spent euthermic has a large impact on survival predictions. For this work, we used estimations from a single study (C. Lausen, *personal Communication*). Data for this parameter is sparse and neither intra-hibernation nor spatial variation were taken into account; and there is also no data yet available on how *Pd* influences arousal duration. Additional data collection, and the refinement of technology with which to collect this data will be paramount to understanding this energy intensive component of hibernation physiology. Finally, as previously mentioned, better understanding of the metabolic demands on emergent bats is critical to understanding not only what it takes to make it through the the winter, but also what challenges remain on the other side.

While large scale population declines are a severe threat to the conservation of *M. lucifugus* and hibernating bats in general, some hope has been found in Eastern populations. Recently, populations that initially suffered declines >50% have begun to rebound [67, 128]. Cheng *et al.* [43] demonstrated that early winter fat stores were significantly higher when sampled post-WNS in 2016 than in 2009, when the infection was absent, by an average of 0.7g. The results from our survival model suggest that the majority of bats predicted to suffer mortality from WNS due to a fat store insufficiency by <0.5g, and a similar increase in fat stores as observed in Eastern populations may be sufficient to tolerate *Pd* infection at most Western locations. These field observations and my results suggest that if populations survive, the selection pressure for bats able to store more fat may be strong.

Chapter 5

Discussion and concluding remarks

5.1 General discussion

5.1.1 Future global emerging infectious disease challenges

The increase in the global pattern of EID occurrence [113] remains a unique public health challenge that will likely only increase as time progresses. In addition to issues relating to emerging infections through increased antimicrobial resistance [245], increased conversion of natural lands, especially primary forests and wetlands, into agricultural and pastoral systems has already facilitated the spillover of a number of high consequence pathogens including Nipah and Hendra viruses [57]. Deforestation and forest fragmentation of the worlds most biodiverese regions will ultimately result in the expatriation and extinction of untold species and an increased risk of zoonotic spillover into human populations from known and unknown pathogens alike during the process [241, 198]. Loss of native biodiversity has been observed to increase the incidence of zoonotic spillover although meta analysis has suggested that this relationship is system specific [201]. Socioeconomic, infrastructural and public heath disparities leave the most vulnerable human communities to act as sentinels for infection at the peridomestic interface [27]. Even within our ever growing urban areas, anthropogenic adapted species and vectors such as *Rattus norvegicus* and *Aedes albopictus* continue to maintain and spread infection [31].

The progression of global climate change is likely to only exacerbate these events. Natural disasters, particularly flooding events, increase incidences of waterborne enteric pathogens and

mosquito-borne disease to communities already in distress due population displacement and unstable sanitation infrastructure [238]. Additionally, shifting thermal patterns have the capacity to alter species distributions effectively opening new regions to the threat of previously absent infectious agents and vectors [3, 153]. Alterations in seasonal patterns brought about by shifting environmental queues may function to bring together novel host species combinations [153]. Even within endemic regions prolonged warm seasons can result in additional generations of reservoir and vector species and extended environmental persistence of infectious agents, leading to increased pathogen pressure across the landscape [3].

5.1.2 One Heath

The interconnectedness between the environmental drivers of infection and health outcomes has lead to the adoptions of various iterations of the One Health framework, acknowledging the inextricable links between environmental, animal and human health [246]. By recognizing the interrelated aspects of health, academics and health workers of all flavors can leverage multiple data streams to develop and implement novel approaches to address infectious disease threats. Identification of occupational risks in facilitating the transmission to the rest of population has been seen within a variety of system. Notable applications of such applications include the identification of livestock as a necessary component linking the transmission of African trypanosomes between sylvatic maintenance hosts and humans [69]. Additionally, date palm sap collectors have been identified to be at high risk for Nipah virus spillover [139], and worker education and surveillance of palm sap worker heath can help prevent transmission to the broader community via infectious food. The One Health framework provides a powerful platform across which the drivers of infection and disease can be identified and preventative measures implemented [138]. Yet, detailed system knowledge is generally required to define the magnitude of hypothesized relationships.

5.1.3 Data challenges

In the so called age of ‘big data’, the main challenge in disease ecology and EID studies, as in many branches of ecology, is the availability of data. The type, quantity, and quality of data available to the research team will define much of what analyses can be carried out, and what conclusions

can be drawn from them and as the aphorism goes, "all models are wrong but some are useful." Specifically within the field of disease ecology one of the primary challenges is the observational unit itself which can present notable challenges. While some infections present pathognomonicly, others have non-specific clinical presentations or non-symptomatic cases which can result in delayed, or misdiagnoses. Notably, observed global patterns of disease emergence may not represent the true diversity of events occurring, especially in regions where health, and/or education resources are low. Within these areas even symptomatic cases may not be detected due to poor surveillance systems resulting in the loss of valuable data and insufficient health interventions [74]. Observational data is the most obvious problem, yet the lack of data on true absences also represents a distinct challenge. Negative results are rarely published in that context, especially for ecological surveys. For example, no data was published on the lack of bats giving birth at locations, but rather only when they were and, as a result, we could infer with some confidence the absence of birthing events at these times and locations. In contrast, within the ebolavirus modeling, low outbreak numbers and a large spatial extent required us to make the assumption that our detection of spillover events was perfect. This can not be true, especially in the case of the non-reservoir spillover hosts where dense biodiverse forests can block direct observation, as recent modeling efforts have shown [74].

5.1.4 Model guided fieldwork

The ideas of model guided fieldwork (MGF) and iterative model development provide a conceptual framework for the integration of diverse data streams within biological systems [194]. Preliminary model development and associated parameter estimation from published values invariably identify gaps in system understanding. By targeting these gaps, and attempting to fill them with explicit mechanistic relationships, validated through fieldwork or experimentation, multidisciplinary research groups can rapidly generate and test hypotheses with limited resources [194]. Continued cyclical development under this methodology was paramount to this dissertation, providing much of the impetus for this research, and actionable next steps for the results obtained within.

While the challenges of case diagnosis may be unique to the epidemiology and disease ecology disciplines, incorporating appropriate covariate data and adequate parameterization of system unknowns are persistent challenges for all ecologists. As progressive leaps are made in remote sensing

and environmental sciences the number, extent, and resolution of available potential environmental covariate has increased dramatically. Accordingly, researchers, especially those within the early model development and hypothesis generation phases need to carefully consider the biological, and ideally mechanistic relationship between the system and modeled phenomenon [159, 194, 88]. A committed and systematic approach to these critical points helps to avoid spurious correlations, limits the number of alternative models that need to be built, and creates an infrastructure within which model assumptions and parameters can be systematically challenged and refined as new data become available. Despite this, even in with the best intentions, early stage parameterization of ecological processes is challenging, relying on access to literature and data spread across academic journals, public, and gray literature across the globe. Gathering comparable data sets describing instraspecific variation between free living animals was a particular challenge through out the entirety of these research project. The decision of what data is comparable, and what simplifications are necessary, must be made by the modeling and 'field' teams, as these early choices can limit what conclusions may be drawn from results.

5.1.4.1 Model guided fieldwork in this project

Spatial and temporally defined models of habitat suitability for bat birthing were created to add additional dimensionality to an existing one dimension study of trait variations across latitude, and retained many of the simplifying assumptions [50]. These results were then used together with all available system knowledge to test the potential reservoir capacity of African fruit bats in chapter 3, thus, continuing the testing of a hypothesis mathematically proposed within Hayman in 2015 [93]. Field researchers are beginning to use these findings to inform their field studies and test these hypotheses further (Hayman, *pers. communication*). The final research chapter of this dissertation represents the most complete example of the iterative model design and MGF philosophies. The original publication by Hayman *et al.,* 2016 [96] demonstrated the predictive power of a mechanistic model of hibernation physiology parameterized with species specific values in predicting the disease outcome for bats suffering from WNS. Sensitivity analysis suggested substantial improvements to predictive models could be made by refining the models use of physiological relationships, adding in spatial variation of host traits and improving estimates of species specific metabolic parameters. To

achieve this, this model became the central focus for a multi-year international collaboration. Within this team, fieldwork was performed and data collected to create species-specific metabolic estimates and model performance was improved through the addition of better, data-driven estimations of energy expenditure during the warming and cooling periods of arousal events [80], and the incorporation of evaporative water loss as a mechanism to trigger arousals [81]. Both additions have significantly improved the individual, mechanistic energetics based component of the model, yet substantial challenges remained in scaling up these results to landscape level predictions. Accordingly, I worked to patch these gaps by reassessing the earlier estimates of winter duration and creating the first estimates for variation in host traits related to body mass and body composition prior to hibernation.

5.2 Chapter discussions

5.2.1 Chapter 2

The models developed within **Chapter 2: Spatial and temporal patterns of birth pulses among African bats** represent the first and only models so far to create a continuous predictions of habitat suitability for the birthing events of African bats defined across both space and time for sub-Saharan Africa. As a component of this, I have also created the most thorough and up-to-date database of African bat birth records for mainland Africa available. Data on these occurrences were spread over nearly a century's worth of ecological research across Africa and required the use of multiple academic databases, search methods, and access to academic journals obscured behind pay-walls. Despite these extensive searches, additional data likely remains untapped within gray literature or proprietary datasets.

Results from the bat birthing models were largely consistent with the previously published literature and also include novel prediction of a single period of habitat suitability about $\pm 10^{\circ}$N and a predicted refinement of the polyestrous/monoestrous further north then suggested by the original analysis [50]. My selection and use of an EMN structure to correlate landscape level phenology with birthing events may represent the first use of such techniques in the ecological literature. This technique allowed me to exploit the mechanistic relationship between food abundance and life history demands of the target species [16]. Additionally, the use of dimensional reduction for the covariates

allowed me to retain biologically relevant variables describing the seasonality of primary resources, while avoiding the inherent co-linearity of temporally explicit covariates.

Early project ideas included the generation of species, or genus level models for bat species, previously implicated in the transmission of ebolaviruses [84, 187], yet preliminary data collection efforts revealed this as an impossibility, and necessitated the use of taxonomic clustering instead. Even with the consolidation of records by taxonomic structure and the use of a recirculating year, per-month data availability required the use of a sliding two month window to achieve usable observation numbers for analysis. Future work will be required to ground truth model predictions and additional data is require to increase model resolution either taxonomically or temporally. Finally, the migratory or nomadic life styles of African bat species were not explicitly considered within this work, yet this nature of detailed system knowledge may be required to fully address intra-taxon variation within the predicted birth pulses.

5.3 Chapter 3

The development of spatially and temporally explicate models to describe the birthing patterns of African bats was paramount to the central hypothesis of **Chapter 3: Predicting Ebola virus disease risk and the role of African bat birthing**. Within this work I successfully tested the hypothesis that African fruit bats, and bi-annually birthing species in particular, are involved in the sylvatic maintenance and spillover of pathogenic ebolaviruses. Our model results reveal that the inclusion of model terms describing bat birthing events improve predictive models of relative risk for both non-reservoir spillover hosts and humans. Additionally, within the human model, when birthing terms were separated by taxon, the use of a down-weighted African fruit bat term (designed to account for the existence of both monoestrous and polyestrous species) improved overall predictive power. While this is no smoking gun in the search for the maintenance reservoir host for ebolaviruses, this is another piece of evidence implicating some species of fruit bat as reservoir hosts(s). Furthermore, this research also provides support for the hypothesis proposed within Hayman 2015 [93] that the the bi-annual birthing of potential host species may be needed to refresh susceptible populations when accounting for acute viremic periods and lower community sizes then those observed for R

aegypticus and the MARV system. The temporal lag terms offsetting predicted births and spillover events are consistent with currently hypothesized mechanisms of MARV spillover (and hypothesized to be shared by ebolaviruses) and include the potential for maternally derived antibody hypothesis. Finally, the identification of a non-molossid microbat related term as significant within the top model suggests that these bat species may play an unrecognized role in ebolavirus maintenance or spillover, especially in light of the description of a punitive new viral species isolated from a non-molossid microbat host by Goldstien *et al.* [75].

Other significant terms identified by this work are largely consistent with existing spillover theory. Local bat diversity was identified as significant within both non-reservoir host and human spillover models (D_{afb} & D_{total}) respectively). Sympatry of bat hosts was identified by Luis *et al.,* [141] as a potential contributor to why bats have a higher viral diversity per-species then rodents. The diversity of non-volant mammals was also identified to be positively correlated with spillover risk in both models, consistent with the concept that pathogens like ebolaviruses often originate within dense, biodiverse regions [241]. This conclusion is further supported by negative correlations with human population density and relative spillover risk although it was only statistically significant in the non-reservoir spillover host model. Finally, our model was proven sensitive to the occurrence of infectious chains from the reservoir host, into a non-volant mammal, and into people by the significance of animal outbreak terms describing spillover events within the non-reservoir host populations the month of, or month preceding a human spillover events.

Relative risk of spillover for both non-reservoir spillover hosts and humans both showed strong seasonal variation in risk and provide the best evidence of seasonality within the ebolavirus system to date. At both locations of human ebolavirus outbreak events in 2018 spillover events likely occurred at, or near local maximums of relative spillover risk. The location of the first outbreak in 2018 (Bikoro, DRC) showed a high degree of seasonality of risk throughout the year. The second location, Beni also displayed predicted seasonality in relative risk, yet also provides evidence towards the existence of persistently at risk locations for ebolavirus spillover. The use of our birth pulse modeling to describe this seasonality of risk is the first of its kind in the field to link seasonality, and a biologically relevant mechanism rather then a purely correlative relationship with environmental covariates [188, 204].

Ultimately, much like chapter 2, results will require ground truthing with field data, yet these results can be used to develop targeted surveillance by indicating locations, times, and species for further investigation. While the use of a recirculation year was necessary to achieve usable data levels, this simplification discounts the potential impacts that inner annual variation, and particularly climatic abnormalities and ecological changes may act as a driver for viral spillover. Short term resource shortages may drive traditionally dispersed populations to localized refugia where resources are concentrated and increasing the potential for infectious transmission. Alternatively, nutritional stress may result in the down regulation of immune function leading to intermittent shedding of infection among chronically infected hosts. Lastly, this work also addresses issues relating to the role bats and other species play as necessary and sufficient hosts for multi-host reservoir communities for pathogens and their role in EVD emergence [197, 69, 164].

5.4 Chapter 4

Previous iterations of the winter energetics and WNS model incorporated spatial heterogeneity of the duration of winter for bats, however this was made *a priori* and never properly investigated within a systematic framework [108, 96]. Additionally, the spatial heterogeneity of body mass and associated body fat had never been described on a species distribution scale, despite the importance to overwinter survival and disease outcome as described by sensitivity analysis within [96, 80, 81]. We hypothesized that by creating improved estimates of these parameters we would be able to increase predictive performance of our hibernation energetics model for both uninfected and *Pd* infected hibernating *Myotis lucifugus*.

By collecting all available data from the literature, public databases, local researchers, and our own fieldwork we were able to better define these high impact parameters. I was able to create a more biologically relevant definition of the duration of winter with predictive capabilities far out stripping those used within the original work [96]. We were also able to create the first species distribution estimates of pre-hibernation body mass for *M. lucifugus*, which when combined with an allometric scaling relationship model, we were able to provide estimates for the fat stores available to bats for the overwinter period. The use of these two improved spatially defined estimations, along with

our improved hibernation energetics model showed major improvements in survival capacity for uninfected bats, more consistent with field observations. While model predictions for infected bats in North America suggest a narrow window of survival for *Myotis lucifugus*, results suggests relatively small short falls in the energy required to survive winter while infected over currently available fat stores.

Similar to all the other chapters, models results for the duration of hibernation, pre-hibernation body mass, fat stores, and the allometric relationship between body mass and fat will need to undergo continued field validation. Each of these parameters likely vary between species, yet species specific estimations of each is unlikely due to the deficiency in data. Even for *M. lucifugus*, one of the most studied species in North America, data was extremely limited, required significant effort to compile, and resulted in wide confidence bounds. Within the survival modeling component, I used narrow range of microclimate parameter values within the hibernation parameter space, using only two sets of temperature and relative humidity values as *M. lucifugus* appears to have a rather narrow range in microhabitat selection [215]. This assumption will likely not be as valid for other species that select more dynamic hibernacula [68] any will lead to more difficult applications to the landscape. Within the simplified hibernacula conditions, *M. lucifugus* were predicted be capable of surviving the predicted durations of winter hibernation. Despite this, it is likely that these specific hibernacula conditions may not be contained within the areas and consequently there may be regions within this distribution where *M. lucifugus* do not overwinter but rather use some nature of local or regional migration to reach more favorable hibernation conditions. Continued research into the fundamental ecology of these bats is required to fully describe this. This chapter, is a significant advance in how we can use individual, mechanistic physiological models to better understand both possible disease outcomes and the likely changes to a realized niche for hosts in the presence of a disease.

5.5 Concluding remarks

5.5.1 Space and time

Overall, a common theme to this thesis is the development of models to understand spatio-temporal processes relating to bats and emerging infectious diseases. In the absence of rich data sets, such as

human measles in the United Kingdom [77], I used a range of statistical approaches to fill gaps in the data while at the same time aiming to use the results of these to inform models that either tested hypotheses regarding mechanisms, such as the relationship between bat birthing and EVD outbreaks, or had mechanistic models embedded within them, such as WNS in bats. Moreover, each of these has some temporal forcing, whether seasonal bat birthing or torpor-arousal bouts nested within the annual overwinter hibernation. It seems necessary to incorporate these processes if we are to make significant advances in our understanding of wildlife infectious disease ecology [2].

5.5.2 The special place for bats in disease ecology

Bats occupy a special place in disease ecology as one of the most biodiverse and widely distributed mammalian taxa. The propensity of some gregarious species to form large dense roosting clusters provides for pathogen permissive environments where multiple pathogens and pathogen strains may be maintained and spillover into novel hosts if circumstances are right [204, 192]. Bats host more zoonotic pathogens per species than other mammalian hosts [141, 171], including many high impact pathogens [79, 134] and are the proposed reservoir host for ebolaviruses. The evolution of flight and a unique metabolic pathways have allowed bats to remain remarkably resistant or tolerant in the face of viral invasion [33, 173], mounting rapid immunizing responses to infections or perhaps tolerating infections that prove fatal in most other mammals [210, 5, 91]. Historically, few mass mortality events for bats have been recorded with most attributed to anthropogenic causes (e.g. wind farms, pest control, or bush meat) yet a cold dwelling fungus has caused the greatest decline in bat populations ever recorded [67]. It seems bats will be a fascinating and important group of animals for infectious disease researchers for the foreseeable future.

References

[1] Adam, J.-P. and Le Pont, F. (1974). Les chiroptères cavernicoles de la République Populaire du Congo : notes bioécologiques et parasitologiques. *Annales de Spéléologie*, 29(1):143–154.

[2] Altizer, S., Dobson, A., Hosseini, P., Hudson, P., Pascual, M., and Rohani, P. (2006). Seasonality and the dynamics of infectious diseases. *Ecology Letters*, 9(4):467–484.

[3] Altizer, S., Ostfeld, R. S., Johnson, P. T. J., Kutz, S., and Harvell, C. D. (2013). Climate change and infectious diseases: from evidence to a predictive framework. *Science (New York, N.Y.)*, 341(6145):514–9.

[4] Amman, B. R., Carroll, S. A., Reed, Z. D., Sealy, T. K., Balinandi, S., Swanepoel, R., Kemp, A., Erickson, B. R., Comer, J. A., Campbell, S., Cannon, D. L., Khristova, M. L., Atimnedi, P., Paddock, C. D., Kent Crockett, R. J., Flietstra, T. D., Warfield, K. L., Unfer, R., Katongole-Mbidde, E., Downing, R., Tappero, J. W., Zaki, S. R., Rollin, P. E., Ksiazek, T. G., Nichol, S. T., and Towner, J. S. (2012). Seasonal Pulses of Marburg Virus Circulation in Juvenile Rousettus aegyptiacus Bats Coincide with Periods of Increased Risk of Human Infection. *PLoS Pathogens*, 8(10).

[5] Amman, B. R., Jones, M. E. B., Sealy, T. K., Uebelhoer, L. S., Schuh, A. J., Bird, B. H., Coleman-McCray, J. D., Martin, B. E., Nichol, S. T., and Towner, J. S. (2015). ORAL SHEDDING OF MARBURG VIRUS IN EXPERIMENTALLY INFECTED EGYPTIAN FRUIT BATS (ROUSETTUS AEGYPTIACUS). *Journal of Wildlife Diseases*, 51(1):113–124.

[6] Anderson, J. and De Winton, W. E. (1902). *Zoology of Egypt: Mammalia*.

[7] Ansell, W. (1986). Some Chiroptera from south-central Africa. *Mammalia*, 50(4):507–520.

[8] Anthony, S. J., Epstein, J. H., Murray, K. A., Navarrete-Macias, I., Zambrana-Torrelio, C. M., Solovyov, A., Ojeda-Flores, R., Arrigo, N. C., Islam, A., Ali Khan, S., Hosseini, P., Bogich, T. L., Olival, K. J., Sanchez-Leon, M. D., Karesh, W. B., Goldstein, T., Luby, S. P., Morse, S. S., Mazet, J. A. K., Daszak, P., and Lipkin, W. I. (2013). A strategy to estimate unknown viral diversity in mammals. *mBio*, 4(5):e00598–13.

[9] Ayouba, A., Ahuka-Mundeke, S., Butel, C., Mbala Kingebeni, P., Loul, S., Tagg, N., Villabona-Arenas, C.-J., Lacroix, A., Ndimbo-Kumugo, S.-P., Keita, A. K., Toure, A., Couacy-Hymann, E., Calvignac-Spencer, S., Leendertz, F. H., Formenty, P., Delaporte, E., Muyembe-Tamfum, J.-J., Mpoudi Ngole, E., and Peeters, M. (2019). Extensive Serological Survey of Multiple African Nonhuman Primate Species Reveals Low Prevalence of Immunoglobulin G Antibodies to 4 Ebola Virus Species. *The Journal of Infectious Diseases*, (Xx Xxxx):1–10.

[10] Barclay, R. M. (1985). Foraging behaviour of the African insectivorous bat, Scotophilus leucogastere. *Biotropica*, 17:65–70.

[11] Barry, A., Ahuka-Mundeke, S., Ali Ahmed, Y., Allarangar, Y., Anoko, J., Archer, B. N., Aruna Abedi, A., Bagaria, J., Belizaire, M. R. D., Bhatia, S., Bokenge, T., Bruni, E., Cori, A., Dabire, E.,

Diallo, A. M., Diallo, B., Donnelly, C. A., Dorigatti, I., Dorji, T. C., Escobar Corado Waeber, A. R., Fall, I. S., Ferguson, N. M., FitzJohn, R. G., Folefack Tengomo, G. L., Formenty, P. B. H., Forna, A., Fortin, A., Garske, T., Gaythorpe, K. A., Gurry, C., Hamblion, E., Harouna Djingarey, M., Haskew, C., Hugonnet, S. A. L., Imai, N., Impouma, B., Kabongo, G., Kalenga, O. I., Kibangou, E., Lee, T. M. H., Lukoya, C. O., Ly, O., Makiala-Mandanda, S., Mamba, A., Mbala-Kingebeni, P., Mboussou, F. F. R., Mlanda, T., Mondonge Makuma, V., Morgan, O., Mujinga Mulumba, A., Mukadi Kakoni, P., Mukadi-Bamuleka, D., Muyembe, J. J., Bathé, N. T., Ndumbi Ngamala, P., Ngom, R., Ngoy, G., Nouvellet, P., Nsio, J., Ousman, K. B., Peron, E., Polonsky, J. A., Ryan, M. J., Touré, A., Towner, R., Tshapenda, G., Van De Weerdt, R., Van Kerkhove, M., Wendland, A., Yao, N. K. M., Yoti, Z., Yuma, E., Kalambayi Kabamba, G., Lukwesa Mwati, J. d. D., Mbuy, G., Lubula, L., Mutombo, A., Mavila, O., Lay, Y., and Kitenge, E. (2018). Outbreak of Ebola virus disease in the Democratic Republic of the Congo, April–May, 2018: an epidemiological study. *The Lancet*.

[12] Bell, G. P., Bartholomew, G. A., and Nagy, K. A. (1986). The roles of energetics, water economy, foraging behavior, and geothermal refugia in the distribution of the bat, Macrotus californicus. *Journal of Comparative Physiology B*, 156(3):441–450.

[13] Bergmans, W. (1976). A revision of the African genus Myonycteris Matschie, 1899 (Mammalia, Megachiroptera). *Beaufortia*, 24(317):189–216.

[14] Bergmans, W. (1979). Taxonomy and Zoogeography of the fruit bats of the peoples republic of Congo, with Notes on their reporductive biology. *Bijdragen tot de Dierkunde*, 48:161–186.

[15] Bernard, R. (1980). Reproductive cycles of Miniopterus schreibersi natalensis (Kuhl, 1819) and Miniopterus fraterculus Thomas and Swann, 1906. *Annals of the Transvaal Museum*, 32(3):55–64.

[16] Bernard, R. and Cumming, G. (1997). African Bats: Evolution of Reproductive Patterns and Delays. *The Quarterly Review of Biology*, 72(3):253–274.

[17] Bernard, R. and Meester, J. (1982). Female reproduction an dthe female reproductive cycle of Hipposideros caffer caffer in Natal, South Africa. *Annals of the Transvaal Museum*, 33(8):131–144.

[18] Bernard, R. F., Willcox, E. V., Parise, K. L., Foster, J. T., and McCracken, G. F. (2017). White-nose syndrome fungus, Pseudogymnoascus destructans, on bats captured emerging from caves during winter in the southeastern United States. *BMC Zoology*, 2(1):1–11.

[19] Bernard, R. T. and Bojarski, C. (1994). Effects of prolactin and hCG treatment on luteal activity and the conceptus during delayed implantation in Schreibers' long-fingered bat (Miniopterus schreibersii). *Journal of reproduction and fertility*, 100(2):359–65.

[20] Bernard, R. T. F. (1981). Monthly changes in the female reproductive organs and the reproductive cycle of Myotis tricolor (Vespertilionidae : Chiroptera). *South African Journal of Zoology*, 17(2):79–84.

[21] Bernard, R. T. F. (1983). Reproduction of Rhinolophus clivosus (Microchiroptera) in Natal, South Africa. *Z. Saugetierkunde*, 48(6):321–329.

[22] Bernard, R. T. F., Cotterill, F. P. D., and Fergusson, R. A. (1996). On the occurance of a short period of delayed implantation in Schreibers' long-fingered bat (Miniopterus schreibersii) from a tropical latitude in Zimbabwe. *Journal of Zoology, London*, 238:13–22.

[23] Bernard, R. T. F. and Tsita, J. N. (1995). Seasonally monoestrous reproduction in the molossid bat, Tadarida aegyptiaca from low temperate... *South African Journal of Zoology*, 30(1):18.

[24] Biek, R., Walsh, P. D., Leroy, E. M., and Real, L. A. (2006). Recent common ancestry of Ebola Zaire virus found in a bat reservoir. *PLoS Pathogens*, 2(10):0885–0886.

[25] Bivand, R., Keitt, T., and Rowlinson, B. (2017). rgdal: Bindings for the Geospatial Data Abstraction Library.

[26] Blehert, D. S., Hicks, A. C., Behr, M., Meteyer, C. U., Berlowski-Zier, B. M., Buckles, E. L., Coleman, J. T. H., Darling, S. R., Gargas, A., Niver, R., Okoniewski, J. C., Rudd, R. J., and Stone, W. B. (2009). Bat White-Nose Syndrome: An Emerging Fungal Pathogen? *Science*, 323(5911):227–227.

[27] Bloomfield, S. F. and Kumar, J. N. (2006). Home Hygiene in Developing Countries Prevention of infection in the home and the peri-domestic setting. Technical report.

[28] Boyles, J. G. and Brack, V. (2009). Modeling Survival Rates of Hibernating Mammals with Individual-Based Models of Energy Expenditure. *Journal of Mammalogy*, 90(1):9–16.

[29] Boyles, J. G., Dunbar, M. B., Storm, J. J., and Brack, V. (2007). Energy availability influences microclimate selection of hibernating bats. *Journal of Experimental Biology*, 210(24):4345–4350.

[30] Bradbury, J. W. (2010). Lek Mating Behavior in the Hammer-headed Bat. *Zeitschrift für Tierpsychologie*, 45(3):225–255.

[31] Bradley, C. A. and Altizer, S. (2007). Urbanization and the ecology of wildlife diseases. *Trends in Ecology and Evolution*, 22(2):95–102.

[32] Briand, S., Bertherat, E., Cox, P., Formenty, P., Kieny, M.-P., Myhre, J. K., Roth, C., Shindo, N., and Dye, C. (2014). The International Ebola Emergency. *New England Journal of Medicine*, 371(13):1180–1183.

[33] Brook, C. E. and Dobson, A. P. (2015). Bats as 'special' reservoirs for emerging zoonotic pathogens. *Trends in Microbiology*, 23(3):172–180.

[34] Brosset, A. (1966). *La biologie des chiropteres*. Masson and Company, Paris.

[35] Brosset, A. (1969). *La vie sociale des oiseaux dans une foret equitoriale du Gabon*.

[36] Brown, J. H., Gillooly, J. F. M., Allen, A. P., Savage, V. M., and West, G. B. (2004). Toward a metabolic theory of ecology. *Ecology*, 85(7):1771–1789.

[37] Brown, V. L., Drake, J. M., Stallknecht, D. E., Brown, J. D., Pedersen, K., and Rohani, P. (2013). Dissecting a wildlife disease hotspot: the impact of multiple host species, environmental transmission and seasonality in migration, breeding and mortality. *Journal of the Royal Society, Interface*, 10(79):20120804.

[38] Buceta, J. and Johnson, K. (2017). Modeling the Ebola zoonotic dynamics: Interplay between enviroclimatic factors and bat ecology. *PLoS ONE*, 12(6):1–14.

[39] Campbell, G. L., Marfin, A. A., Lanciotti, R. S., and Gubler, D. J. (2002). West Nile virus. *The Lancet Infectious Diseases*, 2(9):519–529.

[40] Carey, C. (1993). Why do hibernators periodically arouse? overview. In *Life in teh Cold: Ecological, Physiological and Molecular Mechanism*, pages 25–34. Westview, Boulder, Co.

[41] Chamberlain, S. A. and Szöcs, E. (2013). taxize: taxonomic search and retrieval in R. *F1000Research*, 191:1–28.

[42] Chaturvedi, V., Springer, D. J., Behr, M. J., Ramani, R., Li, X., Peck, M. K., Ren, P., Bopp, D. J., Wood, B., Samsonoff, W. A., Butchkoski, C. M., Hicks, A. C., Stone, W. B., Rudd, R. J., and Chaturvedi, S. (2010). Morphological and molecular characterizations of psychrophilic fungus Geomyces destructans from New York bats with white nose syndrome (WNS). *PLoS ONE*, 5(5).

[43] Cheng, T. L., Gerson, A., Moore, M. S., Reichard, J. D., DeSimone, J., Willis, C. K., Frick, W. F., and Kilpatrick, A. M. (2019). Higher fat stores contribute to persistence of little brown bat populations with white-nose syndrome. *Journal of Animal Ecology*, 88(4):591–600.

[44] (CIESIN), C. f. I. E. S. I. N., University, C., FAO, U. N. F., Programme, A., and (CIAT), C. I. d. A. T. (2005). Gridded Population of the World, Version 3 (GPWv3): Population Count Grid.

[45] Coe, M. (1975). Mammalian ecological studies on Mount Nimbia, Liberia. *Mammalia*, 39(4).

[46] Cohn, S. and Kutalek, R. (2016). Historical Parallels, Ebola Virus Disease and Cholera: Understanding Community Distrust and Social Violence with Epidemics. *PLoS Currents*.

[47] Cotterill, F. P. D. (1998). Female Reproduction in Two Species of Tropical Horseshoe Bats (Rhinolophidae) in Zimbabwe. *Journal of Mammalogy*, 79(4):1306–1316.

[48] Cotterill, F. P. D. and Fergusson, R. A. (1993). Seasonally Polyestrous Reproduction in a Free-Tailed Bat Tadarida fulminans (Microchiroptera: Molossidae) in Zimbabwe. *Biotropica VO - 25*, 25(4):487.

[49] Cotterill, F. P. D. and Fergusson, R. A. (1999). Reproductive ecology of Commerson's leaf-nosed bats Hipposidores commersoni (Chiroptera: Hipposideridae) in South-Central Africa: interactions between seasonality and large body size; and implications for conservation. *South African Journal of Zoology*, 34(2):53–63.

[50] Cumming, G. and Bernard, R. T. F. (1997). Rainfall, Food Abundance and Timing of Parturition in African Bats. *Oecologia*, 111(3):309–317.

[51] Czenze, Z. J., Park, A. D., and Willis, C. K. R. (2013). Staying cold through dinner: cold-climate bats rewarm with conspecifics but not sunset during hibernation. *Journal of Comparative Physiology B*, 183(6):859–866.

[52] De Nys, H. M., Kingebeni, P. M., Keita, A. K., Butel, C., Thaurignac, G., Villabona-Arenas, C.-J., Lemarcis, T., Geraerts, M., Vidal, N., Esteban, A., Bourgarel, M., Roger, F., Leendertz, F., Diallo, R., Ndimbo-Kumugo, S.-P., Nsio-Mbeta, J., Tagg, N., Koivogui, L., Toure, A., Delaporte, E., Ahuka-Mundeke, S., Tamfum, J.-J. M., Mpoudi-Ngole, E., Ayouba, A., and Peeters, M. (2018). Survey of Ebola Viruses in Frugivorous and Insectivorous Bats in Guinea, Cameroon, and the Democratic Republic of the Congo, 2015–2017. *Emerging Infectious Diseases*, 24(12).

[53] Drees, K. P., Lorch, J. M., Puechmaille, S. J., Parise, K. L., Wibbelt, G., Hoyt, J. R., Sun, K., Jargalsaikhan, A., Dalannast, M., Palmer, J. M., Lindner, D. L., Marm Kilpatrick, A., Pearson, T., Keim, P. S., Blehert, D. S., and Foster, J. T. (2017). Phylogenetics of a Fungal Invasion: Origins and Widespread Dispersal of White-Nose Syndrome. *mBio*, 8(6):1–15.

[54] Duke-Sylvester, S. M., Bolzoni, L., and Real, L. a. (2011). Strong seasonality produces spatial asynchrony in the outbreak of infectious diseases. *Journal of the Royal Society, Interface / the Royal Society*, 8(59):817–25.

[55] Elith, J., Phillips, S. J., Hastie, T., Dudík, M., Chee, Y. E., and Yates, C. J. (2011). A statistical explanation of MaxEnt for ecologists. *Diversity and Distributions*, 17(1):43–57.

[56] Epstein, J. H., Baker, M. L., Zambrana-Torrelio, C., Middleton, D., Barr, J. A., DuBovi, E., Boyd, V., Pope, B., Todd, S., Crameri, G., Walsh, A., Pelican, K., Fielder, M. D., Davies, A. J., Wang, L. F., and Daszak, P. (2013). Duration of Maternal Antibodies against Canine Distemper Virus and Hendra Virus in Pteropid Bats. *PLoS ONE*, 8(6):1–8.

[57] Faust, C. L., McCallum, H. I., Bloomfield, L. S. P., Gottdenker, N. L., Gillespie, T. R., Torney, C. J., Dobson, A. P., and Plowright, R. K. (2018). Pathogen spillover during land conversion. *Ecology Letters*, 21(4):471–483.

[58] Fayenuwo, J. O. and Halstead, L. B. (1974). Breeding Cycle of Straw-Colored Fruit Bat, Eidolon helvum, at Ile-Ife, Nigeria. *Journal of Mammalogy*, 55(2):453–454.

[59] Fenton, M., Rautenbach, I., Smith, S., Swanepoel, C., Grosell, J., and van Jaarsveld, J. (1994). Raptors and bats: threats and opportunities. *Animal Behaviour*, 48(1):9–18.

[60] Fenton, M. B., Cumming, D. H. M., Hutton, J. M., and Swanepoel, C. M. (1987). Foraging and habitat use by Nycteris grandis (Chiroptera: Nycteridae) in Zimbabwe. *Journal of Zoology*, 211(4):709–716.

[61] Fischer, R., Judson, S., Miazgowicz, K., Bushmaker, T., Prescott, J., and Munster, V. J. (2015). Ebola Virus Stability on Surfaces and in Fluids in Simulated Outbreak Environments. *Emerging Infectious Diseases*, 21(7):1243–1246.

[62] Fisher, M. C., Henk, D. A., Madoff, L. C., Brownstein, J. S., McCraw, S. L., Briggs, C. J., and Gurr, S. J. (2012). Emerging fungal threats to animal, plant and ecosystem health. *Nature*, 484(7393):186–194.

[63] French, A. R. (1985). Allometries of the durations of torpid and euthermic intervals during mammalian hibernation: A test of the theory of metabolic control of the timing of changes in body temperature. *Journal of Comparative Physiology B*, 156(1):13–19.

[64] Frick, S. and Hijmans, R. J. (2017). Worldclim 2: New 1-km spatial resolution climate surfaces for global land arease. *Internation Journal of Climatology*.

[65] Frick, W. F., Cheng, T. L., Langwig, K. E., Hoyt, J. R., Janicki, A. F., Parise, K. L., Foster, J. T., and Kilpatrick, A. M. (2017). Pathogen dynamics during invasion and establishment of white-nose syndrome explain mechanisms of host persistence. *Ecology*, 98(3):624–631.

[66] Frick, W. F., Pollock, J. F., Hicks, A. C., Langwig, K. E., Reynolds, D. S., Turner, G. G., Butchkoski, C. M., and Kunz, T. H. (2010). An emerging disease causes regional population collapse of a common North American bat species. *Science (New York, N.Y.)*, 329(5992):679–82.

[67] Frick, W. F., Puechmaille, S. J., Hoyt, J. R., Nickel, B. A., Langwig, K. E., Foster, J. T., Barlow, K. E., Bartoni??ka, T., Feller, D., Haarsma, A. J., Herzog, C., Hor????ek, I., van der Kooij, J., Mulkens, B., Petrov, B., Reynolds, R., Rodrigues, L., Stihler, C. W., Turner, G. G., and Kilpatrick, A. M. (2015). Disease alters macroecological patterns of North American bats. *Global Ecology and Biogeography*, 24(7):741–749.

[68] Fuller, N. W., Haase, C. G., Silas, K. A., Olson, S. H., and McGuire, L. P. (2019). Tradeoffs between energy conservation and the costs of torpor: hibernation of Myotis velifer at low latitudes. *Journal of Mammalogy*, Submitted.

[69] Funk, S., Nishiura, H., Heesterbeek, H., Edmunds, W. J., and Checchi, F. (2013). Identifying Transmission Cycles at the Human-Animal Interface: The Role of Animal Reservoirs in Maintaining Gambiense Human African Trypanosomiasis. *PLoS Computational Biology*, 9(1).

[70] Funmilayo, O. (1979). Ecology of the Straw-colored fruit bat Eidolon helvum in Nigeria. *Revue de Zoologie Africaine*, 93(3):589–600.

[71] Geiser, F. and Ruf, T. (1995). Hibernation versus Daily Torpor in Mammals and Birds: Physiological Variables and Classification of Torpor Patterns. *Physiological Zoology*, 68(6):935–966.

[72] Gilbert, A. T., Fooks, A. R., Hayman, D. T., Horton, D. L., Müller, T., Plowright, R., Peel, A. J., Bowen, R., Wood, J. L., Mills, J., Cunningham, A. A., and Rupprecht, C. E. (2013). Deciphering serology to understand the ecology of infectious diseases in wildlife. *EcoHealth*, 10(3):298–313.

[73] Glass, G. E., Shields, T., Cai, B., Yates, T. L., and Parmenter, R. (2007). Persistently highest risk areas for hantavirus pulmonary syndrome: potential sites for refugia. *Ecological applications : a publication of the Ecological Society of America*, 17(1):129–39.

[74] Glennon, E. E., Jephcott, F. L., Restif, O., and Wood, J. L. N. (2019). Estimating undetected Ebola spillovers. *PLOS Neglected Tropical Diseases*, 13(6):e0007428.

[75] Goldstein, T., Anthony, S. J., Gbakima, A., Bird, B. H., Bangura, J., Tremeau-Bravard, A., Belaganahalli, M. N., Wells, H. L., Dhanota, J. K., Liang, E., Grodus, M., Jangra, R. K., DeJesus, V. A., Lasso, G., Smith, B. R., Jambai, A., Kamara, B. O., Kamara, S., Bangura, W., Monagin, C., Shapira, S., Johnson, C. K., Saylors, K., Rubin, E. M., Chandran, K., Lipkin, W. I., and Mazet, J. A. K. (2018). The discovery of Bombali virus adds further support for bats as hosts of ebolaviruses. *Nature Microbiology*, page 1.

[76] Graham, M., Winter, A. K., Ferrari, M., Grenfell, B., Moss, W. J., Azman, A. S., Metcalf, C. J. E., and Lessler, J. (2019). Measles and the canonical path to elimination. *Science*, 364(6440):584–587.

[77] Grenfell, B. T., Bjørnstad, O. N., and Kappey, J. (2001). Travelling waves and spatial hierarchies in measels epidemics. *Nature*, 414(December):716–723.

[78] Guerra, F. M., Bolotin, S., Lim, G., Heffernan, J., Deeks, S. L., Li, Y., and Crowcroft, N. S. (2017). The basic reproduction number (R 0) of measles: a systematic review. *The Lancet Infectious Diseases*, 17(12):e420–e428.

[79] Guo, W.-P., Lin, X.-D., Wang, W., Tian, J.-H., Cong, M.-L., Zhang, H.-L., Wang, M.-R., Zhou, R.-H., Wang, J.-B., Li, M.-H., Xu, J., Holmes, E. C., and Zhang, Y.-Z. (2013). Phylogeny and origins of hantaviruses harbored by bats, insectivores, and rodents. *PLoS pathogens*, 9(2):e1003159.

[80] Haase, C. G., Fuller, N. W., Hranac, C. R., Hayman, D. T., Olson, S. H., Plowright, R. K., and McGuire, L. P. (2019a). Bats are not squirrels: Revisiting the cost of cooling in hibernating mammals. *Journal of Thermal Biology*, 81(January):185–193.

[81] Haase, C. G., Fuller, N. W., Hranac, C. R., Hayman, D. T. S., McGuire, L. P., Norquay, K. J. O., Silas, K. A., Willis, C. K., Plowright, R. K., and Olson, S. H. (2019b). Incorporating evaporative water loss into bioenergetic models of hibernation to test for relative influence of host and pathogen traits on white-nose syndrome. *PLoS Computational Biology*, In Review.

[82] Haase, C. G., Fuller, N. W., Hranac, C. R., Hayman, D. T. S., McGuire, L. P., Norquay, K. J. O., Silas, K. A., Willis, C. K. R., Plowright, R. K., and Olson, S. H. (2019c). Incorporating evaporative water loss into bioenergetic models of hibernation to test for relative influence of host and pathogen traits on white-nose syndrome. *PLOS ONE*, 14(10):e0222311.

[83] Haman, K. and Hibbard, C. (2016). Bat with white-nose syndrome confirmed in Washington state. Technical report, U.S. FISH AND WILDLIFE SERVICE.

[84] Han, B. A., Schmidt, J. P., Alexander, L. W., Bowden, S. E., Hayman, D. T. S., and Drake, J. M. (2016). Undiscovered Bat Hosts of Filoviruses. *PLoS Neglected Tropical Diseases*, 10(7):1–10.

[85] Happold, D. C. and Happold, M. (1989). Reproduction of Angola free-tailed bats (Tadarida condylura) and little free-tailed bats (Tadarida pumila) in Malawi (Central Africa) and elsewhere in Africa. *Journal of reproduction and fertility*, 85(1):133–149.

[86] Happold, D. C. D. and Happold, M. (1990). Reproductive strategies of bats in Africa. *Journal of Zoology*, 222(1990):557–583.

[87] Happold, M. and Happold, D. C. D. (2013). *Mammals of Africa Volume IV - Hedgehogs, Shrews and Bats*. Bloomsbury, London.

[88] Harrison, X. A., Donaldson, L., Correa-Cano, M. E., Evans, J., Fisher, D. N., Goodwin, C. E., Robinson, B. S., Hodgson, D. J., and Inger, R. (2018). A brief introduction to mixed effects modelling and multi-model inference in ecology. *PeerJ*, 6:e4794.

[89] Hassanin, A., Nesi, N., Marin, J., Kadjo, B., Pourrut, X., Leroy, É., Gembu, G.-C., Musaba Akawa, P., Ngoagouni, C., Nakouné, E., Ruedi, M., Tshikung, D., Pongombo Shongo, C., and Bonillo, C. (2016). Comparative phylogeography of African fruit bats (Chiroptera, Pteropodidae) provide new insights into the outbreak of Ebola virus disease in West Africa, 2014–2016. *Comptes Rendus Biologies*, pages 2014–2016.

[90] Haydon, D. T., Cleaveland, S., Taylor, L. H., and Laurenson, M. K. (2002). Identifying reservoirs of infection: A conceptual and practical challenge. *Emerging Infectious Diseases*, 8(12):1468–1473.

[91] Hayman, D. T. (2019a). Bat tolerance to viral infections. *Nature Microbiology*, 4(5):728–729.

[92] Hayman, D. T., Cryan, P. M., Fricker, P. D., and Dannemiller, N. G. (2017). Long-term video surveillance and automated analyses reveal arousal patterns in groups of hibernating bats. *Methods in Ecology and Evolution*, 8(12):1813–1821.

[93] Hayman, D. T. S. (2015). Biannual birth pulses allow filoviruses to persist in bat populations. *Proceedings of the Royal Society B: Biological Sciences*, 282(1803):20142591.

[94] Hayman, D. T. S. (2019b). African Primates: Likely Victims, Not Reservoirs, of Ebolaviruses. *The Journal of Infectious Diseases*, (Xx):1–4.

[95] Hayman, D. T. S., Emmerich, P., Yu, M., Wang, L. F., Suu-Ire, R., Fooks, A. R., Cunningham, A. A., and Wood, J. L. N. (2010). Long-term survival of an urban fruit bat seropositive for ebola and lagos bat viruses. *PLoS ONE*, 5(8):2008–2010.

[96] Hayman, D. T. S., Pulliam, J. R. C., Marshall, J. C., Cryan, P. M., and Webb, C. T. (2016). Environment, host, and fungal traits predict continental-scale white-nose syndrome in bats. *Science Advances*, 2(1):e1500831–e1500831.

[97] Hayman, D. T. S., Yu, M., Crameri, G., Wang, L.-F., Suu-Ire, R., Wood, J. L. N., and Cunningham, A. a. (2012). Ebola virus antibodies in fruit bats, ghana, west Africa. *Emerging infectious diseases*, 18(7):1207–9.

[98] Hennessen, W. (1971). Epidemiology of "Marburg Virus" Disease. In *Marburg Virus Disease*, pages 161–165. Springer Berlin Heidelberg, Berlin, Heidelberg.

[99] Herzig-Straschil, B. and Robinson, G. (1978). On the ecology of the fruit bat, rousettus aegyptiacus leachi (A. Smith, 1829) in the Tsitsikama Coastal National Park. *Koedoe*, 21(1):101–110.

[100] Heukelbach, J., Alencar, C. H., Kelvin, A. A., de Oliveira, W. K., and de Góes Cavalcanti, L. P. (2016). Zika virus outbreak in Brazil. *Journal of Infection in Developing Countries*, 10(2):116–120.

[101] Hijmans, R. J. (2016). raster: Geographic Data Analysis and Modeling. *R package version 2.5-8*.

[102] Hill, J. E. and Morris, P. (1971). Bats from Ethiopoa collected by the great Abbai Expedition. *Zoology*, 21(2):27–49.

[103] Hock, R. J. (1951). THE METABOLIC RATES AND BODY TEMPERATURES OF BATS. *The Biological Bulletin*, 101(3):289–299.

[104] Holm, S. (1978). Board of the Foundation of the Scandinavian Journal of Statistics A Simple Sequentially Rejective Multiple Test Procedure Author (s): Sture Holm Published by : Wiley on behalf of Board of the Foundation of the Scandinavian Journal of Statistics Stable U. *Scandinavian Journal of Statistics*, 6(2):65–70.

[105] Howell, K. (1976). *An ecological study of three species of insectivorous bats near Kisarawe, Tanzania*. PhD thesis, University of Dar es Salaam.

[106] Hoyt, J. R., Sun, K., Parise, K. L., Lu, G., Langwig, K. E., Jiang, T., Yang, S., Frick, W. F., Kilpatrick, A. M., Foster, J. T., and Feng, J. (2015). Widespread Bat White-Nose Syndrome Fungus, Northeastern China. *Emerging Infectious Diseases*, 22(1):140–142.

[107] Huete, A., Didan, K., Miura, T., Rodriguez, E., Gao, X., and Ferreira, L. (2002). Overview of the radiometric and biophysical performance of the MODIS vegetation indices. *Remote Sensing of the Environment*, 83(1-2):195–213.

[108] Humphries, M. M., Thomas, D. W., and Speakman, J. R. (2002). Climate-mediated energetic constraints on the distribution of hibernating mammals. *Nature*, 418(6895):313–316.

[109] IUCN (2016). Terrestrial Mammals Red List Spatial Data. *The IUCN Red List of Threatened Species*.

[110] Jacobsen, N. H. G. and Du Plessis, E. (1976). Observations on the ecology and biology of the Cape Fruit Bat Rousettus aegyptiacus Leachi in the Eastern Transvaal. *South African Journal of Science*, 72:270–273.

[111] Johnson, J. S., Treanor, J. J., Lacki, M. J., Baker, M. D., Falxa, G. A., Dodd, L. E., Waag, A. G., and Lee, E. H. (2016). Migratory and winter activity of bats in Yellowstone National Park. *Journal of Mammalogy*, 98(1):gyw175.

[112] Johnson, P. T., Sutherland, D. R., Kinsella, J., and Lunde, K. B. (2004). Review of the Trematode Genus Ribeiroia (Psilostomidae): Ecology, Life History and Pathogenesis with Special Emphasis on the Amphibian Malformation Problem. pages 191–253.

[113] Jones, K. E., Patel, N. G., Levy, M. a., Storeygard, A., Balk, D., Gittleman, J. L., and Daszak, P. (2008). Global trends in emerging infectious diseases. *Nature*, 451(February):990–993.

[114] Kamins, A. O., Restif, O., Ntiamoa-Baidu, Y., Suu-Ire, R., Hayman, D. T., Cunningham, A. A., Wood, J. L., and Rowcliffe, J. M. (2011). Uncovering the fruit bat bushmeat commodity chain and the true extent of fruit bat hunting in Ghana, West Africa. *Biological Conservation*, 144(12):3000–3008.

[115] King, T. and Dallimer, M. (2010). The fruit bats (Chiroptera: Pteropodidae) of the Lesio-Louna Reserve, Bateke Plateau, Republic of Congo. *Mammalia*, 74(1):63–69.

[116] Kingdon, J. (1974). *East African mammals IIA. Insectivores and bats*. Academic Press, London.

[117] Klüg-Baerwald, B. J. and Brigham, R. M. (2017). Hung out to dry? Intraspecific variation in water loss in a hibernating bat. *Oecologia*, 183(4):977–985.

[118] Klüg-Baerwald, B. J., Lausen, C. L., Willis, C. K. R., and Brigham, R. M. (2017). Home is where you hang your bat: winter roost selection by prairie-living big brown bats. *Journal of Mammalogy*, 98(3):752–760.

[119] Kofron, C. P. and Champan, A. (1994). Reproduction and sexual dimorphism of the West African fruit bat, Epomops buettikoferi, in Liberia. *African Journal of Ecology*, 32(4):308–316.

[120] Kuhn, J. H. (2017). Guide to the Correct Use of Filoviral Nomenclature. In *Current Topics in Microbiology and Immunology*, volume 0, pages 447–460. Springer International Publishing.

[121] Kunz, K. a. and T. H. Kunz (1987). Size of bats at birth and maternal investment during pregnancy.

[122] Kunz, T. H. and Fenton, M. B. (2003). *Bat Ecology*.

[123] Kunz, T. H., Wrazen, J. A., and Burnett, C. D. (1998). Changes in body mass and fat reserves in pre-hibernating little brown bats (Myotis lucifugus). *Ecoscience*, 5(1):8–17.

[124] Kupferschmidt, K. (2019). This bat species may be the source of the Ebola epidemic that killed more than 11,000 people in West Africa.

[125] Kurta, A., Bell, G. P., Nagy, K. A., and Kunz, T. H. (1989). Energetics of Pregnancy and Lactation in Freeranging Little Brown Bats (Myotis lucifugus). *Physiological Zoology*, 62(3):804–818.

[126] Lacki, M. J., Dodd, L. E., Toomey, R. S., Thomas, S. C., Couch, Z. L., and Nichols, B. S. (2015). Temporal Changes in Body Mass and Body Condition of Cave-Hibernating Bats During Staging and Swarming. *Journal of Fish and Wildlife Management*, 6(2):360–370.

[127] Lane, J. E., Kruuk, L. E. B., Charmantier, A., Murie, J. O., and Dobson, F. S. (2012). Delayed phenology and reduced fitness associated with climate change in a wild hibernator. *Nature*, 489(7417):554–557.

[128] Langwig, K. E., Frick, W. F., Bried, J. T., Hicks, A. C., Kunz, T. H., and Marm Kilpatrick, A. (2012). Sociality, density-dependence and microclimates determine the persistence of populations suffering from a novel fungal disease, white-nose syndrome. *Ecology Letters*, 15(9):1050–1057.

[129] LaVal, R. K. and LaVal, M. L. (1977). Reproduction and behaviour of the African Banana Bat, Pipistrellus nanus. *Journal of Mammalogy*, 58(3):403–410.

[130] Leendertz, S. A. J., Gogarten, J. F., Düx, A., Calvignac-Spencer, S., and Leendertz, F. H. (2016). Assessing the evidence supporting fruit bats as the primary reservoirs for ebola viruses. *EcoHealth*, 13(1):18–25.

[131] Leroy, E. M., Kumulungui, B., Pourrut, X., Rouquet, P., Hassanin, A., Yaba, P., Delicat, A., Paweska, J. T., Gonzalez, J.-P., Swanepoel, R., Délicat, A., Paweska, J. T., Gonzalez, J.-P., and Swanepoel, R. (2005). Fruit bats as reservoirs of Ebola virus. *Nature*, 438(7068):575–576.

[132] Leroy, E. M., Rouquet, P., Formenty, P., Kilbourne, A., Froment, J.-m., Bermejo, M., Smit, S., Karesh, W., Swanepoel, R., Zaki, S. R., and Rollin, P. E. (2004). Events and Rapid Decline of Central African Wildlife. *Science*, 303(January):387–390.

[133] Leutner, B. and Horning, N. (2017). RStoolbox: Tools for Remote Sensing Data Analysis.

[134] Li, W., Shi, Z., Yu, M., Ren, W., Smith, C., Epstein, J. H., Wang, H., Crameri, G., Hu, Z., Zhang, H., Zhang, J., Mceachern, J., Field, H., Daszak, P., Eaton, B. T., Zhang, S., and Wang, L.-f. (2005). Supporting Online Material for Bats Are Natural Reservoirs of SARS-like Coronaviruses. *Notes*, 310(September):676–680.

[135] Lilley, T. M. T., Johnson, J. J. S., Ruokolainen, L., Rogers, E. J., Wilson, C. A., Schell, S. M., Field, K. A., Reeder, D. M. D., Coleman, J., Reichard, J., Minnis, A., Lindner, D., Lorch, J., Meteyer, C., Behr, M., Boyles, J., Cryan, P., Hicks, A., Warnecke, L., Turner, J., Bollinger, T., Lorch, J., Misra, V., Cryan, P., Verant, M., Boyles, J., Waldrep, W., Wibbelt, G., Blehert, D., Frick, W., Pollock, J., Hicks, A., Langwig, K., Reynolds, D., Turner, G., Frick, W., Puechmaille, S., Hoyt, J., Nickel, B., Langwig, K., Foster, J., Reichard, J., Fuller, N., Bennett, A., Darling, S., Moore, M., Langwig, K., Carey, H., Andrews, M., Martin, S., Prendergast, B., Freeman, D., Zucker, I., Nelson, R., Bouma, H., Carey, H., Kroese, F., Langwig, K., Frick, W., Bried, J., Hicks, A., Kunz, T., Kilpatrick, A., Meteyer, C., Buckles, E., Blehert, D., Hicks, A., Green, D., Shearn-Bochsler, V., Field, K. A., Johnson, J. J. S., Lilley, T. M. T., Reeder, S., Rogers, E. J., Behr, M., Verant, M., Meteyer, C., Speakman, J., Cryan, P., Lorch, J., Blehert, D., Reeder, D. M. D., Frank, C., Turner, G., Meteyer, C., Kurta, A., Britzke, E., Johnson, J. J. S., Reeder, D. M. D., McMichael, J., Meierhofer, M., Stern, D., Lumadue, S., Turner, J., Warnecke, L., Wilcox, A., Baloun, D., Bollinger, T., Misra, V., Jonasson, K., Willis, C., Boyles, J., Dunbar, M., Whitaker, J., Geiser, F., Thomas, D., Cloutier, D., Gagne, D., Thomas, D., Cloutier, D., Daan, S., Barnes, B., Strijkstra, A., Brownlee-Bouboulis, S., Reeder, D. M. D., Boyles, J., Dunbar, M., Storm, J., Brack, V., Keen, R., Hitchcock, H., Humphries, M., Thomas, D., Speakman, J., Johnson, J. J. S., Reeder, D. M. D., Lilley, T. M. T., Czirják, G., Voigt, C., McMichael, J., Meteyer, C., Barber, D., Mandl, J., Hoyt, J., Langwig, K., Okoniewski, J., Frick, W., Stone, W., Kilpatrick, A., Humphries, M., Speakman, J., Thomas, D., Cryan, P., Meteyer, C., Blehert, D., Lorch, J., Reeder, D. M. D., Turner, G., Kokurewicz, T., Willis, C., Lane, J., Liknes, E., Swanson, D., Brigham, R., Grieneisen, L., Brownlee-Bouboulis, S., Johnson, J. J. S., Reeder, D. M. D., Vonhof, M., Russell, A., Miller-Butterworth, C., Turner, G., Meteyer, C., Barton, H., Gumbs, J., Reeder, D. M. D., Overton, B., Peig, J., and Green, A. (2016). White-nose syndrome survivors do not exhibit frequent arousals associated with Pseudogymnoascus destructans infection. *Frontiers in Zoology*, 13(1).

[136] Lloyd-Smith, J. O., Cross, P. C., Briggs, C. J., Daugherty, M., Getz, W. M., Latto, J., Sanchez, M. S., Smith, A. B., and Swei, A. (2005). Should we expect population thresholds for wildlife disease? *Trends in Ecology & Evolution*, 20(9):511–519.

[137] Lloyd-Smith, J. O., George, D., Pepin, K. M., Pitzer, V. E., Pulliam, J. R. C., Dobson, A. P., Hudson, P. J., and Grenfell, B. T. (2009). Epidemic Dynamics at the Human-Animal Interface. *Science*, 326(5958):1362–1367.

[138] Lo Iacono, G., Cunningham, A. A. A. A. A. A. A., Fichet-Calvet, E., Garry, R. R. F., Grant, D. S. D. D. S. D. D. S., Leach, M., Moses, L. M. L., Nichols, G., Schieffelin, J. J. S. J. J. S. J., Shaffer, J. G. J. J. G. J. J. G., Webb, C. T., Wood, J. L. N. J. J. L. N. J. J. L. N., Jones, K., Patel, N., Levy, M., Storeygard, A., Balk, D., Gittleman, J., Slingenbergh, J., Gilbert, M., de Balogh, K., Wint, W., Lloyd-Smith, J., George, D., Pepin, K., Pitzer, V., Pulliam, J., Dobson, A., Kamara, A., Koroma, B., Gogra, A., Blumberg, S., Lloyd-Smith, J., Kucharski, A., Mills, H., Pinsent, A., Fraser, C., Kerkhove, M., Donnelly, C., Cauchemez, S., Epperson, S., Biggerstaff, M., Swerdlow, D., Finelli, L., Ferguson, N., Kleczkowski, A., Breed, A., Matthews, L., Thronicker, D., de Vries, F., Wood, J. L. N. J. J. L. N. J. J. L. N., Leach, M., Waldman, L., Macgregor, H., Fooks, A., Jones, K., Altizer, S., Ostfeld, R., Johnson, P., Kutz, S., Harvell, C., Iacono, G. L., Cunningham, A. A. A. A. A. A. A., Fichet-Calvet, E., Garry, R. R. F., Grant, D. S. D. D. S. D. D. S., Khan, S., Shaffer, J. G. J. J. G. J. J. G., Grant, D. S. D. D. S. D. D. S., Schieffelin, J. J. S. J. J. S. J., Boisen, M., Goba, A., Hartnett, J., Monath, T., Newhouse, V., Kemp, G., Setzer, H., Cacciapuoti, A., Davis, S., Calvet, E., Leirs, H., Hawkes, A., Oakes, D., Heesterbeek, H., Anderson, R., Andreasen, V.,

Bansal, S., Angelis, D. D., Dye, C., Lloyd-Smith, J., Funk, S., McLean, A., Riley, S., Wood, J. L. N. J. J. L. N. J. J. L. N., Dzingirai, V., Bett, B., Bukachi, S., Lawson, E., Mangwanya, L., Scoones, I., Park, J., Quinn, K., Martin, A., Watanabe, S., Hooten, M., Hobbs, N., Spiegelhalter, D., Best, N., Carlin, B., van der Linde, A., Fichet-Calvet, E., Lecompte, E., Koivogui, L., Soropogui, B., Doré, A., Kourouma, F., Leyequien, E., Verrelst, J., Slot, M., Schaepman-Strub, G., Heitkönig, I., Skidmore, A., Bonney, R., Cooper, C., Dickinson, J., Kelling, S., Phillips, T., Rosenberg, K., Mills, J., Ksiazek, T., Peters, C., Childs, J., Roelke-Parker, M., Munson, L., Packer, C., Kock, R., Cleaveland, S., Carpenter, M., Baker, K., Todd, S., Marsh, G., Crameri, G., Barr, J., Kamins, A., O'Shea, T., Bowen, R., Stanley, T., Shankar, V., Rupprecht, C., Newitt, S., Elliot, A., Morbey, R., Durnall, H., Pietzsch, M., Medlock, J., Andersen, K., Shapiro, B., Matranga, C., Sealfon, R., Lin, A., Moses, L. M. L., Iacono, G. L., van den Bosch, F., Gilligan, C., Brown, J., Ernest, S., Leach, M., Scoones, I., Richards, P., Amara, J., Ferme, M., Kamara, P., Mokuwa, E., Sheriff, A., Redding, D., Moses, L. M. L., Cunningham, A. A. A. A. A. A. A., Wood, J. L. N. J. J. L. N. J. J. L. N., Jones, K., Grant, C., Iacono, G. L., Dzingirai, V., Bett, B., Winnebah, T., Atkinson, P., Brockmann, D., Hufnagel, L., Geisel, T., Colizza, V., Barrat, A., Barthelemy, M., Valleron, A., Vespignani, A., Ni, S., Weng, W., Belik, V., Geisel, T., Brockmann, D., Gibbons, C., Mangen, M., Plass, D., Havelaar, A., Brooke, R., Kramarz, P., and Kingman, J. (2016). A Unified Framework for the Infection Dynamics of Zoonotic Spillover and Spread. *PLOS Neglected Tropical Diseases*, 10(9):e0004957.

[139] Luby, S. P., Rahman, M., Hossain, M. J., Blum, L. S., Husain, M. M., Gurley, E., Khan, R., Ahmed, B.-N., Rahman, S., Nahar, N., Kenah, E., Comer, J. A., and Ksiazek, T. G. (2006). Foodborne transmission of Nipah virus, Bangladesh. *Emerging infectious diseases*, 12(12):1888–94.

[140] Luis, A. D., Hayman, D. T. S., O'Shea, T. J., Cryan, P. M., Gilbert, A. T., Pulliam, J. R. C., Mills, J. N., Timonin, M. E., Willis, C. K. R., Cunningham, A. A., Fooks, A. R., Rupprecht, C. E., Wood, J. L. N., and Webb, C. T. (2013). A comparison of bats and rodents as reservoirs of zoonotic viruses: are bats special? *Proceedings of the Royal Society B: Biological Sciences*, 280(1756):20122753.

[141] Luis, A. D., O'Shea, T. J., Hayman, D. T. S., Wood, J. L. N., Cunningham, A. A., Gilbert, A. T., Mills, J. N., and Webb, C. T. (2015). Network analysis of host-virus communities in bats and rodents reveals determinants of cross-species transmission. *Ecology Letters*, 18(11):1153–1162.

[142] Marshall, A. G. and McWilliam, A. N. (1982). Ecological observations on epomorphorine fruit-bats (Megachiroptera) in West African savanna woodland. *Journal of Zoology*, 198(1):53–67.

[143] McClure, M. L., Haase, C. G., Crowley, D., Hranac, C. R., Hayman, D. T., Mcguire, L. P., Dickson, B. G., Fuller, N. W., Plowright, R. K., Lausen, C. L., and Olson, S. H. (2019). Modeling and Mapping Western Bat Hibernaculum Suitability Before and After Pd Exposure. *In Prep*.

[144] McGuire, L. P., Kelly, L. A., Baloun, D. E., Boyle, W. A., Cheng, T. L., Clerc, J., Fuller, N. W., Gerson, A. R., Jonasson, K. A., Rogers, E. J., Sommers, A. S., and Guglielmo, C. G. (2018). Common condition indices are no more effective than body mass for estimating fat stores in insectivorous bats. *Journal of Mammalogy*, 99(5):1065–1071.

[145] Mcguire, L. P., Turner, J. M., Warnecke, L., Mcgregor, G., Bollinger, T. K., Misra, V., Foster, J. T., Frick, W. F., Kilpatrick, A. M., and Willis, C. K. R. (2016). White-Nose Syndrome Disease Severity and a Comparison of Diagnostic Methods. *EcoHealth*, 13(1):60–71.

[146] Mcwilliam, A. N. (1982). *Adaptive responses to seasonality in four species of insectivorous bats in costal Kenya*. PhD thesis, University of Aberdeen.

[147] Mcwilliam, A. N. (1987). Polyoestry and postpartum oestrus in Tadarida (Chaerephon) pumila (Chiroptera: Molossidae) in northern Ghana, West Africa. *Journal of Zoology*, 213(4):735–739.

[148] Mcwilliam, N. and McWilliam, A. N. (1988). The reproductive cycle of male tomb bats, Taphozous hildegardeae (Chiroptera: Emballonuridae), in a seasonal environment of the African tropics. *Journal of Zoology*, 215(3):433–442.

[149] Menzies, J. I. (1973). A Study of Leaf-Nosed Bats (Hipposideros caffer and Rhinolophus landeri) in a Cave in Northern Nigeria. *Journal of Mammalogy*, 54(4):930–945.

[150] Messenger, A. M., Barnes, A. N., and Gray, G. C. (2014). Reverse zoonotic disease transmission (Zooanthroponosis): A systematic review of seldom-documented human biological threats to animals. *PLoS ONE*, 9(2):1–9.

[151] Mickleburgh, S., Waylen, K., and Racey, P. (2009). Bats as bushmeat: A global review. *Oryx*, 43(2):217–234.

[152] Miranda, M. E. G., Robles, C. G., Peters, C. J., Ksiazek, T. G., Dayrit, M. M., Manaloto, C. R., Hayes, C. G., Barrientos, A. B., Del Rosario, R. A., and Burans, J. P. (1992). Outbreak of Fatal Illness among Captive Macaques in the Philippines Caused by an Ebola-Related Filovirus. *The American Journal of Tropical Medicine and Hygiene*, 46(6):664–671.

[153] Molnár, P. K., Kutz, S. J., Hoar, B. M., and Dobson, A. P. (2013). Metabolic approaches to understanding climate change impacts on seasonal host-macroparasite dynamics. *Ecology letters*, 16(1):9–21.

[154] Monadjem, A., Monadjem, L., and Putnam, J. (1998). Notes and Records. *African Journal of Ecology*, 36(3):280–285.

[155] Monadjem, A. and Reside, A. E. (2012). Breeding Season of Epomophorus walhbergi in the Lowveld of Swaziland. *African Zoology*, 47(2):321–325.

[156] Monadjem, A., Taylor, P. J., Cotterill, F., Schoeman, M. C., and Goodman, S. M. (2010). *Bats of southern and central Africa*. Wits University Press.

[157] Moore, M. S., Reichard, J. D., Murtha, T. D., Zahedi, B., Fallier, R. M., and Kunz, T. H. (2011). Specific alterations in complement protein activity of little brown myotis (Myotis lucifugus) hibernating in White-nose syndrome affected sites. *PLoS ONE*, 6(11).

[158] Morvan, J. M., Deubel, V., Gounon, P., Nakouné, E., Barrière, P., Murri, S., Perpète, O., Selekon, B., Coudrier, D., Gautier-Hion, A., Colyn, M., and Volehkov, V. (1999). Identification of Ebola virus sequences present as RNA or DNA in organs of terrestrial small mammals of the Central African Republic. *Microbes and Infection*, 1(14):1193–1201.

[159] Murray, K. A., Olivero, J., Roche, B., Tiedt, S., and Guégan, J. F. (2018). Pathogeography: leveraging the biogeography of human infectious diseases for global health management. *Ecography*, 41(9):1411–1427.

[160] Mutere, F. A. (1967). The breeding biology of equatorial vertebrates: reproduction in the fruit bat, Eidolon helvum, at latitude 0.20N. *Journal of Zoology*, 153(2):153–161.

[161] Mutere, F. A. (1968). The breeding biology of the fruit bat Rosettuus aegyptiacus living at 0 degrees 22 minutes South. *Acta Tropica1*, 25(2):97–108.

[162] Mutere, F. A. (1973). Reproduction in two species of equatorial free-tailed bats (Molossidae). *African Journal of Ecology*, 11(3-4):271–280.

[163] Ng, M., Ndungo, E., Kaczmarek, M. E., Herbert, A. S., Binger, T., Kuehne, A. I., Jangra, R. K., Hawkins, J. A., Gifford, R. J., Biswas, R., Demogines, A., James, R. M., Yu, M., Brummelkamp, T. R., Drosten, C., Wang, L.-F., Kuhn, J. H., Müller, M. A., Dye, J. M., Sawyer, S. L., and Chandran, K. (2015). Filovirus receptor NPC1 contributes to species-specific patterns of ebolavirus susceptibility in bats. *eLife*, 4.

[164] Nishiura, H., Hoye, B., Klaassen, M., Bauer, S., and Heesterbeek, H. (2009). How to find natural reservoir hosts from endemic prevalence in a multi-host population: A case study of influenza in waterfowl. *Epidemics*, 1(2):118–128.

[165] Norquay, K. J. O. and Willis, C. K. R. (2014). Hibernation phenology of M yotis lucifugus. *Journal of Zoology*, 294(2):85–92.

[166] Nowak, R. M. (1994). *Walker's Bats of the World*. John's Hopkins Iniversity Press, Baltimore.

[167] O'Farrrell, M. J. and Studier, E. H. (1973). Reproduction, Growth, and Development in Myotis Thysanodes and M. Lucifugus (Chiroptera: Vespertilionidae). *Ecology*, 54(1):18–30.

[168] Okia, N. O. (1974). The breeding pattern of the eastern epauletted bat, Epomophorus anurus Heuglin, in Uganda. *Journal of reproduction and fertility*, 37(1):27–31.

[169] Okia, N. O. (1987). Reproductive Cycles of East African Bats. *Journal of Mammalogy*, 68(1):138–141.

[170] Olival, K. J. and Hayman, D. T. S. (2014). Filoviruses in bats: Current knowledge and future directions. *Viruses*, 6(4):1759–1788.

[171] Olival, K. J., Hosseini, P. R., Zambrana-Torrelio, C., Ross, N., Bogich, T. L., and Daszak, P. (2017). Host and viral traits predict zoonotic spillover from mammals. *Nature*, 546(7660):646–650.

[172] Olivier, A., Ramos Perez, J. J., Kalogirou, V., Bontemps, S., Defourny, P., and Van Bogaert, E. (2012). Global Land Cover Map for 2009 (GlobCover 2009).

[173] O'Shea, T. J., Cryan, P. M., Cunningham, A. A., Fooks, A. R., Hayman, D. T. S., Luis, A. D., Peel, A. J., Plowright, R. K., and Wood, J. L. N. (2014). Bat flight and zoonotic viruses. *Emerging Infectious Diseases*, 20(5):741–745.

[174] O'Shea, T. J., Cryan, P. M., Hayman, D. T. S., Plowright, R. K., and Streicker, D. G. (2016). Multiple mortality events in bats: A global review. *Mammal Review*, 46(3):175–190.

[175] O'Shea, T. J., Vaughan, T. A., O'SHEA, T. J., and Vaughan, T. A. (1980). Ecological observations on an East African bat community. *Mammalia*, 44(4):485–496.

[176] Ovaskainen, O. and Soininen, J. (2011). Making more out of sparse data: Hierarchical modeling of species communities. *Ecology*, 92(2):289–295.

[177] Oyston, P. C., Sjostedt, A., and Titball, R. W. (2004). Tularaemia: Bioterrorism defence renews interest in Francisella tularensis. *Nature Reviews Microbiology*, 2(12):967–978.

[178] Pau, G., Fuchs, F., Skylar, O., Boutros, M., and Huber, W. (2010). EBImage—an R package for image processing with applications to cellular phenotypes. *Bioinformatics*, 26(7):979–981.

[179] Pebesma, E. and Bivand, R. (2005). Classes and methods for spatial data in R. *R News*, 5(2):9–13.

[180] Peel, A. J., Baker, K. S., Hayman, D. T. S., Broder, C. C., Cunningham, A. A., Fooks, A. R., Garnier, R., Wood, J. L. N., and Restif, O. (2018). Support for viral persistence in bats from age-specific serology and models of maternal immunity. *Scientific Reports*, 8(1):3859.

[181] Peel, A. J., Sargan, D. R., Baker, K. S., Hayman, D. T. S., Barr, J. A., Crameri, G., Suu-Ire, R., Broder, C. C., Lembo, T., Wang, L.-F., Fooks, A. R., Rossiter, S. J., Wood, J. L. N., and Cunningham, A. A. (2013). Continent-wide panmixia of an African fruit bat facilitates transmission of potentially zoonotic viruses. *Nature communications*, 4:2770.

[182] Peel, A. J., Wood, J. L. N., Baker, K. S., Breed, A. C., Carvalho, A. D., Fernández-Loras, A., Gabrieli, H. S., Gembu, G.-C., Kakengi, V. A., Kaliba, P. M., Kityo, R. M., Lembo, T., Mba, F. E., Ramos, D., Rodriguez-Prieto, I., Suu-Ire, R., Cunningham, A. A., and Hayman, D. T. S. (2017). How Does Africa's Most Hunted Bat Vary Across the Continent? Population Traits of the Straw-Coloured Fruit Bat (Eidolon helvu m) and Its Interactions with Humans. *Acta Chiropterologica*, 19(1):77–92.

[183] Pepin, K. M., Lass, S., Pulliam, J. R. C., Read, A. F., and Lloyd-Smith, J. O. (2010). Identifying genetic markers of adaptation for surveillance of viral host jumps. *Nature Reviews Microbiology*, 8(11):802–813.

[184] Perry, R. W. (2013). A review of factors affecting cave climates for hibernating bats in temperate North America. *Environmental Reviews*, 21(October 2012):28–39.

[185] Peterson, A. T. (2008). Biogeography of diseases: a framework for analysis. *Naturwissenschaften*, 95(6):483–491.

[186] Pigott, D. M., Golding, N., Mylne, A., Huang, Z., Henry, A. J., Weiss, D. J., Brady, O. J., Kraemer, M. U., Smith, D. L., Moyes, C. L., Bhatt, S., Gething, P. W., Horby, P. W., Bogoch, I. I., Brownstein, J. S., Mekaru, S. R., Tatem, A. J., Khan, K., and Hay, S. I. (2014). Mapping the zoonotic niche of Ebola virus disease in Africa. *eLife*, 3(6):366–378.

[187] Pigott, D. M., Millear, A. I., Earl, L., Morozoff, C., Han, B. A., Shearer, F. M., Weiss, D. J., Brady, O. J., Kraemer, M. U., Moyes, C. L., Bhatt, S., Gething, P. W., Golding, N., and Hay, S. I. (2016). Updates to the zoonotic niche map of Ebola virus disease in Africa. *eLife*, 5(2016JULY):1–13.

[188] Pinzon, J. E., Wilson, J. M., Tucker, C. J., Arthur, R., Jahrling, P. B., and Formenty, P. (2004). Trigger events: Enviroclimatic coupling of Ebola hemorrhagic fever outbreaks. *American Journal of Tropical Medicine and Hygiene*, 71(5):664–674.

[189] Plowright, R. K., Eby, P., Hudson, P. J., Smith, I. L., Westcott, D., Bryden, W. L., Middleton, D., Reid, P. A., McFarlane, R. A., Martin, G., Tabor, G. M., Skerratt, L. F., Anderson, D. L., Crameri, G., Quammen, D., Jordan, D., Freeman, P., Wang, L.-F., Epstein, J. H., Marsh, G. A., Kung, N. Y., and McCallum, H. (2015). Ecological dynamics of emerging bat virus spillover. *Proceedings of the Royal Society B: Biological Sciences*, 282(1798):20142124.

[190] Plowright, R. K., Parrish, C. R., Mccallum, H., Hudson, P. J., Ko, A. I., Graham, A. L., and Lloyd-Smith, J. O. (2017). Pathways to zoonotic spillover HHS Public Access. *Nat Rev Microbiol*, 15(8):502–510.

[191] Pourrut, X., Kumulungui, B., Wittmann, T., Moussavou, G., Delicat, A., Yaba, P., Nkoghe, D. D., Gonzalez, J.-P. P., Leroy, E. M., Délicat, A., Yaba, P., Nkoghe, D. D., Gonzalez, J.-P. P., and Leroy, E. M. (2005). The natural history of Ebola virus in Africa. *Microbes and Infection*, 7(7-8):1005–1014.

[192] Pourrut, X., Souris, M., Towner, J. S., Rollin, P. E., Nichol, S. T., Gonzalez, J.-P., and Leroy, E. (2009). Large serological survey showing cocirculation of Ebola and Marburg viruses in Gabonese bat populations, and a high seroprevalence of both viruses in Rousettus aegyptiacus. *BMC infectious diseases*, 9(1):159.

[193] Racey, P. A. (1982). Ecology of bat reproduction. In *Ecology of bats*, pages 57–104. Springer, Boston.

[194] Restif, O., Hayman, D. T. S., Pulliam, J. R. C., Plowright, R. K., George, D. B., Luis, A. D., Cunningham, A. A., Bowen, R. A., Fooks, A. R., O'Shea, T. J., Wood, J. L. N., and Webb, C. T. (2012). Model-guided fieldwork: Practical guidelines for multidisciplinary research on wildlife ecological and epidemiological dynamics. *Ecology Letters*, 15(10):1083–1094.

[195] Reynolds, S. and Kunz, T. H. (2000). Changes in body composition during reproduction and postnatal growth in the little brown bat, Myotis lucifugus (Chiroptera: Vespertilionidae). *Écoscience*, 7(1):10–17.

[196] Richter, H. V. and Cumming, G. S. (2006). Food availability and annual migration of the straw-colored fruit bat (Eidolon helvum). *Journal of Zoology*, 268(1):35–44.

[197] Rothman, K. J. and Greenland, S. (2005). Causation and causal inference in epidemiology. *American Journal of Public Health*, 95(SUPPL. 1):144–150.

[198] Rulli, M. C., Santini, M., Hayman, D. T., and D'Odorico, P. (2017). The nexus between forest fragmentation in Africa and Ebola virus disease outbreaks. *Scientific Reports*, 7(December 2016):1–8.

[199] Ryder, J. J., Miller, M. R., White, A., Knell, R. J., and Boots, M. (2007). Host-parasite population dynamics under combined frequency- and density-dependent transmission. *Oikos*, 116(12):2017–2026.

[200] Saéz, A. M., Weiss, S., Nowak, K., Lapeyre, V., Kaba, M., Regnaut, S., Zimmermann, F., Düx, A., Ku, H. S., Merkel, K., Sachse, A., Thiesen, U., Villányi, L., Boesch, C., Dabrowski, P. W., Nitsche, A., Leendertz, S. A. J., Petterson, S., Becker, S., Krähling, V., Couacy-hymann, E., Akoua-Koffi, C., Weber, N., Schaade, L., Fahr, J., Borchert, M., Gogarten, J. F., Calvignac-spencer, S., Leendertz, F. H., Saez, A. M., Weiss, S., Nowak, K., Lapeyre, V., Zimmermann, F., Dux, A., Kuhl, H. S., Kaba, M., Regnaut, S., Merkel, K., Sachse, A., Thiesen, U., Villanyi, L., Boesch, C., Dabrowski, P. W., Radonic, A., Nitsche, A., Leendertz, S. A. J., Petterson, S., Becker, S., Krahling, V., Couacy-hymann, E., Akoua-Koffi, C., Weber, N., Schaade, L., Fahr, J., Borchert, M., Gogarten, J. F., Calvignac-spencer, S., and Leendertz, F. H. (2014). Investigating the zoonotic origin of the West African Ebola epidemic. *EMBO Molecular Medicine*, 7(1):17–23.

[201] Salkeld, D. J., Padgett, K. a., and Jones, J. H. (2013). A meta-analysis suggesting that the relationship between biodiversity and risk of zoonotic pathogen transmission is idiosyncratic. *Ecology Letters*, 16:679–686.

[202] Scheele, B. C., Pasmans, F., Skerratt, L. F., Berger, L., Martel, A., Beukema, W., Acevedo, A. A., Burrowes, P. A., Carvalho, T., Catenazzi, A., De la Riva, I., Fisher, M. C., Flechas, S. V., Foster, C. N., Frías-Álvarez, P., Garner, T. W. J., Gratwicke, B., Guayasamin, J. M., Hirschfeld, M., Kolby, J. E., Kosch, T. A., La Marca, E., Lindenmayer, D. B., Lips, K. R., Longo, A. V., Maneyro, R., McDonald, C. A., Mendelson, J., Palacios-Rodriguez, P., Parra-Olea, G., Richards-Zawacki, C. L., Rödel, M.-O., Rovito, S. M., Soto-Azat, C., Toledo, L. F., Voyles, J., Weldon, C., Whitfield, S. M., Wilkinson, M., Zamudio, K. R., and Canessa, S. (2019). Amphibian fungal panzootic causes catastrophic and ongoing loss of biodiversity. *Science*, 363(6434):1459–1463.

[203] Schmidt, J. P., Park, A. W., Kramer, A. M., Han, B. A., Alexander, L. W., and Drake, J. M. (2017). Spatiotemporal fluctuations and triggers of ebola virus spillover. *Emerging Infectious Diseases*, 23(3):415–422.

[204] Schuh, A. J., Amman, B. R., Jones, M. E. B., Sealy, T. K., Uebelhoer, L. S., Spengler, J. R., Martin, B. E., Coleman-McCray, J. A. D., Nichol, S. T., and Towner, J. S. (2017). Modelling filovirus maintenance in nature by experimental transmission of Marburg virus between Egyptian rousette bats. *Nature Communications*, 8(1):14446.

[205] Smithers, R. H. N. (1971). *The mammals of Botswana*. Trustees of the National Museums of Rhodesia.

[206] Smithers, R. H. N. and Wilson, V. (1979). *Check list and atlas of the mammals of Zimbabwe Rhodesia*. Trustees of the National Museums and Monuments.

[207] Soberon, J. and Peterson, A. T. (2005). Interpretation of Models of Fundamental Ecological Niches and Species' Distributional Areas. *Biodiversity Informatics*, 2(10):3392–3396.

[208] Speakman, J. R. and Fenton, M. B. (2003). Physiological Ecology and Entergetics of Bats. In Kunz, T. H. and Fenton, M. B., editors, *Bat Ecology*, chapter 10: Physio, pages 430–490. Chiago.

[209] Speakman, J. R. and Rowland, A. (1999). Preparing for inactivity: How insectivorous bats deposit a fat store for hibernation. *Proceedings of the Nutrition Society*, 58(1):123–131.

[210] Swanepoel, R., Leman, P. A., Burt, F. J., Zachariades, N. A., Braack, L. E. O., Ksiazek, T. G., Rollin, P. E., Zaki, S. R., and Peters, C. J. (1996). Experimental Inoculation of Plants and Animals with Ebola Virus. *Emerging Infectious Diseases*, 2(4):321–325.

[211] Swanepoel, R., Smit, S. B., Rollin, P. E., Formenty, P., Leman, P. A., Kemp, A., Burt, F. J., Grobbelaar, A. A., Croft, J., Bausch, D. G., Zeller, H., Leirs, H., Braack, L. E. O., Libande, M. L., Zaki, S., Nichol, S. T., Ksiazek, T. G., and Paweska, J. T. (2007). Studies of reservoir hosts for Marburg virus. *Emerging Infectious Diseases*, 13(12):1847–1851.

[212] Taylor, D. J., Leach, R. W., and Bruenn, J. (2010). Filoviruses are ancient and integrated into mammalian genomes. *BMC Evolutionary Biology*, 10(1).

[213] Team, R. C. (2017). R: A Language and Environment for Statistical Computing.

[214] Thomas, D. W. (1983). The annual migrations of three species of West African fruit bats (Chiroptera: Pteropodidae). *Canadian Journal of Zoology*, 61(10):2266–2272.

[215] Thomas, D. W. and Cloutier, D. (1992). Evaporative Water Loss by Hibernating Little Brown Bats, Myotis lucifugus. *Physiological Zoology*, 65(2):443–456.

[216] Thomas, D. W., Dorais, M., and Bergeron, J.-m. (1990). Winter Energy Budgets and Cost of Arousals for Hibernating Little Brown Bats , Myotis lucifugus. *Journal of Mammalogy*, 71(3):475–479.

[217] Thomas, D. W. and Marshall, A. G. (1984). Reproduction and growth in three species of West African fruit bats. *Journal of Zoology*, 202(2):265–281.

[218] Thuiller, C. W. (2017). biomod2: Ensemble Platform for Species Distribution Modeling.

[219] Trabucco, A. and Zomer, R. J. . (2009). Global Aridity Index (Global-Aridity) and Global Potential Evapo-Transpiration (Global-PET) Geospatial Database. *CGIAR Consortium for Spatial Information*.

[220] van der Merwe, M. (1994). Reproductive biology of the cape serotine bat, Eptesicus capensis in the Transvaal, South Africa. *South African Journal of Zoology*, 29(1):36–39.

[221] van der Merwe, M. and Rautenbach, I. L. (1987). Reproduction in Schlieffen's bat, Nycticeius schlieffenii, in the eastern Transvaal lowveld, South Africa. *Journal of Reproduction & Fertility*, 81(September):41–50.

[222] van der Merwe, M. and Rautenbach, I. L. (1990). Reproduction in the rusty bat, Pipistrellus rusticus, in the northern Transvaal bushveld, South Africa. *Journal of reproduction and fertility*, 89:537–542.

[223] van der Merwe, M., van der Merwe, N. J., and Penzhorn, B. L. (2006). Aspects of reproduction in the seasonally breeding African yellow bat, Scotophilus dinganii (A. Smith, 1833). *African Zoology*, 41(1):67–74.

[224] Van der Merwe, N.J. Rautenbach, I. and Penzhorn, B. (1988). A new pattern of early embryonic development in the seasonally breeding non-hibernating lesser yellow house bat, Scotophilus borbonicus (E. Geoffroy, 1803) (Chiroptera: Vespertilionidae). *Annals of the Transvaal Museum*, 34(24):551–556.

[225] Van derMerwe, M. (1979). Foetal Growth Curves and Seasonal Breeding in the Natal Clinging Bat Miniopterus Schreibersi Natalensis. *South African Journal of Zoology*, 14(1):17–21.

[226] Vaughan, T. A. (1976). Nocturnal Behavior of the African False Vampire Bat (Cardioderma cor). *Journal of Mammalogy*, 57(2):227–248.

[227] Vaughan, T. A., Vaughan, R. P., Bat, Y.-w., Vaughan, T. A., and Vaughan, R. P. (1986). Seasonality and the Behavior of the African Yellow-Winged. *Journal of Mammalogy*, 67(1):91–102.

[228] Verant, M. L., Boyles, J. G., Waldrep, W., Wibbelt, G., and Blehert, D. S. (2012). Temperature-Dependent Growth of Geomyces destructans, the Fungus That Causes Bat White-Nose Syndrome. *PLoS ONE*, 7(9).

[229] Verant, M. L., Meteyer, C. U., Speakman, J. R., Cryan, P. M., Lorch, J. M., and Blehert, D. S. (2014). White-nose syndrome initiates a cascade of physiologic disturbances in the hibernating bat host. *BMC Physiology*, 14(1):10.

[230] Verschuren, J. (1957). Ecologie, biologie, et systématique des Chiroptères. *Journal of Mammalogy1*, 58:469–478.

[231] Vivier, L. and van der Merwe, M. (2001). Aspects of the histology of reproduction in the female Angolan free-tailed bat Mops condylurus (Microchiroptera: Molossidae) in Mpumalanga, South Africa. *Journal of Zoology*, 254(4):495–504.

[232] Walsh, P. D., Biek, R., and Real, L. A. (2005). Wave-like spread of Ebola Zaire. *PLoS Biology*, 3(11):1946–1953.

[233] Wang, L. C. H. (1989). Ecological, physiological , and biochemical aspects of torpor in mammals and birds. In *Advances in comparative and environmental physiology*, pages 361–491. Springer Verlag, Berlin.

[234] Wang, L. C. H. and Lee, T. F. (2011). Torpor and Hibernation in Mammals: Metabolic, Physiological, and Biochemical Adaptations. In *Comprehensive Physiology*, pages 507–532. Wiley.

[235] Wang, T., Hamann, A., Spittlehouse, D., and Carroll, C. (2016). Locally downscaled and spatially customizable climate data for historical and future periods for North America. *PLoS ONE*, 11(6):1–17.

[236] Warnecke, L., Turner, J. M., Bollinger, T. K., Lorch, J. M., Misra, V., Cryan, P. M., Wibbelt, G., Blehert, D. S., and Willis, C. K. R. (2012). Inoculation of bats with European Geomyces destructans supports the novel pathogen hypothesis for the origin of white-nose syndrome. *Proceedings of the National Academy of Sciences*, 109(18):6999–7003.

[237] Warnecke, L., Turner, J. M., Bollinger, T. K., Misra, V., Cryan, P. M., Blehert, D. S., Wibbelt, G., and Willis, C. K. R. (2013). Pathophysiology of white-nose syndrome in bats: a mechanistic model linking wing damage to mortality. *Biology letters*, 9:20130177.

[238] Watson, J. T., Gayer, M., and Connolly, M. A. (2007). Epidemics after natural disasters. *Emerging infectious diseases*, 13(1):1–5.

[239] (WHO), W. H. O. (2018). Cluster of presumptive Ebola cases in North Kivu in the Democratic Republic of the Congo. Technical report, Kinshasa/Geneva.

[240] Wickler, W. and Seibt, U. (1976). Field studies on the African fruit bat Epomophorus wahlbergi (Sundevall), with special reference to male calling. *Zeitschrift für Tierpsychologie*, 40(4):345–376.

[241] Wilkinson, D. A., Marshall, J. C., French, N. P., and Hayman, D. T. S. (2018). Habitat fragmentation, biodiversity loss and the risk of novel infectious disease emergence. *Journal of The Royal Society Interface*, 15(149):20180403.

[242] Wolfe, N. D., Dunavan, C. P., and Diamond, J. (2007). Origins of major human infectious diseases. *Nature*, 447(7142):279–283.

[243] Wolton, R., Arak, P., Godfray, H., and Wilson, R. (1982). Ecological and behavioural studies of the Megachiroptera at Mount Nimba, Liberia, with notes on Microchiroptera. *Mammalia*, 46(4):419–448.

[244] Wood, J. L. N., Leach, M., Waldman, L., Macgregor, H., Fooks, A. R., Jones, K. E., Restif, O., Dechmann, D., Hayman, D. T. S., Baker, K. S., Peel, A. J., Kamins, A. O., Fahr, J., Ntiamoa-Baidu, Y., Suu-Ire, R., Breiman, R. F., Epstein, J. H., Field, H. E., and Cunningham, A. A. (2012). A framework for the study of zoonotic disease emergence and its drivers: spillover of bat pathogens as a case study. *Philosophical transactions of the Royal Society of London. Series B, Biological sciences*, 367(1604):2881–2892.

[245] World Health Organization (2007). The World Health Report 2007: A Safer Future. *Global Public Health*, page 96.

[246] Zinsstag, J., Schelling, E., Waltner-Toews, D., and Tanner, M. (2011). From "one medicine" to "one health" and systemic approaches to health and well-being. *Preventive Veterinary Medicine*, 101(3-4):148–156.

Appendix A

Spatial and temporal patterns of birth pulses among African bats

A.1 Data availability

All R code and data are available at github.com/cReedHranac/FS

A.2 Figures

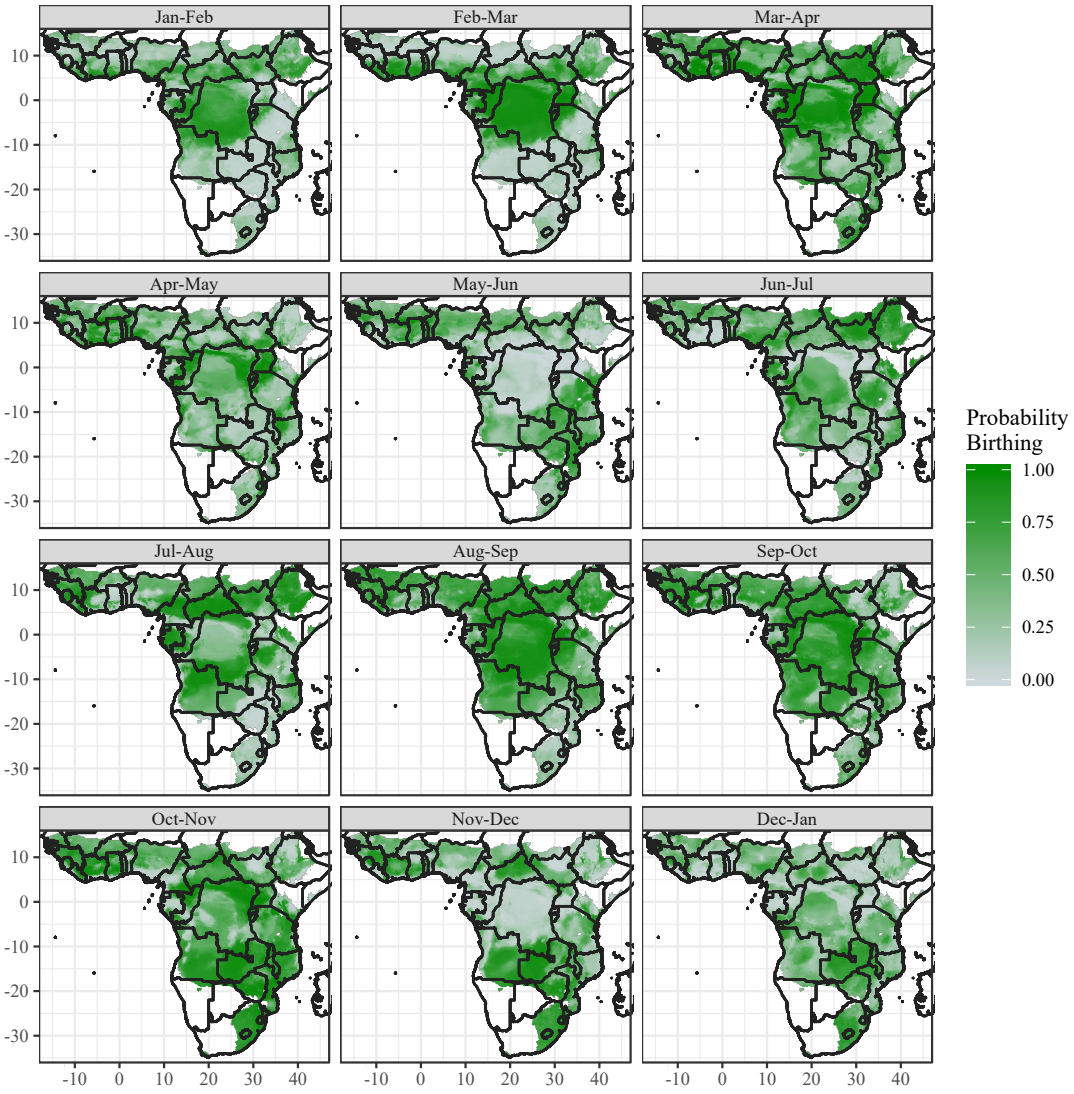


Fig. A.1 Monthly ensemble probability habitat suitability to African fruit bats giving birth.

A.3 Figures

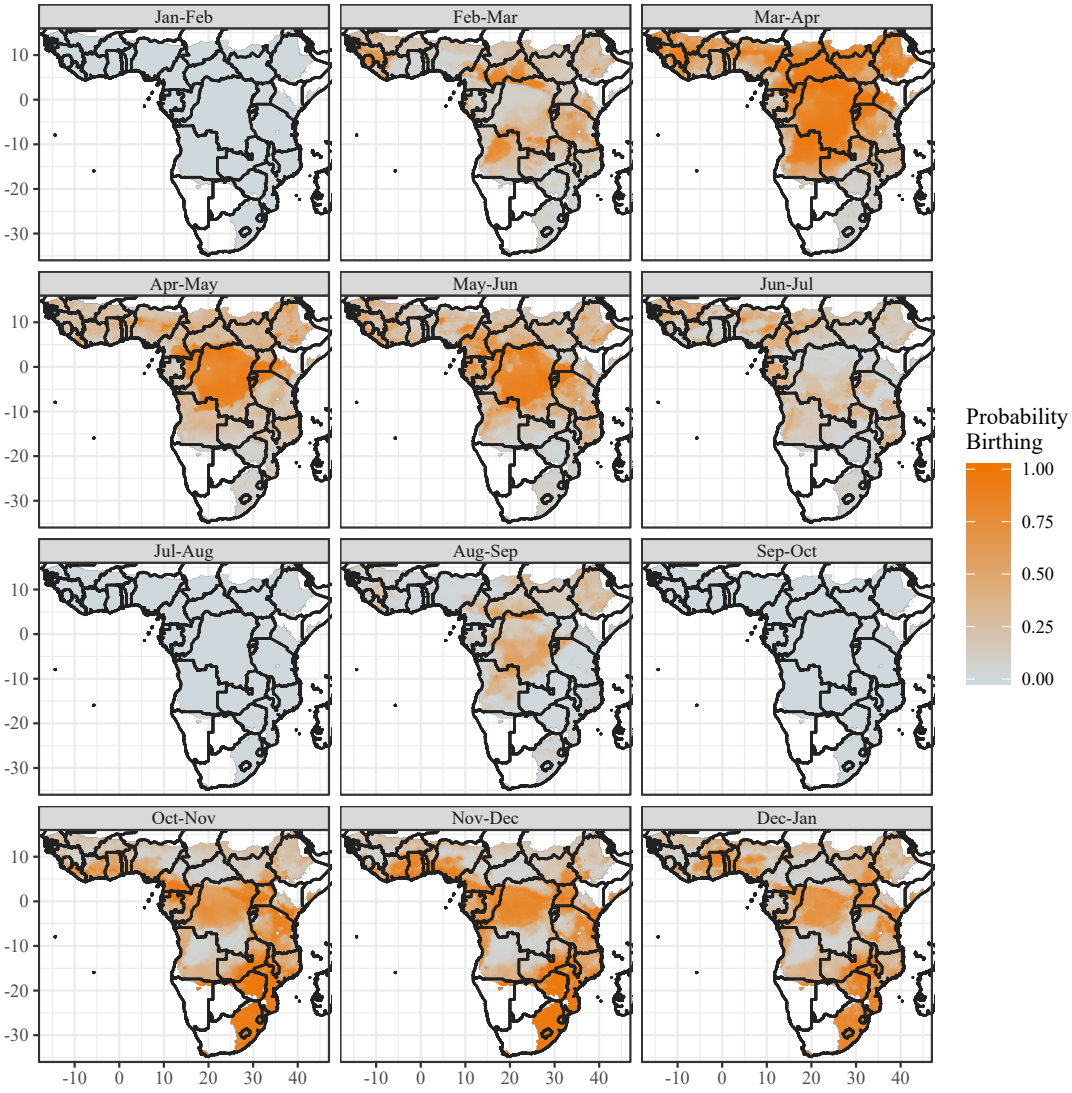


Fig. A.2 Monthly ensemble probability habitat suitability for non-Molossid microbats to give birth. No models were generated for Jan-Feb, Jul-Aug, or Sept-Oct due to the lack of data available.

A.4 Figures

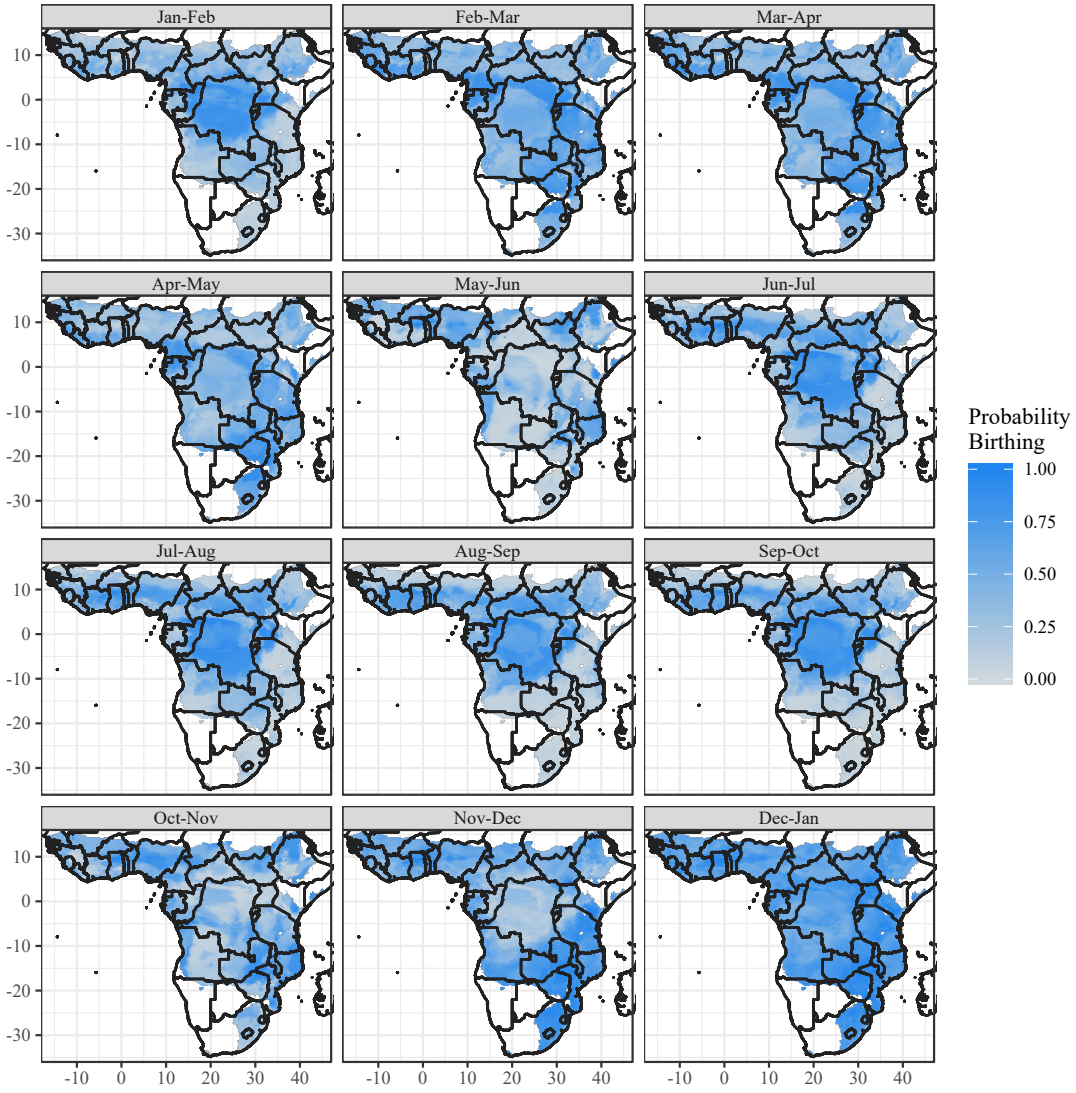


Fig. A.3 Monthly ensemble probability habitat suitability for Molossid bats giving birth.

Appendix B

Spatial and temporal patterns of birth pulses among African bats

B.1 Data availability

All R code and data are available at github.com/cReedHranac/FS

B.2 Tables

Table B.1 Model for all alternative animal spatGLM models. Terms not included in that model are denoted by "-"

Model:	Null		D_{tot}		D_{tax}		P_{tot}		$D_{tot}+P_{tot}$		$D_{tot}\times P_{tot}$		$D_{tax}+P_{tax}$		$D_{tax}\times B_{tax}$	
	Estimate	P value	Estimate	P value	Estimate	P value	Estimate	P value	Estimate	P value	Estimate	P value	Estimate	P value	Estimate	P value
Intercept)	-32.81	<0.001	-30.02	<0.001	-27.56	<0.001	-38.2	0	-36.39	<0.001	-29.63	<0.001	-30.61	<0.001	-31.34	<0.001
P_{afb}	-	-	-	-	-	-	-	-	-	-	-	-	2	0.07	-	-
λ_{afb}	-	-	-	-	-	-	-	-	-	-	-	-	-	-	1.08	0.01
P_{mic}	-	-	-	-	-	-	-	-	-	-	-	-	-0.03	0.98	-	-
λ_{mic}	-	-	-	-	-	-	-	-	-	-	-	-	-	-	0.06	0.79
P_{mol}	-	-	-	-	-	-	-	-	-	-	-	-	-0.28	0.81	-	-
λ_{mol}	-	-	-	-	-	-	-	-	-	-	-	-	-	-	-0.18	0.64
P_{total}	-	-	-	-	-	-	2.11	0.24	1.74	0.31	-	-	-	-	-	-
λ_{total}	-	-	-	-	-	-	-	-	-	-	0.23	0.67	-	-	-	-
P_{afb_2}	-	-	-	-	-	-	-	-	-	-	-	-	1.27	0.25	-	-
λ_{afb_2}	-	-	-	-	-	-	-	-	-	-	-	-	-	-	0.79	0.04
P_{mic_2}	-	-	-	-	-	-	-	-	-	-	-	-	1.67	0.08	-	-
λ_{mic_2}	-	-	-	-	-	-	-	-	-	-	-	-	-	-	0.2	0.3
P_{mol_2}	-	-	-	-	-	-	-	-	-	-	-	-	0.75	0.56	-	-
λ_{mol_2}	-	-	-	-	-	-	-	-	-	-	-	-	-	-	0.47	0.31
P_{total_2}	-	-	-	-	-	-	6.17	0.02	5.65	0.02	-	-	-	-	-	-
λ_{total_2}	-	-	-	-	-	-	-	-	-	-	1.51	0.03	-	-	-	-
P_{afb_4}	-	-	-	-	-	-	-	-	-	-	-	-	-0.72	0.49	-	-
λ_{afb_4}	-	-	-	-	-	-	-	-	-	-	-	-	-	-	0.46	0.19
P_{mic_4}	-	-	-	-	-	-	-	-	-	-	-	-	-1.09	0.28	-	-
λ_{mic_4}	-	-	-	-	-	-	-	-	-	-	-	-	-	-	-0.32	0.09
P_{mol_4}	-	-	-	-	-	-	-	-	-	-	-	-	-0.69	0.55	-	-
λ_{mol_4}	-	-	-	-	-	-	-	-			-	-	-	-	0.02	0.95
P_{total_4}	-	-	-	-	-	-	0.96	0.54	0.57	0.71	-	-	-	-	-	-
λ_{total_4}	-	-	-	-	-	-	-	-	-	-	0	1	-	-	-	-
P_{afb_6}	-	-	-	-	-	-	-	-	-	-	-	-	0.9	0.42	-	-
λ_{afb_6}	-	-	-	-	-	-	-	-	-	-	-	-	-	-	0.6	0.16
P_{mic_6}	-	-	-	-	-	-	-	-	-	-	-	-	-1.69	0.09	-	-
λ_{mic_6}	-	-	-	-	-	-	-	-	-	-	-	-	-	-	-0.31	0.12
P_{mol_6}	-	-	-	-	-	-	-	-	-	-	-	-	-1.15	0.31	-	-
λ_{mol}	-	-	-	-	-	-	-	-	-	-	-	-	-	-	-0.3	0.44
P_{total_6}	-	-	-	-	-	-	2.45	0.17	2.08	0.24	-	-	-	-	-	-
λ_{total_6}	-	-	-	-	-	-	-	-	-	-	0.46	0.4	-	-	-	-
D_{afb}	-	-	-	-	5.52	<0.001	-	-	-	-	-	-	5.93	<0.001	-	-
D_{mic}	-	-	-	-	-2	0.34	-	-	-	-	-	-	-1.54	0.33	-	-
D_{mol}	-	-	-	-	1.5	0.26	-	-	-	-	-	-	1.47	0.13	-	-
D_{bat}	-	-	2.21	0.01	-	-	-	-	0.91	0.36	-	-	-	-	-	-
PopDen	-1.7	<0.001	-1.79	<0.001	-2.03	<0.001	-1.84	<0.001	-1.84	<0.001	-1.84	<0.001	-2.01	<0.001	-1.87	<0.001
fragIndex	0.54	0.15	0.53	0.15	0.03	0.97	0.44	0.34	0.44	0.31	0.46	0.25	0.1	0.84	0.32	0.48
BVD	4.96	<0.001	4.73	<0.001	4.27	<0.001	4.62	<0.001	4.57	<0.001	4.55	<0.001	4.06	<0.001	4.13	<0.001
D_{MNB}	6.34	<0.001	3.97	<0.001	3.74	0.09	6.08	<0.001	5.16	<0.001	4.05	<0.001	3.67	0.04	5.36	<0.001
qAIC	325.99		271.56		481.71		358.26		320.38		272.43		280.96		340.56	
$\hat{c}$	0.82		0.69		1.32		0.92		0.81		0.69		0.71		0.87	

Table B.2 Model for all alternative animal spatGLM models with modified African birth pulse terms. Terms not included in that model are denoted by "-"

Model:	P_{tot*}		$D_{tot} + P_{tot*}$		$D_{tot} \times P_{tot*}$		$D_{tax} + P_{tax*}$		$D_{tax} \times P_{tax*}$	
	Estimate	P value	Estimate	P value	Estimate	P value	Estimate	P value	Estimate	P value
Intercept)	-25.46	<0.001	-27.81	<0.001	-31.44	<0.001	-29.16	<0.001	-33.39	<0.001
P_{afb*}	-	-	-	-	-	-	2.2	0.05	-	-
λ_{afb*}	-	-	-	-	-	-	-	-	2.32	0.06
P_{mic}	-	-	-	-	-	-	-0.13	0.89	-	-
λ_{mic}	-	-	-	-	-	-	-	-	0	1
P_{mol}	-	-	-	-	-	-	-0.79	0.5	-	-
λ_{mol}	-	-	-	-	-	-	-	-	0.13	0.78
P_{total*}	2.41	0.42	3.78	0.17	-	-	-	-	-	-
λ_{total*}	-	-	-	-	2.8	0.04	-	-	-	-
P_{afb*_2}	-	-	-	-	-	-	0.99	0.38	-	-
λ_{afb*_2}	-	-	-	-	-	-	-	-	1.7	0.17
P_{mic_2}	-	-	-	-	-	-	1.58	0.12	-	-
λ_{mic_2}	-	-	-	-	-	-	-	-	0.19	0.41
P_{mol_2}	-	-	-	-	-	-	0.34	0.8	-	-
λ_{mol_2}	-	-	-	-	-	-	-	-	0.49	0.36
P_{total*_2}	-6.27	0.13	-5.04	0.18	-	-	-	-	-	-
λ_{total*_2}	-	-	-	-	-1.6	0.32	-	-	-	-
P_{afb*_4}	-	-	-	-	-	-	-1.57	0.2	-	-
λ_{afb*_4}	-	-	-	-	-	-	-	-	-0.79	0.51
P_{mic_4}	-	-	-	-	-	-	-0.94	0.38	-	-
λ_{mic_4}	-	-	-	-	-	-	-	-	-0.41	0.07
P_{mol_4}	-	-	-	-	-	-	-0.59	0.63	-	-
λ_{mol_4}	-	-			-	-	-	-	-0.12	0.81
P_{total*_4}	-6.03	0.15	-4.81	0.2	-	-	-	-	-	-
λ_{total*_4}	-	-	-	-	-1.55	0.35	-	-	-	-
P_{afb*_6}	-	-	-	-	-	-	0.78	0.51	-	-
λ_{afb*_6}	-	-	-	-	-	-	-	-	1.44	0.28
P_{mic_6}	-	-	-	-	-	-	-1.38	0.18	-	-
λ_{mic_6}	-	-	-	-	-	-	-	-	-0.3	0.16
P_{mol_6}	-	-	-	-	-	-	-1.07	0.36	-	-
λ_{mol}	-	-	-	-	-	-	-	-	-0.25	0.58
P_{total*_6}	2.18	0.48	3.49	0.22	-	-	-	-	-	-
λ_{total*_6}	-	-	-	-	2.68	0.05	-	-	-	-
D_{afb}	-	-	-	-	-	-	5.97	<0.001	-	-
D_{mic}	-	-	-	-	-	-	-1.65	0.31	-	-
D_{mol}	-	-	-	-	-	-	1.6	0.1	-	-
D_{bat}	-	-	2.21	0.01	-	-	-	-	-	-
PopDen	-1.72	<0.001	-1.79	<0.001	-1.78	<0.001	-2.01	<0.001	-1.91	<0.001
fragIndex	0.54	0.15	0.54	0.13	0.54	0.11	0.07	0.88	0.13	0.82
BVD	4.93	<0.001	4.75	<0.001	4.79	<0.001	3.96	<0.001	3.8	<0.001
D_{MNB}	5.97	<0.001	3.89	<0.001	4.1	<0.001	3.54	0.05	4.26	0.02
qAIC	315.64		253.83		252.21		295.64		390.43	
$\hat{c}$	0.79		0.63		0.63		0.75		1.05	

Table B.3 Model for all alternative human spatGLM models. Terms not included in that model are denoted by "-"

Model:	Null		D_{tot}		D_{tax}		B_{tot}		$D+B_{tot}$		$D\times B_{tot}$		$D+B_{tax}$		$D\times B_{tax}$	
	Estimate	P value	Estimate	P value	Estimate	P value	Estimate	P value	Estimate	P value	Estimate	P value	Estimate	P value	Estimate	P value
Intercept)	-29.82	<0.001	-29.03	<0.001	-29.66	<0.001	-28.73	<0.001	-32.76	<0.001	-28.73	<0.001	-31.62	<0.001	-28.62	<0.001
P_{afb}	-	-	-	-	-	-	-	-	-	-	-	-	-1.49	0.14	-	-
λ_{afb}	-	-	-	-	-	-	-	-	-	-	-	-	-	-	-0.25	0.53
P_{mic}	-	-	-	-	-	-	-	-	-	-	-	-	1.48	0.06	-	-
λ_{mic}	-	-	-	-	-	-	-	-	-	-	-	-	-	-	0.23	0.22
P_{mol}	-	-	-	-	-	-	-	-	-	-	-	-	-0.45	0.66	-	-
λ_{mol}	-	-	-	-	-	-	-	-	-	-	-	-	-	-	-0.31	0.43
P_{total}	-	-	-	-	-	-	0.79	0.22	1.88	0.27	-	-	-	-	-	-
λ_{total}	-	-	-	-	-	-	-	-	-	-	0.79	0.22	-	-	-	-
P_{afb_2}	-	-	-	-	-	-	-	-	-	-	-	-	1.39	0.15	-	-
λ_{afb_2}	-	-	-	-	-	-	-	-	-	-	-	-	-	-	0.98	0.01
P_{mic_2}	-	-	-	-	-	-	-	-	-	-	-	-	-0.37	0.63		
λ_{mic_2}	-	-	-	-	-	-	-	-	-	-	-	-	-	-	-0.2	0.23
P_{mol_2}	-	-	-	-	-	-	-	-	-	-	-	-	0.11	0.92		
λ_{mol_2}	-	-	-	-	-	-	-	-	-	-	-	-	-	-	-0.08	0.85
P_{total_2}	-	-	-	-	-	-	1.94	0.01	4.5	0.04	-	-	-	-	-	-
λ_{total_2}	-	-	-	-	-	-	-	-	-	-	1.94	0.01	-	-	-	-
P_{afb_4}	-	-	-	-	-	-	-	-	-	-	-	-	-0.02	0.98	-	-
λ_{afb_4}	-	-	-	-	-	-	-	-	-	-	-	-	-	-	0.5	0.14
P_{mic_4}	-	-	-	-	-	-	-	-	-	-	-	-	-0.95	0.3	-	-
λ_{mic_4}	-	-	-	-	-	-	-	-	-	-	-	-	-	-	-0.17	0.37
P_{mol_4}	-	-	-	-	-	-	-	-	-	-	-	-	0.38	0.73	-	-
λ_{mol_4}	-	-	-	-	-	-					-	-	-	-	0.41	0.35
P_{total_4}	-	-	-	-	-	-	-0.13	0.78	-0.5	0.71	-	-	-	-	-	-
λ_{total_4}	-	-	-	-	-	-	-	-	-	-	-0.13	0.78	-	-	-	-
P_{afb_6}	-	-	-	-	-	-	-	-	-	-	-	-	1.29	0.19	-	-
λ_{afb_6}	-	-	-	-	-	-	-	-	-	-	-	-	-	-	0.68	0.08
P_{mic_6}	-	-	-	-	-	-	-	-	-	-	-	-	-0.23	0.78	-	-
λ_{mic_6}	-	-	-	-	-	-	-	-	-	-	-	-	-	-	0.03	0.86
P_{mol_6}	-	-	-	-	-	-	-	-			-	-	1.48	0.13	-	-
λ_{mol}	-	-	-	-	-	-	-	-	-	-	-	-	-	-	0.53	0.17
P_{total_6}	-	-	-	-	-	-	0.09	0.87	0.29	0.85	-	-	-	-	-	-
λ_{total_6}	-	-	-	-	-	-	-	-	-	-	0.09	0.87	-	-	-	-
D_{afb}	-	-	-	-	3.16	<0.001	-	-	-	-	-	-	2.88	<0.001	-	-
D_{mic}	-	-	-	-	1.99	0.18	-	-	-	-	-	-	1.92	0.18	-	-
D_{mol}	-	-	-	-	-0.43	0.61	-	-	-	-	-	-	-0.63	0.43	-	-
D_{bat}	-	-	3.21	<0.001	-	-	-	-	2.64	0.01	-	-	-	-	-	-
PopDen	-0.23	0.24	-0.29	0.05	-0.25	0.07	-0.28	0.04	-0.28	0.05	-0.28	0.04	-0.23	0.08	-0.27	0.08
fragIndex	-0.21	0.54	-0.26	0.34	-0.38	0.17	-0.31	0.25	-0.3	0.26	-0.31	0.25	-0.4	0.12	-0.36	0.22
BVD	-11.04	0.99	-11.29	0.98	-11.21	0.98	-10.94	0.98	-11.01	0.98	-10.94	0.98	-11.43	0.98	-11.37	0.98
D_{MNB}	5.61	<0.001	2.88	0.02	2.92	0.01	3.37	<0.001	3.36	0.01	3.37	<0.001	3.36	<0.001	4.72	<0.001
OB_{an}	5.17	<0.001	4.96	<0.001	4.47	<0.001	4.74	<0.001	4.74	<0.001	4.74	<0.001	4.5	<0.001	4.73	<0.001
$\text{OB}_{\text{an}_{t-1}}$	2.02	0.28	1.92	0.17	2.03	0.1	1.91	0.14	1.93	0.14	1.91	0.14	2.71	0.02	2.62	0.06
qAIC		1076.48		613.37		512.88		677.95		533.35		522.57		457.58		630.23
$\hat{c}$		1.87	1.08			0.91		1.18		0.93		0.92		0.79		1.10

Table B.4 Model for all alternative human spatGLM models with modified African birth terms. Terms not included in that model are denoted by "-"

Model:	P_{tot*}		$D_{tot} + P_{tot*}$		$D_{tot} \times P_{tot*}$		$D_{tax} + P_{tax*}$		$D_{tax} \times P_{tax*}$	
	Estimate	P value	Estimate	P value	Estimate	P value	Estimate	P value	Estimate	P value
Intercept)	-3.81	<0.001	-9.4	0.29	-29.74	<0.001	-30.63	<0.001	-29.93	<0.001
$P_{\text{afb}*}$	-	-	-	-	-	-	-2.41	0.05	-	-
$\lambda_{\text{afb}*}$	-	-	-	-	-	-	-	-	-1.83	0.06
P_{mic}	-	-	-	-	-	-	1.83	0.89	-	-
λ_{mic}	-	-	-	-	-	-	-	-	0.26	1
P_{mol}	-	-	-	-	-	-	-0.19	0.5	-	-
λ_{mol}	-	-	-	-	-	-	-	-	-0.15	0.78
$P_{\text{total}*}$	-17.59	0.42	-15.29	0.01	-	-	-	-	-	-
$\lambda_{\text{total}*}$	-	-	-	-	-2.23	0.21	-	-	-	-
P_{afb_2*}	-	-	-	-	-	-	0.91	0.38	-	-
$\lambda_{\text{afb}*_2}$	-	-	-	-	-	-	-	-	1.89	0.17
P_{mic_2}	-	-	-	-	-	-	-0.06	0.12	-	-
λ_{mic_2}	-	-	-	-	-	-	-	-	-0.18	0.41
P_{mol_2}	-	-	-	-	-	-	0.29	0.8	-	-
λ_{mol_2}	-	-	-	-	-	-	-	-	-0.09	0.36
$P_{\text{total}*_2}$	-0.29	0.13	0.71	0.84	-	-	-	-	-	-
$\lambda_{\text{total}*_2}$	-	-	-	-	2.65	0.09	-	-	-	-
$P_{\text{afb}*_4}$	-	-	-	-	-	-	-0.39	0.2	-	-
$\lambda_{\text{afb}*_4}$	-	-	-	-	-	-	-	-	0.53	0.51
P_{mic_4}	-	-	-	-	-	-	-0.78	0.38	-	-
λ_{mic_4}	-	-	-	-	-	-	-	-	-0.24	0.07
P_{mol_4}	-	-	-	-	-	-	0.2	0.63	-	-
λ_{mol_4}	-	-			-	-	-	-	0.25	0.81
$P_{\text{total}*_4}$	-2.46	0.15	-0.91	0.8	-	-	-	-	-	-
$\lambda_{\text{total}*_4}$	-	-	-	-	2.14	0.17	-	-	-	-
$P_{\text{afb}*_6}$	-	-	-	-	-	-	1.6	0.51	-	-
$\lambda_{\text{afb}*_6}$	-	-	-	-	-	-	-	-	2.34	0.28
P_{mic_6}	-	-	-	-	-	-	-0.27	0.18	-	-
λ_{mic_6}	-	-	-	-	-	-	-	-	-0.04	0.16
P_{mol_6}	-	-	-	-	-	-	1.34	0.36	-	-
λ_{mol}	-	-	-	-	-	-	-	-	0.44	0.58
$P_{\text{total}*_6}$	-9.41	0.48	-7.28	0.09	-	-	-	-	-	-
$\lambda_{\text{total}*_6}$	-	-	-	-	0.07	0.96	-	-	-	-
D_{afb}	-	-	-	-	-	-	2.87	<0.001	-	-
D_{mic}	-	-	-	-	-	-	1.86	0.19	-	-
D_{mol}	-	-	-	-	-	-	-0.59	0.46	-	-
D_{bat}	-	-	2.1	0.04	-	-	-	-	-	-
PopDen	-0.21	0.2	-0.25	0.09	-0.29	0.07	-2.01	0.07	-0.25	0.08
fragIndex	-0.25	0.43	-0.28	0.33	-0.23	0.41	0.07	0.12	-0.38	0.17
BVD	-11.93	0.98	-11.88	0.98	-11.22	0.98	3.96	0.98	-11.53	0.98
D_{MNB}	4.73	<0.001	3.15	0.01	3.42	0.01	3.54	0.01	4.09	<0.001
OB_{an}	5.14	<0.001	5	<0.001	5.09	<0.001	4.56	<0.001	4.58	<0.001
$OB_{\text{an}_{l-1}}$	2.25	0.14	2.19	0.1	2.1	0.15	2.89	0.01	2.89	0.02
qAIC	757.58		595.88		664.63		454.93		542.84	
$\hat{c}$	1.35		1.06		1.16		0.78		0.96	

B.3 Figures

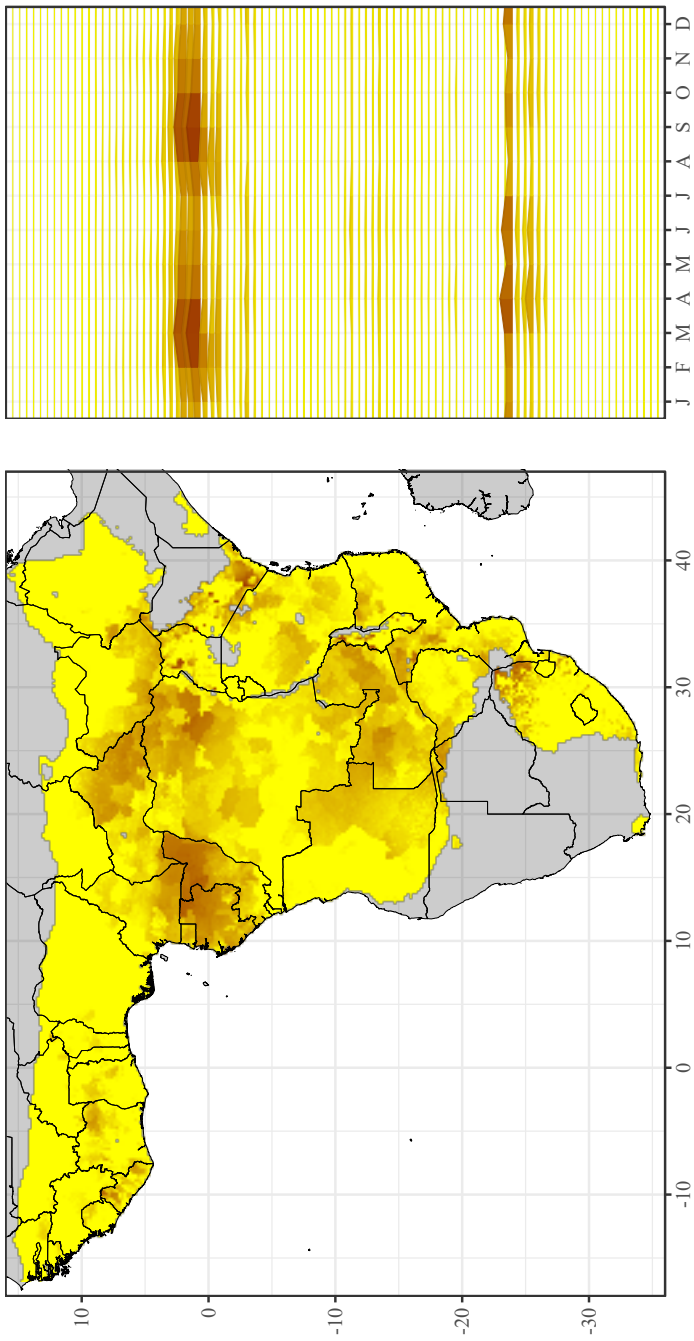


Fig. B.1 *Left:* Mean risk of EVD spillover to non-human reservoir hosts. *Right:* Risk of EVD spillover aggregated by latitude and month.

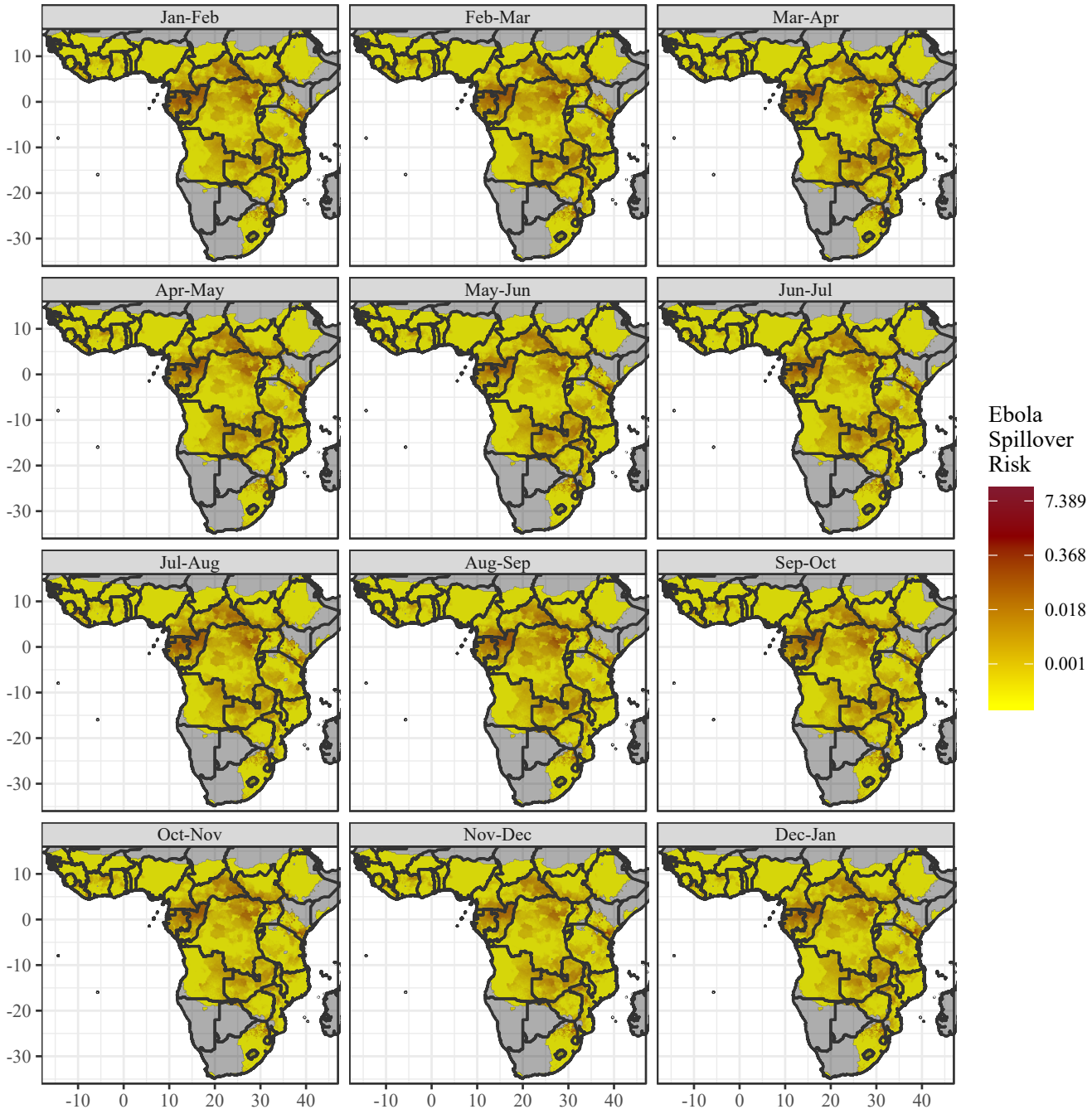


Fig. B.2 Monthly risk of ebolavirus spillover to non-human spillover hosts

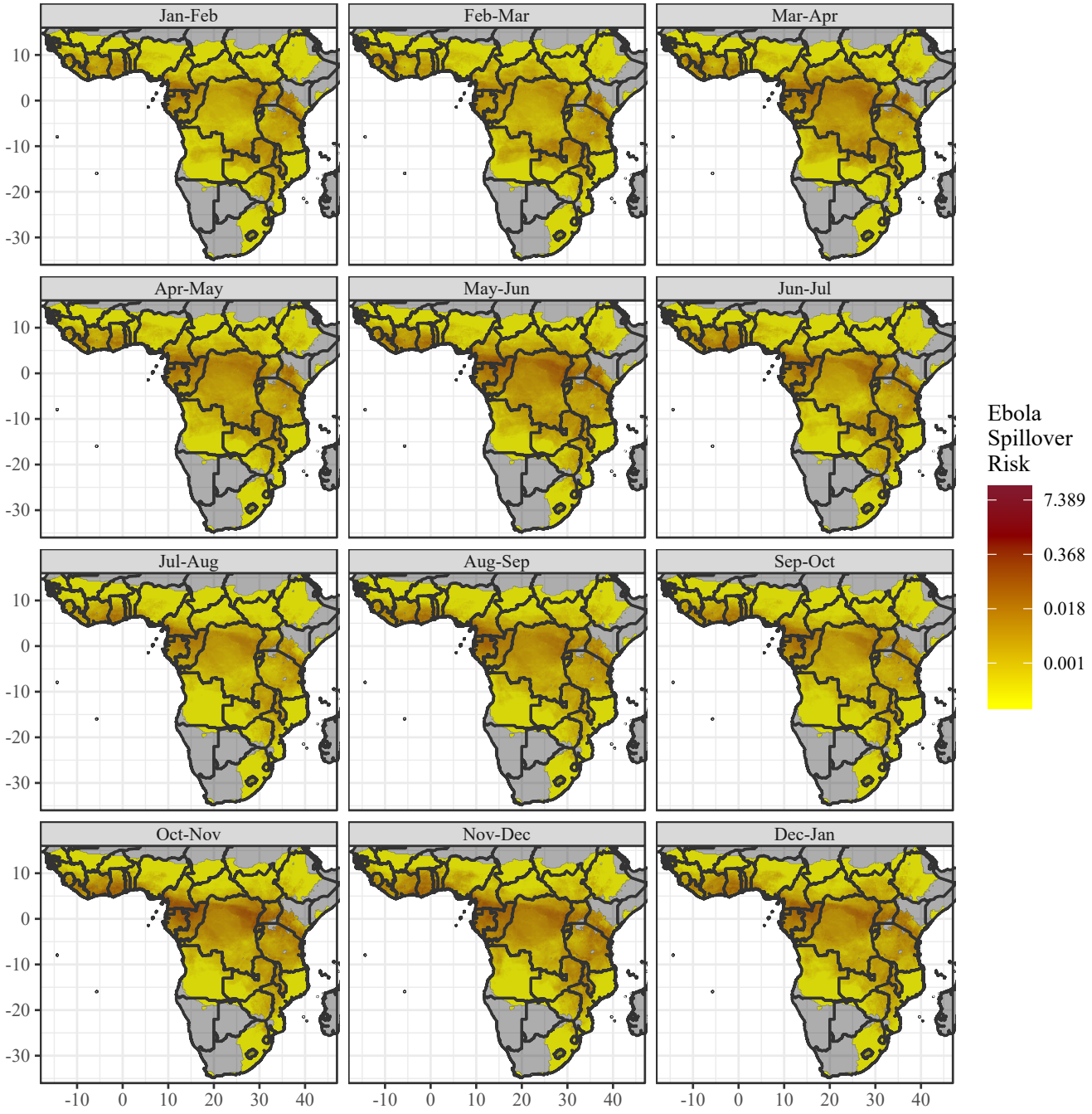


Fig. B.3 Monthly risk ebolavirus spillover into humans

Appendix C

What is a winter? Addressing data deficiencies for vital overwinter bat models

C.1 Tables

Table C.1 Data collection records for the duration of winter for *Myotis lucifugus*

ID	lat	long	Start	End	winter.duration	Ref
L1	53	-99	15/09/2018	15/05/2019	242	Czenze & Willis 2015
L2	51	-97	13/09/2018	15/05/2019	244	Norwuay & Willis 2014
L3	53	-99	15/09/2018	15/05/2019	242	Jonasson and Willis 2012
L4	60	-112	15/10/2018	15/05/2019	212	Reimer, Lausen & Barkley 2014
L5	45	-111	15/10/2018	10/04/2019	177	Johnson et al 2016
L6	39	-92	NA	NA	83	Brack and twente, 1985
L7	37	-84	4/12/2018	1/04/2019	118	Hayman and Cryan 2017
L8	58	-134	24/10/2018	31/03/2019	158	Karen Blejwas
L9	61	-135	30/09/2018	18/04/2019	200	Tom Jung
L10	60	-134	15/10/2018	24/03/2019	160	Cori Lausen
L11	59	-126	21/10/2018	15/04/2019	176	Cori Lausen
L12	59	-126	7/10/2018	7/04/2019	182	Cori Lausen
L13	60	-112	15/10/2018	15/04/2019	182	Sharon Irwin and Cori
L14	54	-117	15/09/2018	15/05/2019	242	Cori Lausen
L15	43	-74	10/10/2018	15/05/2019	217	Davis 1965
L16	61	-117	5/10/2018	20/04/2019	197	Joanna Wilson
L17	47	-111	NA	NA	180	SERDP
Bluff Lake	52	-125	15/10/2015	21/03/2016	158	WCS Recorder
Churn Creek	52	-122	21/10/2015	27/03/2016	158	WCS Recorder
CVWMA Under Interp Centre	49	-117	6/11/2012	27/04/2013	172	WCS Recorder
Des Belton House	55	-129	28/10/2015	1/03/2016	125	WCS Recorder
Dividend Mine Vicinity	49	-119	1/12/2012	11/03/2013	100	WCS Recorder
Fraser Lake	54	-125	25/09/2015	30/03/2016	187	WCS Recorder
Fraser Rock	52	-122	22/10/2015	29/03/2016	159	WCS Recorder
Gilpin Park Grand Forks	49	-118	13/12/2010	4/03/2011	81	WCS Recorder
Hazelton Skeena R	55	-128	11/10/2014	8/04/2015	179	WCS Recorder
Kasiks	54	-129	4/10/2014	16/03/2015	163	WCS Recorder
Kaslo 202 B Avenue	50	-117	20/11/2013	27/03/2014	127	WCS Recorder
Kuskanook	49	-117	28/12/2014	4/03/2015	66	WCS Recorder
Lakelse	54	-129	3/11/2015	5/03/2016	123	WCS Recorder
Lava Beds	55	-129	21/11/2015	25/03/2016	125	WCS Recorder
Liard Hot Springs	59	-126	25/09/2015	24/04/2016	212	WCS Recorder
Lillooet Rosebank Mine	51	-122	26/11/2014	17/04/2015	142	WCS Recorder
Lillooet Scallop Roost	51	-122	4/11/2014	18/04/2015	165	WCS Recorder
Lillooet Wanderers	51	-122	9/12/2014	2/03/2015	83	WCS Recorder
Lot48 Columbia Lake NC	50	-116	31/10/2013	25/03/2014	145	WCS Recorder
Lot48 Columbia Lake NCC	50	-116	21/09/2012	26/03/2013	186	WCS Recorder
Nass Bridge	55	-129	14/10/2014	15/03/2015	152	WCS Recorder
Next Creek NCC	49	-117	17/11/2012	14/03/2013	117	WCS Recorder
Oxbow Park	49	-118	17/12/2011	14/03/2012	88	WCS Recorder
Peachland roost	50	-120	23/10/2013	19/04/2014	178	WCS Recorder
Reclamation House RL	49	-117	17/11/2012	27/04/2013	161	WCS Recorder
Skaha Cave Hill	49	-120	15/06/2012	31/08/2012	77.5	WCS Recorder
Skaha Fortress	49	-120	16/11/2012	23/03/2013	127	WCS Recorder
Tahsis Anabat	50	-127	24/10/2014	1/03/2015	128	WCS Recorder
Telegraph Creek 2015	58	-131	4/10/2015	20/03/2016	168	WCS Recorder
Texada Island	50	-125	3/12/2015	4/03/2016	92	WCS Recorder
Tlingit office in Atlin	60	-134	6/10/2015	2/05/2016	209	WCS Recorder
Tow Hill	54	-132	30/12/2014	4/03/2015	64	WCS Recorder
Vanderhoof Butte	54	-125	18/10/2014	11/03/2015	144	WCS Recorder
Vaseux Lakeshore	49	-120	30/12/2013	4/03/2014	64	WCS Recorder

Table C.2 Data collection records for the mass of *Myotis lucifugus*

Lat	Long	avgMass	Ref	Location
39	-105	8.5	VertNet	NA
40	-122	7	VertNet	NA
40	-108	5.9	VertNet	NA
40	-97	7.3	VertNet	NA
40	-121	7	VertNet	NA
41	-105	7.7	VertNet	NA
43	-78	8.8	VertNet	NA
43	-78	6.9	VertNet	NA
44	-108	5.1	VertNet	NA
44	-76	14.5	VertNet	NA
44	-76	7.35	VertNet	NA
44	-76	9	VertNet	NA
44	-108	6.45	VertNet	NA
45	-90	8.2	VertNet	NA
45	-107	6.9	VertNet	NA
45	-107	5.4	VertNet	NA
45	-94	9.233333	VertNet	NA
48	-122	6.45	VertNet	NA
49	-122	6.725	VertNet	NA
58	-153	6	VertNet	NA
58	-135	6.527273	VertNet	NA
58	-135	6.65	VertNet	NA
59	-157	6.75	VertNet	NA
59	-135	7.08	VertNet	NA
59	-135	7.427273	VertNet	NA
59	-135	7.5	VertNet	NA
60	-135	8.042857	VertNet	NA
65	-148	5.6	VertNet	NA
65	-148	5.4	VertNet	NA
60	-112	8.966667	WCS Canada	Lane Lake-Pine Lake
60	-113	9.913636	WCS Canada	Little Buffalo Hibernaculum
60	-112	9.625	WCS Canada	Parson's Road
60	-112	9.940741	WCS Canada	WalkIn Cave
47	-111	8.221622	SERDP	Lick Creek Cave
42	-112	6.72	SERDP	Logan Cave
53	-117	11.20541	Schowalter 1980	Cadomin
45	-77	11.1	Mcguire 2009	Canada
47	-80	9.55	Fenton 1970	Gowganda
53	-99	12.56	McGuire2016	manatoba
43	-73	9.06	Kunz 1988	Mt. Aerols
43	-73	9.186011	Kunz 1995	Mt. Aerols
45	-77	10	Fenton 1970	Renfrew
49	-87	10.3	Fenton 1970	Schreiber
46	-82	9.5	Fenton 1970	Webbwood
45	-111	7.7625	Johnson 2016	yelowstone
60	-133	11.34	WCS Canada Yukon	Salmo Lake
60	-135	8.733333	WCS Canada Yukon	Wolf Creek

C.2 Figures

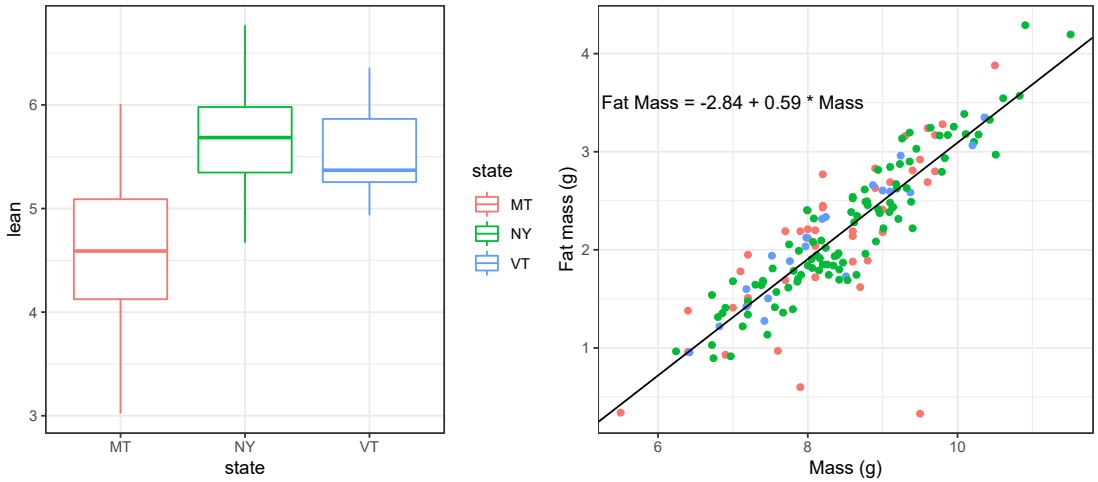


Fig. C.1 text**Compairison of body fat by state for *Myotis lucifugus***. *Left:* Comparison of lean body mass by state. *Right:* Linear relationship between body fat and body mass. Each point represents an individual bat and colors indicate the state each record originated from.

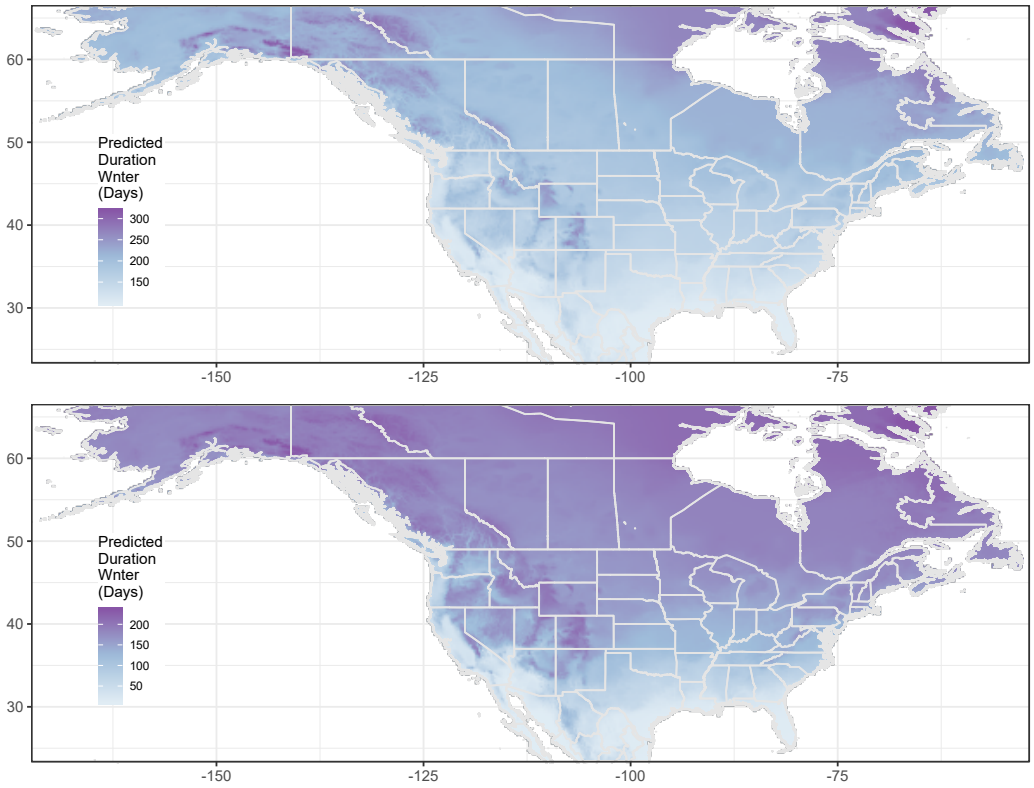


Fig. C.2 **95% Confidence Interval for predicted winter duration** The top panel shows the lower confidence bound, and the lower panel shows the upper confidence bound for the estimate winter duration.

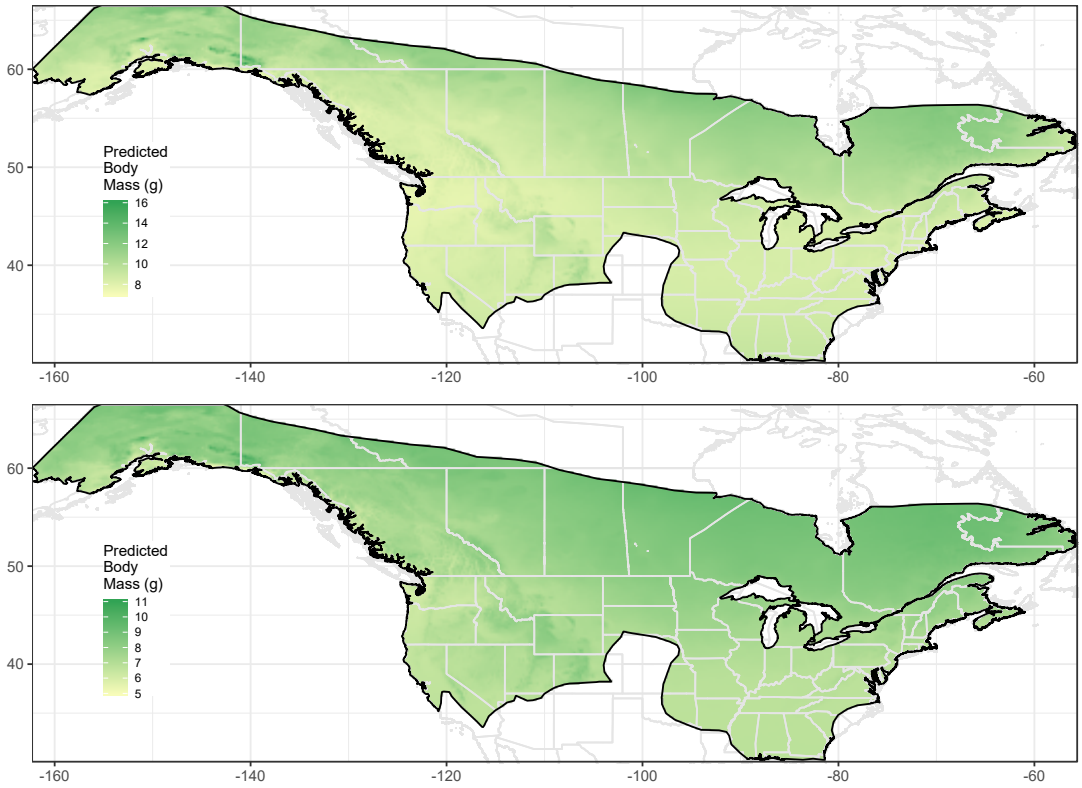


Fig. C.3 **95% Confidence Interval for predicted mass pre-hibernation.** The top panel shows the lower confidence bound, and the lower panel shows the upper confidence bound for the predicted body mass.

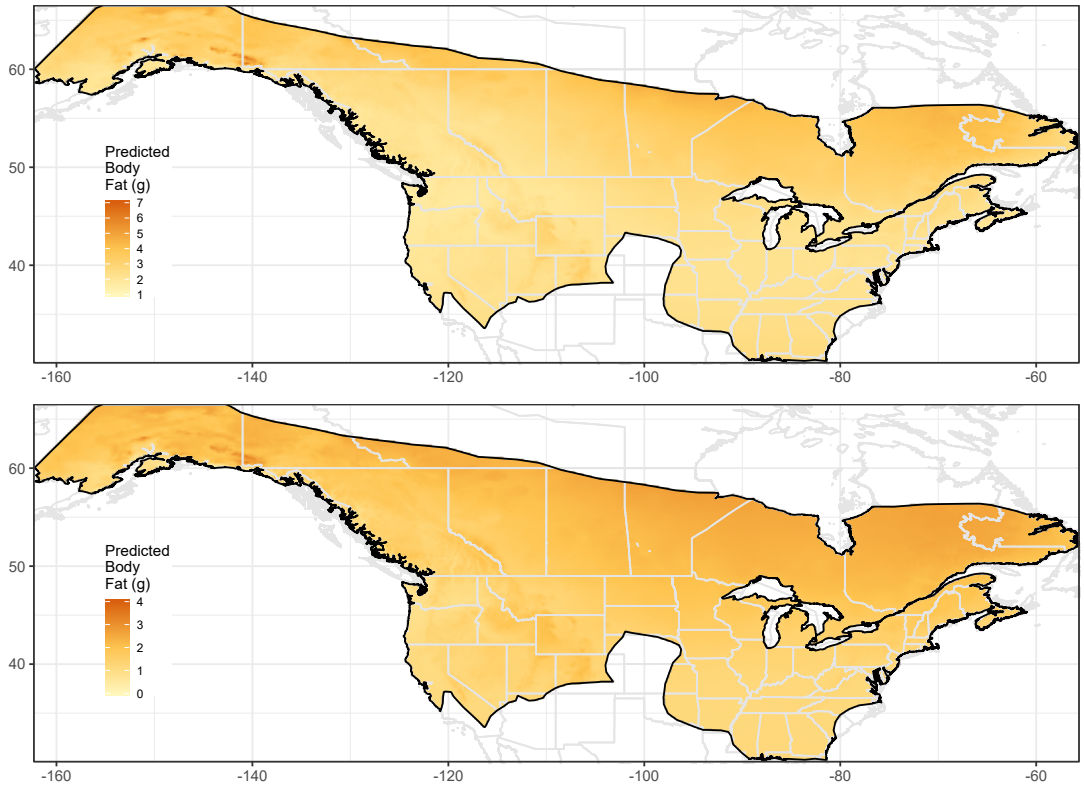


Fig. C.4 **95% Confidence Interval for predicted fat mass pre-hibernation.** The top panel shows the lower confidence bound, and the lower panel shows the upper confidence bound for the predicted fat mass available before hibernation.

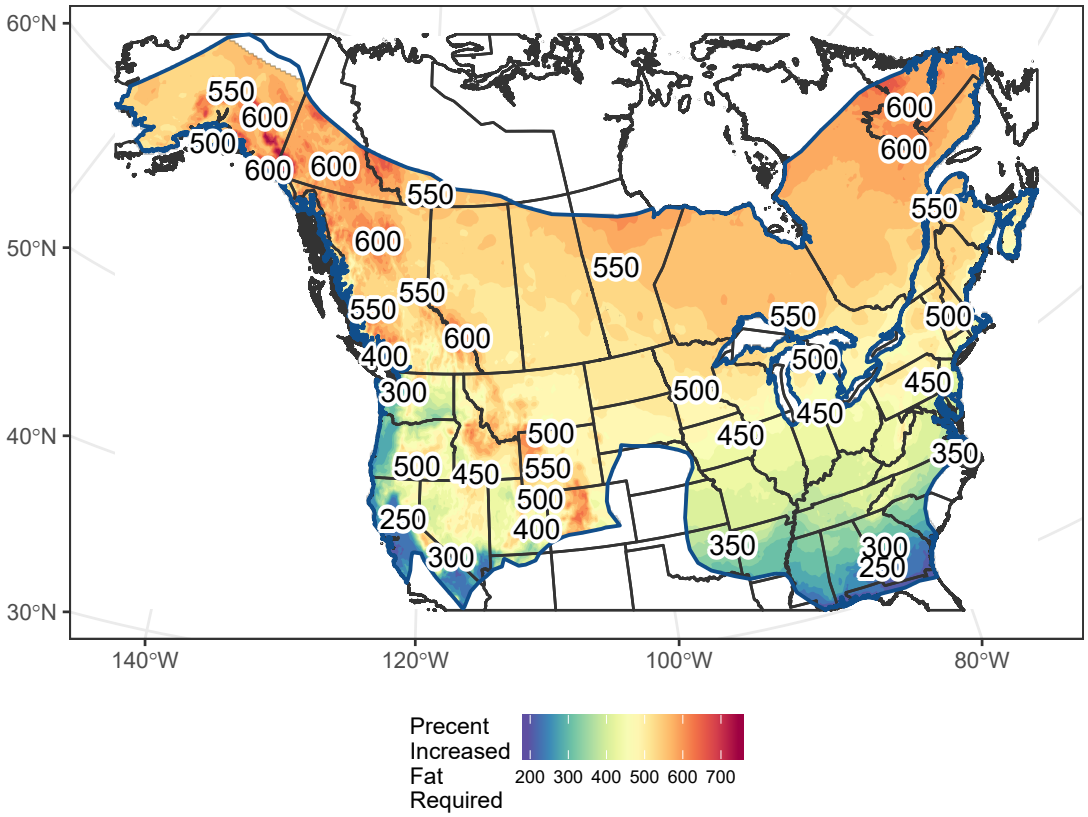


Fig. C.5 **Increased fat consumption due to infection for *Myotis lucifugus* when hibernating at $Ta = 2°$, and $RH = 100\%$.** Values are computed as a percent by $\frac{G_{fat,I}}{G_{fat,N}} * 100$ where I and N represent infected and uninfected (Null) respectively.

Appendix D

Bats are not squirrels: Revisiting the cost of cooling in hibernating mammals

Journal of Thermal Biology 81 (2019) 185–193

Contents lists available at ScienceDirect

Journal of Thermal Biology

journal homepage: www.elsevier.com/locate/jtherbio

Bats are not squirrels: Revisiting the cost of cooling in hibernating mammals

Catherine G. Haase[a,*], Nathan W. Fuller[b], C. Reed Hranac[c], David T.S. Hayman[c], Sarah H. Olson[d], Raina K. Plowright[a], Liam P. McGuire[b]

[a] Department of Microbiology and Immunology, Montana State University, 109 Lewis Hall, PO Box 173520, Bozeman, MT 59717, USA
[b] Department of Biological Sciences, Texas Tech University, 2901 Main St., Lubbock, TX 79409, USA
[c] Molecular Epidemiology and Public Health Laboratory, Hopkirk Research Institute, Massey University, Private Bag, 11 222, Palmerston North 4442, New Zealand
[d] Wildlife Conservation Society, 2300 Southern Boulevard, Bronx, NY 10460, USA

ARTICLE INFO

Keywords:
Bats
Cooling
Energetic model
Hibernation
Torpor
Winter survival

ABSTRACT

Many species use stored energy to hibernate through periods of resource limitation. Hibernation, a physiological state characterized by depressed metabolism and body temperature, is critical to winter survival and reproduction, and therefore has been extensively quantified and modeled. Hibernation consists of alternating phases of extended periods of torpor (low body temperature, low metabolic rate), and energetically costly periodic arousals to normal body temperature. Arousals consist of multiple phases: warming, euthermia, and cooling. Warming and euthermic costs are regularly included in energetic models, but although cooling to torpid body temperature is an important phase of the torpor-arousal cycle, it is often overlooked in energetic models. When included, cooling cost is assumed to be 67% of warming cost, an assumption originally derived from a single study that measured cooling cost in ground squirrels. Since this study, the same proportional value has been assumed across a variety of hibernating species. However, no additional values have been derived. We derived a model of cooling cost from first principles and validated the model with empirical energetic measurements. We compared the assumed 67% proportional cooling cost with our model-predicted cooling cost for 53 hibernating mammals. Our results indicate that using 67% of warming cost only adequately represents cooling cost in ground squirrel-sized mammals. In smaller species, this value overestimates cooling cost and in larger species, the value underestimates cooling cost. Our model allows for the generalization of energetic costs for multiple species using species-specific physiological and morphometric parameters, and for predictions over variable environmental conditions.

1. Introduction

Heterothermy is a thermoregulatory strategy employed by many mammals whereby body temperature (T_b) and metabolic rate are reduced in response to climatic conditions or reduced nutritional availability (Geiser, 1988; Lyman, 2013; Speakman and Thomas, 2003). Hibernation is an extreme form of extended heterothermy, which consists of cycles of torpor, or periods of low metabolic rate and T_b, and arousals, or periods of euthermic T_b (Geiser, 1988; Thomas et al., 1990). Each arousal consists of three phases: (1) warming from torpid T_b to euthermic T_b, (2) maintaining euthermic T_b, (3) and cooling from euthermic T_b back to torpid T_b. The energetics of hibernation are critical to winter survival, and hence this component of life history has been extensively quantified and modeled across many species (Hayman et al., 2016; Humphries et al., 2002; Thomas et al., 1990).

Although only a small fraction of hibernation is spent in euthermia, it accounts for up to 75–90% of winter energy budgets (Thomas et al., 1990). Because of the high energetic cost of arousal, most research has focused on quantifying these costs and how arousal frequency relates to energy budgets and survival (Geiser, 1988; Thomas et al., 1990; Wang, 1978). The energetic cost of warming has been calculated by a variety of models (Table 1), and all of these models focus on the temperature difference between euthermic and torpid T_b. This difference in T_b is scaled by the specific heat of animal tissue, which describes the energy required to warm 1 g of tissue by 1 °C (Wang, 1978). Beyond the cost to warming animal tissue, it is also important to consider the cost of maintaining metabolism during the time it takes to warm (typically against an environmental gradient of cool ambient temperature [T_a] relative to T_b). McKechnie and Wolf (2004) added this additional cost with the calculation of metabolism over the period of warming. Cryan and Wolf (2003) then incorporated the effect of thermal conductance on warming, accounting for heat lost to the environment. Both of these

* Corresponding author.
E-mail address: catherine.haase@montana.edu (C.G. Haase).

https://doi.org/10.1016/j.jtherbio.2019.01.013
Received 16 August 2018; Received in revised form 18 December 2018; Accepted 21 January 2019
Available online 06 March 2019
0306-4565/ © 2019 Elsevier Ltd. All rights reserved.

Table 1
Summary of previous studies that calculated energy expenditure during torpor or arousals, including the various methods by which warming and cooling costs have been considered. Warming models consider the effects of body mass (M_b), specific heat capacity of tissues (S), euthermic (T_{eu}) and torpid (T_b) body temperatures, and resting (RMR) and torpid (TMR) metabolic rates.

Species	Warming model	Cooling use	Reference
Various bats		None	(Prothero and Jürgens, 1986)
Myotis lucifugus	$M_b(T_{eu} - T_{tor})S$	67.2% of warming	(Thomas et al., 1990)
Myotis lucifugus	$(T_{eu} - T_{tor})S$	None	(Humphries et al., 2002)
Lasiurus cinereus	$(T_{eu} - T_{tor})S$	None	(Cryan and Wolf, 2003)
Lasiurus cinereus	$M_b(T_{eu} - T_{tor})S + \int_{t_1}^{t_2} C(T_{eu} - T_a)$	None	(Willis et al., 2006)
Myotis lucifugus	$[M_b(T_{eu} - T_{tor})S] + D^*_{warm}\left(TMR + \frac{RMR - TMR}{2}\right)$	65% of warming	(Frederico, 2007)
Myotis lucifugus	$(T_{eu} - T_{tor})S$	67% of warming	(Boyles and Brack, 2009)
Myotis lucifugus	$(T_{eu} - T_{tor})S$	67% of warming	(Boyles and McKechnie, 2010)
Various bats	$(T_{eu} - T_{tor})S$	67% of warming	(Boyles and Willis, 2010)
Myotis lucifugus	$(T_{eu} - T_{tor})S$	67% of warming	(Jonasson and Willis, 2012)**
Myotis lucifugus	$(T_{eu} - T_{tor})S$	67% of warming	(Ehlman et al., 2013)
Myotis lucifugus	$(T_{eu} - T_{tor})S$	None	(Burles et al., 2014)
Lasionycteris noctivagans	None	67.2% of warming	(McGuire et al., 2014)
Various bats	$M_b(T_{eu} - T_{tor})S + \int_{t_1}^{t_2} C(T_{eu} - T_a)$	None	(Hayman et al., 2016)
Myotis lucifugus	$(T_{eu} - T_{tor})S$	67.2% of warming	(Wilcox and Willis, 2016)
Myotis lucifugus	$[M_b(T_{eu} - T_{tor})S] + D^*_{warm}\left(TMR + \frac{RMR - TMR}{2}\right)$	67.2% of warming	(Czenze et al., 2017)
	$(T_{eu} - T_{tor})S$		

*D_{warm} is defined as the time required to warming tissues, a function of the rate of warming and gradient between euthermic and torpid body temperatures.
**Jonasson and Willis (2012) also used models published by Thomas et al. (1990) and Humphries et al. (2002) listed in the table.

models also incorporated the effects of warming rate, which is found to scale with body mass in both mammals and birds (Geiser and Baudinette, 1990; McKechnie and Wolf, 2004).

Cooling is also an important phase of the torpor-arousal cycle; however, this phase has been overlooked in modeling hibernation energetics (Henshaw, 1968; Kleiber, 1972). Most models of hibernation energetics have either used an assumed cost of cooling calculated from the cost of warming or excluded the cooling phase entirely (Table 1). Cooling is typically considered a passive process (but see discussions of metabolic suppression: Drew et al., 2007; Geiser, 2004; Heldmaier and Ruf, 1992; Snapp and Heller, 1981; Staples, 2014) and therefore requires less energy than warming (Geiser, 2004, 1988). However, the cooling phase still requires energy for metabolism over the period of time it takes to cool (Thomas et al., 1990; Wang, 1978), which can vary among taxa.

The energetic cost of cooling was first measured by Wang (1978) in Richardson's ground squirrels (*Urocitellus richardsonii*, formerly *Spermophilus richardsonii*) across winter hibernation at a range of T_a. Thomas et al. (1990) used Wang's measurements to calculate cooling cost as a proportion of warming cost, regardless of temperature, and found cooling costs were equivalent to 65–67% of the cost of warming. As the Thomas et al. (1990) energetic model has been frequently applied and revised, many subsequent hibernation energetic models have assumed the same proportional cost of cooling (Table 1). It is unclear whether this proportion is broadly representative across taxa.

We suspect that assuming proportional cooling costs could be problematic in other taxa for three reasons: differences in body size, differences in thermal conductance, and the influence of T_a on cooling rate. Estimates of cooling cost by the 67% proportion may overestimate cost in small-bodied species or underestimate cost for larger species due to the relationship between body mass and surface area (Berman, 2003; Gouma et al., 2012; Meeh, 1879). The higher surface area to volume ratio in smaller species lead to a greater rate of heat loss, and thus, for species smaller than Richardson's ground squirrels (the basis for the proportional cost estimate), there is a potential for a lower cooling cost than that predicted by 67% of warming. Additionally, thermal conductance has been observed to scale with body mass (Aschoff, 1981; Kleiber, 1972), and thus large-bodied species not only have greater body mass to cool, but are more resistant to heat loss. Thermal conductance can also vary within similar-sized species that reside in variable environments (Aschoff, 1981; Anon, 1987). Thus, it is possible that cooling rate may be more affected by T_a than warming rate due

Table 2
Measured and modeled costs (ml O_2 g^{-1}) of cooling into torpor from euthermia. Measured costs are reported from the referenced papers and modeled costs are from Eq. (2).

Species	T_a (°C)	Measured Costs	Modeled Costs	Data Reference
Erinaceus europaeus	5	4.73	4.65	Webb and Ellison (1998)
Glis glis	4	2.65	2.86	Wilz and Heldmaier (2000)
Marmota flaviventris	6	9.25	8.53	Armitage et al. (2003)
Marmota marmota	7	3.76	3.86	Heldmaier et al. (2004)
Urocitellus richardsonii	13–15	4.22[a]	4.50[b]	Wang (1978)
Urocitellus richardsonii	8–10	3.16[a]	3.85[b]	Wang (1978)
Urocitellus richardsonii	2–6	4.09[a]	3.98[b]	Wang (1978)
Zapus princeps	5	5.09	5.17	Cranford (1983)

[a] mean over all individuals.
[b] mean over all temperatures.

differences in physical and physiological processes in each phase (Nicol and Andersen, 2007), and therefore cooling cost may have higher variation with T_a compared to warming cost.

Many applications of the 67% cooling cost assumption have focused on bats (Table 1), which may have very different physiologies and cooling properties compared to ground squirrels (Bakken, 1976a; Strunk, 1971). Appropriately modeling hibernation energetics is important for understanding the impacts of white-nose syndrome (WNS) (Hayman et al., 2016), a disease of hibernating bats caused by an invasive fungal pathogen (Blehert et al., 2009; Lorch et al., 2013; Warnecke et al., 2012). WNS causes an increase in arousal frequency (Reeder et al., 2012; Warnecke et al., 2012), leading to premature depletion of fat stores and death (Hayman et al., 2016). Many studies have focused on the energetics associated with hibernation and WNS (Hayman et al., 2016; Mayberry et al., 2018; McGuire et al., 2017; Warnecke et al., 2013; Willis, 2015; Willis et al., 2011), and therefore energetic models represent an important tool for understanding the costs and consequences of the disease. This approach is especially timely as evidence suggests species differ in their susceptibility and response to WNS, due in part to interspecific variation in morphology and physiology, and microclimate selection during hibernation (Langwig et al., 2016; Langwig et al., 2012; Willis, 2015).

We investigated the energetic cost of cooling to determine if previous estimates are applicable across taxa. We developed a mathematical model to calculate the cost of cooling given the change in metabolic rate between euthermia and torpor and the rate at which an animal cools. Cooling rate was calculated using Newton's law of cooling (Bakken, 1976a; Newton, 1701; Prothero and Jürgens, 1986), which considers body mass, surface area, and thermal conductance in addition to the difference between euthermic T_b and T_a. We also determined if mass-specific cooling cost could be predicted by cooling rate. We then applied our model to a variety of species to test whether modeled cooling cost matched the oft cited 67% of warming cost and determined if any variation in the relationship is better described by differences in body size. Finally, given the scaling relationship found between body mass and warming rate, we determined if cooling rate could be predicted by body mass.

2. Materials and methods

2.1. Energetic costs of cooling

We modeled the energetic cost of cooling (E_{cool}) as a function of the difference between euthermic and torpid T_b, the decrease in metabolic rate over that temperature range, and the cooling rate. We assumed that cooling occurred passively; that is, the reduction in metabolic rate is due to an effect of temperature, rather than physiological inhibition (but see Geiser, 2016, 2004).

We calculated the total cost of cooling as the energy required for metabolism during steady-state torpor, plus the additional costs to maintain metabolism above torpid T_b as the body cools from euthermic T_b (Prothero and Jürgens, 1986; Strunk, 1971). We calculated this change using Q_{10}, or the change in metabolic rate over a 10 °C change in temperature, with a scaling equation with body mass (M_b; g)(Geiser, 1988):

$$Q_{10} = 3.82 - 0.507\log_{10}M_b \quad (1)$$

The cost of cooling was therefore calculated as the sum of this reduction in euthermic metabolic rate in response to the difference between torpid and euthermic T_b, and the metabolic rate of steady-state torpor:

$$E_{cool} = D_{cool}\left[TMR_{min} + \left(RMR \bullet Q_{10}^{\frac{T_{tor}-T_{eu}}{10}}\right)\right] \quad (2)$$

where TMR_{min} is the mass-specific minimum torpid metabolic rate (ml O_2 g^{-1} h^{-1}), RMR is the mass-specific resting metabolic rate at T_a (ml O_2 g^{-1} h^{-1}), T_{tor} and T_{eu} are torpid and euthermic T_b (°C), respectively, and D_{cool} is the duration of the cooling phase (h). We estimated RMR by increasing allometrically predicted BMR (Schmidt-Nielsen, 1984; Speakman and Thomas, 2003) in response to T_a and scaled by euthermic thermal conductance (C):

$$RMR = BMR + C(T_{eu} - T_a) \quad (3)$$

The duration of the cooling phase (D_{cool}) was determined by the cooling rate (CR) and the temperature difference between T_b:

$$D_{cool} = \frac{\log(T_{eu} - T_{tor})}{CR} \quad (4)$$

We assumed that cooling followed an exponential decay (Newton, 1701). Therefore we modeled the rate of cooling as a derivation from Newton's Law of Cooling (Henshaw, 1968; Kleiber, 1972; Newton, 1701; Strunk, 1971), which assumes the rate of heat loss from a body is directly proportional to body size, conductance, and temperature difference between the body and the surrounding environment (Bakken, 1976a; Prothero and Jürgens, 1986). We calculated the cooling rate as:

$$CR = \frac{C \bullet M_b^{0.67} \bullet \log(T_{eu} - T_a)}{S \bullet M_b} \quad (5)$$

where C is the thermal conductance during euthermia (ml O_2 g^{-1} $°C^{-1}$ h^{-1}), $M_b^{0.67}$ represents the surface area of the animal as defined by body mass, $T_{eu} - T_a$ is the difference between euthermic T_b and T_a (°C), and S is the specific heat of animal tissue (0.1728 ml O_2 g^{-1} $°C^{-1}$; Hart, 1951). By taking the log of the temperature difference in both Eqs. 4 and 5, we account for the exponential change in the rate of cooling as T_b is reduced to torpid body temperature. Rather than estimating an instantaneous cooling rate, this equation allowed for the consideration of body size and insulation of the animal (i.e. thermal conductance), as well as environmental influences (e.g., rapid cooling in cold environments).

Table 3
Parameters used to apply cooling model across mammalian species: cooling rate (CR; °C h^{-1}), warming rate (*WR*; °C h^{-1}), body mass (M_b; g), thermal conductance (C; ml O_2 g^{-1} °C^{-1}), euthermic (T_{eu}; °C) and torpid (T_{tor}; °C) body temperature, air temperature (T_a; °C), and Q_{10} rates.

Species, by order	CR	*WR*	M_b	C	T_{eu}	T_{tor}	T_a	Q_{10}	Reference [Conductance Reference]
Chiroptera									
Chalinolobus gouldii	1.29	84.0	12	0.34	36	6	5	3.27	Hosken and Withers (1997)
Corynorhinus townsendii	0.80	91.2[a]	10	0.20	37	9	8	3.32	CGH et al. (Unpublished data) Speakman and Thomas (2003)
Eptesicus fuscus	0.61	90.0[b]	18	0.20	37	16	15	3.19	Halsall et al. (2012) and Willis (2015)
Lasionycteris noctivagans	0.59	162.0[b]	11	0.15	35	6	5	3.30	Dunbar (2007)
Lasiurus borealis	0.46	106.8[b]	13	0.13	35	6	5	3.26	Dunbar and Tomasi (2006)
Lasiurus cinereus	0.53	128.4[b]	25	0.18	35	6	5	3.11	Cryan and Wolf (2003)
Myotis californicus	1.26	77.4[a]	5	0.26	35	11	10	3.47	CGH et al. (Unpublished data) Speakman and Thomas (2003)
Myotis lucifugus	1.11	64.0[a]	9	0.26	37	5	4	3.33	Czenze and Willis (2015) and Hayman et al. (2016)
Myotis myotis	0.51	24.2[a]	25	0.20	35	17	16	3.11	Wojciechowski et al. (2007)
Myotis nattereri	0.77	63.0[a]	8	0.18	35	10	8	3.36	Hope and Jones (2012) and Speakman and Thomas (2003)
Myotis velifer	0.70	50.0	14	0.20	37	9	8	3.23	CGH et al. (Unpublished data) Hirshfeld and O'Farrell (1976)
Myotis yumanensis	0.72	27.6	6	0.15	37	9	8	3.44	Licht and Leitner (1967) and O'Farrell and Studier (1970)
Nyctalus noctula	0.21	94.8[a]	27	0.07	37	5	5	3.09	Kayser (1964)
Nyctophilus geoffroyi	1.57	80.4[b]	8	0.36	36	6	6	3.37	Geiser and Brigham (2000) and Herreid and Kessel (1967)
Pipistrellus pipistrellus	1.10	57.0[a]	6	0.23	37	6	5	3.43	Kayser (1964)
Tadarida brasiliensis	0.90	43.8[a]	12	0.25	36	11	10	3.27	Herreid and Schmidt-Nielsen (1966)
Tadarida teniotis	0.45	46.8[a]	30	0.18	35	22	15	3.07	Marom et al. (2006)
Dasyuromorphia									
Dasyuroides byrnei	0.21	33.0[a]	120	0.13	34	11	10	2.77	Geiser and Baudinette (1987)
Planigale gilesi	1.19	57.0	8	0.33	33	10	15	3.36	Geiser and Baudinette (1988) and Stone and Purvis (1992)
Sminthopsis macroura	0.50	8.0[a]	28	0.22	34	21	19	3.09	Song et al. (1995)
Diprotodontia									
Burramys parvus	0.32	26.4[a]	54	0.14	36	3	2	2.94	Fleming (1985) and Herreid and Kessel (1967)
Cercartetus concinnus	0.70	47.4[a]	17	0.21	34	6	5	3.20	Geiser (1987)
Cercartetus lepidus	0.78	54.0[a]	12	0.21	34	6	5	3.27	Geiser (1987)
Cercartetus nanus	0.22	24.0[a]	70	0.11	35	6	5	2.88	Song et al. (1997)
Eulipotyphla									
Crocidura leucodon	0.61	54.0[a]	12	0.20	36	24	20	3.27	Nagel (1977)
Crocidura russula	0.69	54.0[a]	14	0.20	36	19	10	3.24	Nagel (1977)
Crocidura suaveolens	1.56	54.0[a]	8	0.37	36	20	10	3.38	Nagel (1977)
Erinaceus europaeus	0.19	10.2	505	0.18	34	11	10	2.45	Webb and Ellison (1998)
Rodentia									
Baiomys taylori	1.44	20.4	6	0.39	36	22	20	3.41	Hudson (1965)
Callospermophilus lateralis	0.18	20.0	137	0.12	35	16	15	2.74	Larkin and Heller (1996) and Snapp and Heller (1981)
Chaetodipus californicus	0.70	54.6	22	0.23	34	11	5	3.14	Tucker (1965)
Chaetodipus hispidus	0.47	21.0	40	0.21	38	18	17	3.01	Wang and Hudson (1970)
Cricetus cricetus	0.15	30.0[a]	370	0.13	35	10	8	2.52	Waßmer and Wollnik (1997) and Kayser (1964)
Eliomys quercinus	0.34	54.0[a]	80	0.17	33	6	5	2.86	Pajunen (1970) and Kayser (1964)
Glis glis	0.20	51.0[a]	100	0.11	36	8	8	2.81	Wilz and Heldmaier (2000) and Kayser (1961)
Ictidomys mexicanus	0.18	21.0[a]	190	0.14	36	15	17	2.66	Neumann and Cade (1965) and Snyder and Nestler (1990)
Ictidomys tridecemlineatus	0.16	27.0[a]	190	0.11	35	7	6	2.66	Pohl and Hart (1965) and Aschoff (1981)
Marmota broweri	0.03	2.9	2400	0.04	30	10	2	2.11	Lee et al. (2016)
Marmota flaviventris	0.02	2.3	3405	0.04	36	9	8	2.03	Arnold (1988) and Florant and Heller (1977)
Marmota marmot	0.02	5.0[a]	3870	0.04	34	10	7	2.00	Ortmann and Heldmaier (2000) and Kayser (1964)
Mesocricetus auratus	0.35	25.8[a]	80	0.17	37	5	4	2.86	Lyman (1948)
Microdipodops pallidus	0.53	48.0[a]	15	0.15	39	9	8	3.22	Bartholomew and MacMillen (1961)
Muscardinus avellanarius	0.87	66.0[a]	15	0.26	36	11	10	3.22	Pretzlaff and Dausmann (2012)
Otospermophilus beecheyi	0.11	2.6	502	0.12	32	15	14	2.45	Strumwasser (1959) and Aschoff (1981)
Perognathus longimembris	1.18	24.0[a]	8	0.27	35	5	3	3.35	Bartholomew and Cade (1957)
Phodopus sungorus	0.32	8.7	31	0.13	32	18	12	3.07	Heldmaier et al. (2004)
Sicista betulina	1.53	72.0[a]	10	0.38	38	6	5	3.31	Johansen and Krog (1959)
Spermophilus citellus	0.15	24.0[a]	290	0.11	36	6	1	2.57	Hut et al. (2002) and Aschoff (1981)
Tamias amoenus	0.52	56.0[a]	50	0.21	38	3	1	2.96	Geiser and Kenagy (1988) and Kenagy and Vleck (1982)
Tamias striatus	0.25	60.0[a]	92	0.13	35	6	5	2.82	Neal (1976) and Wang and Hudson (1970)
Urocitellus parryii	0.14	7.0	406	0.11	35	0	− 2	2.50	Boyer and Barnes (1999) and Hock (1960)
Urocitellus richardsonii	0.19	9.4	400	0.17	37	10	10	2.50	Wang (1978) and Snyder and Nestler (1990)
Zapus princeps	0.72	60.0[a]	26	0.25	33	6	5	3.10	Cranford (1983)
Monotremata									
Tachyglossus aculeatus	0.01	4.3	4600	0.03	33	2	2	1.96	Grigg et al. (1992) and Nicol and Andersen (2007)

[a] Geiser and Baudinette (1990).
[b] Menzies et al. (2016).

2.2. Model validation

To validate the cooling equation, we compiled data from published papers that presented metabolic rate and skin temperature curves over time and compared the total energetic cost of torpor entry (i.e., cooling) with modeled cost (Table 2). For publications where data was only presented in figures, we used plot digitizing software (WebPlotDigitizer 4.1; https://apps.automeris.io/wpd) to extract metabolic rate and skin temperature over the period of cooling. We calculated the mean of euthermic and torpid skin temperatures and defined the onset of

cooling when skin temperature dropped at least 2 °C below mean euthermic skin temperature and the end of cooling when skin temperature was within 0.5 °C of mean torpid skin temperature. We extracted metabolic rate for the cooling curve at one-hour intervals from the start and end of cooling and summed the values over the entire cooling period.

Using Eq. (2), we then modeled the energetic cost of cooling given morphometric, physiological, and environmental parameters reported in each publication. We obtained body mass, torpid and euthermic T_b, and thermal conductance (if available) for each species; if thermal conductance was not available, we calculated conductance using methodology described by McNab (1969) and Speakman and Thomas (2003). RMR was predicted using Eq. (3) and TMR was predicted using the Q_{10} decrease in BMR in response to torpid T_b (Geiser, 1988). One publication (Wang, 1978) reported cooling costs for multiple individuals over three ranges of T_a. Therefore, we calculated the mean cost for each temperature range over individuals (for the measured cost) and temperatures (for modeled cost). In instances where multiple data sources existed for the same species (as in the case of *Myotis lucifugus*), we chose the source that reported as many model parameters as possible.

We compared our modeled values to measured values using linear regression in R version 3.3.3 (R Development Core Team, 2009). We assumed that if our cooling model adequately represented measured cooling cost, the slope of the relationship would not be different than 1 (Glantz and Slinker, 2000). We did not run a sensitivity analysis of the model to changes in parameters, as a preliminary analysis showed that the model was sensitive to all parameters equally.

We examined the relationship between mass-specific cooling cost and both body size and thermal conductance to determine the effects of each variable on cooling. We also determined if a scaling relationship with body size and mass-specific cooling cost existed with cooling rate, similar to the relationships observed with warming rate (Geiser and Baudinette, 1990; McKechnie and Wolf, 2004).

2.3. Comparison between 67% proportion and cooling model

We compared the energetic cost of cooling for 53 species (Table 3) using both our cooling model (Eq. (2)) and the commonly-assumed 67% proportion of warming cost. We defined the energy required to warm from torpor to euthermia (E_{warm}) as a function of the cost to raise the temperature of animal tissue from torpid to euthermic T_b (McKechnie and Wolf, 2004), in addition to the metabolic costs required to balance heat lost to the environment over the period of warming (Cryan and Wolf, 2003). Thus, the cost of warming was calculated as:

$$E_{warm} = S\bullet(T_{eu} - T_{lor}) + D_{warm}[C(T_{eu} - T_a)] \quad (6)$$

where D_{warm} is the duration of time required to warm from torpid to euthermic T_b (h). Assuming warming occurs linearly (Cryan and Wolf, 2003; McKechnie and Wolf, 2004), we calculated D_{warm} as:

$$D_{warm} = \frac{T_{eu} - T_{tor}}{WR} \quad (7)$$

where WR is the warming rate for the species (°C h^{-1}). We obtained warming rates for each species from multiple sources (Geiser and Baudinette, 1990; Hirshfeld and O'Farrell, 1976; Menzies et al., 2016; Willis, 2008). All other model parameters were acquired as described above.

We compared both estimates of cooling, predicted from Eq. (2) and estimated as 67% of warming, using linear regression. If 67% of warming sufficiently described the cost of cooling, we assumed the slope of the relationship not to be different from 1 (Glantz and Slinker, 2000). We regressed the difference between the two estimates against body mass to examine differences in predicted cooling costs in the context of body size.

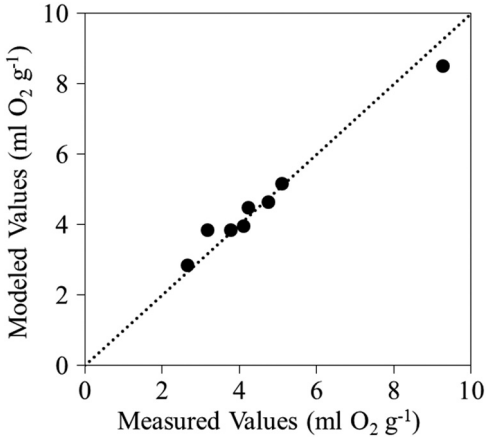


Fig. 1. Measured and modeled cooling cost (ml O_2 g^{-1}) of hibernating species used to validate a cooling cost model. Dashed line represents 1:1 line. Modeled cost was not different from measured cost (*slope* = 0.99 [0.939, 1.04], $F_{1,7}$ = 1220, p = < 0.001, r^2 = 0.99).

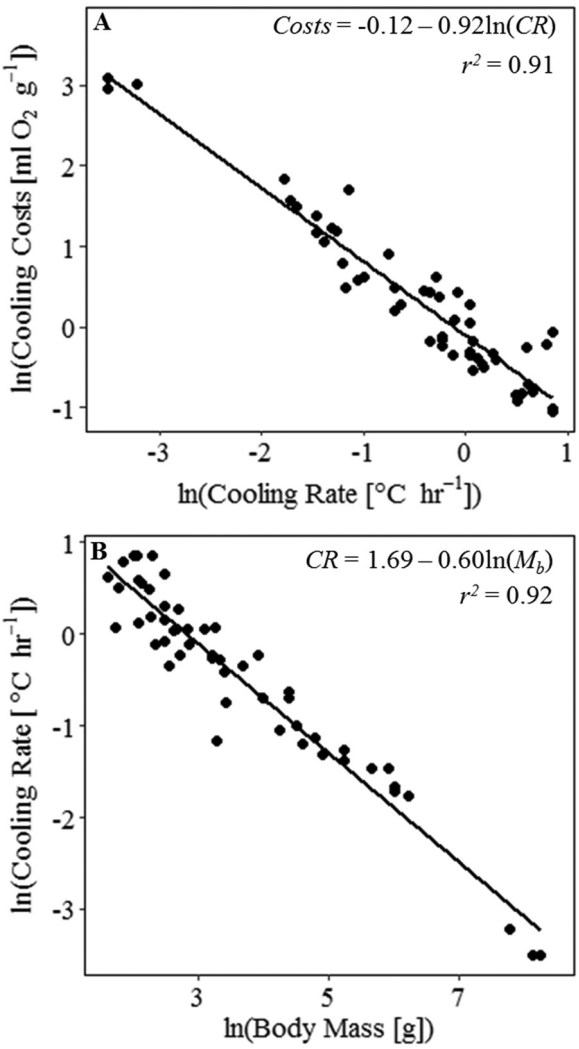


Fig. 2. Relationship between cooling rate (CR; °C h^{-1}) and A) body mass (g) and B) mass-specific cooling cost per arousal (ml O_2 g^{-1}) for 53 mammalian hibernators.

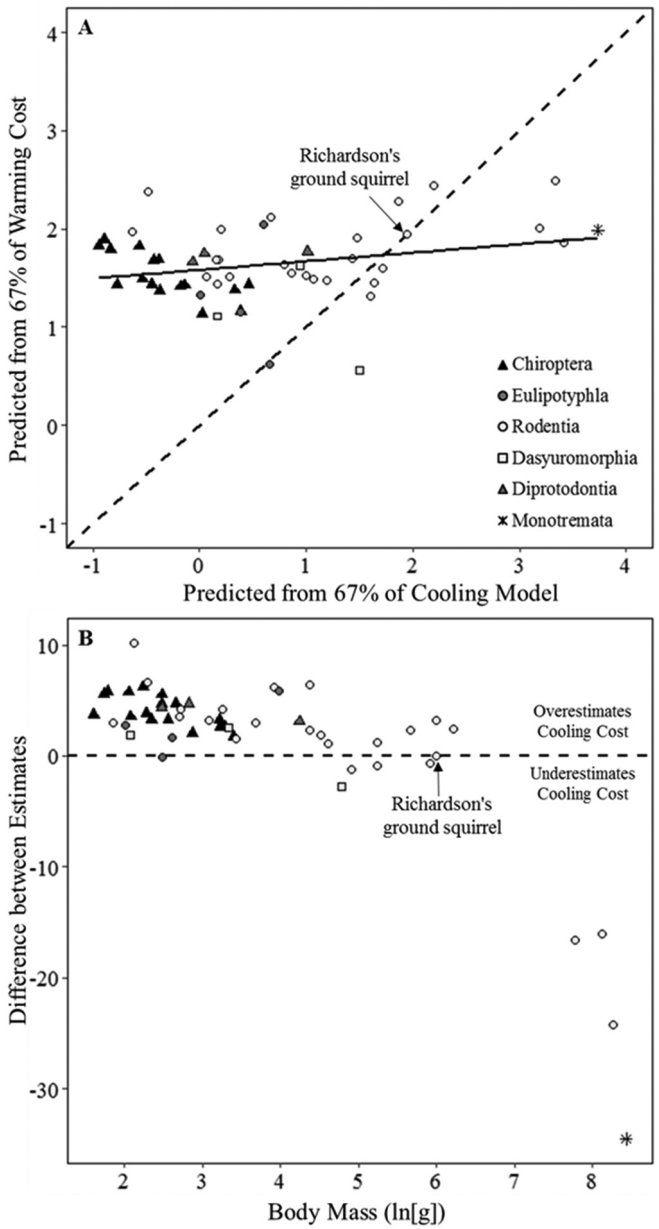


Fig. 3. A) Energetic cost of cooling (ln[ml O_2 g^{-1}]) for 53 mammalian species grouped by order and predicted from our cooling model and estimated from the commonly assumed 67% of warming costs. Dashed line represents one-to-one relationship between estimates and solid line is the fitted relationship. B) Relationship of the difference between cooling cost estimates (predicted from 67% of warming cost – cooling model; ml O_2 g^{-1}) and body mass (ln[*g*]). Dashed line represents 0 difference between estimates.

3. Results

Cooling cost from our model was not different from measured cost (*slope* = 0.99 [0.93, 1.04], $F_{1,7}$ = 1220, p = < 0.001, r^2 = 0.99; Table 2, Fig. 1). Mass-specific costs of cooling ranged from 0.36 ml O_2 g^{-1} in the Northern birch mouse (*Sicista betulina* [10 g]), one of the smallest species, to 41.9 ml O_2 g^{-1} in the short-beaked echidna (*Tachyglossus aculeatus* [4600 g]), the largest species in our dataset. Warming ranged from 2.8 ml O_2 g^{-1} in the bicolored shrew (*Crocidura leucodon* [12 g]) to 26.4 ml O_2 g^{-1} in the arctic ground squirrel (*Urocitellus parryii* [406 g]). Cooling was more energetically costly than warming in four species (*Marmota flaviventris*, *M. broweri, M. marmota,* and *T. aculeatus*), all of which had low thermal conductance values (< 0.05 ml O_2 g^{-1} °C^{-1} h^{-1}), large body sizes (> 2000 g), and thus slow cooling rates (< 0.5 °C h^{-1}).

Both body mass and thermal conductance were significant predictors of mass-specific cooling cost ($F_{1,51}$ =226.4, p < 0.001, r^2 = 0.90), with body mass and thermal conductance accounting for 88.9% and 10% of the variation in cooling cost across species, respectively. Mass-specific cooling cost decreased with increased cooling rate ($F_{1,51}$ = 506.4, p < 0.001, r^2 = 0.91; Fig. 2a), and cooling rate was inversely proportional to body mass ($F_{1,51}$ = 611.1, p < 0.001, r^2 = 0.92; Fig. 2b).

The oft-used 67% proportion of warming cost estimate of cooling cost did not describe cooling cost across taxa (*slope* = 0.07 [-0.03, 0.16], $F_{1,51}$ = 1.83, p = 0.18, r^2 = 0.03; Fig. 3a). Body mass, however, explained 47% of the variation in the difference between the two calculations ($F_{1,51}$ = 44.36, p < 0.001; Fig. 3b). The mean cooling cost was 47.9 ± 18% of warming cost, ranging from 3.8% in *Perognathus longimembris* (8.4 g), the little pocket mouse, to 383% in *T. aculeatus* (4600 g). Cooling cost represented 67% of warming cost in all ground squirrel species and one other species of similar body size: *Callospermophilus lateralis* (137 g, 58% [48–68%]), *Cricetus cricetus* (370 g, 76% [66–86%]), *Ictidomys mexicanus* (190 g, 74% [64–84%]), *I. tridecemlineatus* (190 g, 70% [60–80%]), *Otospermophilus beecheyi* (502 g, 57% [47–67%]), *Spermophilus citellus* (290 g, 58% [48–68%]), *U. parryii* (406 g, 60% [50–70%]), and *U. richardsonii* (406 g, 67% [57–77%]).

4. Discussion

The common assumption that the cost of cooling is equal to 67% of the cost of warming during arousal in hibernation is not broadly applicable across taxa. The cost of cooling scaled with body mass, which was expected given the relationship between the rate of heat loss and surface area to volume ratio (Bakken, 1976a). Consequently, cooling rate was inversely related to mass-specific cooling cost (Fig. 2a), suggesting cooling rate, as a function of body size and thermal conductance, is an important factor in hibernation energetics.

We attributed the mismatch between the two estimates of cooling cost to the fact that the 67% proportion relied on metabolic measurements from a squirrel species (*U. richardsonii*), which has a body mass that is not representative of the body size of most hibernating mammals. Due to the scaling relationship between body mass and surface area (Schmidt-Nielsen, 1984), smaller species have a greater amount of surface exposed to the environment per unit volume compared to larger species (Kleiber, 1972; Strunk, 1971). Greater surface area leads to greater heat loss and thus faster cooling rates, which we observed in the relationship between cooling rate and body mass (Fig. 2b). Therefore, the estimated 67% of the cost of warming overestimated the cost of cooling in species smaller than ground squirrels and underestimated the cost of cooling in larger species (Fig. 3). The fact that most of the variation in the relationship between both cooling cost calculations was described by body mass also supports these patterns. Incorporating both body size and surface area (scaled from body mass) in the calculation of cooling cost leads to more accurate estimates of the differences in cooling across taxa.

In addition to body size differences, body shape can affect cooling cost. Behavioral changes such as posture adjustments may be as important to heat exchange as the physiological properties of an animal (Satinoff, 1978; Stelzner and Hausfater, 1986). Even small postural changes can reduce exposed surface area and alter the amount of heat lost to the environment (Adair, 1976; Sale, 1970). For instance, when exposed to cold environments, captive pigs decrease heat loss by posture adjustments that reduce surface area by as much as 35% (Mount, 1964; Turnpenny et al., 2000). Similarly, *U. richardsonii* curl into a sphere when hibernating (Wang, 1978), whereas other species, such as bats, often remain cylindrical (Gouma et al., 2012). Our model does not consider differences in postural changes, but as the sphere has the least amount of surface area per unit of volume of all geometric shapes (Schmidt-Nielsen, 1970), species of the same body mass may have

considerable differences in heat loss due to changes in posture. However, as body size and thermal conductance account for almost 99% of the variation in cooling cost, postural changes could account for only 1% of the variation.

Air temperature can greatly influence the energetic costs associated with both the cooling and warming phases of hibernation: colder environments facilitate a faster rate of cooling and thus lower cooling cost (Bakken, 1976b; Henshaw, 1968) but substantially increase the cost of warming. Therefore, it is no surprise that deriving cooling cost from estimates of warming cost would not be accurate in most species across environments, as T_a has opposite effects on each phase. Though the proportion holds true for *U. richardsonii* in the environments that were measured in the Wang (1978) study, it may misrepresent cooling cost in other environments. By including the effect of T_a in both the cooling and warming models, we include a mechanistic influence of the environment on animal physiology.

The physiological mechanisms behind the cooling and warming processes also suggest it is inappropriate to estimate cooling cost from warming estimates. Warming is considered to be an active process in our analysis, where animals increase T_b using endogenous heat production to warm tissues (Geiser, 2004; but see discussion of passive rewarming below). In placental mammals, brown adipose tissue provides high metabolic heat production for nonshivering thermogenesis (Smalley and Dryer, 1963; Smith and Hock, 1963), while non-placentals (monotremes and marsupials) and birds generate heat by shivering (Johnston, 1971; Schmidt-Nielsen, 1987). Nonshivering thermogenesis has been reported to produce as much heat as shivering in species that do both (Janský, 2008), but the energetic costs of brown fat consumption compared to muscular activity required by shivering have yet to be compared. Differences in the efficiency between these two processes may potentially lead to interspecific differences in warming costs, which makes assumptions inaccurate for some species.

In contrast with active warming, our model assumed that entry into torpor was a passive process – that is, cooling was driven by heat loss rather than active metabolic suppression (Snapp and Heller, 1981). Snapp and Heller (1981) observed that the rate of metabolism decreases in response to temperature, i.e. the Q_{10} effect, supports the hypothesis that most mammals passively enter torpor. However, active metabolic inhibition (e.g. suppression of enzyme activity) may be required for deep torpor (Geiser, 2016, 2004). If active suppression is required for the cooling phase to occur, then cooling rate would also be driven by the ability to inhibit metabolism rather than just body size and thermal conductance. Due to the uncertainty behind when and in which species metabolic inhibition occurs, we assumed passive cooling, and did not account for any changes to metabolic rate. However, our model can be revised to include alterations to input parameters (e.g. metabolic rate) if active suppression alters metabolic rate for a species of interest.

Behavioral mechanisms, such as social thermoregulation, are not considered in our model and may limit model applicability. Social thermoregulation can occur when individuals cluster in hibernation. Social thermoregulation can potentially lead to passive rewarming, which occurs when individuals use increasing T_b of neighbors to synchronize their warming and decrease costs of arousal (Geiser, 2004). Passive rewarming can influence our calculations of warming costs in two different ways. First, lower efficiency of passive rewarming (Arnold, 1988) results in reduced warming rates. Second, because passive rewarming does not have the same energetic requirements of active rewarming, the total energetic cost of warming would be lower in these species (Currie et al., 2015). Although social thermoregulation has been hypothesized to reduce energetic costs associated with arousals and euthermia (Boyles et al., 2008), there has not been an indication of how it may influence cooling. Clustering can increase insulation of individuals and decrease surface area, both of which impede heat loss (Boyles et al., 2008). Though we do not specifically address these issues here, the use of equations to model both cooling and warming allows for modification of functional body size, thermal conductance, or cooling/warming rate once the effect of clustering on these parameters is determined. Using a mathematical equation to predict cooling costs, rather than a general assumption, allows for incorporation of thermoregulatory behavior into energetic modeling.

5. Conclusion

A common assumption used to predict the energetic cost of cooling may not represent cooling cost of all hibernators due to interspecific variation in body size, thermal conductance, and T_a exposure. We considered how mechanisms differed between the cooling and warming processes and how these differences may lead to a mismatch between the assumed proportion and modeled costs. We found that cooling rate scaled linearly with body mass and was a strong predictor of overall cooling cost. Our model allows for generalization of energetic cost for multiple taxa using species-specific physiological and morphometric parameters, and for predictions over variable environmental conditions. Accurate predictions are especially important in the context of wildlife conservation, as the case with predicting the energetic effects of white-nose syndrome on bat species across North America.

Acknowledgements

This project has been funded in part with Federal funds from the Department of Defense Strategic Environmental Research and Development Program [Contract Number W912HQ-16-C-0015]. RP was supported by Defense Advanced Research Projects Agency D16AP00113, National Science Foundation DEB-1716698, National Institutes of Health P20GM103474 and National Institutes of Health P30GM110732. Any opinions, findings, and conclusions or recommendations expressed in this publication are those of the author(s) and do not necessarily reflect the views of the Government.

References

Adair, E.R., 1976. Autonomic thermoregulation in squirrel monkey when behavioral regulation is limited. J. Appl. Physiol. 40, 694–700. https://doi.org/10.1152/jappl.1976.40.5.694.

Armitage, K.B., Blumstein, D.T., Woods, B.C., 2003. Energetics of hibernating yellow-bellied marmots (*Marmota flaviventris*). Comp. Biochem. Physiol. A. Mol. Integr. Physiol. 134, 101–114. https://doi.org/10.1016/S1095-6433(02)00219-2.

Arnold, W., 1988. Social thermoregulation during hibernation in alpine marmots (*Marmota marmota*). J. Comp. Physiol. B 158, 151–156. https://doi.org/10.1007/BF01075828.

Aschoff, J., 1981. Thermal conductance in mammals and birds: its dependence on body size and crcadian phase. Comp. Biochem. Physiol. A Physiol. 69, 611–619. https://doi.org/10.1016/0300-9629(81)90145-6.

Bakken, G.S., 1976a. A heat transfer analysis of animals: unifying concepts and the application of metabolism chamber data to field ecology. J. Theor. Biol. 60, 337–384. https://doi.org/10.1016/0022-5193(76)90063-1.

Bakken, G.S., 1976b. An improved method for determining thermal conductance and equilibrium body temperature with cooling curve experiments. J. Therm. Biol. 1, 169–175. https://doi.org/10.1016/0306-4565(76)90009-7.

Bartholomew, G.A., Cade, T.J., 1957. Temperature regulation, hibernation, and Aestivation in the little pocket mouse, *Perognathus longimembris*. J. Mammal. 38, 60–72. https://doi.org/10.2307/1376476.

Bartholomew, G.A., MacMillen, R.E., 1961. Oxygen consumption, estivation, and hibernation in the kangaroo mouse, *Microdipodops pallidus*. Physiol. Zool. 34, 177–183.

Berman, A., 2003. Effects of body surface area estimates on predicted energy requirements and heat stress. J. Dairy Sci. 86, 3605–3610. https://doi.org/10.3168/jds.S0022-0302(03)73966-6.

Blehert, D.S., Hicks, A.C., Behr, M., Meteyer, C.U., Berlowski-Zier, B.M., Buckles, E.L., Coleman, J.T.H., Darling, S.R., Gargas, A., Niver, R., Okoniewski, J.C., Rudd, R.J., Stone, W.B., 2009. Bat white-nose syndrome: an emerging fungal pathogen? (227–227). Science 323. https://doi.org/10.1126/science.1163874.

Boyer, B.B., Barnes, B.M., 1999. Molecular and metabolic aspects of mammalian hibernation: expression of the hibernation phenotype results from the coordinated regulation of multiple physiological and molecular events during preparation for and entry into torpor. BioScience 49, 713–724. https://doi.org/10.2307/1313595.

Boyles, J.G., Brack, V., 2009. Modeling survival rates of hibernating mammals with individual-based models of energy expenditure. J. Mammal. 90, 9–16. https://doi.org/10.1644/08-MAMM-A-205.1.

Boyles, J.G., McKechnie, A.E., 2010. Energy conservation in hibernating endotherms: why “suboptimal” temperatures are optimal. Ecol. Model. 221, 1644–1647. https://doi.org/10.1016/j.ecolmodel.2010.03.018.

Boyles, J.G., Storm, J.J., Brack, V., 2008. Thermal benefits of clustering during hibernation: a field test of competing hypotheses on *Myotis sodalis*. Funct. Ecol. 22, 632–636.
Boyles, J.G., Willis, C.K., 2010. Could localized warm areas inside cold caves reduce mortality of hibernating bats affected by white-nose syndrome? Front. Ecol. Environ. 8, 92–98. https://doi.org/10.1890/080187.
Burles, D.W., Fenton, M.B., Barclay, R.M., Brigham, R.M., Volkers, D., 2014. Aspects of the winter ecology of bats on Haida Gwaii, British Columbia. Northwest. Nat 95, 289–299. https://doi.org/10.1898/12-32.1.
Cranford, J.A., 1983. Body temperature, heart rate and oxygen consumption of normothermic and heterothermic western jumping mice (*Zapus princeps*). Comp. Biochem. Physiol. A 74, 595–599.
Cryan, P.M., Wolf, B.O., 2003. Sex differences in the thermoregulation and evaporative water loss of a heterothermic bat, *Lasiurus cinereus*, during its spring migration. J. Exp. Biol. 206, 3381–3390. https://doi.org/10.1242/jeb.00574.
Currie, S.E., Noy, K., Geiser, F., 2015. Passive rewarming from torpor in hibernating bats: minimizing metabolic costs and cardiac demands. Am. J. Physiol. Regul. Integr. Comp. Physiol. 308, R34–R41. https://doi.org/10.1152/ajpregu.00341.2014.
Czenze, Z.J., Jonasson, K.A., Willis, C.K.R., 2017. Thrifty females, frisky males: winter energetics of hibernating bats from a cold climate. Physiol. Biochem. Zool. 90, 502–511. https://doi.org/10.1086/692623.
Czenze, Z.J., Willis, C.K.R., 2015. Warming up and shipping out: arousal and emergence timing in hibernating little brown bats (*Myotis lucifugus*). J. Comp. Physiol. [B] 185, 575–586. https://doi.org/10.1007/s00360-015-0900-1.
Drew, K.L., Buck, C.L., Barnes, B.M., Christian, S.L., Rasley, B.T., Harris, M.B., 2007. Central nervous system regulation of mammalian hibernation: implications for metabolic suppression and ischemia tolerance. J. Neurochem. 102, 1713–1726. https://doi.org/10.1111/j.1471-4159.2007.04675.x.
Dunbar, M.B., 2007. Thermal energetics of torpid silver-haired bats *Lasionycteris noctivagans*. Acta Theriol. (Warsz.) 52, 65–68. https://doi.org/10.1007/BF03194200.
Dunbar, M.B., Tomasi, T.E., 2006. Arousal patterns, metabolic rate, and an energy budget of Eastern red bats (*Lasiurus borealis*) in winter. J. Mammal. 87, 1096–1102.
Ehlman, S.M., Cox, J.J., Crowley, P.H., 2013. Evaporative water loss, spatial distributions, and survival in white-nose-syndrome-affected little brown myotis: a model. J. Mammal. 94, 572–583. https://doi.org/10.1644/12-MAMM-A-111.1.
Fleming, M.R., 1985. The thermal physiology of the feathertail glider *Acrobates pygmaeus* (Marsupialia: burramyidae). Aust. J. Zool. 33, 667–681.
Florant, G.L., Heller, H.C., 1977. CNS regulation of body temperature in euthermic and hibernating marmots *(Marmota flaviventris*). Am. J. Physiol. 232, R203–R208. https://doi.org/10.1152/ajpregu.1977.232.5.R203.
Frederico, P., 2007. Bat Population Dynamics: an Individual-based Model Approach (Ph.D. Dissertation). University of Tennessee.
Geiser, F., 2016. Conserving energy during hibernation. J. Exp. Biol. 219, 2086–2087. https://doi.org/10.1242/jeb.129171.
Geiser, F., 2004. Metabolic rate and body temperature reduction during hibernation and daily torpor. Annu. Rev. Physiol. 66, 239–274. https://doi.org/10.1146/annurev.physiol.66.032102.115105.
Geiser, F., 1988. Reduction of metabolism during hibernation and daily torpor in mammals and birds: temperature effect or physiological inhibition? J. Comp. Physiol. B 158, 25–37. https://doi.org/10.1007/BF00692726.
Geiser, F., 1987. Hibernation and daily torpor in two pygmy possums (*Cercartetus* Spp., Marsupialia). Physiol. Zool. 60, 93–102.
Geiser, F., Baudinette, R.V., 1990. The relationship between body mass and rate of rewarming from hibernation and daily torpor in mammals. J. Exp. Biol. 151, 349–359.
Geiser, F., Baudinette, R.V., 1988. Daily torpor and thermoregulation in the small Dasyurid marsupials *Planigale gilesi* and *Ningaui yvonneae*. Aust. J. Zool. 36, 473–481.
Geiser, F., Baudinette, R.V., 1987. Seasonality of torpor and thermoregulation in three dasyurid marsupials. J. Comp. Physiol. B 157, 335–344. https://doi.org/10.1007/BF00693360.
Geiser, F., Brigham, R.M., 2000. Torpor, thermal biology, and energetics in Australian long-eared bats (*Nyctophilus*). J. Comp. Physiol. B 170, 153–162. https://doi.org/10.1007/s003600050270.
Geiser, F., Kenagy, G.J., 1988. Torpor duration in relation to temperature and metabolism in hibernating ground squirrels. Physiol. Zool. 61, 442–449.
Glantz, S., Slinker, B., 2000. Primer of Applied Regression & Analysis of Variance, 2 ed. McGraw-Hill Education / Medical, New York.
Gouma, E., Simos, Y., Verginadis, I., Lykoudis, E., Evangelou, A., Karkabounas, S., 2012. A simple procedure for estimation of total body surface area and determination of a new value of Meeh's constant in rats. Lab. Anim. 46, 40–45. https://doi.org/10.1258/la.2011.011021.
Grigg, G.C., Augee, M.L., Beard, L.A., 1992. Thermal Relations of Free-living Echidnas During Activity and in Hibernation in a Cold Climate. pp. 160–173.
Halsall, A.L., Boyles, J.G., Whitaker, J.O., 2012. Body temperature patterns of big brown bats during winter in a building hibernaculum. J. Mammal. 93, 497–503. https://doi.org/10.1644/11-MAMM-A-262.1.
Hart, J.S., 1951. Calorimetric determination of average body temperature of small mammals and its variation with environmental conditions. Can. J. Zool. 29, 224–233. https://doi.org/10.1139/z51-021.
Hayman, D.T.S., Pulliam, J.R.C., Marshall, J.C., Cryan, P.M., Webb, C.T., 2016. Environment, host, and fungal traits predict continental-scale white-nose syndrome in bats. Sci. Adv. 2, e1500831. https://doi.org/10.1126/sciadv.1500831.
Heldmaier, G., Ortmann, S., Elvert, R., 2004. Natural hypometabolism during hibernation and daily torpor in mammals. Respir. Physiol. Neurobiol. 141, 317–329. https://doi.org/10.1016/j.resp.2004.03.014.
Heldmaier, G., Ruf, T., 1992. Body temperature and metabolic rate during natural hypothermia in endotherms. J. Comp. Physiol. B 162, 696–706. https://doi.org/10.1007/BF00301619.
Henshaw, R.E., 1968. Thermoregulation during hibernation: application of Newton's law of cooling. J. Theor. Biol. 20, 79–90. https://doi.org/10.1016/0022-5193(68)90093-3.
Herreid, C.F., Kessel, B., 1967. Thermal conductance in birds and mammals. Comp. Biochem. Physiol. 21, 405–414. https://doi.org/10.1016/0010-406X(67)90802-X.
Herreid, C.F., Schmidt-Nielsen, K., 1966. Oxygen consumption, temperature, and water loss in bats from different environments. Am. J. Physiol. 211, 1108–1112.
Hirshfeld, J.R., O'Farrell, M.J., 1976. Comparisons of differential warming rates and tissue temperatures in some species of desert bats. Comp. Biochem. Physiol. A 55, 83–87.
Hock, R.J., 1960. Seasonal variations in physiologic functions of arctic ground squirrels and black bears. Bull. Mus. Comp. Zool. 124, 155–171.
Hope, P.R., Jones, G., 2012. Warming up for dinner: torpor and arousal in hibernating Natterer's bats (*Myotis nattereri*) studied by radio telemetry. J. Comp. Physiol. B 182, 569–578. https://doi.org/10.1007/s00360-011-0631-x.
Hosken, D.J., Withers, P.C., 1997. Temperature regulation and metabolism of an Australian bat, *Chalinolobus gouldii* (Chiroptera: vespertilionidae) when euthermic and torpid. J. Comp. Physiol. [B] 167 71–80.
Hudson, J.W., 1965. Temperature regulation and torpidity in the pygmy mouse, *Baiomys taylori*. Physiol. Zool. 38, 243–254.
Humphries, M.M., Thomas, D.W., Speakman, J.R., 2002. Climate-mediated energetic constraints on the distribution of hibernating mammals. Nature 418, 313–316. https://doi.org/10.1038/nature00828.
Hut, R.A., Barnes, B.M., Daan, S., 2002. Body temperature patterns before, during, and after semi-natural hibernation in the European ground squirrel. J. Comp. Physiol. [B] 172, 47–58.
Janský, L., 2008. Non-shivering thermogenesis and its thermoregulatory significance. Biol. Rev. 48, 85–132. https://doi.org/10.1111/j.1469-185X.1973.tb01115.x.
Johansen, K., Krog, J., 1959. Diurnal body temperature variations and hibernation in the birchmouse, *Sicista betulina*. Am. J. Physiol. -Leg. Content 196, 1200–1204. https://doi.org/10.1152/ajplegacy.1959.196.6.1200.
Johnston, D.W., 1971. The absence of brown adipose tissue in birds. Comp. Biochem. Physiol. A Physiol. 40, 1107–1108. https://doi.org/10.1016/0300-9629(71)90298-2.
Jonasson, K.A., Willis, C.K.R., 2012. Hibernation energetics of free-ranging little brown bats. J. Exp. Biol. 215, 2141–2149. https://doi.org/10.1242/jeb.066514.
Kayser, C., 1964. La depense d'energie des mammiferes en hibernation. Arch. Sci. Physiol. (Paris) 18, 137–150.
Kayser, C., 1961. The Physiology of Natural Hibernation. Pergamon Press.
Kenagy, G.J., Vleck, D., 1982. Daily temporal organization of metabolism in small mammals: adaptation and diversity. In: Vertebrate Circadian Systems, Proceedings in Life Sciences. Springer, Berlin, Heidelberg, pp. 322–338. https://doi.org/10.1007/978-3-642-68651-1_35.
Kleiber, M., 1972. Body size, conductance for animal heat flow and Newton's law of cooling. J. Theor. Biol. 37, 139–150. https://doi.org/10.1016/0022-5193(72)90120-8.
Langwig, K.E., Frick, W.F., Bried, J.T., Hicks, A.C., Kunz, T.H., Marm Kilpatrick, A., 2012. Sociality, density-dependence and microclimates determine the persistence of populations suffering from a novel fungal disease, white-nose syndrome. Ecol. Lett. 15, 1050–1057. https://doi.org/10.1111/j.1461-0248.2012.01829.x.
Langwig, K.E., Frick, W.F., Hoyt, J.R., Parise, K.L., Drees, K.P., Kunz, T.H., Foster, J.T., Kilpatrick, A.M., 2016. Drivers of variation in species impacts for a multi-host fungal disease of bats. Philos. Trans. R. Soc. B 371, 20150456. https://doi.org/10.1098/rstb.2015.0456.
Larkin, J.E., Heller, H.C., 1996. Temperature sensitivity of sleep homeostasis during hibernation in the golden-mantled ground squirrel. Am. J. Physiol. 270, R777–R784. https://doi.org/10.1152/ajpregu.1996.270.4.R777.
Lee, T.N., Kohl, F., Buck, C.L., Barnes, B.M., 2016. Hibernation strategies and patterns in sympatric arctic species, the Alaska marmot and the arctic ground squirrel. J. Mammal. 97, 135–144. https://doi.org/10.1093/jmammal/gyv163.
Licht, P., Leitner, P., 1967. Physiological responses to high environmental temperatures in three species of microchiropteran bats. Comp. Biochem. Physiol. 22, 371–387. https://doi.org/10.1016/0010-406X(67)90601-9.
Lorch, J.M., Muller, L.K., Russell, R.E., O'Connor, M., Lindner, D.L., Blehert, D.S., 2013. Distribution and environmental persistence of the causative agent of white-nose syndrome, *Geomyces destructans*, in bat hibernacula of the eastern United States. Appl. Environ. Microbiol. 79, 1293–1301. https://doi.org/10.1128/AEM.02939-12.
Lyman, C.P., 2013. Hibernation and Torpor in Mammals and Birds. Elsevier.
Lyman, C.P., 1948. The oxygen consumption and temperature regulation of hibernating hamsters. J. Exp. Zool. 109, 55–78. https://doi.org/10.1002/jez.1401090105.
Marom, S., Korine, C., Wojciechowski, M.S., Tracy, C.R., Pinshow, B., 2006. Energy metabolism and evaporative water loss in the European free-tailed bat and Hemprich's long-eared bat (Microchiroptera): species sympatric in the Negev Desert. Physiol. Biochem. Zool. PBZ 79, 944–956. https://doi.org/10.1086/505999.
Mayberry, H.W., McGuire, L.P., Willis, C.K.R., 2018. Body temperatures of hibernating little brown bats reveal pronounced behavioural activity during deep torpor and suggest a fever response during white-nose syndrome. J. Comp. Physiol. [B] 188, 333–343. https://doi.org/10.1007/s00360-017-1119-0.
McGuire, L.P., Jonasson, K.A., Guglielmo, C.G., 2014. Bats on a budget: torpor-assisted migration saves time and energy. PLoS One 9, e115724. https://doi.org/10.1371/journal.pone.0115724.
McGuire, L.P., Mayberry, H.W., Willis, C.K.R., 2017. White-nose syndrome increases torpid metabolic rate and evaporative water loss in hibernating bats. Am. J. Physiol. Regul. Integr. Comp. Physiol. 313, R680–R686. https://doi.org/10.1152/ajpregu.00058.2017.
McKechnie, A.E., Wolf, B.O., 2004. The energetics of the rewarming phase of avian

torpor. In: Barnes, B.M., Carey, H.V. (Eds.), Life in the Cold: Evolution, Mechanisms, Adaptiation, and Applications. International Hibernation Symposium Institute of Arctic Biology, University of Alaska, Fairbanks, Alaska.
Meeh, K., 1879. Oberflächenmessungen des menschlichen Körpers. Z. Biol. 15, 425–458.
Menzies, A.K., Webber, Q.M.R., Baloun, D.E., McGuire, L.P., Muise, K.A., Coté, D., Tinkler, S., Willis, C.K.R., 2016. Metabolic rate, latitude and thermal stability of roosts, but not phylogeny, affect rewarming rates of bats. Physiol. Behav. 164, 361–368. https://doi.org/10.1016/j.physbeh.2016.06.015.
Mount, L.E., 1964. Radiant and convective heat loss from the new-born pig. J. Physiol. 173, 96–113.
Nagel, A., 1977. Torpor in the European white-toothed shrews. Experientia 33, 1455–1456. https://doi.org/10.1007/BF01918804.
Neal, C.M., 1976. Energy budget of the eastern chipmunk (*Tamias striatus*): convective heat loss. Comp. Biochem. Physiol. A 54, 157–160.
Neumann, R.L., Cade, T.J., 1965. Torpidity in the Mexican ground squirrel *Citellus mexicanus parvidens* (mearns). Can. J. Zool. 43, 133–140. https://doi.org/10.1139/z65-011.
Newton, I., 1701. Scala graduum caloris, Calorum descriptiones & signa (scale of the degrees of heat). Philos. Trans. 22, 74–829.
Nicol, S.C., Andersen, N.A., 2007. Cooling rates and body temperature regulation of hibernating echidnas (*Tachyglossus aculeatus*). J. Exp. Biol. 210, 586–592. https://doi.org/10.1242/jeb.02701.
O'Farrell, M.J., Studier, E.H., 1970. Fall metabolism in relation to ambient temperatures in three species of Myotis. Comp. Biochem. 35–697.
Ortmann, S., Heldmaier, G., 2000. Regulation of body temperature and energy requirements of hibernating alpine marmots (*Marmota marmota*). Am. J. Physiol. Regul. Integr. Comp. Physiol. 278, R698–R704.
Pajunen, I., 1970. Body temperature, heart rate, breathing pattern, weight loss and periodicity of hibernation in the Finnish garden dormouse, *Eliomys quercinus* L. Ann. Zool. Fenn. 7, 251–266.
Pohl, H., Hart, J.S., 1965. Thermoregulation and cold acclimation in a hibernator, *Citellus tridecemlincatus*. J. Appl. Physiol. 20, 398–404. https://doi.org/10.1152/jappl.1965.20.3.398.
Pretzlaff, I., Dausmann, K.H., 2012. Impact of climatic variation on the hibernation physiology of *Muscardinus avellanarius*. In: Living in a Seasonal World. Springer, Berlin, Heidelberg, pp. 85–97. https://doi.org/10.1007/978-3-642-28678-0_8.
Prothero, J., Jürgens, K.D., 1986. An energetic model of daily torpor in endotherms. J. Theor. Biol. 121, 403–415. https://doi.org/10.1016/S0022-5193(86)80099-6.
R Development Core Team, 2009. R: a Language and Environment for Statistical Computing. R Foundation for Statistical Computing, Vienna, Austria.
Reeder, D.M., Frank, C.L., Turner, G.G., Meteyer, C.U., Kurta, A., Britzke, E.R., Vodzak, M.E., Darling, S.R., Stihler, C.W., Hicks, A.C., Jacob, R., Grieneisen, L.E., Brownlee, S.A., Muller, L.K., Blehert, D.S., 2012. Frequent arousal from hibernation linked to severity of infection and mortality in bats with white-nose syndrome. PLoS One 7, e38920. https://doi.org/10.1371/journal.pone.0038920.
Sale, J.B., 1970. The behaviour of the resting rock hyrax in relation to its environment. Zool. Afr. 5, 87–99. https://doi.org/10.1080/00445096.1970.11447383.
Satinoff, E., 1978. Neural organization and evolution of thermal regulation in mammals. Science 201, 16–22.
Schmidt-Nielsen, K., 1987. Animal Physiology: Adaptation and Environment, 3rd ed. Cambridge University Press, London ; New York.
Schmidt-Nielsen, K., 1984. Scaling: Why is Animal Size so Important?, 1 ed. Cambridge University Press, Cambridge ; New York.
Schmidt-Nielsen, K., 1970. Energy metabolism, body size, and problems of scaling. Fed. Proc. 29, 1524–1532.
Smalley, R.L., Dryer, R.L., 1963. Brown fat: thermogenic effect during arousal from hibernation in the bat. Science 140, 1333–1334.
Smith, R.E., Hock, R.J., 1963. Brown fat: thermogenic effector of arousal in hibernators. Science 140, 199–200.
Snapp, B.D., Heller, H.C., 1981. Suppression of metabolism during hibernation in ground squirrels (*Citellus lateralis*). Physiol. Zool. 54, 297–307. https://doi.org/10.1086/physzool.54.3.30159944.
Snyder, G.K., Nestler, J.R., 1990. Relationships between body temperature, thermal conductance, Q10 and energy metabolism during daily torpor and hibernation in rodents. J. Comp. Physiol. B 159, 667–675. https://doi.org/10.1007/BF00691712.
Song, X., Körtner, G., Geiser, F., 1997. Thermal relations of metabolic rate reduction in a hibernating marsupial. Am. J. Physiol. 273, R2097–R2104.
Song, X., Körtner, G., Geiser, F., 1995. Reduction of metabolic rate and thermoregulation during daily torpor. J. Comp. Physiol. B 165, 291–297. https://doi.org/10.1007/BF00367312.
Speakman, J.R., Thomas, D.W., 2003. Physiological ecology and energetics of bats. In: Kunz, T.H., Fenton, M.B. (Eds.), Bat Ecology. University Of Chicago Press, Chicago and London, pp. 430–490.
Staples, J.F., 2014. Metabolic suppression in mammalian hibernation: the role of mitochondria. J. Exp. Biol. 217, 2032–2036. https://doi.org/10.1242/jeb.092973.
Stelzner, J.K., Hausfater, G., 1986. Posture, microclimate, and thermoregulation in yellow baboons. Primates 27, 449–463. https://doi.org/10.1007/BF02381890.
Stone, G.N., Purvis, A., 1992. Warm-up rates during arousal from torpor in heterothermic mammals: physiological correlates and a comparison with heterothermic insects. J. Comp. Physiol. B 162, 284–295.
Strumwasser, F., 1959. Thermoregulatory, brain and behavioral mechanisms during entrance into hibernation in the squirrel, *Citellus beecheyi*. Am. J. Physiol. 196, 15–22.
Strunk, T.H., 1971. Heat loss from a Newtonian animal. J. Theor. Biol. 33, 35–61. https://doi.org/10.1016/0022-5193(71)90215-3.
Thomas, D.W., Dorais, M., Bergeron, J.-M., 1990. Winter energy budgets and cost of arousals for hibernating little brown bats, *Myotis lucifugus*. J. Mammal. 71, 475–479. https://doi.org/10.2307/1381967.
Tucker, V.A., 1965. Oxygen consumption, thermal conductance, and torpor in the California pocket mouse *Perognathus californicus*. J. Cell. Comp. Physiol. 65, 393–403. https://doi.org/10.1002/jcp.1030650313.
Turnpenny, J.R., Wathes, C.M., Clark, J.A., McArthur, A.J., 2000. Thermal balance of livestock: 2. applications of a parsimonious model. Agric. For. Meteorol. 101, 29–52. https://doi.org/10.1016/S0168-1923(99)00157-4.
Wang, L., Hudson, J.W., 1970. Some physiological aspects of temperature regulation in the normothermic and torpid hispid pocket mouse, *Perognathus hispidus*. Comp. Biochem. Physiol. 32, 275–293. https://doi.org/10.1016/0010-406X(70)90941-2.
Wang, L.C.H., 1978. Energetics and field aspects of mammalian torpor: the Richardson's ground squirrel. In: Wang, L.C.H., Hudson, J.W. (Eds.), Strategies in the Cold. Academic Press, New York, pp. 109–145.
Warnecke, L., Turner, J.M., Bollinger, T.K., Lorch, J.M., Misra, V., Cryan, P.M., Wibbelt, G., Blehert, D.S., Willis, C.K.R., 2012. Inoculation of bats with European *Geomyces destructans* supports the novel pathogen hypothesis for the origin of white-nose syndrome. Proc. Natl. Acad. Sci. USA 109, 6999–7003. https://doi.org/10.1073/pnas.1200374109.
Warnecke, L., Turner, J.M., Bollinger, T.K., Misra, V., Cryan, P.M., Blehert, D.S., Wibbelt, G., Willis, C.K.R., 2013. Pathophysiology of white-nose syndrome in bats: a mechanistic model linking wing damage to mortality. Biol. Lett. 9, 20130177. https://doi.org/10.1098/rsbl.2013.0177.
Waßmer, T., Wollnik, F., 1997. Timing of torpor bouts during hibernation in European hamsters (*Cricetus cricetus L.*). J. Comp. Physiol. B 167, 270–279. https://doi.org/10.1007/s003600050074.
Webb, P.I., Ellison, J., 1998. Normothermy, torpor, and arousal in hedgehogs (*Erinaceus europaeus*) from Dunedin. N. Z. J. Zool. 25, 85–90. https://doi.org/10.1080/03014223.1998.9518139.
Wilcox, A., Willis, C.K., 2016. Energetic benefits of enhanced summer roosting habitat for little brown bats (*Myotis lucifugus*) recovering from white-nose syndrome. Conserv. Physiol. 4, cov070.
Willis, C.K., 2015. Conservation physiology and conservation pathogens: white-nose syndrome and integrative biology for host–pathogen systems. Integr. Comp. Biol. 55, 631–641.
Willis, C.K.R., 2008. Do roost type or sociality predict warming rate? A phylogenetic analysis of torpor arousal. In: Lovegrove, B.G., McKechnie, A.E. (Eds.), Hypometabolism in Animals: Hibernation, Torpor and Cryobiology. School of Biological and Conservation Sciences, University of KwaZulu-Natal, Pietermaritzburg, pp. 373–384.
Willis, C.K.R., Brigham, R.M., Geiser, F., 2006. Deep, prolonged torpor by pregnant, free-ranging bats. Naturwissenschaften 93, 80–83. https://doi.org/10.1007/s00114-005-0063-0.
Willis, C.K.R., Menzies, A.K., Boyles, J.G., Wojciechowski, M.S., 2011. Evaporative water loss is a plausible explanation for mortality of bats from white-nose syndrome. Integr. Comp. Biol. 51, 364–373. https://doi.org/10.1093/icb/icr076.
Wilz, M., Heldmaier, G., 2000. Comparison of hibernation, estivation and daily torpor in the edible dormouse, *Glis glis*. J. Comp. Physiol. B 170, 511–521. https://doi.org/10.1007/s003600000129.
Wojciechowski, M.S., Jefimow, M., Tegowska, E., 2007. Environmental conditions, rather than season, determine torpor use and temperature selection in large mouse-eared bats (*Myotis myotis*). Comp. Biochem. Physiol. A. Mol. Integr. Physiol. 147, 828–840. https://doi.org/10.1016/j.cbpa.2006.06.039.

Appendix E

Incorporating evaporative water loss into bioenergetic models of hibernation to test for relative influence of host and pathogen traits on white-nose syndrome

PLOS ONE

RESEARCH ARTICLE

Incorporating evaporative water loss into bioenergetic models of hibernation to test for relative influence of host and pathogen traits on white-nose syndrome

Catherine G. Haase[1¤]*, Nathan W. Fuller[2], C. Reed Hranac[3], David T. S. Hayman[3], Liam P. McGuire[2], Kaleigh J. O. Norquay[4], Kirk A. Silas[5], Craig K. R. Willis[4], Raina K. Plowright[1‡], Sarah H. Olson[5‡]

1 Department of Microbiology and Immunology, Montana State University, Bozeman, Montana, United States of America, **2** Department of Biological Sciences, Texas Tech University, Lubbock, Texas, United States of America, **3** Molecular Epidemiology and Public Health Laboratory, Hopkirk Research Institute, Massey University, Palmerston North, New Zealand, **4** Department of Biology, University of Winnipeg, Winnipeg, Canada, **5** Wildlife Conservation Society, Wildlife Health Program, Bronx, New York, United States of America

¤ Current address: Department of Biology, Austin Peay State University, Clarksville, Tennessee, United States of America
‡ RKP and SHO are joint senior authors on this work.
* haasec@apsu.edu

Check for updates

OPEN ACCESS

Citation: Haase CG, Fuller NW, Hranac CR, Hayman DTS, McGuire LP, Norquay KJO, et al. (2019) Incorporating evaporative water loss into bioenergetic models of hibernation to test for relative influence of host and pathogen traits on white-nose syndrome. PLoS ONE 14(10): e0222311. https://doi.org/10.1371/journal.pone.0222311

Editor: De-Hua Wang, Institute of Zoology, CHINA

Received: August 22, 2019

Accepted: October 8, 2019

Published: October 31, 2019

Copyright: © 2019 Haase et al. This is an open access article distributed under the terms of the Creative Commons Attribution License, which permits unrestricted use, distribution, and reproduction in any medium, provided the original author and source are credited.

Data Availability Statement: All bat morphometric and physiological data files are available from the Dyrad database at doi: 10.5061/dryad.2280gb5n2.

Funding: This study was supported with equipment from Texas Tech University. This project has been funded in part with Federal funds from the Department of Defense Strategic Environmental Research and Development Program, under Contract Number W912HQ-16-C-0015 to SHO. RKP was supported by DARPA

Abstract

Hibernation consists of extended durations of torpor interrupted by periodic arousals. The 'dehydration hypothesis' proposes that hibernating mammals arouse to replenish water lost through evaporation during torpor. Arousals are energetically expensive, and increased arousal frequency can alter survival throughout hibernation. Yet we lack a means to assess the effect of evaporative water loss (EWL), determined by animal physiology and hibernation microclimate, on torpor bout duration and subsequent survival. White-nose syndrome (WNS), a devastating disease impacting hibernating bats, causes increased frequency of arousals during hibernation and EWL has been hypothesized to contribute to this increased arousal frequency. WNS is caused by a fungus, which grows well in humid hibernaculum environments and damages wing tissue important for water conservation. Here, we integrated the effect of EWL on torpor expression in a hibernation energetics model, including the effects of fungal infection, to determine the link between EWL and survival. We collected field data for *Myotis lucifugus*, a species that experiences high mortality from WNS, to gather parameters for the model. In saturating conditions, we predicted healthy bats experience minimal mortality. Infected bats, however, suffer high fungal growth in highly saturated environments, leading to exhaustion of fat stores before spring. Our results suggest that host adaptation to humid environments leads to increased arousal frequency from infection, which drives mortality across hibernaculum conditions. Our modified hibernation model provides a tool to assess the interplay between host physiology, hibernaculum microclimate, and diseases such as WNS on winter survival.

D16AP00113, NSF DEB-1716698, NIH P20GM103474, and NIH P30GM110732. DTSH is supported by RDF-MAU1701. CKRW and KJON were supported by NSERC, Canada, USFWS, and Species at Risk Research Fund of Ontario. The funders had no role in study design, data collection and analysis, decision to publish, or preparation of the manuscript.

Competing interests: The authors have declared that no competing interests exist.

Introduction

In periods of food scarcity, hibernators conserve energy by entering torpor, during which body temperature (T_b) is maintained near hibernaculum temperature and metabolic rate is lowered to reduce energy demands [1]. There are several hypotheses proposed to explain periodic arousals, but two of the most prominent are linked to water balance: 1) the dehydration hypothesis [2,3]; and 2) the need to excrete metabolic byproducts [4]. The dehydration hypothesis suggests that hibernators arouse periodically after a threshold of total body water is reached [5,6]. The metabolic byproducts hypothesis suggests that bats accumulate byproducts from biochemical reactions during torpor, and these byproducts need to be excreted as waste as they can be damaging to cellular function [4]. Both of these hypotheses are affected by microclimate, which is supported by empirical evidence of the relationship between hibernaculum temperature and relative humidity and torpor bout duration [3,5,7,8]. Hibernators do not normally defecate or urinate during torpor [9], thus water lost during inactive periods of hibernation is assumed to be from evaporation. Evaporative water loss (EWL) is comprised of respiratory and cutaneous water loss [10,11] and is driven by the difference in water vapor pressure between the surface of an animal and the surrounding air, which, in turn, is determined by the saturation of the air given air temperature [12]. The dehydration hypothesis is supported by correlations between torpor bout duration/arousal frequency and hibernaculum temperature and relative humidity in both free living and laboratory conditions [2,5,13].

Though arousals only make up a small portion of hibernation time, these periods account for the majority of the winter energy budget [1,14]. Therefore, the influence of microclimate on arousal frequency is critical for over-winter fat loss. However, the influence of microclimate has recently become an important question in the context of white-nose syndrome (WNS). WNS is a rapidly spreading infectious disease that has led to high mortality rates in hibernating bats across eastern and central North America. It has been proposed that increased EWL from infection could be a trigger of increased arousals associated with WNS [13,15].

The causal agent of WNS is a psychrophilic fungus, *Pseudogymnoascus destructans*, which erodes wing tissue [16,17]. Mechanistic models and empirical evidence connecting *P. destructans* infection to altered torpor-arousal cycles suggest that ulceration of the highly vascularized wing tissues causes increased fluid and water loss [13,18–21]. The growth rate of *P. destructans* is linked to both ambient temperature [22] and humidity [23], with higher fungal growth rates in environmental conditions frequently found in bat hibernacula.

Although studies have linked arousal frequency with survival, and hibernaculum microclimate and EWL with arousal frequency, none have explicitly considered the effect of EWL on survival to our knowledge. Hibernation energetic models are commonly used to understand energy consumption over winter but have yet to account for water balance and its effect on arousal behavior. With the current threat of WNS, a disease that potentially directly impacts water balance, it is important to understand the implications surrounding the association of EWL, energy consumption, and survival. We therefore developed a hibernation energetics model that incorporates water balance to assess the effects of the dehydration hypothesis on survival of *Myotis lucifugus*, a wide-ranging species that is heavily impacted by WNS. Using WNS as a study system, we tested the hypothesis that increased EWL from fungal infection results in greater energy consumption due to increased arousal frequency and, therefore, reduced survival. We predicted that hibernaculum conditions that reduce EWL (cold temperatures, high relative humidity) would increase our modeled survival rates. We also predicted that model parameters that influence EWL (surface area, area-specific rate of EWL), would have greater effects on modeled survival rates compared to other parameters.

Building on equations developed by Thomas et al. [1], Humphries et al. [24], and Hayman et al. [25], we included the effects of hibernaculum microclimate on fungal growth, EWL, torpor bout duration, and total fat loss. We parameterized the model using morphometric and physiological characteristics collected from *M. lucifugus* captured in the field. We validated the modified model components using a variety of data sources, determined the most influential parameters using a sensitivity analysis, and predicted fat loss over a range of hibernaculum conditions for both healthy and *P. destructans*-infected bats. Finally, in the context of winter duration, we inferred the impact of WNS on survival by comparing pre-hibernation fat stores to fat loss estimated by the energy expenditure model.

Methods

Ethics statement

All procedures were approved by the Texas Tech University Institutional Animal Care and Use Committee (protocol 16031–05) and followed guidelines of the Guide for the Care and Use of Laboratory Animals. We obtained proper permits from the Montana Department of Fish, Wildlife & Parks (permits 2016–104, 2017–018, and 2018–008).

Study species

M. lucifugus is a common insectivorous bat species found across most of North America [26]. The hibernation behavior of *M. lucifugus* is well-studied. During the winter, *M. lucifugus* hibernate in caves and abandoned mines, often in large colonies [26]. Most hibernacula have stable microclimates, with high humidity ($\geq$ 90% RH) and temperatures ranging from 2 to 8˚C [8,27,28]. Many energetic models have determined energy expenditure during hibernation in response to microclimate selection, sex, and location [1,8,24,29–35]. Energetic models have been used to predict energy expenditure from WNS with alterations to arousal frequency [21,32]. *M. lucifugus* is also one of the most studied species in terms of WNS impacts. Since the discovery of WNS in 2006, millions of *M. lucifugus* have died across the species' range and have faced upwards of 99% mortality rates [28,36,37]. Populations across eastern and mid-western North America affected by WNS remain at severely reduced population sizes and reduced population growth rates [36,38,39].

Field data collection for model parameters

We captured *M. lucifugus* during the pre-hibernation (September-November) swarming and mid-hibernation (January-February) periods from 2016–2018 at a cave in central Montana. We used mist nets placed at the cave entrance to capture bats during swarming and hand-captured bats from hibernaculum walls during mid-hibernation. We transported bats in cloth bags to a mobile laboratory at the field site location for morphometric measurements. We weighed each bat (± 0.1 g) and used quantitative magnetic resonance (Echo-MRI-B, Echo Medical Systems, Houston, TX) to measure fat mass and lean mass [40]. We measured torpid metabolic rate (TMR) and EWL using open-flow respirometry at 2, 5, 8, and 10˚C (S1 File; [41]). We calculated the mean body mass, fat mass, and lean mass across all fall field seasons and the mean of mass-specific TMR across both seasons among all individuals across to use as parameters in the hibernation model (Table 1).

We measured hibernaculum temperature and relative humidity over each hibernation period using HOBO (Model U23-001, ± 0.001˚C, ± 0.001% RH, Onset Computer Corporation) and iButton (temperature only; Model DS1921Z-F5, ± 0.05˚C, Maxim Integrated Products) dataloggers. We placed four HOBO and ten iButton dataloggers throughout the

Table 1. Parameters for the energetics model for the little brown bat (*Myotis lucifugus*), their units, and the reference.

Parameter Name	Parameter	Value	Units	Reference
Basal metabolic rate	BMR	2.6	ml O_2 g^{-1} h^{-1}	Calculated from [55]
Minimum torpid metabolic rate	TMR_{min}	0.03	ml O_2 g^{-1} h^{-1}	Measured in this study
Lower defended temperature during torpor	$T_{tor\text{-}min}$	2	˚C	[48–50]
Lower critical temperature	T_{lc}	32	˚C	[48–50]
Euthermic body temperature	T_{eu}	37	˚C	[1,48–50]
Change in torpid metabolism	Q_{10}	$1.6 + 0.26\ T_a — 0.006T_a^2$	-	[48]
Torpid thermal conductance	C_t	0.20	ml O_2 g^{-1}˚C^{-1} h^{-1}	Calculated from [73]
Euthermic thermal conductance	C_{eu}	0.26	ml O_2 g^{-1}˚C^{-1} h^{-1}	Calculated from [27]
Wing surface area	SA_{wing}	19.68	cm^{-2}	Calculated in this study
Body surface area	SA_{body}	39.26	cm^{-2}	Calculated from [53]
Area-specific rate of evaporative water loss for wing	$rEWL_{wing}$	0.33	mg hr^{-1} ΔWVP^{-1} cm^{-2}	Calculated in this study
Area-specific rate of evaporative water loss for body	$rEWL_{body}$	0.10	mg hr^{-1} ΔWVP^{-1} cm^{-2}	Calculated in this study
Time in euthermia per arousal	t_{eu}	1.10	h	[31,74,75]
Maximum time in torpor	$t_{tor\text{-}max}$	1300	h	[51]
Specific heat of tissue	S	0.173	ml O_2 g^{-1}˚C^{-1}	[14]
Rewarming rate	WR	0.80	˚C min^{-1}	[44,58,76,77]
Body mass	M_b	7.60	g	Measured in this study
Proportion of lean mass	pLean	0.55	g	Measured in this study
Proportion of fat mass	pFat	0.25	g	Measured in this study
Proportion of body water threshold	pMass	0.027	mg	Calculated in this study
Humidity-dependent fungal growth parameter	μ_1	1.51×10^{-4}	-	[25]
Humidity-dependent fungal growth parameter	μ_2	-9.92×10^{-3}	-	[25]
Temperature-dependent fungal growth parameter	β_1	1.15×10^{-3}	-	[25]
Temperature-dependent fungal growth parameter	β_2	0.27	-	[25]

https://doi.org/10.1371/journal.pone.0222311.t001

hibernaculum in the fall and recorded conditions at 3 h intervals. We determined the main winter roosting location from personal communication with U.S. Forest Service and Montana Department of Fish, Wildlife, and Parks personnel. We placed two HOBO loggers in the main roost, a large cathedral room at the back of the cave (one logger at the far end, one at the entrance), one within 3 m of the entrance of the cave, and one attached to a tree immediately outside the cave entrance (< 10 m). We spaced the iButtons evenly throughout the cave system from the entrance to the cathedral room. We suspended HOBO loggers with copper wire and used pantyhose to attach each iButton to a projected rock to suspend the logger in the air column. We collected loggers from the hibernaculum in the spring of each year.

We estimated winter duration for central Montana by acoustically monitoring bat activity at the entrance to the cave (Anabat Roost Logger RL1, Titley Scientific). The acoustic logger operated between 30 min before sunset and 30 min following sunrise. We used AnaLookW software (v4.3) to digitize calls and count the number of bat passes per day [42]. We were not interested in species-specific calls, but rather use the calls as an index of winter duration so we counted passes that contained calls of *Myotis* species (minimum frequency [f_{min}] > 30 kHz) to filter out noise [43]. We were also not interested in the number of individual bats passing the detector, but rather if there was general activity outside the cave; we thus used a threshold of 50 passes day^{-1}, defining the lower end of the 95% of bat counts, to determine the onset and end of the hibernation period [43].

Incorporating evaporative water loss into the hibernation energetics model

We revised the hibernation energetics model first described by Thomas et al. [1] and Humphries [24], and then modified to include fungal growth by Hayman et al. [25]. The model estimates the amount of fat consumed during hibernation as a summation of the energy expended during multiple torpor-arousal bouts across a winter period (full model presented in S1 File). We derived estimates of the energy required during torpor (E_{tor}), euthermia (E_{eu}), and the warming (E_{warm}) and cooling (E_{cool}) periods between torpid and euthermic temperatures. We estimated the period of each arousal spent within euthermia from literature (Table 1) and the time to warm and cool were calculated given published warming and cooling rates, respectively [44].

We incorporated a mechanistic link between EWL and torpor bout duration. We estimated torpor bout duration (t_{tor}) in two ways: 1) as a function of torpid metabolic rate in response to ambient temperature (T_a) as described in Hayman et al. [25], and 2) as a function of EWL. Our revised model uses the shorter of the two estimates given hibernaculum conditions (Fig A in S1 File), either arousing as a consequence of EWL or TMR, whichever comes first. By including both calculations in our estimates of torpor bout duration, we considered both the effect of EWL and metabolism on torpor physiology [45,46].

To estimate torpor bout duration as a function of metabolic rate (t_{torTMR}), we modified the existing equations developed by Hayman et al. [25] that scale maximum possible time in torpor (t_{torMax}) by the effects of metabolic rate given T_a:

$$t_{torTMR} = t_{torMax} / Q_{10}^{\left(\frac{T_a - T_{torMin}}{10}\right)} \qquad \text{if } T_a > T_{torMin} \tag{1}$$

$$t_{torTMR} = \frac{t_{torMax}}{1 + (T_{torMin} - T_a) \cdot \left(\frac{C_t}{TMR_{min}}\right)} \qquad \text{if } T_a \leq T_{torMin} \tag{2}$$

where Q_{10} is the change in metabolism with a 10˚C change in temperature [47], T_{torMin} is the minimum defended T_b in torpor, TMR_{min} is the associated metabolic rate at T_{torMin}, and C_t is the thermal conductance during torpor. Minimum defended T_b [48–50] and the maximum time in torpor (t_{torMax}) were estimated from literature [51], and minimum torpid metabolic rate and thermal conductance were measured in the field using respirometry (S1 File).

To calculate torpor bout duration as a function of EWL (t_{torEWL}), we assumed bats arouse when the total body water pool was depleted to a threshold [5]. The hourly rate of total EWL (mg H_2O h^{-1}) is comprised of both cutaneous and respiratory rates of EWL and is dependent on the water vapor pressure deficit between the bat and the surrounding environment. The hourly rate of cutaneous evaporative water loss (CEWL; mg H_2O h^{-1}) is a function of the difference between water vapor pressure at the surface of the bat and the environment (ΔWVP):

$$\Delta WVP = WVP_{bat} - WVP_{air} \tag{3}$$

where WVP_{bat} is the water vapor pressure at the skin surface and WVP_{air} is the water vapor pressure of the surrounding air (both in kPa). We assumed WVP_{bat} was at saturation, which can be calculated as:

$$WVP_{bat} = 0.611 \cdot e^{\left[\frac{17.503 \cdot T_b}{(T_b + 240.97)}\right]} \tag{4}$$

where T_b is the body temperature of the bat in torpor [52]. We then calculated WVP_{air} at T_a and given relative humidity. We modeled cutaneous EWL as a function of ΔWVP and the area-specific rate of EWL from bodily tissue (rEWL; mg H_2O h^{-1} cm^{-2} per ΔWVP^{-1}) across the

surface area (SA; cm^2) of the bat:

$$CEWL = SA \cdot rEWL \cdot \Delta WVP \quad (5)$$

We used a surface area scaling equation [53] to calculate body surface area (SA_{body}) and photos of bat wings to estimate the total surface area of the wings and tail (SA_{wing}; S1 File). Assuming that a furred body and naked wing have biophysical differences that would affect cutaneous EWL, we used different values of the area-specific rate of EWL for the body ($rEWL_{body}$) and wing ($rEWL_{wing}$), estimated from respirometry (S1 File). Therefore, we rewrote Eq 5 as:

$$CEWL = [(SA_{body} \cdot rEWL_{body}) + (SA_{wing} \cdot rEWL_{wing})] \cdot \Delta WVP \quad (6)$$

Respiratory EWL (REWL; mg H_2O h^{-1}) is a function of the saturation deficit between inspired and expired air. We assumed that inspired air is at T_a and is expired as saturated air at torpid T_b [5]. Therefore, we calculated respiratory EWL as:

$$REWL = respired\ air\ volume \cdot saturation\ deficit \quad (7)$$

The volume of air that a bat breathes per hour was calculated as a function of the respiration rate of oxygen (i.e. TMR_{min}) in ml O_2 g^{-1} h^{-1} and body mass:

$$respired\ air\ volume = \frac{TMR_{min} \cdot M_b}{0.2095 \cdot 0.30 \cdot 10^3} \quad (8)$$

assuming the fractional concentration of oxygen in air is 0.2095 and that oxygen extraction efficiency is 30% [5]. Using the ideal gas law [52], we converted the water vapor pressure deficit (ΔWVP; Eq 3) from kPa to mg L^{-1} to determine the saturation deficit.

We validated the rate of total EWL (cutaneous EWL and respiratory EWL) by comparing modeled EWL (from Eqs 5 and 7) to measured EWL from each individual during our respirometry procedures. We used individual body mass (Eqs 5 and 6), metabolic rate (Eqs 7 and 8), area-specific rate of EWL (Eqs 5 and 6), and predicted surface area given body mass (Eqs 5 and 6). We modeled the hourly rate of total EWL given the measured T_a and WVP experienced by each individual. We used linear regression to compare modeled EWL to measured EWL rates, assuming that if the model was accurate, the slope of the relationship should be equal to 1.

Given total EWL, we calculated torpor bout duration (t_{torEWL}) based on the reduction of the total body water pool, setting the threshold at 2.7% of lean mass (assuming no body water in fat stores):

$$t_{torEWL} = \frac{0.027 \cdot LeanMass \cdot 1000}{CEWL + REWL} \quad (9)$$

Including the effects of fungal growth on hibernation

We further adjusted the hibernation model by including a link between fungal growth and reduced torpor bout duration through an increase in both metabolic rate and EWL (modifying Eqs 1, 2 and 9). We first altered the estimation of torpor bout duration from T_a (t_{torTMR}; Eqs 1 and 2) by scaling t_{torTMR} by the proportion the bat wing surface affected by the fungus. When

fungal growth > 0, t_{torTMR} was calculated as:

$$t_{torTMR} = \left[\frac{t_{torMax}}{Q_{10}^{\left(\frac{T_a - T_{torMin}}{10}\right)}}\right] \Big/ \left(\frac{area_{Pd}}{SA_{wing}}\right) \quad \text{if } T_a > T_{torMin} \tag{10}$$

$$t_{torTMR} = \left[\frac{t_{tor-max}}{1 + (T_{torMin} - T_a) \cdot \left(\frac{C_t}{TMR_{min}}\right)}\right] \Big/ \left(\frac{area_{Pd}}{SA_{wing}}\right) \quad \text{if } T_a \leq T_{torMin} \tag{11}$$

where $area_{Pd}$ is the area (cm^2) of fungal growth calculated as a function of T_b and relative humidity given equations from Hayman et al. [25].

We adjusted the calculation of torpor bout duration in response to EWL (t_{torEWL}; Eq 9) by increasing CEWL and REWL as a function of fungal growth. We used data from McGuire et al. [20], who directly measured an increase in TMR and EWL in *M. lucifugus* infected with *P. destructans* (S1 File). We increased CEWL by including a linear increase to the rate of EWL of bat wings ($rEWL_{wing}$) in response to the proportion the bat wing surface affected by the fungus (from Eq 6):

$$CEWL_{wing} = \left[\left(SA_{body} \cdot rEWL_{body}\right) + \left(SA_{wing} \cdot \left[rEWL_{wing} + \left(0.16 \cdot \frac{area_{Pd}}{SA_{wing}} \cdot 100\right)\right]\right)\right] \cdot \Delta WVP \tag{12}$$

where 0.16 is the rate of increase in $rEWL_{wing}$, given the proportion the bat wing surface affected by the fungus, determined from data presented in McGuire et al. [20] (S1 File). REWL also is hypothesized to increase in response to fungal growth with an increase in TMR; we included this linear increase by adjusting Eq 8:

$$respired\ air\ volume = \frac{\left[TMR_{min} + \left(0.015 \cdot \frac{area_{Pd}}{SA_{wing}} \cdot 100\right)\right] \cdot M_b}{0.2095 \cdot 0.30 \cdot 10^3} \tag{13}$$

where 0.015 is the linear increase of torpid metabolic rate given the proportion the bat wing surface affected by the fungus (S1 File).

To validate the adjustment to the estimation of torpor bout duration in response to fungal growth (Eqs 10, 11 and 13), we used an independent dataset of skin temperature measurements from a captive hibernation study by McGuire et al. [54]. Skin temperature data were measured from thirteen *M. lucifugus* infected with *P. destructans* prior to hibernating in a controlled environment (T_a = 7˚C, relative humidity = 98%). Using methodology from Jonasson and Willis [31], we defined torpor and arousal periods based on cut-off temperatures and calculated the total time in each hibernation phase. We then estimated torpor bout duration (Eqs 10–13) at each measured torpor bout from each individual given individual morphometric parameters (initial body mass, predicted surface area). We estimated TMR from body mass and T_b [55] and allowed for variation in lean mass (to determine threshold of body water) by sampling from a normal distribution with mean and standard deviation from our capture data. We predicted fungal growth area at each torpor bout given the time since inoculation and Eqs 2–4 in Hayman et al [25]. We then used a linear model to compare modeled torpor bout duration to measured torpor bout duration, assuming that if the prediction was accurate, the slope of the relationship should be equal to 1. To determine if including EWL improved our description of torpor expression, we also predicted torpor bout duration without the contribution of EWL using only Eqs 10 and 11. We then compared these predictions to measured

bout duration to determine model accuracy. Finally, we compared the R^2 values of both fitted relationships to determine which model had better precision in predicting torpor bout duration.

Estimation of total fat loss and survival for *M. lucifugus* in Montana

Using our modified hibernation model and model parameters obtained from our field captures and literature (Table 1), we estimated time until total fat exhaustion for *M. lucifugus* over the range of hibernaculum microclimate conditions measured at our field site. Torpor bout duration changes with body condition and fungal growth so we used differential equations to estimate energy consumption over the winter. We assumed that bats require energy to arouse at the end of hibernation and to leave the hibernaculum in order to obtain food. Therefore, we included energy required to warm (E_{warm}) and spend 24 h in euthermia (24 x E_{eu}) at the end of winter hibernation. We used the lsoda function of the *deSolve* package, which allowed torpor bout duration to change over time given fungal growth, bat parameters (Table 1), and hibernaculum microclimate. We converted total energy consumed over time from ml O_2 g^{-1} to the amount of fat expended (g) as:

$$fat_{winter} = (E_{winter} \cdot 19.6)/(37.6 \cdot 1000) \quad (14)$$

assuming that 1 ml O_2 releases 19.6 J of energy and the energy content of fat is 37.6 J mg^{-1} [30]. We calculated time until fat exhaustion (t_{fatEx}) as the time when total fat exhaustion (fat_{winter}), became greater than mean fat stores measured during our fall field captures. Finally, we compared the estimated t_{fatEx} for both healthy and infected bats over the range of hibernaculum conditions to the duration of winter for central Montana estimated from our acoustic data. We assumed that mortality would occur if t_{fatEx} was less than winter duration; that is, the mean fat stores did not provide enough fat for a bat to survive through winter, as measured above.

We validated the entirety of the hibernation energetic model by comparing measured mass loss from 56 free-living hibernating *M. lucifugus* (Norquay and Willis, unpublished data, but see [56] for description of capture methodology and locations) to predicted fat loss from our model. We used this dataset because data from captive animals may not accurately reflect field conditions of free-living animals. We used individuals in which mass was measured during both swarming (August-September) and emergence (April-May). We estimated fat loss using the bioenergetic model for the time between swarming and emergence capture dates, given the hibernaculum conditions where each bat was captured [57,58]. We took the mean and standard deviation of T_a and water vapor pressure of each capture location and sampled random values from a normal distribution for each individual. We estimated TMR from body mass and T_b [55] and allowed for variation in lean mass by sampling from a normal distribution set at the mean and standard deviation from our capture data. We compared estimated fat loss with measured mass loss (assuming all mass change is due to fat loss) using linear regression, assuming if the two values were the same, the slope of the relationship would be no different than 1. We also predicted fat loss for the validation dataset given the hibernation model without the inclusion of EWL; more specifically, we only included Eqs 1 and 2 in our calculations of torpor bout duration. We compared these predictions to measured mass loss and determined both model accuracy (slope = 1) and precision (R^2) to compare against our modified model including EWL.

Following Hayman et al. [25], we used a multi-parameter sensitivity analysis to assess the impact of each parameter on estimations of time until mortality. Using Latin hypercube sampling in R package *lhs*, we created 100 random parameter sets sampled from a uniform

distribution of potential values ranging from 10% lower or higher than the default value (Table 1). By constraining the minimum and maximum values of the parameters, and including a joint distribution within the Latin hypercube sampling, we considered the potential for correlations between parameters. We determined the relative importance of each variable by comparing partial rank correlation coefficients (PRCC) values. Positive PRCC values indicate an increase in the model output with an increase in the parameter value, while negative PRCC values indicate a decrease in the model output with an increase in parameter value [25].

Results

We captured 183 *M. lucifugus* over the capture periods of 2016–2018 (140 during fall, 43 during winter; Table 2). There was minimal variation in hibernaculum microclimate measured by the HOBO and iButton loggers within the hibernaculum (temperature: mean = 4.80 ± 0.60˚C, range = 2.77–5.68˚C; water vapor pressure deficit: mean = 0.11 ± 0.26 kPa, range = 0.00–2.57 kPa) across winters (Fig 1). We found all bats roosting in the cathedral room, where hibernaculum microclimate was stable throughout the winter (Ta = 4.8˚C, RH = 100%). Activity decreased $<$ 50 passes day^{-1} by mid-October (mean date among years 14 October) and increased beyond 50 passes day^{-1} by mid-April (mean date among years 13 April). We therefore concluded that hibernation duration in central Montana was 181 days.

Measured EWL from our respirometry procedures in dry air (0% relative humidity) ranged from 0.31 to 1.53 mg H_2O h^{-1} g^{-1} (mean: 0.71 ± 0.25 mg H_2O h^{-1} g^{-1}) depending on temperature and individual. Our model accurately predicted EWL for *M. lucifugus* in Montana ($F_{1,61}$ = 570.3, $p < 0.001$, *slope* = 0.97 [0.89, 1.06]; Fig 2A). Given the hibernaculum conditions measured at the roosting location (T_a = 4.8˚C, RH = 100%), we predicted EWL from *M. lucifugus* as 0.06 ± 0.40 mg H_2O h^{-1} g^{-1} in healthy bats (Fig B in S1 File). *P. destructans* had no impact on EWL early in infection, but by late hibernation had increased EWL to 2.19 mg H_2O h^{-1} g^{-1} (Fig B in S1 File).

Our model accurately estimated torpor bout duration in captive bats infected with *P. destructans* ($F_{1,32}$ = 18.64, p = 0.0001, *slope* = 0.65 [0.43, 1.16]; Fig 2B), but the estimates had a wide variance and lacked precision (only 25% of the variation in the data was explained by the model). Without the inclusion of EWL, however, the model did not accurately describe torpor bout duration ($F_{1,32}$ = 0.40, p = 0.53, *slope* = -0.15 [-0.59, 0.30]) and did not describe variation in the data (R^2 = 0.02). We therefore predicted torpor bout duration using our modified model including EWL. For healthy bats, torpor bouts lasted 16.10 ± 5.04 days within the microclimate conditions of the hibernaculum at the field site (range: 4.54–18.3 days; Fig C in S1 File). Torpor bouts ranged from $<$ 1 day to 18.3 days (mean: 6.20 ± 5.40 days) for bats infected with *P. destructans* (Fig C in S1 File).

Our modified hibernation model accurately predicted mass loss in healthy wild bats ($F_{1,47}$ = 74.38, $p < 0.0001$, *slope* = 0.87 [0.67, 1.07]; Fig 2C). Though there was a lack of individual

Table 2. Morphometric and physiological data measured from *Myotis lucifugus* captured at a hibernaculum in central Montana. *N* = sample size, TMR: mass-specific torpid metabolic rate, EWL: mass-specific evaporative water loss.

Variable	Value ± SD	*N*
Body mass (g)	7.61 ± 1.08	183
Fat mass (g)	2.11± 0.82	46
Lean mass (g)	4.54 ± 0.93	46
TMR (ml O_2 g^1 h^{-1})	0.03 ± 0.07	33
EWL (mg H_2O g^{-1} h^{-1})	0.81 ± 0.38	26

https://doi.org/10.1371/journal.pone.0222311.t002

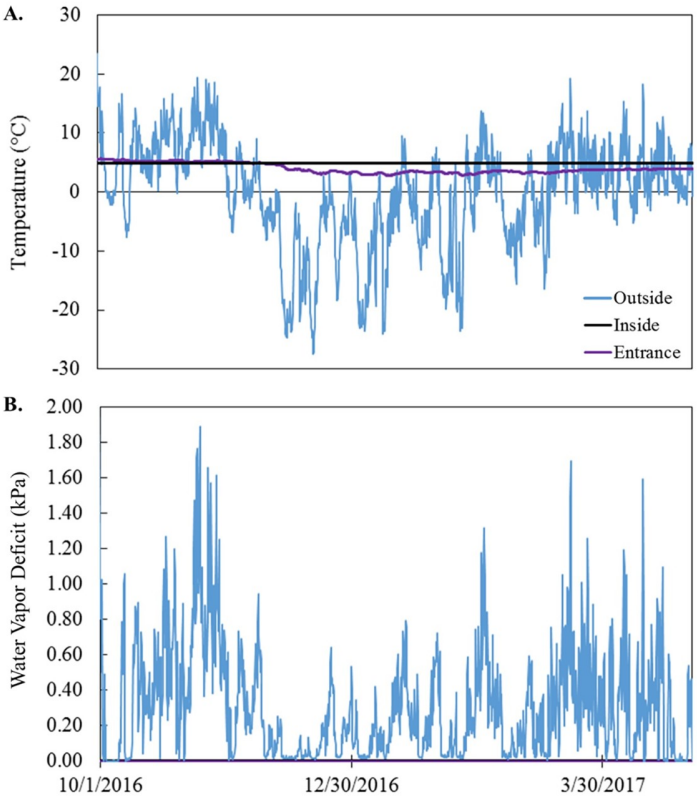


Fig 1. Hibernaculum microclimate conditions. (A) Hibernaculum temperature (˚C) and (B) water vapor pressure deficit (kPa) deep within the hibernaculum where *Myotis lucifugus* are found during hibernation (black line), at the entrance of the hibernaculum (purple line), and outside the hibernaculum entrance (blue line). Both the entrance (purple) and inside the hibernaculum (black) were at saturation the entire winter period (therefore the inside line is not visible). Note that the inside temperature was almost completely stable at 4.8˚C.

https://doi.org/10.1371/journal.pone.0222311.g001

metabolic rate and EWL data for the bats used in this validation procedure, our model still explained 62% of the variation in the dataset. Our model was also more precise than the hibernation model that lacked EWL, which was not accurate ($F_{1,47}$ = 1.04, p = 0.84, *slope* = -0.02 [-0.18, 0.15]) and described less than 1% of the variation in the data. Using the model with EWL, the mean time until total fat exhaustion for healthy *M*. *lucifugus* predicted in the hibernaculum microclimate conditions at our field site in Montana was 317.5 ± 105.50 days (Fig 3A) at a rate of 0.006 ± 0.002 g day^{-1}. Bats were predicted to survive for over 360 days in the microclimate selected for roosting (T_a = 4.8˚C, RH = 100%). The shortest time until fat exhaustion (176 days) was at the warmest temperature available in the hibernaculum (5.5˚C) and lowest humidity (90%). Almost all other available microclimate conditions within the hibernaculum (2–5˚C and > 90% RH) result in predicted hibernation duration greater than winter duration (181 days).

Within the hibernaculum conditions available at our field site, we predicted a higher and more variable rate of fat loss (range: 0.006–0.32 g day^{-1}) for infected bats. In the specific hibernaculum conditions selected for roosting within these conditions, infected bats lost 0.01 ± 0.001 g day^{-1} at the beginning of hibernation (< 14 days) while the rate of fat loss increased to 0.03 ± 0.01 g day^{-1} at the end of hibernation (181 days). Almost all microclimate conditions available at our field site resulted in mortality for infected bats as time until fat

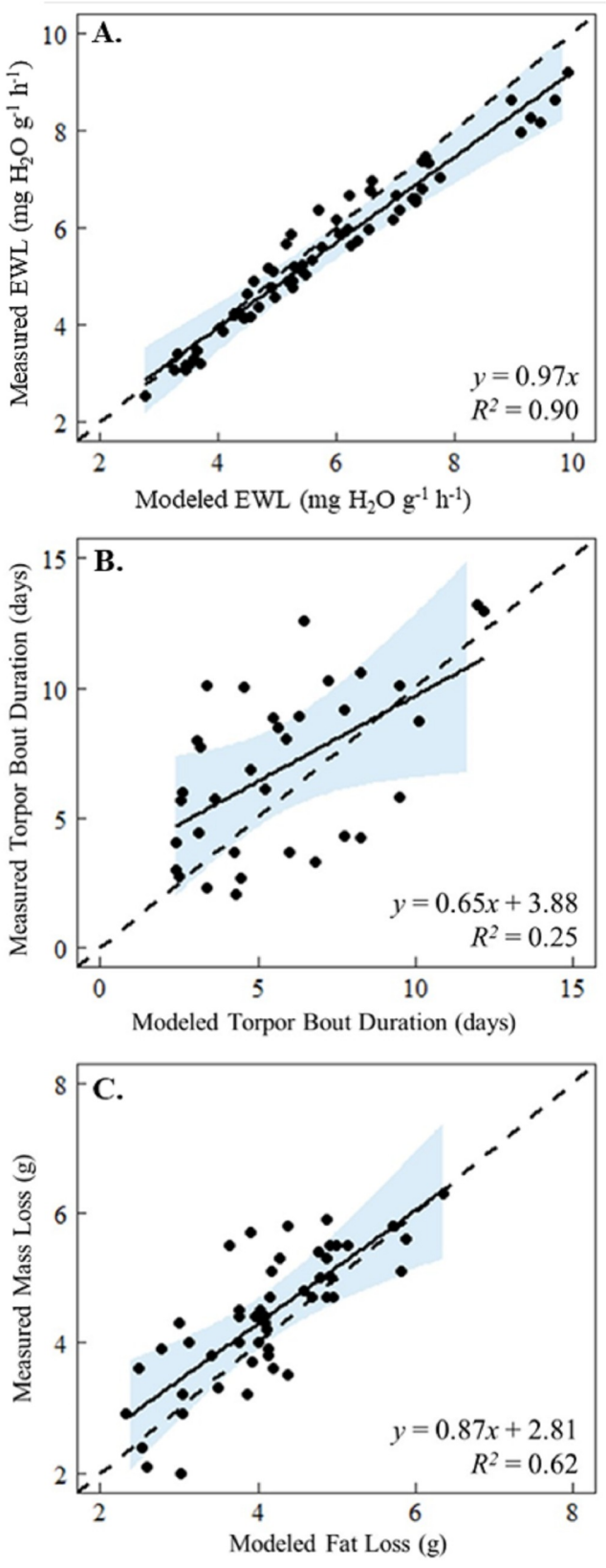

A.
Measured EWL (mg H2O g-1 h-1)
Modeled EWL (mg H2O g-1 h-1)
y = 0.97x
R2 = 0.90
B.
Measured Torpor Bout Duration (days)
Modeled Torpor Bout Duration (days)
y = 0.65x + 3.88
R2 = 0.25
C.
Measured Mass Loss (g)
Modeled Fat Loss (g)
y = 0.87x + 2.81
R2 = 0.62

Fig 2. Validation of model components. Comparison of measured and modeled (A) evaporative water loss (EWL), (B) torpor bout duration, and (C) fat loss in *Myotis lucifugus*. EWL and fat loss were measured/modeled in healthy bats, while torpor bout duration was measured/modeled in bats that were inoculated with *P. destructans*. Dashed lines represent one-to-one line and solid lines represent fitted relationship with 95% confidence intervals (shaded blue).

https://doi.org/10.1371/journal.pone.0222311.g002

exhaustion was less than hibernation duration (mean: 131.23 ± 38.40 days; Fig 3B). The only available microclimate conditions that permitted survival were at the lowest temperatures (2–3˚C) and highest humidity conditions (96–100%) but these locations were not selected by any healthy bats within this hibernaculum. Bats selected saturated environments that were within the temperature range that allowed fungal growth, resulting in increased energy expenditure and ultimately decreased time until total fat exhaustion.

Our sensitivity analysis revealed that fat loss was influenced by host-specific parameters, including body mass, the proportions of body mass comprised of fat and lean mass, and parameters that influenced EWL, including wing surface area and the area-specific rates of cutaneous EWL (Fig 4). Model parameters that were most influential to survival were physical traits that vary both within and among species. There was little effect of metabolic rate during torpor or euthermia, nor time spent euthermic.

Discussion

With the continued spread of WNS, it is imperative to understand the effects of hibernaculum microclimate (temperature and humidity) on fungal growth, host physiology, and winter survival. A model that includes effects of EWL on arousal frequencies within the study system of WNS, can improve understanding of the role of EWL on the evolution of hibernation and the interplay of host physiology with the environment. We showed that host parameters, particularly body mass, fat mass, and area-specific rate of EWL, were important drivers of torpor bout duration. Our results suggest that factors associated with EWL and arousal frequency are key elements for predicting the effects of WNS on hibernating bats.

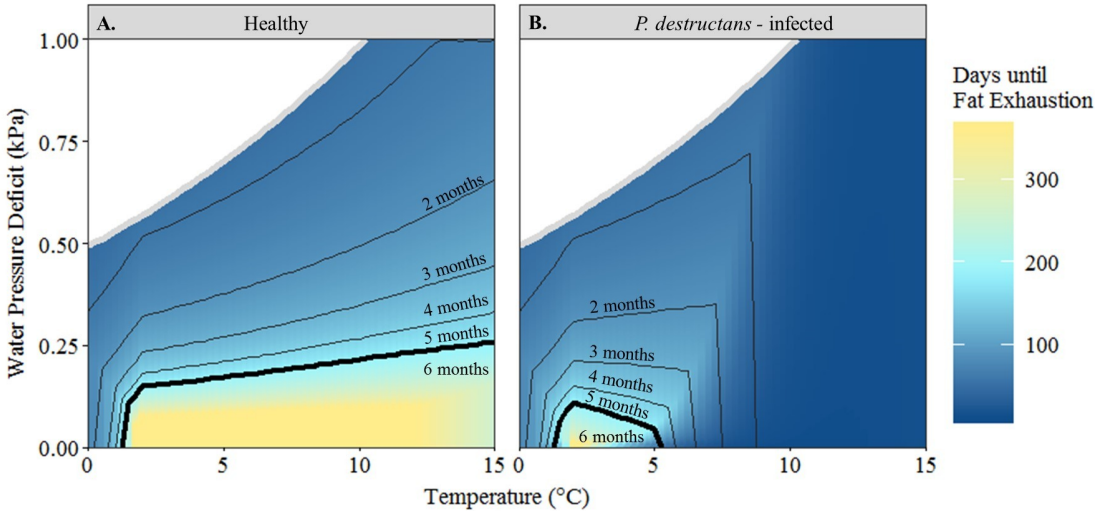


Fig 3. Predicted time until fat exhaustion. Predicted number of days until fat exhaustion for (**A**) healthy and (**B**) *P. destructans*—infected little brown bats (*Myotis lucifugus*) over a range of hibernaculum temperature (˚C) and water vapor deficit (kPa) values. Contours represent hibernaculum conditions that allow survival for specific winter duration (in months); dark black contour indicates 6 months, the estimated hibernation duration at our study site in central Montana. White area bounded by grey line represents impossible parameters space for each temperature (e.g. at 2˚C, air is saturated at 0.50 kPa and cannot hold more water).

https://doi.org/10.1371/journal.pone.0222311.g003

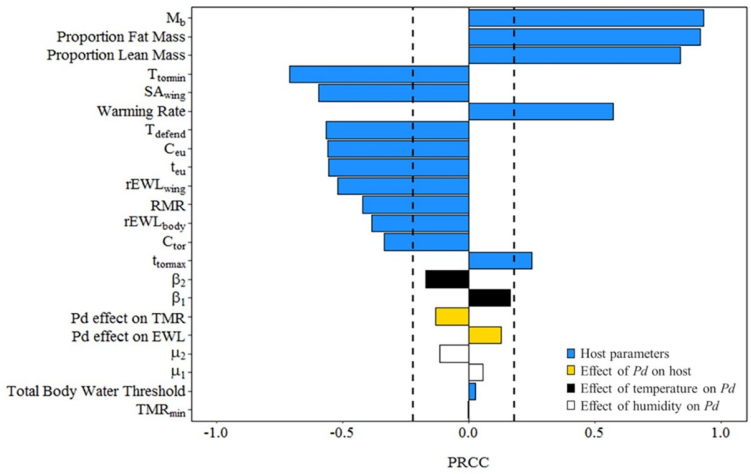


Fig 4. Sensitivity analysis of hibernation energetics model. Sensitivity analysis for model calculating total fat exhaustion in hibernating bats infected with *P. destructans*. Dashed lines signify confidence intervals ($\alpha = 0.05$). Positive PRCC values indicate an increase in predicted time until total fat exhaustion with an increase in parameter value; negative values indicate a decrease in predicted time until fat exhaustion with an increase in parameter value.

https://doi.org/10.1371/journal.pone.0222311.g004

Our modified hibernation bioenergetic model predicted torpor behavior similar to torpor-arousal behavior observed in wild *M. lucifugus* populations. For instance, Reeder et al. [59] measured torpor bouts of 16.32 ± 6.65 days and Czenze et al. [35] measured bouts of 16.2 ± 11.4 days in similar conditions where we predicted bouts of 16.1 ± 5.04 days in the Montana cave system (Fig B in S1 File). Observations of torpor behavior in WNS-affected bats corroborated our predictions of torpor bout duration (6.20 ± 5.40 days; Fig B in S1 File): wild populations of *M. lucifugus* remained in torpor for 7.93 ± 2.49 days [59], while captive populations averaged 6.48 ± 0.76 days [60]. Similarly, Reeder et al. [59] determined a negative relationship between wing damage due to fungal growth and torpor bout duration, which is aligned with how we incorporated the effect of infection in our model. Overall, the fidelity of the model implies that our prediction of torpor bout duration as a function of EWL is biologically relevant and representative of hibernation physiology and behavior.

We showed complete survival capacity (100% survival) in the entire microclimate space inhabited by healthy *M. lucifugus* in a cave system in central Montana (Fig 3A). Unfortunately, these hibernaculum temperatures and predicted torpor bout durations are comparable to hibernacula inhabited by highly impacted *M. lucifugus* populations in WNS-affected regions [28,35,39]. We predicted almost complete mortality (11% survival) for *M. lucifugus* within the current hibernaculum conditions in this cave system, in part because the high humidity selected by hibernating bats also results in high fungal growth [22,23]. Our predictions are consistent with population trends observed in WNS-affected regions in eastern North America, where similar hibernaculum microclimates have resulted in high mortality (80–98%) [39]. However, our model predicts a small window of microclimate space that would allow for survival, where cooler temperatures and moderate humidity reduce fungal growth, resulting in longer torpor bout duration and decreased arousal frequency (Fig 3B; Fig B in S1 File). Our model predictions are consistent with observations of WNS-affected bats roosting in colder temperatures compared to unaffected bats [59,61]. These observations, in conjunction with our predictions, suggest that *M. lucifugus* within the Montana cave system would be highly impacted by WNS, but could potentially survive if individuals seek out cooler microclimates. Alternatively, if there are cooler microclimates available, those individuals that already prefer

these conditions will survive while others will not. If microclimate preference is heritable, there is the potential for evolutionary rescue [62,63].

Our modified hibernation energetics model relies on measurements of the response of *P. destructans* to temperature from the lab and modeled response to relative humidity based on previous work [25]. Multiple studies reported diverse *P. destructans* responses to microclimate conditions [22,23,37,64,65], potentially due to subtle differences in laboratory procedures, and thus our predictions of fungal growth may not perfectly represent wild conditions. Additionally, parameters we used to estimate the increase in both metabolic rate and the rate of cutaneous EWL were derived from a single captive study [20]. However, results of studies of the effects of WNS on torpor patterns in wild and free-ranging bats are similar [59,66]. Additionally, our sensitivity analysis indicates that the predictions did not change significantly in response to changes in the temperature and humidity-dependent fungal growth rates or the increase to metabolic rate and EWL (Fig 4). Although future research into humidity-dependent fungal growth rate parameters on wild bats within natural conditions is warranted to increase our understanding of these dynamics, our predictions are consistent with the data currently available.

Evidence of at least some *M. lucifugus* populations with greater fat stores persisting post-WNS [67–71] corroborates our findings from our sensitivity analysis that fat mass is a major driver of WNS-survival (Fig 4). Large fat stores allow for increased arousal frequency associated with infection with *P. destructans* and extend the time until total fat exhaustion. Currently, we assess the costs of infection on the mean parameters–that is, body mass, fat mass, and lean mass represent the center of the distribution of morphometric characteristics if we assume a symmetrical distribution. Given evidence of the importance of body mass and fat, we would expect that some individuals from the Montana population would survive in the sampled hibernaculum if they had greater fat stores. It is therefore important that we further our research on the drivers of intra- and interspecific variation in overwintering survival from WNS.

The relationship between water vapor pressure and fungal growth indicates the potential for mitigation of WNS impacts if bats roost in microclimates below saturation–that is, infected individuals may trade-off water conservation with energy minimization. In healthy bats, maximum survival was at saturation (100% RH; Fig 3A). As saturation leads to negligible EWL [5], bats can remain in torpor longer before dehydration leads to arousal [46]; thus, roosting in saturated microclimates minimizes energetic costs. However, because *P. destructans* growth increases with water vapor pressure [23], infected bats had lower survival at saturation compared to less humid environments (Fig 3B). This hypothesis is supported by evidence of a relationship between increased population growth rate in multiple species and decreased relative humidity in regions post-WNS infection [39]; hibernacula with less than 90% relative humidity were the only microclimates to have population growth rates above zero, which aligns with our predictions of reduced survival at saturation.

Our model supports the role of EWL as a driver of periodic arousals in hibernation, and contributes to addressing one of the longest-standing questions in hibernation biology. It also showcases how interactions between host and pathogen physiology, and the environment can exacerbate or mitigate the costs of a disease. The relationship between EWL, fungal growth, and humidity suggests that bats found in some parts of western North America, where hibernacula are often drier than eastern hibernacula, may not be as impacted by WNS as eastern populations. Additionally, species and populations that inhabit more arid environments tend to have lower rates of EWL [72] due to adaptations to allow maintenance of water balance in sub-optimal conditions, and thus may not experience high WNS-related mortality [23]. The non-linear interplay of temperature, humidity, and behavior (selecting roosting conditions)

needs further analysis, and our model provides a tool to address these questions. The model allows for species-specific parameterization and interspecific variation in morphometrics, physiology, and roosting habitats, suggesting that morphometric and physiological data from western bat species is needed. With this modified hibernation energetics model, we now have the tool to assess the potential impact of WNS on populations that have different hibernation behaviors than previously impacted species.

Supporting information

S1 File. Supporting information. Additional methodology regarding determining parameters for the hibernation energetics model and respirometry measurements.
(DOCX)

Acknowledgments

We thank Quinn Fletcher and other members of the U. of Winnipeg bat lab for help with field data on mass loss of hibernating bats. We thank L. Hanauska-Brown for helping obtain permits and B. Maxwell and D. Bachen for site identification. We appreciate the field help from H. D. Bobbitt, D. Taylor, D. Jones, D. Crowley, E. Brandell, G. Botto, E. Lee, K. Smucker, and D. Bishop.

Author Contributions

Conceptualization: David T. S. Hayman, Liam P. McGuire, Raina K. Plowright, Sarah H. Olson.

Data curation: Catherine G. Haase, Kaleigh J. O. Norquay, Kirk A. Silas, Craig K. R. Willis.

Formal analysis: Catherine G. Haase, Nathan W. Fuller, C. Reed Hranac, Liam P. McGuire.

Funding acquisition: David T. S. Hayman, Liam P. McGuire, Raina K. Plowright, Sarah H. Olson.

Investigation: Catherine G. Haase, David T. S. Hayman, Liam P. McGuire, Raina K. Plowright, Sarah H. Olson.

Methodology: Catherine G. Haase, Nathan W. Fuller, Liam P. McGuire.

Project administration: David T. S. Hayman, Liam P. McGuire, Raina K. Plowright, Sarah H. Olson.

Resources: Nathan W. Fuller, David T. S. Hayman, Liam P. McGuire, Raina K. Plowright, Sarah H. Olson.

Software: David T. S. Hayman, Liam P. McGuire, Raina K. Plowright, Sarah H. Olson.

Supervision: Nathan W. Fuller, David T. S. Hayman, Liam P. McGuire, Raina K. Plowright, Sarah H. Olson.

Validation: Catherine G. Haase, Nathan W. Fuller, Liam P. McGuire.

Visualization: Catherine G. Haase.

Writing – original draft: Catherine G. Haase.

Writing – review & editing: Catherine G. Haase, Nathan W. Fuller, C. Reed Hranac, David T. S. Hayman, Liam P. McGuire, Craig K. R. Willis, Raina K. Plowright, Sarah H. Olson.

References

1. Thomas DW, Dorais M, Bergeron J-M. Winter energy budgets and cost of arousals for hibernating little brown bats, *Myotis lucifugus*. Journal of Mammalogy. 1990; 71: 475–479. https://doi.org/10.2307/1381967
2. Ben-Hamo M, Muñoz-Garcia A, Williams JB, Korine C, Pinshow B. Waking to drink: rates of evaporative water loss determine arousal frequency in hibernating bats. Journal of Experimental Biology. 2013; 216: 573–577. https://doi.org/10.1242/jeb.078790 PMID: 23364570
3. Thomas DW, Geiser F. Periodic arousals in hibernating mammals: is evaporative water loss involved? Functional Ecology. 1997; 11: 585–591. https://doi.org/10.1046/j.1365-2435.1997.00129.x
4. Fisher KC. On the mechanism of periodic arousal in the hibernating ground squirrel. *Annales Academiae scientiarum fennicae* Ser A. 1964; 71: 143–156.
5. Thomas DW, Cloutier D. Evaporative water loss by hibernating little brown bats, *Myotis lucigugus*. Physiological Zoology. 1992; 65: 443–456.
6. Kallen FC. Some aspects of water balance in the hibernating bat. Annales Academie Scientiarum Fennicae. *Suomalainen Tiedeakatemia*; 1964. pp. 259–267.
7. Humphries MM, Thomas DW, Speakman JR. Climate-mediated energetic constraints on the distribution of hibernating mammals. Nature. 2002; 418: 313–316. https://doi.org/10.1038/nature00828 PMID: 12124621
8. Boyles JG, McKechnie AE. Energy conservation in hibernating endotherms: Why "suboptimal" temperatures are optimal. Ecological Modelling. 2010; 221: 1644–1647. https://doi.org/10.1016/j.ecolmodel.2010.03.018
9. Nelson RA. Nitrogen turnover and its conservation in hibernation. Living in the Cold. Paris: John Libbey Eurotext; 1989. pp. 299–307.
10. Herreid CF, Schmidt-Nielsen K. Oxygen consumption, temperature, and water loss in bats from different environments. Am J Physiol. 1966; 211: 1108–1112. https://doi.org/10.1152/ajplegacy.1966.211.5.1108 PMID: 5924031
11. Morris S, Curtin AL, Thompson MB. Heterothermy, torpor, respiratory gas exchange, water balance and the effect of feeding in Gould's long-eared bat *Nyctophilus gouldi*. Journal of Experimental Biology. 1994; 197: 309–335. PMID: 7852907
12. Schmidt-Nielsen K, editor. Animal Physiology: Adaptation and Environment. 3rd ed. London; New York: Cambridge University Press; 1987.
13. Cryan PM, Meteyer CU, Blehert DS, Lorch JM, Reeder DM, Turner GG, et al. Electrolyte depletion in white-nose syndrome bats. Journal of Wildlife Diseases. 2013; 49: 398–402. https://doi.org/10.7589/2012-04-121 PMID: 23568916
14. Wang LCH. Energetics and field aspects of mammalian torpor: the Richardson's ground squirrel. In: Wang LCH, Hudson JW, editors. Strategies in the Cold. New York: Academic Press; 1978. pp. 109–145.
15. Willis CKR, Menzies AK, Boyles JG, Wojciechowski MS. Evaporative water loss is a plausible explanation for mortality of bats from white-nose syndrome. Integr Comp Biol. 2011; 51: 364–373. https://doi.org/10.1093/icb/icr076 PMID: 21742778
16. Cryan PM, Meteyer CU, Boyles JG, Blehert DS. Wing pathology of white-nose syndrome in bats suggests life-threatening disruption of physiology. BMC Biology. 2010; 8: 135. https://doi.org/10.1186/1741-7007-8-135 PMID: 21070683
17. Meteyer CU, Buckles EL, Blehert DS, Hicks AC, Green DE, Shearn-Bochsler V, et al. Histopathologic criteria to confirm white-nose syndrome in bats. Journal of Veterinary Diagnostic Investigation. 2009; 21: 411–414. https://doi.org/10.1177/104063870902100401 PMID: 19564488
18. Warnecke L, Turner JM, Bollinger TK, Misra V, Cryan PM, Blehert DS, et al. Pathophysiology of white-nose syndrome in bats: a mechanistic model linking wing damage to mortality. Biology Letters. 2013; 9: 20130177. https://doi.org/10.1098/rsbl.2013.0177 PMID: 23720520
19. Verant ML, Meteyer CU, Speakman JR, Cryan PM, Lorch JM, Blehert DS. White-nose syndrome initiates a cascade of physiologic disturbances in the hibernating bat host. BMC Physiology. 2014; 14: 10. https://doi.org/10.1186/s12899-014-0010-4 PMID: 25487871
20. McGuire LP, Mayberry HW, Willis CKR. White-nose syndrome increases torpid metabolic rate and evaporative water loss in hibernating bats. Am J Physiol Regul Integr Comp Physiol. 2017; 313: R680–R686. https://doi.org/10.1152/ajpregu.00058.2017 PMID: 28835446
21. Boyles JG, Willis CK. Could localized warm areas inside cold caves reduce mortality of hibernating bats affected by white-nose syndrome? Frontiers in Ecology and the Environment. 2010; 8: 92–98. https://doi.org/10.1890/080187

22. Verant ML, Boyles JG, Waldrep W, Wibbelt G, Blehert DS. Temperature-dependent growth of Geomyces destructans, the fungus that causes bat white-nose syndrome. PLOS ONE. 2012; 7: e46280. https://doi.org/10.1371/journal.pone.0046280 PMID: 23029462

23. Marroquin CM, Lavine JO, Windstam ST. Effect of humidity on development of *Pseudogymnoascus destructans*, the causal agent of bat white-nose syndrome. Northeastern Naturalist. 2017; 24: 54–64. https://doi.org/10.1656/045.024.0105

24. Humphries MM, Thomas DW, Speakman JR. Climate-mediated energetic constraints on the distribution of hibernating mammals. Nature. 2002; 418: 313–316. https://doi.org/10.1038/nature00828 PMID: 12124621

25. Hayman DTS, Pulliam JRC, Marshall JC, Cryan PM, Webb CT. Environment, host, and fungal traits predict continental-scale white-nose syndrome in bats. Science Advances. 2016; 2: e1500831. https://doi.org/10.1126/sciadv.1500831 PMID: 27152322

26. Fenton MB, Barclay RMR. Myotis lucifugus. Mammalian Species. 1980; 1–8. https://doi.org/10.2307/3503792

27. Fenton MB. Population studies of *Myotis lucifugus* (Chiroptera: Vespertilionidae) in Ontario. Toronto, Canada: The Royal Ontario Museum; 1970. Available: https://www.biodiversitylibrary.org/item/111399

28. Langwig KE, Frick WF, Hoyt JR, Parise KL, Drees KP, Kunz TH, et al. Drivers of variation in species impacts for a multi-host fungal disease of bats. Phil Trans R Soc B. 2016; 371: 20150456. https://doi.org/10.1098/rstb.2015.0456 PMID: 28080982

29. Frederico P. Bat Population Dynamics: An Individual-based Model Approach. Ph.D. Dissertation, University of Tennessee. 2007.

30. Boyles JG, Brack V. Modeling survival rates of hibernating mammals with individual-based models of energy expenditure. J Mammal. 2009; 90: 9–16. https://doi.org/10.1644/08-MAMM-A-205.1

31. Jonasson KA, Willis CKR. Hibernation energetics of free-ranging little brown bats. J Exp Biol. 2012; 215: 2141–2149. https://doi.org/10.1242/jeb.066514 PMID: 22623203

32. Ehlman SM, Cox JJ, Crowley PH. Evaporative water loss, spatial distributions, and survival in white-nose-syndrome-affected little brown myotis: a model. J Mammal. 2013; 94: 572–583. https://doi.org/10.1644/12-MAMM-A-111.1

33. Burles DW, Fenton MB, Barclay RM, Brigham RM, Volkers D. Aspects of the winter ecology of bats on Haida Gwaii, British Columbia. Northwestern Naturalist. 2014; 95: 289–299. https://doi.org/10.1898/12-32.1

34. Wilcox A, Willis CK. Energetic benefits of enhanced summer roosting habitat for little brown bats (*Myotis lucifugus*) recovering from white-nose syndrome. Conservation Physiology. 2016; 4: cov070. https://doi.org/10.1093/conphys/cov070 PMID: 27293749

35. Czenze ZJ, Jonasson KA, Willis CKR. Thrifty females, frisky males: Winter energetics of hibernating bats from a cold climate. Physiological and Biochemical Zoology. 2017; 90: 502–511. https://doi.org/10.1086/692623 PMID: 28641050

36. Frick WF, Pollock JF, Hicks AC, Langwig KE, Reynolds DS, Turner GG, et al. An emerging disease causes regional population collapse of a common North American bat species. Science. 2010; 329: 679–682. https://doi.org/10.1126/science.1188594 PMID: 20689016

37. Blehert DS, Hicks AC, Behr M, Meteyer CU, Berlowski-Zier BM, Buckles EL, et al. Bat white-nose syndrome: An emerging fungal pathogen? Science. 2009; 323: 227–227. https://doi.org/10.1126/science.1163874 PMID: 18974316

38. Dzal Y, McGuire LP, Veselka N, Fenton MB. Going, going, gone: the impact of white-nose syndrome on the summer activity of the little brown bat (*Myotis lucifugus*). Biol Lett. 2011; 7: 392–394. https://doi.org/10.1098/rsbl.2010.0859 PMID: 21106570

39. Langwig KE, Frick WF, Bried JT, Hicks AC, Kunz TH, Marm Kilpatrick A. Sociality, density-dependence and microclimates determine the persistence of populations suffering from a novel fungal disease, white-nose syndrome. Ecol Lett. 2012; 15: 1050–1057. https://doi.org/10.1111/j.1461-0248.2012.01829.x PMID: 22747672

40. McGuire LP, Guglielmo CG. Quantitative magnetic resonance: a rapid, noninvasive body composition analysis technique for live and salvaged bats. J Mammal. 2010; 91: 1375–1380. https://doi.org/10.1644/10-MAMM-A-051.1

41. Fuller NW, Haase CG, Silas KA, Olson SH, McGuire LP. Tradeoffs between energy conservation and the costs of torpor: hibernation of Myotis velifer at low latitudes. Journal of Comparative Physiology B. In press;

42. Corben C. AnaBat (version 6.0) and AnaLook (version 4.9 j)[computer programs]. 2004.

43. Lausen CL, Barclay RMR. Winter bat activity in the Canadian prairies. Can J Zool. 2006; 84: 1079–1086. https://doi.org/10.1139/z06-093

44. Haase CG, Fuller NW, Hranac CR, Hayman DTS, Olson S, Plowright R, et al. Bats are not squirrels: revisiting the cost of cooling in hibernating mammals. Journal of Thermal Biology. 2019; 81: 185–193. https://doi.org/10.1016/j.jtherbio.2019.01.013 PMID: 30975417

45. Geiser F, Kenagy GJ. Torpor duration in relation to temperature and metabolism in hibernating ground squirrels. Physiological Zoology. 1988; 61: 442–449.

46. Thomas DW, Geiser F. Periodic arousals in hibernating mammals: is evaporative water loss involved? Functional Ecology. 11: 585–591. https://doi.org/10.1046/j.1365-2435.1997.00129.x

47. Geiser F. Metabolic rate and body temperature reduction during hibernation and daily torpor. Annu Rev Physiol. 2004; 66: 239–274. https://doi.org/10.1146/annurev.physiol.66.032102.115105 PMID: 14977403

48. Hock RJ. The metabolic rates and body temperatures of bats. The Biological Bulletin. 1951; 101: 289–299. https://doi.org/10.2307/1538547

49. Hanus K. Body temperatures and metabolism of bats at different environmental tempereatures. Physiol Bohemoslov. 1959; 8: 250–259.

50. Speakman JR, Webb PI, Racey PA. Effects of disturbance on the energy expenditure of hibernating bats. Journal of Applied Ecology. 1991; 28: 1087–1104. https://doi.org/10.2307/2404227

51. Brack V, Twente JW. The duration of the period of hibernation of three species of vespertilionid bats. I. Field studies. Can J Zool. 1985; 63: 2952–2954. https://doi.org/10.1139/z85-442

52. Campbell GS, Norman JM. An Introduction to Environmental Biophysics [Internet]. New York: Springer-Verlag; 1998. Available: http://www.springer.com/us/book/9780387949376

53. Gouma E, Simos Y, Verginadis I, Lykoudis E, Evangelou A, Karkabounas S. A simple procedure for estimation of total body surface area and determination of a new value of Meeh's constant in rats. Laboratory Animals. 2012; 46: 40–45. https://doi.org/10.1258/la.2011.011021 PMID: 22008848

54. McGuire LP, Mayberry HW, Fletcher QE, Willis CKR. An experimental test of energy and electrolyte supplementation as a mitigation strategy for white-nose syndrome. Conserv Physiol. 2019; 7. https://doi.org/10.1093/conphys/coz006 PMID: 30805191

55. Speakman JR, Thomas DW. Physiological Ecology and Energetics of Bats. In: Kunz TH, Fenton MB, editors. Bat Ecology. First. Chicago and London: University Of Chicago Press; 2003. pp. 430–490.

56. Norquay KJO, Martinez-Nuñez F, Dubois JE, Monson KM, Willis CKR. Long-distance movements of little brown bats (Myotis lucifugus). J Mammal. 2013; 94: 506–515. https://doi.org/10.1644/12-MAMM-A-065.1

57. Bilecki LC. Bat Hibernacula in the Karst Landscape of Central Manitoba: Protecting Critical Wildlife Habitat while Managing for Resource Development. M.S. Thesis, University of Manitoba. 2003.

58. Czenze ZJ, Willis CKR. Warming up and shipping out: arousal and emergence timing in hibernating little brown bats (Myotis lucifugus). J Comp Physiol B, Biochem Syst Environ Physiol. 2015; 185: 575–586. https://doi.org/10.1007/s00360-015-0900-1 PMID: 25809999

59. Reeder DM, Frank CL, Turner GG, Meteyer CU, Kurta A, Britzke ER, et al. Frequent arousal from hibernation linked to severity of infection and mortality in bats with white-nose syndrome. PLOS ONE. 2012; 7: e38920. https://doi.org/10.1371/journal.pone.0038920 PMID: 22745688

60. Brownlee-Bouboulis SA, Reeder DM. White-nose syndrome-affected little brown myotis (Myotis lucifugus) increase grooming and other active behaviors during arousals from hibernation. J Wildl Dis. 2013; 49: 850–859. https://doi.org/10.7589/2012-10-242 PMID: 24502712

61. Storm JJ, Boyles JG. Body temperature and body mass of hibernating little brown bats Myotis lucifugus in hibernacula affected by white-nose syndrome. Acta Theriol. 2011; 56: 123–127. https://doi.org/10.1007/s13364-010-0018-5

62. Maslo B, Fefferman NH. A case study of bats and white-nose syndrome demonstrating how to model population viability with evolutionary effects. Conservation Biology. 2015; 29: 1176–1185. https://doi.org/10.1111/cobi.12485 PMID: 25808080

63. Andrew Gonzalez, Ophélie Ronce, Regis Ferriere, Hochberg Michael E. Evolutionary rescue: an emerging focus at the intersection between ecology and evolution. Philosophical Transactions of the Royal Society B: Biological Sciences. 2013; 368: 20120404. https://doi.org/10.1098/rstb.2012.0404 PMID: 23209175

64. Bandouchova H, Bartonička T, Berkova H, Brichta J, Kokurewicz T, Kovacova V, et al. Alterations in the health of hibernating bats under pathogen pressure. Scientific Reports. 2018; 8: 6067. https://doi.org/10.1038/s41598-018-24461-5 PMID: 29666436

65. Chaturvedi V, Springer DJ, Behr MJ, Ramani R, Li X, Peck MK, et al. Morphological and molecular characterizations of psychrophilic fungus *Geomyces destructans* from New York bats with white nose syndrome (WNS). PLOS ONE. 2010; 5: e10783. https://doi.org/10.1371/journal.pone.0010783 PMID: 20520731

66. Warnecke L, Turner JM, Bollinger TK, Lorch JM, Misra V, Cryan PM, et al. Inoculation of bats with European *Geomyces destructans* supports the novel pathogen hypothesis for the origin of white-nose syndrome. PNAS. 2012; 109: 6999–7003. https://doi.org/10.1073/pnas.1200374109 PMID: 22493237

67. Cheng TL, Gerson A, Moore MS, Reichard JD, DeSimone J, Willis CKR, et al. Higher fat stores contribute to persistence of little brown bat populations with white-nose syndrome. Journal of Animal Ecology. 2019; 88: 591–600. https://doi.org/10.1111/1365-2656.12954 PMID: 30779125

68. Dunbar MB, Brigham RM. Thermoregulatory variation among populations of bats along a latitudinal gradient. J Comp Physiol B. 2010; 180: 885–893. https://doi.org/10.1007/s00360-010-0457-y PMID: 20213177

69. Speakman JR, Racey PA. Hibernal Ecology of the Pipistrelle Bat: Energy Expenditure, Water Requirements and Mass Loss, Implications for Survival and the Function of Winter Emergence Flights. Journal of Animal Ecology. 1989; 58: 797–813. https://doi.org/10.2307/5125

70. Jonasson KA, Willis CKR. Changes in Body Condition of Hibernating Bats Support the Thrifty Female Hypothesis and Predict Consequences for Populations with White-Nose Syndrome. PLOS ONE. 2011; 6: e21061. https://doi.org/10.1371/journal.pone.0021061 PMID: 21731647

71. Boyles JG, Dunbar MB, Storm JJ, Brack V. Energy availability influences microclimate selection of hibernating bats. Journal of Experimental Biology. 2007; 210: 4345–4350. https://doi.org/10.1242/jeb.007294 PMID: 18055623

72. Klüg-Baerwald BJ, Brigham RM. Hung out to dry? Intraspecific variation in water loss in a hibernating bat. Oecologia. 2017; 183: 977–985. https://doi.org/10.1007/s00442-017-3837-0 PMID: 28213638

73. McNab BK. On estimating thermal conductance in endotherms. Physiological Zoology. 1980; 53: 145–156.

74. French AR. Allometries of the durations of torpid and euthermic intervals during mammalian hibernation: A test of the theory of metabolic control of the timing of changes in body temperature. J Comp Physiol B. 1985; 156: 13–19. https://doi.org/10.1007/BF00692921 PMID: 3836228

75. French AR. Effects of temperature on the duration of arousal episodes during hibernation. J Appl Physiol Respir Environ Exerc Physiol. 1982; 52: 216–220. PMID: 7061268

76. Geiser F, Baudinette RV. The relationship between body mass and rate of rewarming from hibernation and daily torpor in mammals. J Exp Biol. 1990; 151: 349–359. PMID: 2380659

77. Hirshfeld JR, O'Farrell MJ. Comparisons of differential warming rates and tissue temperatures in some species of desert bats. Comp Biochem Physiol A Comp Physiol. 1976; 55: 83–87. https://doi.org/10.1016/0300-9629(76)90127-4 PMID: 8251

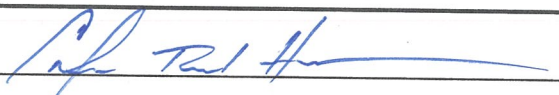
Appendix F

Statements of contribution and copyright declarations

MASSEY UNIVERSITY
GRADUATE RESEARCH SCHOOL

STATEMENT OF CONTRIBUTION
DOCTORATE WITH PUBLICATIONS/MANUSCRIPTS

We, the candidate and the candidate's Primary Supervisor, certify that all co-authors have consented to their work being included in the thesis and they have accepted the candidate's contribution as indicated below in the *Statement of Originality*.

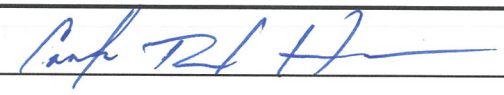
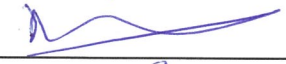
Name of candidate:	CARTER. R. HRANAC
Name/title of Primary Supervisor:	DAVID T.S. HAYMAN, PROFESSOR
Name of Research Output and full reference:	
HRANAC, CR., MARSHALL, J.C., MONADJEM, A, HAYMAN, D.T.S. (2019) PREDICTING EBOLAVIRUS DISEASE RISK AND THE ROLE OF AFRICAN BAT BIRTHING. EPIDEMICS, IN REVIEW	
In which Chapter is the Manuscript /Published work:	2 & 3
Please indicate:	
• The percentage of the manuscript/Published Work that was contributed by the candidate:	90%
and	
• Describe the contribution that the candidate has made to the Manuscript/Published Work:	
- Developed methods, compiled data, wrote code, ran the analysis, wrote the first draft	
For manuscripts intended for publication please indicate target journal:	
Epidemics	
Candidate's Signature:	
Date:	20/08/2019
Primary Supervisor's Signature:	
Date:	20/08/2019

(This form should appear at the end of each thesis chapter/section/appendix submitted as a manuscript/ publication or collected as an appendix at the end of the thesis)

MASSEY UNIVERSITY
GRADUATE RESEARCH SCHOOL

STATEMENT OF CONTRIBUTION
DOCTORATE WITH PUBLICATIONS/MANUSCRIPTS

We, the candidate and the candidate's Primary Supervisor, certify that all co-authors have consented to their work being included in the thesis and they have accepted the candidate's contribution as indicated below in the *Statement of Originality*.

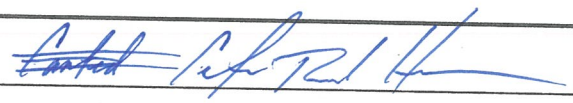
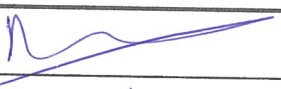
Name of candidate:	Carter Reed Hranac
Name/title of Primary Supervisor:	David T.S. Hayman, Professor
Name of Research Output and full reference:	
Hranac, CR, Haase, CG, Fuller, NW, Marshall, JC, Jansen, CL, McGuire, LP, Olsen, S. Hayman, DTS What is Winter? Addressing data deficiencies for wintering bats, (INPrep)	
In which Chapter is the Manuscript /Published work:	4
Please indicate:	
• The percentage of the manuscript/Published Work that was contributed by the candidate:	90
and	
• Describe the contribution that the candidate has made to the Manuscript/Published Work:	
•Conceived of work, developed methods, compiled data, wrote code, ran analyses, wrote draft	
For manuscripts intended for publication please indicate target journal:	
Proceedings of the Royal society B	
Candidate's Signature:	
Date:	20/08/2019
Primary Supervisor's Signature:	
Date:	20/08/2019

(This form should appear at the end of each thesis chapter/section/appendix submitted as a manuscript/ publication or collected as an appendix at the end of the thesis)

MASSEY UNIVERSITY
GRADUATE RESEARCH SCHOOL

STATEMENT OF CONTRIBUTION
DOCTORATE WITH PUBLICATIONS/MANUSCRIPTS

We, the candidate and the candidate's Primary Supervisor, certify that all co-authors have consented to their work being included in the thesis and they have accepted the candidate's contribution as indicated below in the *Statement of Originality*.

Name of candidate:	Carter Reed Hranac
Name/title of Primary Supervisor:	David T.S. Hayman, Professor
Name of Research Output and full reference:	
Haase, CG, Fuller, NW, Hayman, DTS, Hranac, CR, Olson, SH, Plowright, RK, McGuire LP. (2019), Journal of Thermal Biology, (81) 185-193	
In which Chapter is the Manuscript /Published work:	Appendix D
Please indicate:	
• The percentage of the manuscript/Published Work that was contributed by the candidate:	24%
and	
• Describe the contribution that the candidate has made to the Manuscript/Published Work:	
wrote code, analysed data, commented on manuscript	
For manuscripts intended for publication please indicate target journal:	
Candidate's Signature:	
Date:	20/08/2019
Primary Supervisor's Signature:	
Date:	20/08/2019

(This form should appear at the end of each thesis chapter/section/appendix submitted as a manuscript/ publication or collected as an appendix at the end of the thesis)

MASSEY UNIVERSITY
GRADUATE RESEARCH SCHOOL

STATEMENT OF CONTRIBUTION
DOCTORATE WITH PUBLICATIONS/MANUSCRIPTS

We, the candidate and the candidate's Primary Supervisor, certify that all co-authors have consented to their work being included in the thesis and they have accepted the candidate's contribution as indicated below in the *Statement of Originality*.

Name of candidate:	Carter Reed Hranac
Name/title of Primary Supervisor:	David T.S. Hayman, Professor
Name of Research Output and full reference: (Author list same as Appendix D)	
Incorporating evaporative water loss into bioenergetic models of hibernation to test for realistic influence of host and pathogen traits of white nose syndrome	
In which Chapter is the Manuscript /Published work:	
Please indicate: Appendix E	
• The percentage of the manuscript/Published Work that was contributed by the candidate:	25%
and	
• Describe the contribution that the candidate has made to the Manuscript/Published Work:	
wrote code, ran analysis, reviewed manuscript	
For manuscripts intended for publication please indicate target journal:	
PLOS Computational Biology	
Candidate's Signature:	Carter R Hranac
Date:	
Primary Supervisor's Signature:	
Date:	20/08/2019

(This form should appear at the end of each thesis chapter/section/appendix submitted as a manuscript/ publication or collected as an appendix at the end of the thesis)

SPRINGER NATURE LICENSE TERMS AND CONDITIONS

Aug 21, 2019

This Agreement between Mr. Carter Hranac ("You") and Springer Nature ("Springer Nature") consists of your license details and the terms and conditions provided by Springer Nature and Copyright Clearance Center.

License Number	4653850261143
License date	Aug 21, 2019
Licensed Content Publisher	Springer Nature
Licensed Content Publication	Nature Reviews Microbiology
Licensed Content Title	Pathways to zoonotic spillover
Licensed Content Author	Raina K. Plowright, Colin R. Parrish, Hamish McCallum, Peter J. Hudson, Albert I. Ko et al.
Licensed Content Date	May 30, 2017
Licensed Content Volume	15
Licensed Content Issue	8
Type of Use	Thesis/Dissertation
Requestor type	academic/university or research institute
Format	print and electronic
Portion	figures/tables/illustrations
Number of figures/tables /illustrations	1
High-res required	no
Will you be translating?	no
Circulation/distribution	<501
Author of this Springer Nature content	no
Title	Ecology of infectious disease in wild bats
Institution name	Massey University
Expected presentation date	Nov 2019
Order reference number	Figure 2
Portions	Figure number 2 the barriers to spillover and the figure caption
Requestor Location	Mr. Carter Hranac 8 Worcester St West End Palmerston North, Manawatu-wanganui 4410 New Zealand Attn: Mr. Carter Hranac
Total	0.00 USD
Terms and Conditions	

Springer Nature Customer Service Centre GmbH
Terms and Conditions

This agreement sets out the terms and conditions of the licence (the **Licence**) between you and **Springer Nature Customer Service Centre GmbH** (the **Licensor**). By clicking 'accept' and completing the transaction for the material (**Licensed Material**), you also confirm your acceptance of these terms and conditions.

1. Grant of License

1. 1. The Licensor grants you a personal, non-exclusive, non-transferable, world-wide licence to reproduce the Licensed Material for the purpose specified in your order only. Licences are granted for the specific use requested in the order and for no other use, subject to the conditions below.

1. 2. The Licensor warrants that it has, to the best of its knowledge, the rights to license reuse of the Licensed Material. However, you should ensure that the material you are requesting is original to the Licensor and does not carry the copyright of another entity (as credited in the published version).

1. 3. If the credit line on any part of the material you have requested indicates that it was reprinted or adapted with permission from another source, then you should also seek permission from that source to reuse the material.

2. Scope of Licence

2. 1. You may only use the Licensed Content in the manner and to the extent permitted by these Ts&Cs and any applicable laws.

2. 2. A separate licence may be required for any additional use of the Licensed Material, e.g. where a licence has been purchased for print only use, separate permission must be obtained for electronic re-use. Similarly, a licence is only valid in the language selected and does not apply for editions in other languages unless additional translation rights have been granted separately in the licence. Any content owned by third parties are expressly excluded from the licence.

2. 3. Similarly, rights for additional components such as custom editions and derivatives require additional permission and may be subject to an additional fee. Please apply to Journalpermissions@springernature.com/bookpermissions@springernature.com for these rights.

2. 4. Where permission has been granted **free of charge** for material in print, permission may also be granted for any electronic version of that work, provided that the material is incidental to your work as a whole and that the electronic version is essentially equivalent to, or substitutes for, the print version.

2. 5. An alternative scope of licence may apply to signatories of the STM Permissions Guidelines, as amended from time to time.

3. Duration of Licence

3. 1. A licence for is valid from the date of purchase ('Licence Date') at the end of the relevant period in the below table:

Scope of Licence	Duration of Licence
Post on a website	12 months
Presentations	12 months

Books and journals	Lifetime of the edition in the language purchased

4. Acknowledgement

4. 1. The Licensor's permission must be acknowledged next to the Licenced Material in print. In electronic form, this acknowledgement must be visible at the same time as the figures/tables/illustrations or abstract, and must be hyperlinked to the journal/book's homepage. Our required acknowledgement format is in the Appendix below.

5. Restrictions on use

5. 1. Use of the Licensed Material may be permitted for incidental promotional use and minor editing privileges e.g. minor adaptations of single figures, changes of format, colour and/or style where the adaptation is credited as set out in Appendix 1 below. Any other changes including but not limited to, cropping, adapting, omitting material that affect the meaning, intention or moral rights of the author are strictly prohibited.

5. 2. You must not use any Licensed Material as part of any design or trademark.

5. 3. Licensed Material may be used in Open Access Publications (OAP) before publication by Springer Nature, but any Licensed Material must be removed from OAP sites prior to final publication.

6. Ownership of Rights

6. 1. Licensed Material remains the property of either Licensor or the relevant third party and any rights not explicitly granted herein are expressly reserved.

7. Warranty

IN NO EVENT SHALL LICENSOR BE LIABLE TO YOU OR ANY OTHER PARTY OR ANY OTHER PERSON OR FOR ANY SPECIAL, CONSEQUENTIAL, INCIDENTAL OR INDIRECT DAMAGES, HOWEVER CAUSED, ARISING OUT OF OR IN CONNECTION WITH THE DOWNLOADING, VIEWING OR USE OF THE MATERIALS REGARDLESS OF THE FORM OF ACTION, WHETHER FOR BREACH OF CONTRACT, BREACH OF WARRANTY, TORT, NEGLIGENCE, INFRINGEMENT OR OTHERWISE (INCLUDING, WITHOUT LIMITATION, DAMAGES BASED ON LOSS OF PROFITS, DATA, FILES, USE, BUSINESS OPPORTUNITY OR CLAIMS OF THIRD PARTIES), AND
WHETHER OR NOT THE PARTY HAS BEEN ADVISED OF THE POSSIBILITY OF SUCH DAMAGES. THIS LIMITATION SHALL APPLY NOTWITHSTANDING ANY FAILURE OF ESSENTIAL PURPOSE OF ANY LIMITED REMEDY PROVIDED HEREIN.

8. Limitations

8. 1. ***BOOKS ONLY:***Where **'reuse in a dissertation/thesis'** has been selected the following terms apply: Print rights of the final author's accepted manuscript (for clarity, NOT the

published version) for up to 100 copies, electronic rights for use only on a personal website or institutional repository as defined by the Sherpa guideline (www.sherpa.ac.uk/romeo/).

9. Termination and Cancellation

9. 1. Licences will expire after the period shown in Clause 3 (above).

9. 2. Licensee reserves the right to terminate the Licence in the event that payment is not received in full or if there has been a breach of this agreement by you.

Appendix 1 — Acknowledgements:

For Journal Content:
Reprinted by permission from [**the Licensor**]: [**Journal Publisher** (e.g. Nature/Springer/Palgrave)] [**JOURNAL NAME**] [**REFERENCE CITATION** (Article name, Author(s) Name), [**COPYRIGHT**] (year of publication)

For **Advance Online Publication papers:**
Reprinted by permission from [**the Licensor**]: [**Journal Publisher** (e.g. Nature/Springer/Palgrave)] [**JOURNAL NAME**] [**REFERENCE CITATION** (Article name, Author(s) Name), [**COPYRIGHT**] (year of publication), advance online publication, day month year (doi: 10.1038/sj.[JOURNAL ACRONYM].)

For Adaptations/Translations:
Adapted/Translated by permission from [**the Licensor**]: [**Journal Publisher** (e.g. Nature/Springer/Palgrave)] [**JOURNAL NAME**] [**REFERENCE CITATION** (Article name, Author(s) Name), [**COPYRIGHT**] (year of publication)

Note: For any republication from the British Journal of Cancer, the following credit line style applies:

Reprinted/adapted/translated by permission from [**the Licensor**]: on behalf of Cancer Research UK: : [**Journal Publisher** (e.g. Nature/Springer/Palgrave)] [**JOURNAL NAME**] [**REFERENCE CITATION** (Article name, Author(s) Name), [**COPYRIGHT]** (year of publication)

For **Advance Online Publication** papers:
Reprinted by permission from The [**the Licensor**]: on behalf of Cancer Research UK: [**Journal Publisher** (e.g. Nature/Springer/Palgrave)] [**JOURNAL NAME**] [**REFERENCE CITATION** (Article name, Author(s) Name), [**COPYRIGHT**] (year of publication), advance online publication, day month year (doi: 10.1038/sj.[JOURNAL ACRONYM])

For Book content:
Reprinted/adapted by permission from [**the Licensor**]: [**Book Publisher** (e.g. Palgrave Macmillan, Springer etc) [**Book Title**] by [**Book author**(s)] [**COPYRIGHT**] (year of publication)

Other Conditions:

Version 1.2

Questions? customercare@copyright.com or +1-855-239-3415 (toll free in the US) or +1-978-646-2777.

Appendix G

Predicting Ebola virus disease risk and the role of African bat birthing

Epidemics xxx (xxxx) xxxx

Contents lists available at ScienceDirect

Epidemics

journal homepage: www.elsevier.com/locate/epidemics

Predicting Ebola virus disease risk and the role of African bat birthing

C. Reed Hranac[a,*], Jonathan C. Marshall[b], Ara Monadjem[c,d], David T.S. Hayman[a,*]

[a] Molecular Epidemiology and Public Health Laboratory, Hopkirk Research Institute, Massey University, Private Bag, 11 222, Palmerston North 4442, New Zealand
[b] Institute of Fundamental Sciences, Massey University, Private Bag 11 222, Palmerston North 4442, New Zealand
[c] Department of Biological Sciences, University of Eswatini, Private Bag 4, Kwaluseni, Eswatini
[d] Mammal Research Institute, Department of Zoology and Entomology, University of Pretoria, Pretoria, Republic of South Africa

ARTICLE INFO

Keywords:
Ebolavirus
Chiroptera
Pteropodidae
Spillover
Viral ecology
Spatio-temporal Poisson point process
Ecological niche model

ABSTRACT

Ebola virus disease (EVD) presents a threat to public health throughout equatorial Africa. Despite numerous 'spillover' events into humans and apes, the maintenance reservoirs and mechanism of spillover are poorly understood. Evidence suggests fruit bats play a role in both instances, yet data remain sparse and bats exhibit a wide range of life history traits. Here we pool sparse data and use a mechanistic approach to examine how birthing cycles of African fruit bats, molossid bats, and non-molossid microbats inform the spatio-temporal occurrence of EVD spillover. We create ensemble niche models to predict spatio-temporally varying bat birthing and model outbreaks as spatio-temporal Poisson point processes. We predict three distinct annual birthing patterns among African bats along a latitudinal gradient. Of the EVD spillover models tested, the best by quasi-Akaike information criterion (qAIC) and by out of sample prediction included significant African bat birth-related terms. Temporal bat birthing terms fit in the best models for both human and animal outbreaks were consistent with hypothesized viral dynamics in bat populations, but purely spatial models also performed well. Our best model predicted risk of EVD spillover at locations of the two 2018 EVD outbreaks in the Democratic Republic of the Congo was within the top 12–35% and 0.1% of all 25 × 25 km spatial cells analyzed in sub-Saharan Africa. Results suggest that sparse data can be leveraged to help understand complex systems.

1. Introduction

Since the first reports of Ebola virus disease (EVD) in the late 1970s outbreaks have occurred sporadically (Pourrut et al., 2005), with 34 identified human index cases to date (Fig. 1). The 2013–2016 West African EVD epidemic caused the death of at least 11,310 people and was a Public Health Emergency of International Concern (Briand et al., 2014). Outbreaks have been unpredictable, sometimes including more than one primary transmission or 'spillover' event, and together with high case fatality rates cause significant strain on public health authorities in typically resource poor settings (Pigott et al., 2016). Additional conservation concerns have arisen such as the large scale great ape die-offs linked to EVD in central Africa (Leroy et al., 2004). Despite decades of research the ecology, sylvatic maintenance, and mechanisms of spillover of these viruses to humans, or non-humans, have remained undetermined (Olival and Hayman, 2014).

The genus *Ebolavirus* (family *Filoviridae*) is composed of five recognized viral species, four of which are agents of EVD (Olival and Hayman, 2014). An additional proposed sixth *Ebolavirus* species with unknown ability to cause EVD was also described recently (Goldstein et al., 2018). For the four *Ebolavirus* species known to cause EVD mounting evidence implicates African Old World fruit bat species (Order Chiroptera; family Pteropodidae) as potential reservoirs as defined by Haydon et al. (2002) in maintaining and propagating infection on the landscape (De Nys et al., 2018; Leroy et al., 2005; Han et al., 2016; Pourrut et al., 2009). However, different bats may play roles as both necessary and sufficient hosts in reservoir host communities (Nishiura et al., 2009). To date no full EVD-causing *Ebolavirus* has been isolated from a bat host. Possible reasons for this, if they are true maintenance reservoir hosts, include: the remote geographic locations of the EVD outbreaks; nomadic or migratory nature of bats (Nowak, 1994); potentially acute viremic periods (Swanepoel et al., 1996); spatio-temporal extinction and recolonization dynamics, the unknown role of viral persistence and intermittent viral shedding (Schuh et al., 2017), and possibly biased samples unrepresentative of true bat diversity (Leendertz et al., 2016).

Despite these limitations, RNA viral fragments of ebolaviruses causing EVD have been recovered from three African fruit bat species: Franquet's epauletted fruit bat (*Epomops franqueti*), the Hammer-headed bat (*Hypsignathus monstrosus*), and the Little collared fruit bat

* Corresponding authors.
E-mail addresses: c.r.hranac@massey.ac.nz (C. Reed Hranac), d.t.s.hayman@massey.ac.nz (D.T.S. Hayman).

https://doi.org/10.1016/j.epidem.2019.100366
Received 14 February 2019; Received in revised form 19 August 2019; Accepted 22 August 2019
1755-4365/ © 2019 The Authors. Published by Elsevier B.V. This is an open access article under the CC BY-NC-ND license (http://creativecommons.org/licenses/BY-NC-ND/4.0/).

Please cite this article as: C. Reed Hranac, et al., Epidemics, https://doi.org/10.1016/j.epidem.2019.100366

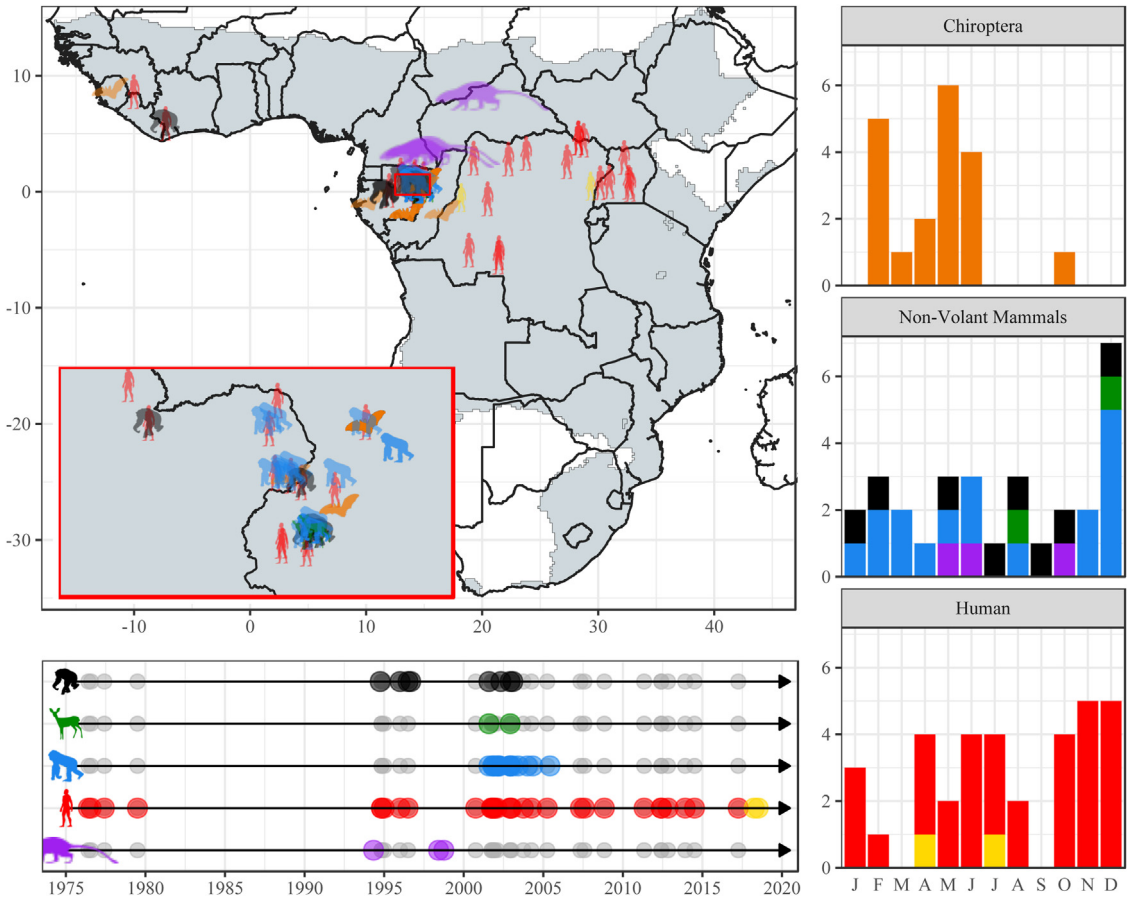


Fig. 1. Spatial and temporal detection of ebolavirus by host taxonomic group. *Top left*: Location of all EVD index spillover events and detections within bat populations. Zoom panel focuses in on the border of Gabon and Republic of Congo. *Bottom left*: Viral detection by taxonomic classes (non-human timeline grey points are human events for reference). *Right*: Frequency of viral detection by taxonomic host collapsed into a single year and aggregated by month. Bats are orange, chimpanzees black, duikers green, gorillas blue, rodents purple and humans red. In all cases except for the bats detections represent unique spillover events. For bats, a detection represents the recovery of an ebolavirus viral RNA gene fragment. The two most recent outbreaks in the DRC are denoted in gold. All references, are available within the online material. (For interpretation of the references to color in this figure legend, the reader is referred to the web version of this article.)

(*Myonycteris torquata*) (Leroy et al., 2005). *Ebolavirus* fragments were also detected in four rodent species: two *Praomys sp.*, two *Mus sp.* and one shrew *Sylvisorex ollula* (family: Soricidae) (Morvan et al., 1999), although there is some contention whether these species could effectively act as reservoir hosts (Swanepoel et al., 1996) and whether these were in fact active infections (Taylor et al., 2010). Phylogenetic analyses have also suggested that fruit bats have played some role in the recent evolutionary history of *Zaire ebolavirus* (Walsh et al., 2005; Biek et al., 2006). Most recently 20% of an *Ebolavirus* has reportedly been sequenced from an insectivorous greater long-fingered bat (*Miniopterus inflatus*), captured in 2016 in Liberia (Kupferschmidt, 2019).

Much of what is postulated about the ecological niche and sylvatic maintenance of ebolaviruses is inferred from a member of its sister genus, *Marburgvirus marburgvirus* (MARV). MARV circulates within cave dwelling Egyptian fruit bat (*Rousettus aegyptiacus*) colonies with seasonal increases in viral shedding among juvenile bats and the high birthing synchrony (Amman et al., 2012), although the inclusion of persistent infection with intermittent viral shedding has still to be explored for ebolaviruses. Anti-marburgvirus antibodies have also been detected within co-roosting insectivorous bats, which to date play an unknown role in sylvatic maintenance. Machine learning and infection dynamic simulations have both identified biannual, synchronous birth-pulses as potentially important host life history traits for filovirus maintenance, all traits found within African bat species (Han et al., 2016; Hayman, 2015).

While there are many similarities between MARV and ebolavirus systems, the principal suspected ebolavirus reservoirs are primarily tree roosting bat species with far lower colony densities compared to the Egyptian fruit bat. The sporadic occurrence of outbreaks, lifestyles of putative reservoirs, viral dynamics and subsequent antibody production in bats (Swanepoel et al., 1996) suggest a potential reliance on meta-populations within a larger reservoir community to sustain sylvatic ebolavirus transmission (Brown et al., 2013; Grenfell et al., 2001; Han et al., 2016; Hassanin et al., 2016). Strong, spatially asynchronous seasonal forcing events, including birthing, likely add additional layers of complexity in disease outbreak events (Duke-Sylvester et al., 2011).

Spatial risk models have previously identified regions of realized and unrealized risk throughout equatorial sub-Saharan Africa, linked to a variety of drivers, including forest fragmentation and vegetation index (Rulli et al., 2017; Pigott et al., 2014, 2016). Additional temporal risk models have suggested that EVD spillover risk across the region is greatest during transitions between wet and dry seasons (Schmidt et al., 2017), periods also associated with African bat species birthing events (Cumming and Bernard, 1997). One hypothesis of filovirus spillover risk posits that synchronous shifts in population demographics may be responsible for periods of increased viral shedding similar to those witnessed in the MARV system (Hayman, 2015; Pourrut et al., 2009).

In this work we test the hypothesis that birthing among some African bat species is linked to EVD spillover events to humans and forest dwelling animals susceptible to EVD, hereafter referred to as “non-human spillover hosts.” Due to the rarity of EVD outbreak events we were not able to model each EVD-causing *Ebolavirus* species

separately, and therefore combined them all together to represent a single, general, "ebolavirus" capable of infecting and causing EVD in mammalian hosts. We created two general model frameworks: a model describing the birthing patterns of African bats; and another to describe the relative spillover risk. We assumed bats were reservoir hosts and that non-human spillover hosts have different habitat use, risk factors and contact patterns with the potential reservoir host(s) than humans. Subsequently we modeled spillover into non-human spillover hosts independently of humans. We then used the two most recent outbreaks of EVD in the Democratic Republic of the Congo (DRC) (Barry et al., 2018; WHO, 2018), which were excluded from our modeling procedures (but see methods), to test the predictive power of our generated models.

2. Materials and methods

Evolutionary, environmental, and phenological processes undoubtedly drive the timing and location of bat breeding and birthing, yet these intricacies have yet to be fully described. Sparse data exist for the timing bat births, especially in mainland tropical Africa (Cumming and Bernard, 1997; Monadjem et al., 2010). To circumvent these issues we compiled the better part of 50 years of ecological research into a single, recirculating year of spatio-temporally defined bat birthing events (full data mining methods in SI Methods). Bat species were subset into three groups: African fruit bats (family Pteropodidae), molossid bats (family Molossidae), and non-molossid microbats, as described by Cumming and Bernard (1997). These taxonomic clusters tend to share key life history traits such as diet and reproductive strategies making them useful subgroups for this analysis. Combining these occurrence data with static and temporally explicit geographic covariate layers (see SI Table 2) allowed us to construct temporally defined ecological niche models (ENMs) of bat birthing across a subset of sub-Saharan Africa. This subset was restricted to locations in mainland Africa receiving more than 500 mL of precipitation annually, as suggested by Schmidt et al. (2017). While outbreaks have not been observed in much of this region and hypothesized reservoir species use subsets of these regions making them a potentially unrealized viral niche. Unlike most ENMs that correlate a probably of occurrence with environmental conditions at any given location, we modified our procedure to correlate dynamic phenological signals focused on changing environments with bat birthing cycles (see full details for covariate selection and processing in SI methods and SI Table 2). We used a sliding two month observation window to estimate the probability of wild species giving birth across space and time for all pairs of consecutive months where sufficient data existed (see full ENM description in SI Methods).

The ENM results were used and combined with bat diversity in a number of different ways. First and most intuitively, the probability of birthing for the three different taxonomic class were used as covariates where probability of birth occurrence is $P_{T,i,t}$ for each taxonomic group T, at location i and time t. Next the ENM results were combined with local species diversity estimates to create a "force of birthing" ($\lambda_{T,i,t}$) metric, representing the relative number of taxon member species giving birth at any time and space, as defined by:

$$\lambda_{T,i,t} = P_{T,i,t}\mathrm{D}_{T,i}$$

where the number of taxonomic members is given by $\mathrm{D}_{T,i}$. The abbreviations *afb*, *mic* and *mol* were used to represent African fruit bats, non-molossid microbats, and molossid bats respectively. Third, the total conditional probability $P_{total,i,t}$ of any bat birthing from any of the three taxonomic groups at location i and time t, assuming independence, defined by:

$$P_{\mathrm{total},i,t} = 1 - \prod_{T=1}^{n}(1 - P_{T,i,t})$$

A total "force of birthing" ($\lambda_{total,i,t}$) metric representing the number of bats of all taxons giving birth at any time and space as defined by:

$$\lambda_{\mathrm{total},i,t} = P_{\mathrm{total},i,t}\sum_{T=1}^{n}\mathrm{D}_{T,i}$$

Finally, a modified version of the probability of birth was made for the African fruit bats in which we accounted for variation within taxonomic classes in the first annual birthing pulse of the year. Previous work has indicated that the bi-annually polyestrous breeding African fruit bats will have a birth pulse proceeding the start of the short dry period in addition to giving birth following the long dry season like all monoestrous species. Historically phenomena was only seen above ~18° S, south of which all fruit bat populations only had a single annual birth associated with the long-dry season (Cumming and Bernard, 1997). However, our modeling results suggested a threshold of ~10° S and therefore we used this value. We accounted for this by down-weighting the probability of birth on the first six months of the calendar year by a ratio of biannual genera:total genera $\left(\frac{5}{9}\right)$, as determined by our data-mining results. This information was not available on a comparable scale for any other taxonomic group. This modification allowed us to further probe the involvement of African fruit bat births on ebolavirus spillover events and is denoted throughout with the * symbol.

To test the hypothesized link between spillover events and bat birthing we collapsed the 42 year history of EVD outbreaks into the same recirculating year used in the birthing ENM. We then treated outbreaks as a spatio-temporal Poisson point process, with rate (herein, risk) estimated using a spatially weighted, over-dispersed general linear model (spatGLM). To assess the hypothesized temporal lags between birth pulses and outbreak events due to shifting population demographics we included lag terms for bat birthing terms. In the model with most parameters, the risk of EVD spillover into non-human spillover hosts was defined as:

$$\begin{aligned}\log(R_{\mathrm{an},i,t}) \sim\ & \beta_1 P_{\mathrm{afb}*,i,t} + \beta_2 P_{\mathrm{mic},l,i,t} + \beta_3 P_{\mathrm{mol},i,t} \\ & + \beta_4 P_{\mathrm{afb}*,i,t-2} + \beta_5 P_{\mathrm{mic},i,t-2} + \beta_6 P_{\mathrm{mol},i,t-2} \\ & + \beta_7 P_{\mathrm{afb}*,i,t-4} + \beta_8 P_{\mathrm{mic},i,t-4} + \beta_9 P_{\mathrm{mol},i,t-4} \\ & + \beta_{10} P_{\mathrm{afb}*,i,t-6} + \beta_{11} P_{\mathrm{mic},i,t-6} + \beta_{12} P_{\mathrm{mol},i,t-6} \\ & + \beta_{13}\mathrm{D}_{\mathrm{afb},i} + \beta_{14}\mathrm{D}_{\mathrm{mic},i} + \beta_{15}\mathrm{D}_{\mathrm{mol},i} \\ & + \beta_{16}\mathrm{NBMdiv}_i + \beta_{17}\mathrm{PopDen}_i + \beta_{18}\mathrm{fragIndex}_i \\ & + \beta_{19}\mathrm{BVD}_{i,t}\end{aligned}$$

where $R_{\mathrm{an},i,t}$ represented the risk of EVD spillover at spatial location i, and month t. Potential sources of infection on the landscape were defined as times and locations where RNA fragments had been recovered from wild bats, our hypothesized reservoir hosts, and were included by the term $\mathrm{BVD}_{i,t}$. Seropositive animals were not included because the timing of infection is unknown. Non-bat mammalian diversity and a forest fragmentation index (Wilkinson et al., 2018) were also included as the terms NBMdiv_i and $\mathrm{fragIndex}_i$. Human population density, PopDen_i was included to represent the human-wildlife interface (Plowright et al., 2015). The transformation $\log(x + 1)$ was used to treat all variables (with the exception of $\mathrm{BVD}_{i,t}$) on the log scale while allowing that they might be zero.

Human outbreak events are not exclusively linked to direct exposure to proposed bat reservoir host(s) (Pourrut et al., 2005) and so outbreaks in non-humans were included within the human spillover model to capture these transmission chains. A lag term of a single month was included for non-human outbreaks to describe the transmission chain and incubation periods of non-human spillover hosts acting as amplifying hosts and transmitting virus to humans (Swanepoel et al., 1996). The risk of EVD spillover into humans (R_{hum}) was therefore described as:

$$\begin{aligned}\log(R_{\text{hum},i,t})\sim\ & \beta_1 P_{\text{afb}*,i,t} + \beta_2 P_{\text{mic},l,i,t} + \beta_3 P_{\text{mol},i,t} \\ & + \beta_4 P_{\text{afb}*,i,t-2} + \beta_5 P_{\text{mic},i,t-2} + \beta_6 P_{\text{mol},i,t-2} \\ & + \beta_7 P_{\text{afb}*,i,t-4} + \beta_8 P_{\text{mic},i,t-4} + \beta_9 P_{\text{mol},i,t-4} \\ & + \beta_{10} P_{\text{afb}*,i,t-6} + \beta_{11} P_{\text{mic},i,t-6} + \beta_{12} P_{\text{mol},i,t-6} \\ & + \beta_{13} \text{D}_{\text{afb},i} + \beta_{14} \text{D}_{\text{mic},i} + \beta_{15} \text{D}_{\text{mol},i} \\ & + \beta_{16} \text{NBMdiv}_i + \beta_{17} \text{PopDen}_i + \beta_{18} \text{fragIndex}_i \\ & + \beta_{19} \text{BVD}_{i,t} + \beta_{20} \text{OB}_{\text{an},i,t} + \beta_{21} \text{OB}_{\text{an},i,t-1}\end{aligned}$$

where OB_{an} is the occurrence of an EVD spillover into a non-human spillover host at spatial location i, and month t.

Within alternative models, bat diversity terms were tested as both combined (read: any bat species), and separated by taxon to test the relative contribution of each tax group to overall spillover risk. "Null" models in which all bat birth associated terms ($P_{T,i,t}$, $P_{toal,i,t}$, $\lambda_{T,i,t}$, and $\lambda_{total,i,t}$) were excluded were also computed and model comparison and selection were completed though qAIC (see SI Methods for details).

Additional validation was provided by testing our model predictions using the two most recent EVD outbreaks in the DRC, which were not included in the analysis. To do so, we estimated relative risk as $R_{\text{hum},i,t}/g_{\text{mean}}(R_{\text{hum},i,t})$, where g_{mean} is the geometric mean, and percent risk rank, which was calculated for all cells across all 12 months. Values were extracted for all cells covering the health districts where the spillover cases were purported to have occurred (Barry et al., 2018; WHO, 2018) and visually compared. Because the outbreak numbers are low, we also checked the model sensitivity to the inclusion of these two data points, and performed the same analyses as above.

Model forms for both human, and non-humans spillover host spatGLMs are available from SI Tables 5 and 6. All work was completed using custom code written for R (version 3.4.3 R Core Team, 2017) and is available at github.com/cReedHranac/FS.

3. Results

A total of 63 articles provided information on 14 African fruit bat species, 7 molossid species, and 43 non-molossid microbats at 75 unique locations, totaling 164 event records (Fig. 2, SI Table S1). Of these, 89% were retained with 8 records discarded as outside of our study extent within mainland Africa. EMNs were generated for all three bat taxonomic groups for 34 of 36 possible month pairs, and full model results are summarize in SI Table S2 and visualized in SI Figures 1–3.

At equatorial latitudes (± 10°) some African fruit bats and non-molossid microbats were predicted to experience conditions suitable for biannual birthing seasons, while molossid bat species had suitable conditions for birth nearly continuously throughout the year (Fig. 3). Above ~10° N the signal of habitat suitability was reduced for the non-molossid microbats and fruit bat species to two periods and one more broad period of habitat suitable for birth respectively. Results for molossid bats still suggested the suitability for two birth pulses although the signal for the period following the long dry season was less intense than at equatorial latitudes. At more southern latitudes (> ~10° S) molossid species results suggested suitability for biannual birthing patterns with a high degree of synchronicity in following to the long dry season. Both fruit bats and the non-molossid microbats were predicted to reduce births to a monoestrous reproductive cycle with births prior end the long dry season at southern latitudes. These results are largely consistent with previous work (Bernard and Cumming, 1997; Happold and Happold, 1990, 2013; Monadjem et al., 2010), but critically provide a continuous metric describing both the spatial and temporal aspects of the phenomenon.

The inclusion of bat terms improved the qAIC and predictive ability of our spatGLM models compared to the "null" models without bat terms for all human and the majority of animal models (Fig. 4, SI Tables 5 and 6). The top animal spillover model by qAIC included product terms of the conditional probability of bat birth (including the modified fruit bat term) and total bat diversity. The African fruit bat terms describing bat birthing events 5–6 months prior and both the molossid and fruit bat terms the month before and the month of spillover events were both significant and positively related to spillover risk to other mammals. Diversity of non-volant mammals is identified as a significant predictor and human population density had the only inverse significant relationship identified with spillover risk (see SI Table 5). The spatial and temporal locations of viral RNA detections in bats was also found to be a significant term providing credence to some of our

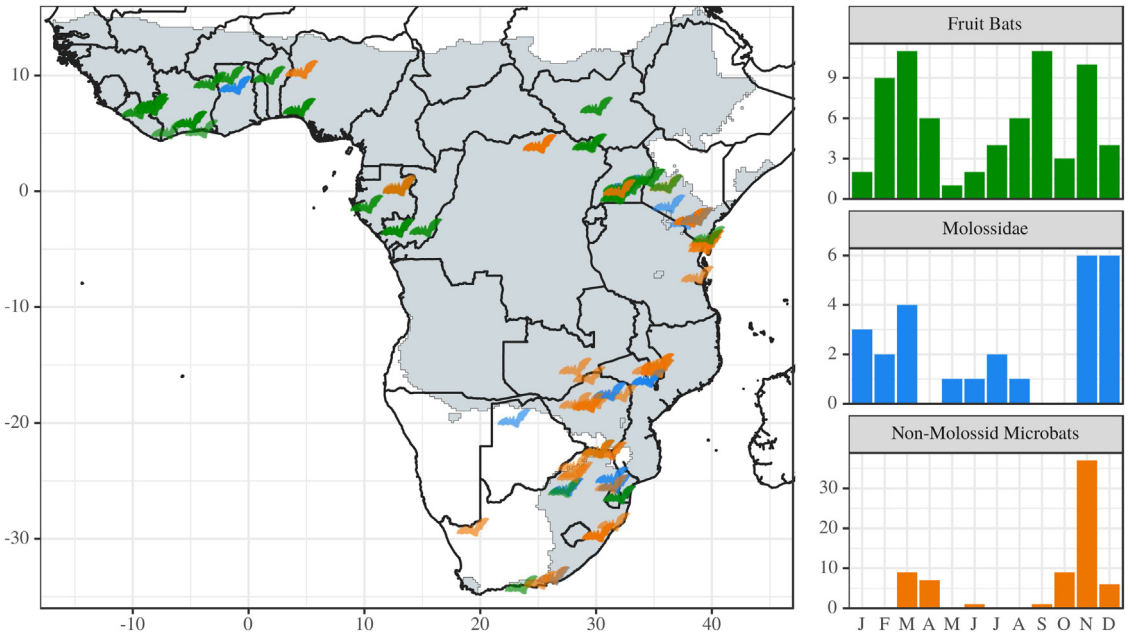


Fig. 2. Spatial and temporal occurrence of bat birthing records obtained from the literature. All results from mainland sub-Saharan Africa for the date and location of bat birth events. African fruit bat species are in green, molossid species in blue, and non-molossid microbats in orange. The gray background represents the study region and regions in white were excluded from this analysis. *Left*: Spatial locations of recorded observations. *Right*: Number of birthing observations in the literature by taxonomic group collapsed into a single year and aggregated by month. (For interpretation of the references to color in this figure legend, the reader is referred to the web version of this article.)

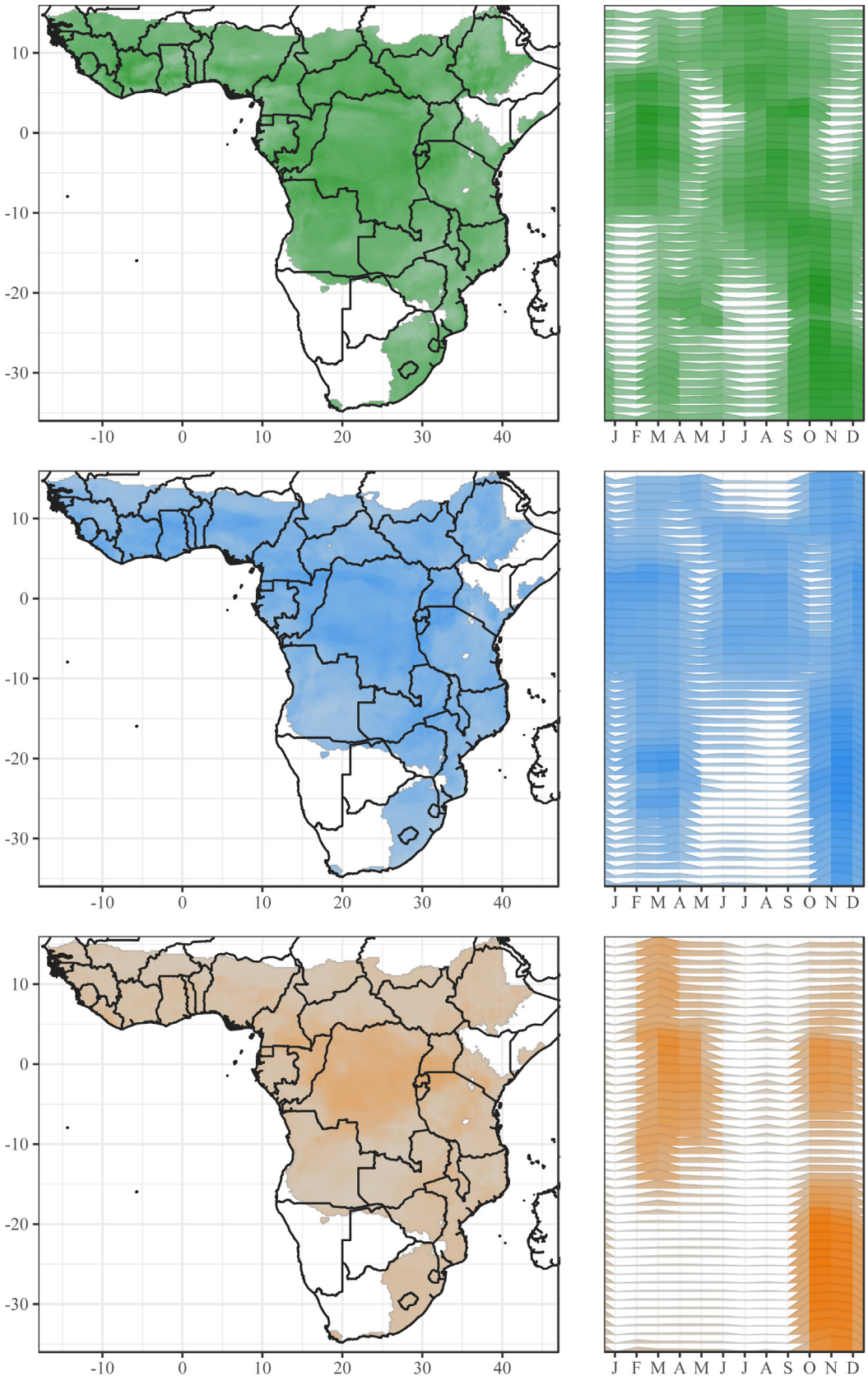


Fig. 3. Probability of birth of African bats. *Top row*: African fruit bats. *Middle row*: Molossid bats. *Bottom row*: Non-molossid microbats. *Left*: Mean annual probability of a bat giving birth spatially. Grey represents low values while more intense colors denote regions where a environmental conditions correlated with bat birth events are met. White regions were excluded from this study. *Right*: Probability of birth by latitude and month. Height and color intensity are proportional to relative number of species giving birth within the latitudinal window. (For interpretation of the references to color in this figure legend, the reader is referred to the web version of this article.)

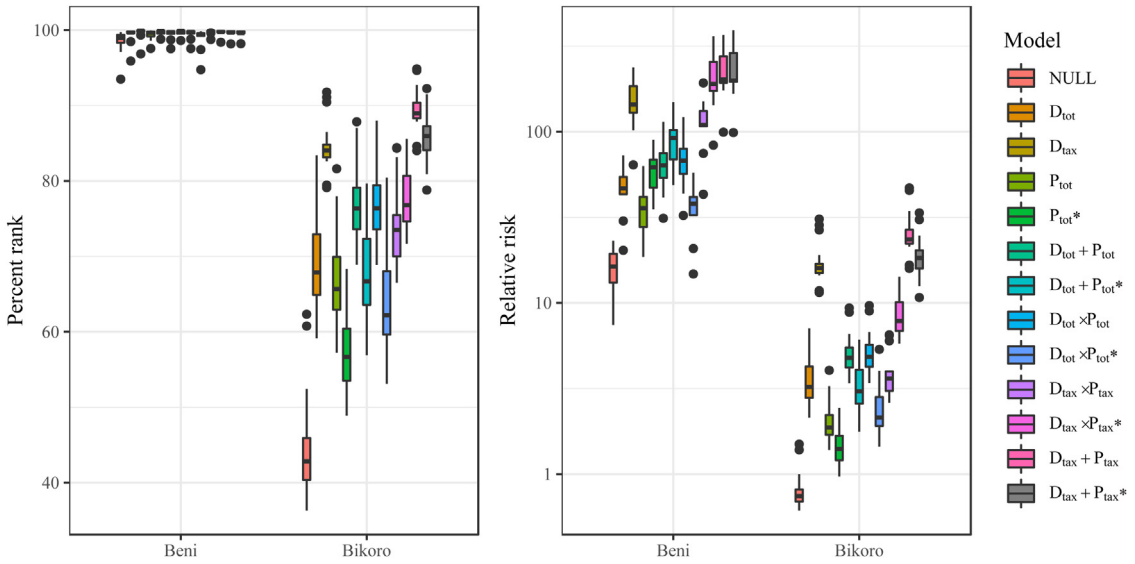


Fig. 4. Model prediction comparison. All proposed models predictive scores for the cells covering the health districts in which the two most recent DRC outbreaks occurred for the month of outbreak occurrence (July and April respectively). *Left*: Percent rank against all cells in all months, *Right*: relative risk of *Ebolavirus* spillover in to human populations. Models contain different covariate combinations of bat diversity (*D*), and bat birth terms (*B*) with were either separated by taxonomic group ($_{tax}$) or combined as ($_{tot}$). Alternative models that contain the down-weighted fruit bat term are denoted by *. (For interpretation of the references to color in this figure legend, the reader is referred to the web version of this article.)

hypotheses. Risk of EVD spillover to non-human spillover hosts was largely focused on Central Africa with high annual probability of infection across Gabon and the Republic of the Congo (RoC), the Eastern region of the Central African Republic (CAR), Northeastern DRC and included pockets in Western Africa covering Liberia, northern Côte d'Ivoire, and Ghana (SI Figure S4). Additional regions of potential risk were predicted throughout South Sudan, Uganda, and parts of Kenya. At equatorial latitudes risk was constantly elevated over the rest of the study area with seasonal peaks centered around May and September. Another region of elevated annual risk was predicted at 25° S covering Angola, Zambia, eastern Mozambique and Northern South Africa despite no known occurrences of eboalviruses south of 10° S. Seasonal fluctuations in risk peaked between May to July in a single annual pulse rather then the bi-modal pattern observed further North.

The top model for human spillover risk by qAIC used the taxonomically separated probability of birth terms and included the down-weighted fruit bat modification (*). Significant terms identified included EVD spillover into a non-human host in the month of and month prior to an outbreak, suggesting the model's sensitivity to the stuttering infection chains within the system and supporting observed patterns of infection transmission. The down-weighted probability of birthing term for the African fruit bat group 5–6 months prior, and the month of and month proceeding spillover events for both the fruit bats and non-molossid microbats were significant to predictions and top two models are summarized in Table 1 (See SI Table 6 for full alternative model results). Diversity of non-bat mammals was again identified as a significant predictor although neither viral detection in bats, nor the effect of forest fragmentation were identified as significant predictors of ebolavirus spillover to humans within this analysis. Risk of EVD spillover to humans was somewhat different to that of spillover into the non-human spillover hosts, as annual risk was more diffuse across Central Africa and more evenly distributed across areas of Western Africa (Fig. 5). Similar to the non-human spillover hosts, the highest risk zones occurred around the border of Gabon and the RoC, although Cameroon was included and the high risk of spillover within the CAR were missing from the human model results. The associated temporal analysis (Fig. 5 *right*) suggest seasonality within the system with two distinct periods of increased risk centered around the months of June and November just north of the equator. Acknowledging possible

Table 1
Top two human Ebola virus disease risk model results.

Model	$D_{tax} + P_{tax*}$			$D_{tax} + P_{tax}$		
	Estimate	± 95 CI	*P* value	Estimate	± 95 CI	*P* value
Intercept	−30.63	10.04	< 0.001	−31.62	10.00	< 0.001
P_{afb}	−2.41	2.16	0.04	−1.49	1.98	0.14
P_{mic}	1.83	1.53	0.02	1.48	1.50	0.06
P_{mol}	−0.19	2.00	0.84	−0.45	2.02	0.66
P_{afb_2}	0.91	2.04	0.29	1.39	1.88	0.15
P_{mic_2}	−0.06	1.55	0.93	−0.37	1.51	0.63
P_{mol_2}	0.29	2.14	0.73	0.11	2.18	0.92
P_{afb_4}	−0.39	1.96	0.9	−0.02	1.84	0.98
P_{mic_4}	−0.78	1.84	0.35	−0.95	1.80	0.3
P_{mol_4}	0.20	2.16	0.85	0.38	2.16	0.73
P_{afb_6}	1.60	1.88	0.05	1.29	1.94	0.19
P_{mic_6}	−0.27	1.61	0.67	−0.23	1.63	0.78
P_{mol_6}	1.34	1.98	0.2	1.48	1.94	0.13
D_{afb}	2.87	1.59	< 0.001	2.88	1.63	< 0.001
D_{mic}	1.86	2.76	0.18	1.92	2.78	0.18
D_{mol}	−0.59	1.57	0.46	−0.63	1.57	0.43
PopDen	−0.23	0.25	0.07	−0.23	0.255	0.08
fragIndex	−0.39	0.51	0.12	−0.4	0.51	0.12
BVD	−11.54	937.31	0.98	−11.43	944.88	0.98
D_{MNB}	3.23	2.31	< 0.001	3.36	2.33	< 0.001
OB_{an}	4.56	1.57	< 0.001	4.5	1.58	< 0.001
$OB_{an_{l-1}}$	2.89	2.20	0.01	2.71	2.23	0.02
qAIC		454.93			457.58	
$\hat{c}$		0.78			0.79	

surveillance bias, the difference in peak relative risk between the human and non-human spillover host models suggest potential differences in spillover mechanisms between human and non-reservoir mammal host systems.

The two most recent EVD outbreaks in the DRC provided a test of the predictive power of our model (Fig. 6). The EVD outbreak announced by the WHO in July likely started in April within the Bikoro health district in the northeastern part of the country close to the border with RoC (Barry et al., 2018). This health district showed seasonality with peaks and troughs in the relative risk of viral spillover into humans

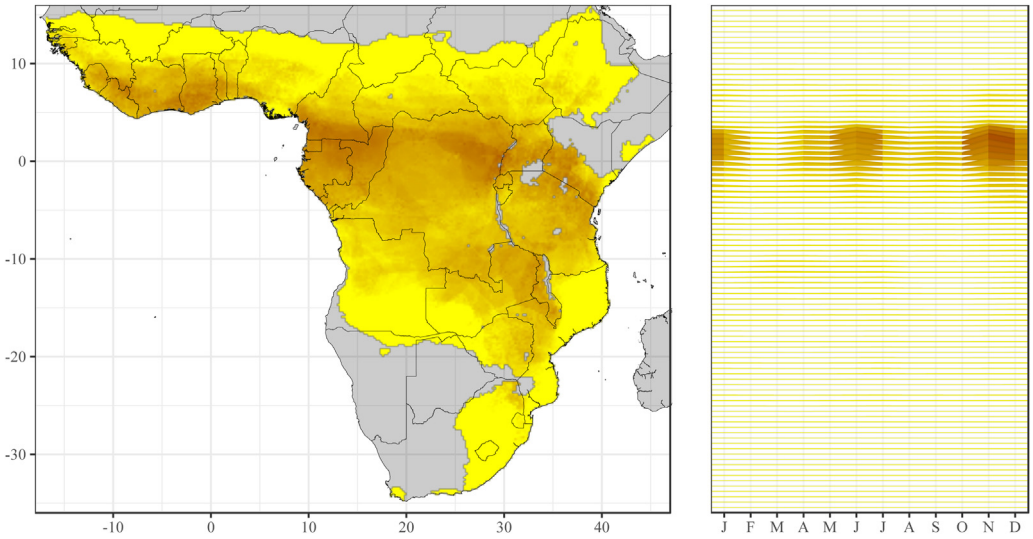


Fig. 5. Risk of Ebola virus disease outbreaks among people. *Left*: Mean annual risk of EVD emergence in humans across the study area. Low values are in yellow, high values in red, and grey zones were not included in the analysis. *Right*: Risk of EVD aggregated by latitude and month. Height and color intensity are proportional to the risk of EVD within the latitudinal window. (For interpretation of the references to color in this figure legend, the reader is referred to the web version of this article.)

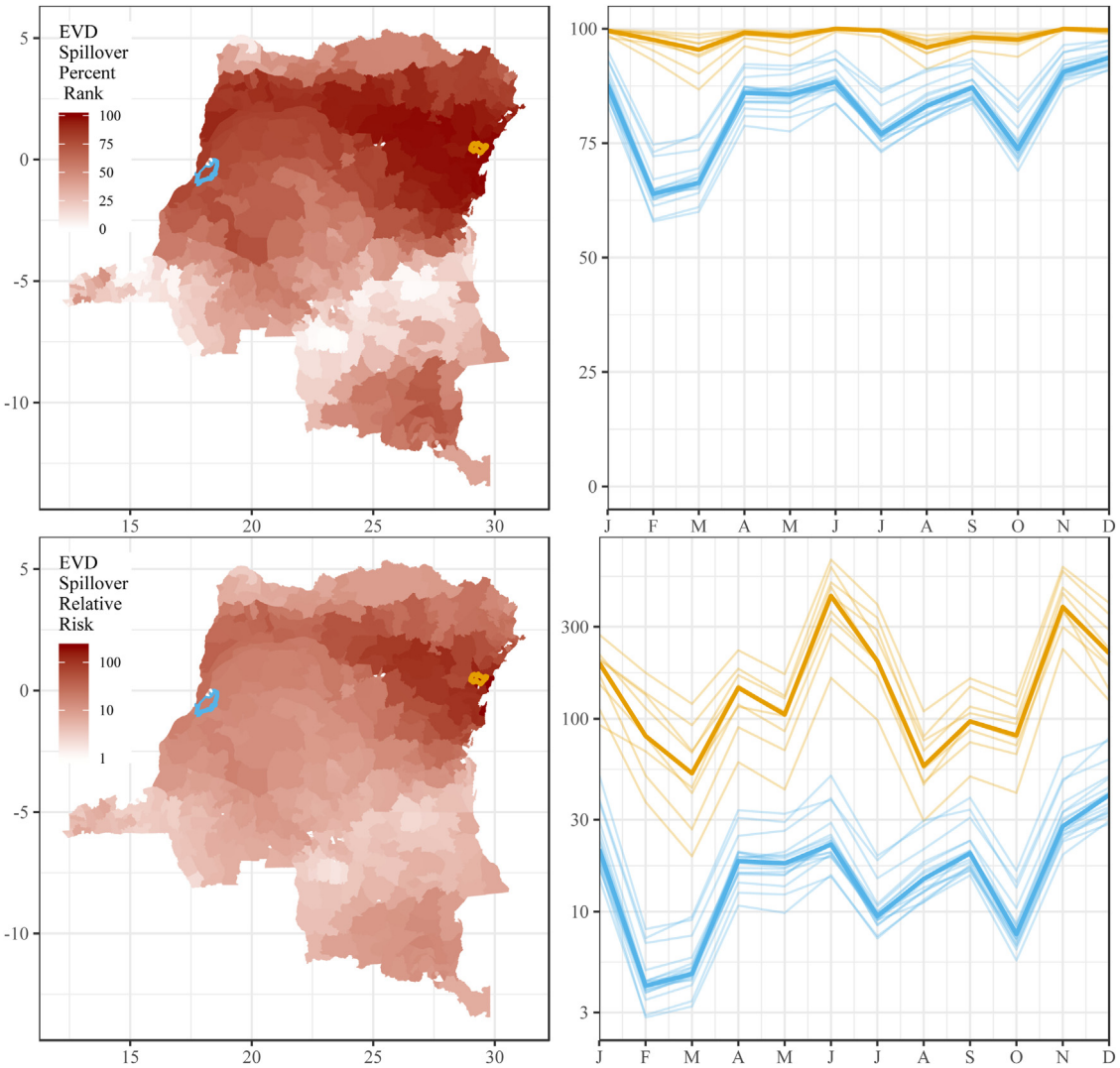


Fig. 6. Model results in the context of the most recent EVD outbreaks. In 2018 there were two recognized EVD outbreaks in the Democratic Republic of the Congo (DRC).The district of Bikoro where the July 2018 outbreak occurred is highlighted in blue, and highlighted in orange is the district of Beni where the outbreak announced in August 2018 started. The index case for the Bikoro epidemic was believed to be in April, while the Beni outbreak is believed to have begun in July. *Upper*: Percent risk ranking against all cells and all months (not just the DRC). *Lower*: Relative risk of viral spillover. *Left*: Annual average risk by district health zone. *Right*: Risk with in the health districts throughout the year. Each line represents a cell within the district and the median value is bolded. (For interpretation of the references to color in this figure legend, the reader is referred to the web version of this article.)

(Fig. 6). Of the 16 cells that covered the Bikoro health district there was a median percent rank scores of 88.3% compared to all cells in all months. Relative risk of ebolavirus spillover fluctuated between minimum, median, and high of 14.9, 21.3 and 50.4 respectively. The more recent EVD outbreak occurred in the district of Beni, a persistently highly ranked region. The district in northwestern DRC near the border with Uganda announced the outbreak on first of August with the index case was presumably in July or June (WHO, 2018). The smaller region was covered by only nine cells and risk percent rank values extracted from the model covering July were among the highest ranking of all cells with a median of 99.6%, minimum of 98.0% and maximum of 99.8%. Relative risk for the region was considerable with minimal values of 93.0, a median of 195.0 and a high of 273 across the year. Percent rank and relative risk scores were very similar between $D + B_{tax}*$ and $D + B_{tax}$ models with the later preforming slightly better in both metrics at the Bikoro site. We ultimately chose the $D + B_{tax}*$ model as our top model due to it's inclusion of more precise information related to our *a priori* hypotheses, and its comparable predictive power over all other alternative models.

4. Discussion

The spatial and temporal occurrence of ebolavirus on the landscape is complex, with seasonal drivers likely modifying the behaviors of both the (yet unidentified) maintenance reservoir host(s) and susceptible non-maintenance host populations. The inability of outbreak investigation teams to determine a definitive source of infection in all but a small number of cases has severely hindered the ability of public health officials to generate actionable measures against future EVD outbreak events. Infections from non-human spillover hosts to humans have only been confirmed from great apes and duikers, despite ebolavirus sequence detection in some Rodentia species (Morvan et al., 1999), Chiropteran species and the wide diversity of susceptible species within the biome (Leroy et al., 2004; Swanepoel et al., 1996). Here we predict the continental birthing patterns of African bats and find some statistical support for bats births, and African fruit bats in particular, being correlated with EVD outbreaks. Together we use these to predict the spatio-temporal risk of EVD outbreaks in non-human mammals and humans across the African continent.

The natural history, distributions and diversity of African bat species are broad yet through this analysis we are able to generate the first comprehensive spatio-temporal predictions for bat parturition events. Data availability ultimately required the use of several simplifying assumptions, most notably the consolidation of species into the taxonomic groups. This simplification creates scenarios in which within a single location two taxonomic members can give birth at different, non-overlapping times during a single birth pulse, or that a single species at two separate locations can give birth at different times again within a broader birth pulse. Despite this, the patterns predicted were largely consistent with previous work (Cumming and Bernard, 1997) with only minor deviations. The reduction in predictive signal from a biannual, or continual birthing above 10° is novel, although potentially an artefact of scare data availability at the northern most latitudes of our study extent. Our analysis also refined the latitudinal threshold from polyestrous to monoestrous from the 18° S to 10° S and was supported by more observations than the northern phenomenon. Data mining and collection highlighted the spatial and taxonomic bias of observations with extremely limited data availability for some of the largest, densest forests in continental Africa, and low representation of the most diverse taxonomic groups. However, models with terms describing the birth pulses of bats preformed highly for both the human and non-reservoir spillover host spatGLM. Furthermore the inclusion of the proportionally down-weighted birth term for the African fruit bats species improved predictive ability in most cases.

The discovery of statistical support for some African fruit bats species being correlated with ebolavirus outbreaks supports a number of previously disparate hypotheses (Hayman, 2015; Walsh et al., 2005; Han et al., 2016). The historical association of EVD spillover events and African fruit bats has been more anecdotal than factual in most cases, and to date no hunters targeting fruit bats have been confirmed index cases despite the widespread practice (Kamins et al., 2011; Mickleburgh et al., 2009; Peel et al., 2017). This may be because the species most hunted, *Eidolon helvum* (Kamins et al., 2011; Mickleburgh et al., 2009), is likely not a reservoir species, possibly due in part to its single annual birth pulse (in contrast to some other African fruit bats species) (Hayman et al., 2012, 2010) and unique cellular mechanisms (Ng et al., 2015). The large geographic spread by viral subtypes, such as that observed in the 2014 outbreak in West Africa, could be facilitated by other broad ranging African fruit bats such as the hammer-headed bat, whose population spans both Central to West African regions with little measurable population genetic structure (Hassanin et al., 2016). Until recently the only potential reservoir species from which EVD-causing Ebola virus viral fragments have been recovered were Pteropodidae members (Leroy et al., 2005; Olival and Hayman, 2014). Serological surveys have implicated molossid and non-molossid species, however serological data are difficult to interpret (Gilbert et al., 2013). Our analysis also identified molossid birthing events as a potential contributor to human risk of EVD spillover and serological findings are consistent with the patterns observed in MARV infected *R. aegyptiacus* (Pourrut et al., 2009; Amman et al., 2012). Recent detections of ebolavirus fragments in molossid species and our analyses suggest the role of molossid bats in ebolavirus sylvatic maintenance is an important area for potential research (Kupferschmidt, 2019; Goldstein et al., 2018).

Seasonality of EVD events has been noted (Schmidt et al., 2017), however the abiotic conditions (such as rainfall) used within these analyses are likely not directly driving spillover, especially for unstable RNA viruses in tropical environments (Fischer et al., 2015). We hypothesized viral persistence within bat populations themselves, meaning viral sylvatic dynamics, are also unlikely to be directly attributable to exogenous pressures. By exchanging the traditional abiotic metrics of seasonality with a derived metric such as seasonality of birth we are able to explore a mechanistically plausible driver of seasonality within the sylvatic EVD system (Altizer et al., 2006) and aim to understand both necessary and sufficient causes of EVD emergence and contributions of bats as reservoirs (Nishiura et al., 2009; Rothman, 1976). Temporally varying bat birth terms identified by both our non-human spillover host and human risk models support the hypothesis that birthing may facilitate transmission into non-human mammals (Pourrut et al., 2009; Schuh et al., 2017). In our best models for ebolavirus spillover the birthing term for both fruit bats and non-molossid microbats were significant. The later of the lag terms identified for the African fruit bats is consistent with the maternally derived anti-body (MDA) hypothesis of Pourrut et al. (2009) and Peel et al. (2018), dynamics predicted by generic filovirus models (Hayman, 2015), and observed in empirical MARV data (Amman et al., 2012).

Risk of spillover to non-human spillover hosts was strongly driven by human population density and responsible for much of the patchy geographic risk distribution (see SI Figure 4). This negative human population density-EVD risk relationship was still significant, but the effect size was much smaller, within the human system. This may be expected given many outbreaks in animals are identified in forest-dwelling species, such as gorillas, and concurrently with human cases where index cases are reported to have had contact with other species such as gorillas (Leroy et al., 2004). The correlation of non-bat mammalian diversity in both spillover models could indicate simply that both the bat hosts and the non-reservoir spillover hosts live in the biodiverse tropical forests. Temporally lagged terms that describe chains of infection, both from bats to non-humans spillover hosts and from them to humans, were significant in our models as expected. In contrast to other work, however, we did not find habitat fragmentation to be predictive of EVD spillover risk (Rulli et al., 2017), perhaps because we are not modeling changes in forest through time or because

we are modeling risk at a much larger scale than those studies (but see also Wilkinson et al. (2018)) and thus Simpson's paradox applies, using slightly different methods, or because the other terms in our models are more important. It is difficult to consider how instances of Simpson's paradox may be influencing our results, but clearly the interactions between habitat change, bat birthing, ebolavirus emergence and disease emergence in general are areas for future research (Rulli et al., 2017; Wilkinson et al., 2018; Han et al., 2016). Data sets to test these relationships, such as one populated with animal infections independent of human outbreak events, however, present serious hurdles in these regards.

The DRC has seen more EVD outbreak events than any other country, and the two most recent outbreaks exemplify the country's ongoing struggle to combat a complex system. While the seasonality of relative risk is largely similar between the two locations, there are distinct and potentially important local peaks and troughs within the local seasonality of risk for each location and both outbreaks occurred at, or close to, local maximal values of relative risk. These seasonal patterns may be linked to the biannual birth pulses of the local fruit bat or molossid species, but are also likely tied to extremely local shifts in behavioral, phenological, and climatic factors that modify both the reservoir host(s) and susceptible populations.

Analyses of EVD emergence, including ours, are clearly limited by sparse data. This includes information on other possible host species such as apes, swine and other small mammals, which may warrant further investigation if data become available. Most recent serological analyses of African primates, however, support our assumptions that they are unlikely to be maintenance hosts (Ayouba et al., 2019; Hayman, 2019). The lack of detailed species specific bat birthing data hampered our ability to test some hypotheses and necessitated the aggregation of data by host taxonomic traits rather than a species, or genus level. While these groupings have proved useful (Cumming and Bernard, 1997), we do acknowledge that the patterns discussed may not be fully representative for all members (i.e. *E. helvum*) and was our primary motivation for creating down-weighted variation. However, despite individual bat variations, our model still broadly captures when species such as *E. helvum* give birth in space and time, even if the particular species only gives birth annually (Peel et al., 2017). Despite the significance of only fruit bat associated diversity terms, non-molossid microbats are under sampled virologically (Leendertz et al., 2016) and ecologically (this study) for such a diverse taxonomic group. Increased data may change our understanding of their role in EVD, especially in light of the recent news of ebolavirus viral fragments in the *Miniopterus inflatus* microbat and isolation of a potentially new *Ebolavius* species by Goldstein et al. (2018) from a molossid species, demonstrate the undiscovered viral diversity within the system. We were also unable to include bat abundance terms, and clearly host abundance will affect the likelihood of viral persistence in populations (Hayman, 2015; Pourrut et al., 2009). These ecological gaps, however, can be filled without additional virological work, although contemporaneous ecological and virological data collection will provide advantages for data integration and improved system understanding (Rulli et al., 2017; Pourrut et al., 2009; Amman et al., 2012; Restif et al., 2012). Because of the limited number of viral detections, all *Ebolavirus* species were combined into a generic definition of ebolavirus despite the probably that each species has its own intricacies of sylvatic persistence, distribution, reservoir host and spillover. Further, the reliance on symptomatic EVD has increased these biases if viruses had different pathological consequences in man. Only increased virological studies in hosts and unfortunately outbreaks in people will allow us to disentangle these species level intricacies. Despite these weaknesses, we believe we have successfully captured the overall patterns of birth pulses of African bats and provide potentially useful insights in the ecology of ebolaviruses and how seasonal changes in EVD risk may be driven by bat reservoir host ecology.

Author contributions

D.T.S.H. conceived the study; D.T.S.H., C.R.H., J.C.M. developed the methods; C.R.H. & A.M. compiled the data; C.R.H. & J.C.M. wrote the code; C.R.H. ran the analysis; A.M. provided critiques; C.R.H. wrote the first draft with all authors editing and reviewing the manuscript.

Funding

D.T.S.H would like to acknowledge funding by Rutherford Discovery FellowshipRDF-MAU1701 and MarsdenMAU1503.

Conflicts of interest

The authors declare no conflicts of interest.

Acknowledgements

We would like to acknowledge Dr. David Wilkinson for all his help, along with the many reviewers who helped.

Appendix A. Supplementary data

Supplementary data associated with this article can be found, in the online version, at https://doi.org/10.1016/j.epidem.2019.100366.

References

Altizer, S., Dobson, A., Hosseini, P., Hudson, P., Pascual, M., Rohani, P., 2006. Seasonality and the dynamics of infectious diseases. Ecol. Lett. 9 (4), 467–484.

Amman, B.R., Carroll, S.A., Reed, Z.D., Sealy, T.K., Balinandi, S., Swanepoel, R., et al., 2012. Seasonal pulses of Marburg virus circulation in Juvenile Rousettus aegyptiacus bats coincide with periods of increased risk of human infection. PLoS Pathog. 8 (10).

Ayouba, A., Ahuka-Mundeke, S., Butel, C., Mbala Kingebeni, P., Loul, S., Tagg, N., et al., 2019. Extensive serological survey of multiple African nonhuman primate species reveals low prevalence of immunoglobulin G antibodies to 4 Ebola virus species. J. Infect. Dis.

Barry, A., Ahuka-Mundeke, S., Ali Ahmed, Y., Allarangar, Y., Anoko, J., Archer, B.N., et al., 2018. Outbreak of Ebola virus disease in the democratic republic of the Congo, April–May, 2018: an epidemiological study. Lancet.

Bernard, R.T.F., Cumming, G.S., 1997. African bats: evolution of reproductive patterns and delays. Q. Rev. Biol. 72 (3), 253–274.

Biek, R., Walsh, P.D., Leroy, E.M., Real, L.A., 2006. Recent common ancestry of Ebola Zaire virus found in a bat reservoir. PLoS Pathog. 2 (10), 0885–0886.

Briand, S., Bertherat, E., Cox, P., Formenty, P., Kieny, M.P., Myhre, J.K., et al., 2014. The international Ebola emergency. New Engl. J. Med. 371 (September (13)), 1180–1183. https://doi.org/10.1056/NEJMp1409903. http://www.nejm.org/doi/10.1056/NEJMp1409858.

Brown, V.L., Drake, J.M., Stallknecht, D.E., Brown, J.D., Pedersen, K., Rohani, P., 2013. Dissecting a wildlife disease hotspot: the impact of multiple host species, environmental transmission and seasonality in migration, breeding and mortality. J. R. Soc. Interface 10 (79), 20120804. Available from: http://www.pubmedcentral.nih.gov/articlerender.fcgi?artid=3565696&tool=pmcentrez&rendertype=abstract.

Cumming, G.S., Bernard, R.T.F., 1997. Rainfall, food abundance and timing of parturition in African bats. Oecologia 111 (3), 309–317.

De Nys, H.M., Kingebeni, P.M., Keita, A.K., Butel, C., Thaurignac, G., Villabona-Arenas, C.J., et al., 2018. Survey of Ebola Viruses in frugivorous and insectivorous bats in Guinea, Cameroon, and the democratic republic of the Congo, 2015–2017. Emerg. Infect. Dis. 24 (December (12)). Available from: http://wwwnc.cdc.gov/eid/article/24/12/18-0740_article.htm.

Duke-Sylvester, S.M., Bolzoni, L., Real, La., 2011. Strong seasonality produces spatial asynchrony in the outbreak of infectious diseases. J. R. Soc. Interface/R. Soc. 8 (59), 817–825. Available from: http://www.pubmedcentral.nih.gov/articlerender.fcgi?artid=3104344&tool=pmcentrez&rendertype=abstract.

Fischer, R., Judson, S., Miazgowicz, K., Bushmaker, T., Prescott, J., Munster, V.J., 2015. Ebola virus stability on surfaces and in fluids in simulated outbreak environments. Emerg. Infect. Dis. 21 (July (7)), 1243–1246. Available from: http://www.ncbi.nlm.nih.gov/pubmed/26079114 http://www.pubmedcentral.nih.gov/articlerender.fcgi?artid=PMC4480404.

Gilbert, A.T., Fooks, A.R., Hayman, D.T.S., Horton, D.L., Müller, T., Plowright, R., et al., 2013. Deciphering serology to understand the ecology of infectious diseases in wildlife. EcoHealth 10 (3), 298–313.

Goldstein, T., Anthony, S.J., Gbakima, A., Bird, B.H., Bangura, J., Tremeau-Bravard, A., et al., 2018. The discovery of Bombali virus adds further support for bats as hosts of ebolaviruses. Nat. Microbiol. 1. Available from: http://www.nature.com/articles/s41564-018-0227-2.

Grenfell, B.T., Bjørnstad, O.N., Kappey, J., 2001. Travelling waves and spatial hierarchies

in measles epidemics. Nature 414 (December), 716–723.
Han, B.A., Schmidt, J.P., Alexander, L.W., Bowden, S.E., Hayman, D.T.S., Drake, J.M., 2016. Undiscovered bat hosts of Filoviruses. PLOS Negl. Trop. Dis. 10 (7), 1–10.
Happold, D.C.D., Happold, M., 1990. Reproductive strategies of bats in Africa. J. Zool. 222 (December (1990)), 557–583. https://doi.org/10.1111/j.1469-7998.1990.tb06014.x.
Happold, M., Happold, D.C.D., 2013. Mammals of Africa Volume IV – Hedgehogs, Shrews and Bats. Bloomsbury, London.
Hassanin, A., Nesi, N., Marin, J., Kadjo, B., Pourrut, X., Leroy É, et al., 2016. Comparative phylogeography of African fruit bats (Chiroptera, Pteropodidae) provide new insights into the outbreak of Ebola virus disease in West Africa, 2014–2016. C. R. Biol. (October), 2014–2016. Available from: http://www.ncbi.nlm.nih.gov/pubmed/27746072http://linkinghub.elsevier.com/retrieve/pii/S1631069116301287.
Haydon, D.T., Cleaveland, S., Taylor, L.H., Laurenson, M.K., 2002. Identifying reservoirs of infection: a conceptual and practical challenge. Emerg. Infect. Dis. 8 (12), 1468–1473.
Hayman, D.T.S., Emmerich, P., Yu, M., Wang, L.F., Suu-Ire, R., Fooks, A.R., et al., 2010. Long-term survival of an urban fruit bat seropositive for Ebola and Lagos bat viruses. PLoS ONE 5 (8), 2008–2010.
Hayman, D.T.S., Yu, M., Crameri, G., Wang, L.F., Suu-Ire, R., Wood, J.L.N., et al., 2012. Ebola virus antibodies in fruit bats, Ghana, West Africa. Emerg. Infect. Dis. 18 (7), 1207–1209. Available from: http://www.pubmedcentral.nih.gov/articlerender.fcgi?artid=3376795&tool=pmcentrez&rendertype=abstract.
Hayman, D.T.S., 2015. Biannual birth pulses allow filoviruses to persist in bat populations. Proc. R. Soc. B Biol. Sci. 282 (1803). https://doi.org/10.1098/rspb.2014.2591.
Hayman, D.T.S., 2019. African primates: likely victims, not reservoirs, of Ebolaviruses. J. Infect. Dis. https://doi.org/10.1093/infdis/jiz007.
Kamins, A.O., Restif, O., Ntiamoa-Baidu, Y., Suu-Ire, R., Hayman, D.T.S., Cunningham, A.A., et al., 2011. Uncovering the fruit bat bushmeat commodity chain and the true extent of fruit bat hunting in Ghana, West Africa. Biol. Conserv. 144 (12), 3000–3008. https://doi.org/10.1016/j.biocon.2011.09.003.
Kupferschmidt, K., 2019. This Bat Species May be the Source of the Ebola Epidemic That Killed More Than 11,000 People in West Africa. Available from: http://www.sciencemag.org/news/2019/01/bat-species-may-be-source-ebola-epidemic-killed-more-11000-people-west-africa.
Leendertz, S.A.J., Gogarten, J.F., Düx, A., Calvignac-Spencer, S., Leendertz, F.H., 2016. Assessing the evidence supporting fruit bats as the primary reservoirs for Ebola viruses. EcoHealth 13 (1), 18–25.
Leroy, E.M., Rouquet, P., Formenty, P., Kilbourne, A., Froment Jm, Bermejo, M., et al., 2004. Events and rapid decline of central African wildlife. Science 303 (January), 387–390.
Leroy, E.M., Kumulungui, B., Pourrut, X., Rouquet, P., Hassanin, A., Yaba, P., et al., 2005. Fruit bats as reservoirs of Ebola virus. Nature 438 (December (7068)), 575–576. https://doi.org/10.1038/438575a.
Mickleburgh, S., Waylen, K., Racey, P., 2009. Bats as bushmeat: a global review. Oryx 43 (2), 217–234.
Monadjem, A., Taylor, P.J., Cotterill, F., Schoeman, M.C., Goodman, S.M., 2010. Bats of Southern and Central Africa. Wits University Press.
Morvan, J.M., Deubel, V., Gounon, P., Nakouné, E., Barrière, P., Murri, S., et al., 1999. Identification of Ebola virus sequences present as RNA or DNA in organs of terrestrial small mammals of the Central African Republic. Microbes Infect. 1 (14), 1193–1201.
Ng, M., Ndungo, E., Kaczmarek, M.E., Herbert, A.S., Binger, T., Kuehne, A.I., et al., 2015. Filovirus receptor NPC1 contributes to species-specific patterns of Ebolavirus susceptibility in bats. eLife 4 (December). Available from: https://elifesciences.org/articles/11785.
Nishiura, H., Hoye, B., Klaassen, M., Bauer, S., Heesterbeek, H., 2009. How to find natural reservoir hosts from endemic prevalence in a multi-host population: a case study of influenza in waterfowl. Epidemics 1 (2), 118–128.
Nowak, R.M., 1994. Walker's Bats of the World. John's Hopkins Iniversity Press, Baltimore.
Olival, K.J., Hayman, D.T.S., 2014. Filoviruses in bats: current knowledge and future directions. Viruses 6 (4), 1759–1788.
Peel, A.J., Wood, J.L.N., Baker, K.S., Breed, A.C., Carvalho, A.D., Fernández-Loras, A., et al., 2017. How does Africa's most hunted bat vary across the continent? Population traits of the straw-coloured fruit bat (*Eidolon helvu* m) and Its Interactions with Humans. Acta Chiropterol. 19 (1), 77–92. https://doi.org/10.3161/15081109ACC2017.19.1.006.
Peel, A.J., Baker, K.S., Hayman, D.T.S., Broder, C.C., Cunningham, A.A., Fooks, A.R., et al., 2018. Support for viral persistence in bats from age-specific serology and models of maternal immunity. Sci. Rep. 8 (1), 3859. Available from: http://www.nature.com/articles/s41598-018-22236-6.
Pigott, D.M., Golding, N., Mylne, A., Huang, Z., Henry, A.J., Weiss, D.J., et al., 2014. Mapping the zoonotic niche of Ebola virus disease in Africa. eLife 3 (September (6)), 366–378. https://doi.org/10.7554/eLife.04395.
Pigott, D.M., Millear, A.I., Earl, L., Morozoff, C., Han, B.A., Shearer, F.M., et al., 2016. Updates to the zoonotic niche map of Ebola virus disease in Africa. eLife 5 (2016 July), 1–13.
Plowright, R.K., Eby, P., Hudson, P.J., Smith, I.L., Westcott, D., Bryden, W.L., et al., 2015. Ecological dynamics of emerging bat virus spillover. Proc. R. Soc. B: Biol. Sci. 282 (1798), 20142124. https://doi.org/10.1098/rspb.2014.2124.
Pourrut, X., Kumulungui, B., Wittmann, T., Moussavou, G., Delicat, A., Yaba, P., et al., 2005. The natural history of Ebola virus in Africa. Microbes Infect. 7 (June (7–8)), 1005–1014. Available from: http://linkinghub.elsevier.com/retrieve/pii/S1286457905001437.
Pourrut, X., Souris, M., Towner, J.S., Rollin, P.E., Nichol, S.T., Gonzalez, J.P., et al., 2009. Large serological survey showing cocirculation of Ebola and Marburg viruses in gabonese bat populations, and a high seroprevalence of both viruses in Rousettus aegyptiacus. BMC Infect. Dis. 9 (1), 159. Available from: http://www.biomedcentral.com/1471-2334/9/159.
Restif, O., Hayman, D.T.S., Pulliam, J.R.C., Plowright, R.K., George, D.B., Luis, A.D., et al., 2012. Model-guided fieldwork: practical guidelines for multidisciplinary research on wildlife ecological and epidemiological dynamics. Ecol. Lett. 15 (10), 1083–1094.
Rothman, K.J., 1976. Causes. Am. J. Epidemiol. 104 (6), 587–592.
Rulli, M.C., Santini, M., Hayman, D.T.S., D'Odorico, P., 2017. The nexus between forest fragmentation in Africa and Ebola virus disease outbreaks. Sci. Rep. 7 (December (2016)), 1–8. https://doi.org/10.1038/srep41613.
Schmidt, J.P., Park, A.W., Kramer, A.M., Han, B.A., Alexander, L.W., Drake, J.M., 2017. Spatiotemporal fluctuations and triggers of ebola virus spillover. Emerg. Infect. Dis. 23 (3), 415–422.
Schuh, A.J., Amman, B.R., Jones, M.E.B., Sealy, T.K., Uebelhoer, L.S., Spengler, J.R., et al., 2017. Modelling filovirus maintenance in nature by experimental transmission of Marburg virus between Egyptian rousette bats. Nat. Commun. 8 (February (1)), 14446. https://doi.org/10.1038/ncomms14446.. Available from: https://doi.org/10.1038/s41598-017-07824-2.
Swanepoel, R., Leman, P.A., Burt, F.J., Zachariades, N.A., Braack, L.E.O., Ksiazek, T.G., et al., 1996. Experimental inoculation of plants and animals with Ebola virus. Emerg. Infect. Dis. 2 (4), 321–325.
Taylor, D.J., Leach, R.W., Bruenn, J., 2010. Filoviruses are ancient and integrated into mammalian genomes. BMC Evolut. Biol. 10 (1).
Team RC, 2017. R: A Language and Environment for Statistical Computing. Vienna, Austria. Available from: https://www.r-project.org/.
Walsh, P.D., Biek, R., Real, L.A., 2005. Wave-like spread of Ebola Zaire. PLoS Biol. 3 (11), 1946–1953.
(WHO) WHO, 2018. Cluster of Presumptive Ebola Cases in North Kivu in the Democratic Republic of the Congo. Kinshasa/Geneva. Available from: http://www.who.int/news-room/detail/01-08-2018-cluster-of-presumptive-ebola-cases-in-north-kivu-in-the-democratic-republic-of-the-congo.
Wilkinson, D.A., Marshall, J.C., French, N.P., Hayman, D.T.S., 2018. Habitat fragmentation, biodiversity loss and the risk of novel infectious disease emergence. J. R. Soc. Interface 15 (149), 20180403. https://doi.org/10.1098/rsif.2018.0403.